Dissertation zur Erlangung des Doktorgrades
der Fakultät für Chemie und Pharmazie
der Ludwig-Maximilians-Universität München

The *Arabidopsis* glucosyltransferase UGT76B1 as a major hub in salicylic acid-related plant defence

Sibylle Bauer

aus
Regensburg

2020

Erklärung

Diese Dissertation wurde im Sinne von § 7 der Promotionsordnung vom 28.November 2011 von Herrn PD Dr. Anton R. Schäffner betreut.

Eidesstattliche Versicherung

Diese Dissertation wurde eigenständig und ohne unerlaubte Hilfe erarbeitet.

München, den **14.08.2020**

.....

(Sibylle Bauer)

Dissertation eingereicht am **26.05.2020**

1. Gutachter: PD Dr. Anton Rudolf Schäffner

2. Gutachter: Prof. Dr. Jörg Durner

Mündliche Prüfung am **16.07.2020**

Publications and conference contributions related to this thesis:

Bauer S, Mekonnen DW, Geist B, Lange B, Zhang W, Schäffner AR (2020) The isoleucic acid triad: distinct impacts on plant defense, root growth and formation of reactive oxygen species, *Journal of Experimental Botany* **71:** 4258-4270, https://doi.org/10.1093/jxb/eraa160

Bauer S, Mekonnen DW, Hartmann M, Janowski R, Lange B, Geist B, Zeier J, Schäffner AR (2020) UGT76B1, a promiscuous hub of small molecule-based immune signaling, glucosylates N-hydroxypipecolic acid and controls basal pathogen defense (submitted to *The Plant Cell*)

Bauer S, Georgii E, Lange B, Maksym RP, Janowski R, Geist B, Schäffner AR Functional relationships of UDP glucosyltransferases in salicylic acid metabolism of *Arabidopsis thaliana* (in preparation)

Bauer S, Maksym RP, Geist B, Lange B, Mekonnen DW, Zhang W, Schäffner AR (2019) The 2-hydroxy carboxylic acid isoleucic acid modulates defense and growth in *Arabidopsis thaliana*, 14th International Conference on Reactive Oxygen and Nitrogen Species in Plants, München, Germany, Oral presentation.

Bauer S, Maksym RP, Ghirado A, Geist B, Lange B, Mekonnen DW, Zhang W, Schäffner AR (2018) Isoleucic acid enhances SA-related and SA-independent defense responses, The International Conference on Arabidopsis Research (ICAR), Turku, Finland, Oral presentation

Bauer S, Maksym RP, Geist B, von Saint Paul V, Zhu X, Schmiesing A, Georgii E, Schäffner AR (2017) Roots of defense - belowground impact of the small molecule glucosyltransferase UGT76B1, Topic Day: Terrestial Environment, München, Germany, Poster presentation

Abstract

Plants are sessile organisms which are continuously challenged with a diverse range of environmental stress stimuli. Thus, plants have developed a plethora of ways to adapt and survive. Salicylic acid (SA) is a crucial phytohormone involved in various aspects of plant life, notably in inducing plant defence against biotrophic pathogens. However, high concentrations of endogenous SA and the subsequent activation of defence inversely correlate with plants growth. Consequently, free SA levels are controlled at the biosynthetic level and by various downstream chemical modifications. One important modification of SA is the formation of physiologically inactive SA glucosides. At least three UDP-dependent glucosyltransferases (UGTs), UGT74F1, UGT74F2, and UGT76B1 of *Arabidopsis thaliana* were shown to glucosylate SA *in vitro*. However, their impact on SA glucosylation and plant defence *in vivo* was inconclusive and not proven.

A complete mutant set of single, double, and the triple mutants of the three UGTs was produced in Col background to understand the influence of each UGT towards free SA levels and pathogen defence responses. Targeted metabolic analysis revealed that *ugt76b1* contained enhanced levels of free SA under non stressed conditions, whereas the mutation of UGT74F1 or UGT74F2 did not lead to changes in free SA levels compared to the wild type. In addition, transcriptomic studies showed that UGT76B1 plays a major role in plant defence responses by regulating SA biosynthesis and SA signalling. Bacterial infection of single mutants exhibited a higher disease resistance of the *ugt76b1* mutant compared to that of the *ugt74f1* or *ugt74f2* mutants. Even though SAG production was mainly dependent on UGT74F1, the attempt to replace UGT76B1 by the coding region of UGT74F1 in the *ugt76b1* background did not rescue the phenotypes of the *ugt76b1* mutant. This shows that UGT76B1 has different tasks than UGT74F1 and both enzymes are not redundant. In summary, UGT76B1 suppressed free SA levels and SA signalling under non-stressed conditions, whereas UGT74F1 and UGT74F2 had no major influence.

The role of UGT76B1 in plant defence was not only related to the ability of UGT76B1 to glucosylate SA, but also to its ability to glucosylate two other pathogen defence activating compounds: isoleucic acid (ILA) and N-hydroxy pipecolic acid (N-OH-Pip). Both compounds were shown to induce plant resistance towards pathogens. ILA was already known as a substrate of UGT76B1, whereas N-OH-Pip was discovered as a third and new substrate. UGT74F1 and UGT74F2 seem to not glucosylate these two compounds. By competitive

inhibition of UGT76B1, ILA as well as N-OH-Pip could influence the free SA pool and thereby SA-dependent plant defence responses.

To understand the role of ILA in SA-mediated defence, the interaction of these two compounds was further analysed. ILA synergistically activated SA-responsive gene expression in a UGT76B1-dependent manner, in agreement with the observed competitive ILA-dependent repression of SA glucosylation by UGT76B1.

In addition to N-OH-Pip, a hexoside of N-OH-Pip was also found in infected plant tissue. The presence of N-OGLC-Pip was completely abolished and N-OH-Pip levels were increased by the mutation of UGT76B1. The action of UGT76B1 as an N-OH-Pip glucosyltransferase was confirmed *in vitro* and *in vivo*. Furthermore, an interaction between ILA and N-OH-Pip was found, as the exogenous application of ILA promoted N-OH-Pip biosynthesis and accumulation.

UGT76B1 was shown to glucosylate the three pathogen defence activators SA, ILA, and N-OH-Pip and thereby controlled SA-related defence responses. All three activators were enriched in the *ugt76b1* knockout mutant and consequently plant defence responses enhanced. In summary, this work demonstrates the importance of UGT76B1 to suppress SA-related defence responses in the absence of pathogens.

Table of contents

Figures

Tables

Abbreviations

A. thaliana	*Arabidopsis thaliana*
B. napus	*Brassica napus*
BCAA	Branched chain amino acid
BTH	Benzo (1,2,3) thiadiazole-7-carbothioc acid S-methyl ester
ILA	Isoleucic acid
Ile	Isoleucine
JA	Jasmonic acid
LA	Leucic acid
MeSA	Methyl salicylate
MS	Murashige and Skoog
N-OH-Pip	N-hydroxy pipecolic acid
N-OGLC-Pip	N-hydroxy pipecolic acid glycoside
OE	Overexpressor
PCR	Polymerase chain reaction
Pip	Pipecolic acid
Pst	*Pseudomonas syringae*
ROS	Reactive oxygen species
SA	Salicylic acid
SAG	SA-2-O-β-glucoside
SAR	Systemic acquired resistance
SGE	Salicyloyl glucose ester
UGT	UDP-glycosyltransferase
WT	Wild type

1 Introduction

Salicylic acid (SA; 2-hydroxybenzoic acid) is an important secondary phenolic compound occurring in a broad range of prokaryotic and eukaryotic organisms. In plants, SA is involved in a multitude of developmental processes and stress responses, playing an essential role during the lifespan of the organism (Liu *et al.*, 2015). For instance, SA is involved in seed germination (Rajjou *et al.*, 2006), fruit yield (Larqué-Saavedra & Martin-Mex, 2007), leaf senescence (Morris *et al.*, 2000), stomatal aperture (Miura *et al.*, 2013) and salt tolerance (Ashraf *et al.*, 2010). Most important, on both a local and systemic level plant resistance towards biotrophic pathogens is mediated through SA (Vlot *et al.*, 2009; Yan & Dong, 2014; Lu *et al.*, 2016). Biotrophic pathogen infection leads to an increase in the endogenous levels of SA which in turn activate defence mechanisms (Pieterse *et al.*, 2009). However, high concentrations of endogenous SA and the activation of defence inversely correlate with plants growth. For example, plants with constitutively elevated basal SA levels exhibit both an enhanced disease resistance and a reduced growth phenotype (Rivas-San Vicente & Plasencia, 2011; Chandran *et al.*, 2014). Plants are sessile organisms, which are continuously challenged with a range of environmental stress stimuli, such as pathogens. Therefore, plants have to be able to respond to pathogenic attacks as well as continuing their developmental programme. As a result, plants have developed a trade-off between plant growth and plant defence by controlling the levels of free endogenous SA content (Huot *et al.*, 2014). The enhanced biosynthesis of SA during plant defence leads to higher free SA levels and, once synthesised, free SA is thought to be inactivated by glucosylation (Song, 2006; Song *et al.*, 2008; Vlot *et al.*, 2009; Zhang *et al.*, 2013; Dempsey & Klessig, 2017). Based on current knowledge at least three UDP-dependent glycosyltransferases (UGTs) have been identified *in vitro* as having a potential role in SA glucosylation in the model plant *A. thaliana*: UGT74F1, UGT74F2, and UGT76B1 (von Saint Paul *et al.*, 2011; Dempsey & Klessig, 2017).

1.1 Biosynthesis of salicylic acid during pathogen defence

In plants, SA can be synthesised via two different pathways, the isochorismate and the phenylalanine ammonia-lyase pathway (Liu *et al.*, 2015). In both pathways, SA is synthesised from chorismate, the final product of the shikimate pathway (Dempsey *et al.*, 2011). In *A. thaliana*, it has been reported that during pathogen defence SA is produced primarily by the isochorismate pathway in the chloroplast (Wildermuth *et al.*, 2001; Dempsey & Klessig, 2017). The quadruple *pal* (PHENYLALANINE AMMONIA LYASE) mutants still exhibited 50 % of wild-type SA levels after pathogen infection, whereas in ISOCHORISMATE SYNTHASE1

(ICS1) mutant SA levels were reduced to around 5 % (Huang *et al.*, 2010). The *A. thaliana* genome contains two ICS genes, ICS1 and ICS2, but only *ICS1* (ISOCHORISMATE SYNTHASE1 or SALICYLIC ACID INDUCTION DEFICIENT2 = SID2) accumulates rapidly after pathogen infection (Wildermuth *et al.*, 2001).

The synthesised SA is transported to the cytoplasm by ENHANCED DISEASE SUSCEPTIBILITY 5 (EDS5), where it acts as a signal for initiation of defence responses (Dempsey *et al.*, 2011). For the regulation of ICS1 and thereby SA synthesis under stress, a complex transcriptional regulation is present. Two key transcription factors, SAR DEFICIENT1 (SARD1) and CAM-BINDING PROTEIN 60-LIKE G (CBP60g), induce expression of *ICS1* (Zhang *et al.*, 2010). Many additional regulatory elements involved in SA biosynthesis have been reported, including those that negatively regulate *ICS1* expression. For example, the double knockout mutant of ETHYLENE INSENSITIVE3 (EIN3) and ETHYLENE INSENSITIVE3-LIKE1 (EIL1) revealed enhanced *ICS1* expression, SA enrichment, and were more resistant towards pathogen infection. It was shown that EIN3 directly targets the *ICS1* promoter to suppress plant defence response. By introgression of *sid2* mutation in the *ein3 eil1* double mutant susceptibility to pathogens was restored (Chen *et al.*, 2009). Antagonistically acting compounds as jasmonic acid (JA) and ethylene are involved in SA content regulation (Pieterse & van Loon, 1999). In general, the SA- and JA/ethylene-mediated defence pathways are thought to negatively influence each other and undergo extensive cross-talk (Pieterse *et al.*, 2009). Nevertheless, synergistic effects were also reported (Mur *et al.*, 2006). In summary, SA biosynthesis and signalling is tightly controlled by various processes including positive and negative regulations/interactions.

1.2 SA perception and downstream signalling

One mode of SA perception is presumed to be dependent on the cytosolic protein NONEXPRESSOR OF PATHOGENESIS-RELATED PROTEIN1 (NPR1). NPR1 plays a major and central role in regulation of SA-mediated transcription during plant immune response (Zhang *et al.*, 1999; Fu & Dong, 2013; Seyfferth & Tsuda, 2014). SA influences the expression of more than 1,000 genes (Vidhyasekaran, 2015). A genome-wide gene expression study showed that the *npr1* mutant is almost completely deficient in SA-mediated transcriptional reprogramming (Wang *et al.*, 2006).

In addition to high accumulation of SA, accumulation of reactive oxygen species (ROS) was found to be an early response towards pathogens (Overmyer *et al.*, 2003). Pathogens induce apoplastic ROS production through plasma membrane localised NADPH-oxidases (RESPIRATORY BURST OXIDASE HOMOLOGs, RBOHs) (Grant & Loake, 2000; Qi *et al.*, 2017). In

A. thaliana ten isoforms of RBOHs are known with different tissue-specific expression patterns. Only RBOHD and RBOHF are highly expressed throughout the plant (Orman-Ligeza *et al.*, 2016). In plant defence major attention has been given to RBOHD and RBOHF, since the loss of both genes leads to susceptibility against pathogens (Torres *et al.*, 2006; Morales *et al.*, 2016). During pathogen recognition RBOHD can be activated via Ca^{2+} binding to EF-hand motifs or phosphorylation by Ca^{2+}-DEPENDENT PROTEIN KINASE5 (CPK5), leading to enhanced levels of ROS provoking plant immune responses (Dubiella *et al.*, 2013). It was shown that BOTRYTIS-INDUCED KINASE1 (BIK1) can also phosphorylate ROBHD in a Ca^{2+}-independent manner (Kadota *et al.*, 2014) and recently CYSTEIN-RICH RECEPTOR-LIKE PROTEIN KINASE2 (CRK2) was found to be required for full pathogen-induced ROS bursts (Kimura *et al.*, 2019). Both antagonistic and synergistic effects between RBOHs activity, ROS and SA signalling have been found during pathogen resistance response (Durner & Klessig, 1996; Durrant & Dong, 2004; Herrera-Vásquez *et al.*, 2015; Pandey *et al.*, 2017). In addition to the role of ROS in plant defence, plant growth, and development, such as cell proliferation and differentiation, programmed cell death, senescence, and root hair growth, can be also affected (Singh *et al.*, 2016). For example, pathogen-induced SA accumulation leads to local programmed cell death (Fu & Dong, 2013). *A. thaliana rbohd rbohf* double mutant showed reduced cell death control (Torres *et al.*, 2005) and impaired stomatal closure (Kwak *et al.*, 2003).

1.3 Regulation of cytosolic SA levels

In addition to the regulation of SA biosynthesis, the amount of free bioactive SA within the cytoplasm is regulated. SA content can be regulated by the conjugation of free SA to hydrophilic molecules such as glucose, resulting in the alteration of reactivity, lipophilicity, and biological activity of the molecule. Thus, enzymes involved in SA modification influence the level of free SA content, and thereby control plant defence (Dempsey *et al.*, 2011). Several diverse forms of modification, which are thought to inactivate SA, are depicted in Fig. 1. For instance, SA is glucosylated by cytosolic UDP-dependent glycosyltransferases (UGTs). SA can either be glucosylated at its hydroxyl group to produce 2-*O*-β-D-glucoside (SAG) or glucosylation at its carboxyl group, generating salicyloyl glucose ester (SGE) (Lim *et al.*, 2002). Most of the SA *in planta* is converted into SAG in the cytoplasm and then transported to the vacuole for storage (Vlot *et al.*, 2009). In contrast, the SGE generated in plants remains outside the vacuole (Vaca *et al.*, 2017). It has been speculated that this SAG can be easily hydrolysed and used as a rapidly accessible source to generate bioactive free SA under pathogen attack (Fu & Dong, 2013). Additionally, the inhibition of the conversion of SA to its glucosides leads

to enhanced disease resistance (Dean *et al.*, 2005; Zhang & Li, 2019). Based on current knowledge at least three UGTs are potentially involved in SA glucosylation *in vitro*, UGT74F2, UGT74F1, and UGT76B1 (von Saint Paul *et al.*, 2011; Noutoshi *et al.*, 2012). The function of these enzymes *in vivo* are discussed in detail in section 1.4.

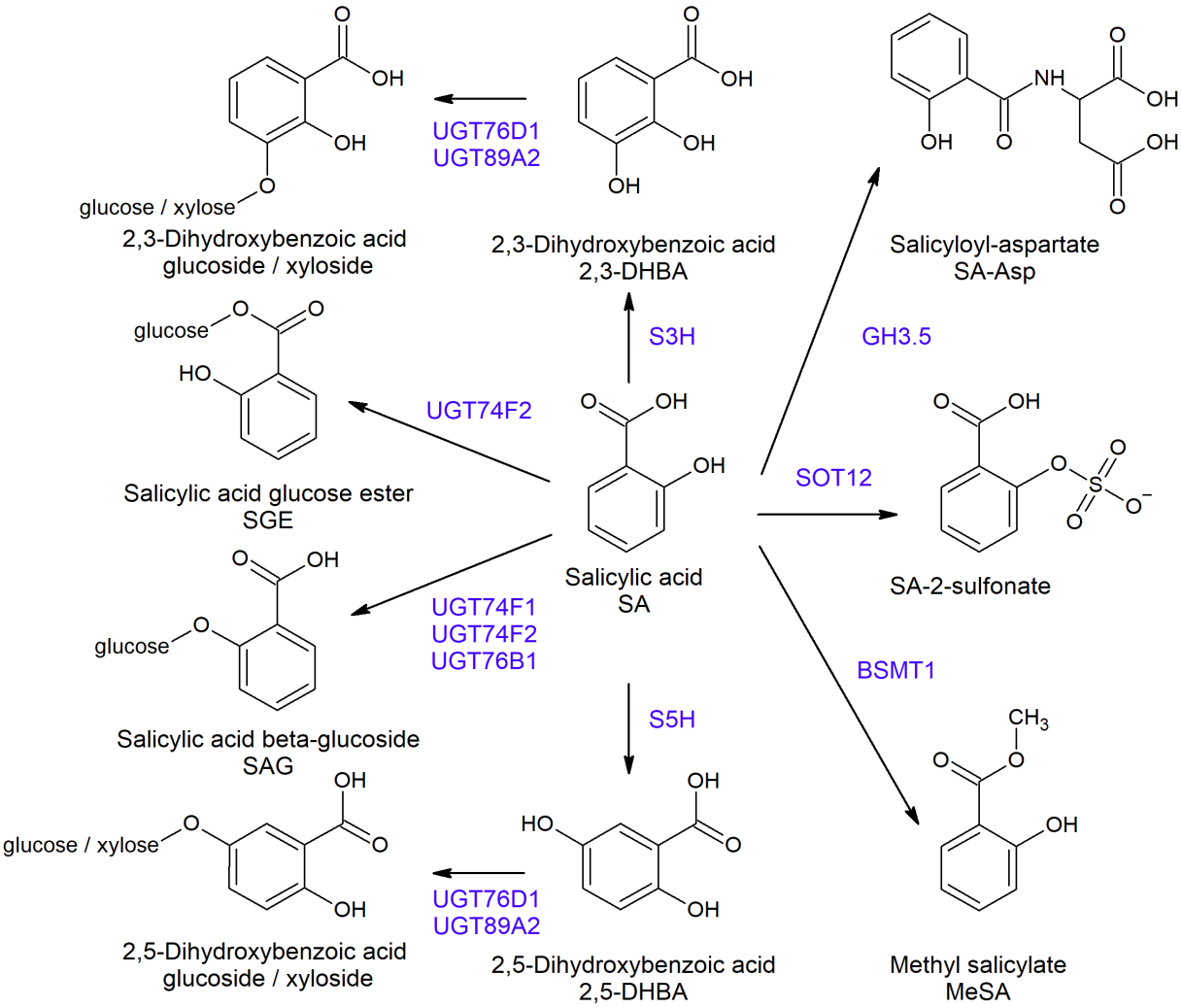

Fig. 1: Regulation of cytosolic SA levels by different modifications

Free SA levels are thought to be controlled by several diverse forms of modifications, which may inactivate free SA. Thereby the control of glucosylation of SA by UGT74F1/UGT74F2 and UGT76B1 were shown to play a major role during pathogen attack. Next to this methylation, sulphonation and amino acid conjugation were also discussed. Furthermore, hydroxylation was shown to influence plant response during pathogen attack.

In addition to glucosylation, other modifications of SA are known. Sulphonation of SA *in vitro* by SULFOTRANSFERASE12 (SOT12) has been described. During infection of plants with *Pseudomonas syringae pv. tomato* (*Pst*), *sot12* knockout mutants accumulated less SA, and SOT12 overexpression revealed enhanced SA levels, indicating that sulphonation of SA may positively regulate free SA levels (Baek *et al.*, 2010). Furthermore, the conjugation of SA to salicyloyl-aspartate (SA-Asp) has been reported. This is the only amino acid conjugate of SA

reported up to date (Mackelprang *et al.*, 2017). The acyl acid amido synthetase GRETCHEN-HAGEN3.5 (GH3.5) conjugates SA to its aspartyl conjugate, but also indole-3-acetic acid (IAA), to balance SA and IAA signalling during pathogen infection (Zhang *et al.*, 2007; Westfall *et al.*, 2016). It was shown that the concentration of Asp determined the preference of GH3.5 between the two compounds (Mackelprang *et al.*, 2017).

In addition, SA can also be oxidised to 2,3-dihydroxybenzoic acid (2,3-DHBA) and 2,5-dihydroxybenzoic acid (2,5-DHBA). 2,3-DHBA was shown to accumulate in an *EDS1*-dependent way in response to pathogens and during senescence, whereas 2,5-DHBA accumulated to a lesser extent. In addition, exogenously applied 2,3-DHBA slightly induced *PR1* expression (Pandey *et al.*, 2017). Formation of 2,3-DHBA is catalysed by SA 3-HYDROXYLASE (S3H), whereas 2,5-DHBA is derived by SA 5- HYDROXYLASE (S5H). The s*3h s5h* knockout mutant accumulated SA. Thus, 2,3-DHBA and 2,5-DHBA might be involved in a feedback loop with SA biosynthesis, preventing too high levels of SA (Zhang *et al.*, 2013; Zhang *et al.*, 2017). Mostly glucosylated forms of DHBAs were found *in planta*. UGT89A2 was responsible for the formation of 2,5-DHBA xyloside (Li *et al.*, 2014) and UGT76D1 was found to glycosylate 2,3-DHBA and 2,5-DHBA with glucose or xylose (Huang *et al.*, 2018). In mutant lines overexpressing *UGT76D1*, DHBAs and SA levels were enhanced (Huang *et al.*, 2018). In total, DHBAs and their glucosylation seem to influence SA homeostasis and plant immune responses.

As well as the generation of inactive SA compounds, certain modifications enable SA transport throughout the plant. For example, methylation of SA by BENZOIC ACID/SA CARBOXYL METHYLTRANSFERASE1 (BSMT1) to methyl salicylate leads to the increase of membrane permeability and enables long distance transport of SA signals (Chen *et al.*, 2003). It was implicated that methyl salicylate (MeSA) is a phloem-based mobile signal in systemic acquired resistance (SAR) dependent on SA (Park *et al.*, 2007).

1.4 Glucosyltransferases in *Arabidopsis*

Glycosyltransferases catalyse the transfer of sugar molecules to a broad and diverse range of molecules, such as lipids, proteins, nucleic acids, and antibiotics, as well as secondary metabolites (Bowles *et al.*, 2005; Lairson *et al.*, 2008; Wang & Hou, 2009). For instance, plant secondary metabolite UGTs catalyse glucosylation of small molecule acceptors (Li *et al.*, 2001). UGTs are therefore thought to be managers of small molecules, including hormones such as SA, JA, and abscisic acid (Bowles *et al.*, 2005). As previously mentioned, the incorporation of a sugar moiety influences properties such as solubility, stability, bioactivity, subcellular localisation, and binding with other molecules. Glucosylation of different sub-

strates contributes to the complexity and variety of its substrates, and is thereby one of the most important modifications especially regarding plant secondary metabolites (Lim & Bowles, 2004; Tiwari *et al.*, 2016). For example, it plays major roles in maintaining cell homoeostasis, plant growth, development, responses to abiotic and biotic stresses, and transport properties of the substrate (Ross *et al.*, 2001; Wang & Hou, 2009; von Saint Paul *et al.*, 2011; Caputi *et al.*, 2012; Saema *et al.*, 2016).

Glycosyltransferases are a diverse multigene family categorised into more than 100 families based on the characteristics of the enzymes (Yonekura-Sakakibara & Hanada, 2011, GT1: GT110; May 2020). Family 1, the largest family of plant kingdom, consists of glycosyltransferases transferring UDP-activated sugar moieties and is characterised by a sequence motif near the C-terminus. It consists of a 44-amino acid consensus and is called PLANT SECONDARY PRODUCT GLYCOSYLTRANSFERASE (PSPG) motif, which defines the nucleotide-diphosphate-sugar binding site of the enzymes (Gachon *et al.*, 2005). This was confirmed by co-crystallisation of UGTs in plants (Yonekura-Sakakibara & Hanada, 2011). UDP-glucose and UDP-rhamnose (in plants) and UDP-glucuronic (in mammalian species) are regarded as the major donor molecules, alongside e.g. UDP-xylose and UDP-galactose. Furthermore, a single UGT can recognise multiple substrates and similarly, a single substrate can be recognized by multiple UGTs (Vogt & Jones, 2000; Lim *et al.*, 2002). In the model plant *A. thaliana* 120 UGT genes were identified as belonging to family 1 (Li *et al.*, 2001), mostly thought to be localised in the cytosol (Bowles *et al.*, 2006). Many different hormones and other substrates are regulated by UGTs, such as auxins, cytokinins, phenylpropanoids, and flavonoids (Bowles *et al.*, 2005). Therefore, UGTs play crucial roles in regulating responses of plants to biotic and abiotic stresses. As mentioned above SA and the content of free SA levels during and after pathogen attack are regulated by glucosylation influencing defence status of plants (1.3). Based on current knowledge at least three UGTs, which all belong to family 1, are potentially involved in SA glucosylation *in vitro:* UGT74F1, UGT74F2, and UGT76B1 (Dean & Delaney, 2008; von Saint Paul *et al.*, 2011).

1.4.1. UGT74F1

In vitro UGT74F1 was able to form SAG (Lim *et al.*, 2002; Dean & Delaney, 2008; Noutoshi *et al.*, 2012), but other substrates were also converted: anthranilate (Quiel & Bender, 2003), flavonoid quercetin (Cartwright *et al.*, 2008), and phenylacetothiohydroximate (Grubb *et al.*, 2014). UGT74F1 and UGT74F2 are 77 % identical, however UGT74F1 is not able to produce SGE, whereas UGT74F2 mainly produces SGE (George Thompson *et al.*, 2017). It was shown that one mutation of a threonine in UGT74F1 (T365A) led to 75 % decreased production of SAG, whereas SGE formation was increased three fold (George Thompson *et al.*,

2017). Noutoshi *et al.* (2012) reported higher levels of free SA in the *ugt74f1-1* mutant and a slightly more resistant phenotype towards virulent and avirulent *Pst* strains compared to the wild type. This is consistent with the *in vitro* and *in vivo* studies of Dean & Delaney (2008), concluding that UGT74F1 plays a role in SA glucosylation. In contrast to these outcomes, in another study, *ugt74f1-1* mutants contained lower levels of free SA and SAG and consequently exhibit higher susceptibility towards pathogens (Boachon *et al.*, 2014). In both studies SAG levels were reduced, but still present. This implies that next to UGT74F1 another enzyme is involved in SAG production. At the transcriptional level *UGT74F1* was not induced by application of exogenous SA or *Pst* infection (Song, 2006; Song *et al.*, 2008; Okamoto *et al.*, 2009). Since contradicting results about the resistance phenotype of *ugt74f1-1* were found, a role of UGT74F1 in controlling free SA levels is less clear. In addition, expression patterns observed via GUS straining of UGT74F1 were not enhanced by *Pst*, SA or BTH treatment (Meßner & Schäffner, unpublished).

1.4.2. UGT74F2

Although *in vitro* studies exhibited that UGT74F2 can form SAG, UGT74F2 mostly catalyses SGE formation (Lim *et al.*, 2002; Dean & Delaney, 2008; Noutoshi *et al.*, 2012; George Thompson *et al.*, 2017). Besides this, it was shown that UGT74F2 also glucosylates different substrates other than SA with higher affinity. For example, observations in both *in vitro* and *in vivo* assays, anthranilate glucosylation is tenfold more efficient than SA glucosylation (Quiel & Bender, 2003). Furthermore, the flavonoid quercetin (Cartwright *et al.*, 2008), phenylacetothiohydroximate (Grubb *et al.*, 2014), benzoic acid, and nicotinate (Li *et al.*, 2015) were used as acceptors. In a comparative study, recombinant UGT74F2 was most active with anthranilate, followed by benzoic acid and nicotinate, whereas activity towards SA was not detected (Li *et al.*, 2015). To test SA glucosylation by UGT74F2, *ugt74f2-1* knockdown plants were fed with radiolabeled [7-^{14}C]-SA and metabolites were measured at different time points. It was shown that wild-type leaves will form SAG and SGE, whereby SGE is exclusively formed by UGT74F2 activity (Dean & Delaney, 2008). Li *et al.* (2015) compared uninfected and infected wild-type plants to the same *ugt74f2-1* knockdown used by Dean & Delaney (2008). They found increased SA, SAG, and SGE levels in wild type after infection, whereas in the *ugt74f2-1* knockdown line, all three substances were less abundant. In addition, they detected higher levels of free nicotinate and lower levels of nicotinate glucosides, demonstrating multi-functionality of UGT74F2. Because of the lower level of SGE in *ugt74f2-1* leaves infected with *Pst,* they concluded that UGT74F2 also catalysed the glucosylation of SA in response to pathogen infection, even though free SA content was reduced. In contrast to this finding, Boachon *et al.* (2014) observed higher levels of free SA in *ugt74f2-1* mutants

after infection. This in turn would suggest that UGT74F2 negatively influences the accumulation of free SA. In addition, SGE levels were abolished, whereas SAG levels were enhanced, demonstrating the SAG measured was catalysed by other UGTs. Infection assays of a UGT74F2 overexpression line led to an increased susceptibility to *Pst* (Song *et al.*, 2008). In accordance with these results, the *ugt74f2-1* knockdown mutant showed slightly higher resistance three days after infection (Boachon *et al.*, 2014). At the transcriptional level, *UGT74F2* expression was induced by pathogen infection, SA, and BTH treatment (BTH = benzo (1,2,3) thiadiazole-7-carbothioc acid S-methyl ester, used as a SA analogue (Song, 2006; Song *et al.*, 2008; Okamoto *et al.*, 2009, Meßner & Schäffner, unpublished). In summary, UGT74F2 could be involved in SA conversion, but the catalytic promiscuity makes it more complicated to connect an observed phenotype to a single compound, if also other processes maybe affected.

1.4.3. UGT76B1

Expression studies on plants exposed to biotic and abiotic stress showed a notably higher expression of *UGT76B1* compared to the other UGTs found in *A. thaliana* (von Saint Paul *et al.*, 2011). In addition, UGT76B1 is among the top 10 highly expressed transcripts following exogenous treatment with SA (Krinke *et al.*, 2007). *In vitro* studies indicate that UGT76B1 possesses glucosylation activity towards SA (von Saint Paul *et al.*, 2011; Noutoshi *et al.*, 2012). In *ugt76b1* knockout mutants elevated SA levels and SA-related marker gene expression were found (von Saint Paul *et al.*, 2011). Therefore, the loss of UGT76B1 function led to enhanced resistance to the biotrophic pathogen *Pst*. Collectively, these results indicate that UGT76B1 plays an important role during stress conditions. Since *in vitro* activity of UGT76B1 towards SA resulted in SAG formation, it can be hypothesised that the loss-of-gene function in *planta* would lead to reduced SAG levels. Unexpectedly, *ugt76b1-1* mutants generated in *Columbia* (Col) exhibited increased basal levels of SAG relative to the wild type. This argued against a role of UGT76B1 in SA glucosylation *in vivo* (von Saint Paul *et al.*, 2011). In contrast, in *ugt76b1-3* mutants generated in the *Wassilekija* (Ws) background, reduced SAG levels in leaves were observed (Noutoshi *et al.*, 2012). However, using the Ws-based *ugt76b1* mutants, this experiment was repeated in our laboratory and no repression of SA glucosides formation was observed (Maksym, 2018). Nevertheless, although the function *in vivo* of UGT76B1 is yet to be elucidated, in both studies *ugt76b1* knockout led to enhanced levels of SA and, consequently, higher resistance towards pathogens. For SA glucosylation in *ugt76b1* background, other UGTs seem to be involved. A non-targeted metabolome analysis of *ugt76b1*, wild type and UGT76B1 overexpressor revealed that another possible substrate of UGT76B1 is isoleucic acid (ILA) (von Saint Paul *et al.*, 2011). Correlation between

UGT76B1 expression, isoleucic acid glucoside (ILAG) formation, and modulation of plant defence were demonstrated. The role of isoleucine in plant defence is discussed in the next section.

1.5 Isoleucic acid - a novel regulator of plant defence

In addition to SA, ILA was discovered as a substrate of UGT76B1 (von Saint Paul *et al.*, 2011; Maksym *et al.*, 2018). Firstly, ILA glucoside was found in plants by non-targeted metabolome analysis as a possible product of UGT76B1 (von Saint Paul *et al.*, 2011). Application of ILA led to an enhanced expression of *PR1* and to higher resistance towards biotrophic pathogens (von Saint Paul *et al.*, 2011). It was considered as a new compound involved in plant defence.

Several defensive compounds are produced from amino acid precursors and amino acid metabolism was connected to plant resistance (Huang *et al.*, 2011; Zeier, 2013). Due to its chemical structure and evidence provided by Maksym *et al.* (2018) ILA is likely linked to the metabolism of the branched-chain amino acid (BCAA) isoleucine (Ile), although this has not yet been unequivocally demonstrated. In humans, ILA was identified in association with the maple syrup urine disease, originating from Ile (Mamer & Reimer, 1992). Genetic defects in the BCKDH complex of the degradation pathway of BCAAs repressed the breakdown of isoleucine, leucine, and valine. Consequently, BCAAs, 2-keto acids and other related products like ILA and related 2-hydroxy acids, valic acid (VA) and leucic acid (LA), accumulate with severe impact on human health (Mamer & Reimer, 1992; Podebrad *et al.*, 1997).

Analyses of different plant species revealed that ILA was found in all plants examined, whereas LA and VA were only found in some species. In *A. thaliana* only ILA and LA were detectable. *In vitro* LA, but not VA, could be also used by UGT76B1 as a substrate (von Saint Paul *et al.*, 2011; Maksym *et al.*, 2018). However, ILA was inversely related to UGT76B1 expression *in planta*, whereas LA was not affected. LA content was not altered in infected plants, while ILA showed reduced levels after infection (Maksym *et al.*, 2018). These results indicate that regulation of ILA is independent to the regulation of LA. How ILA is produced, which tasks are fulfilled by ILA in plants and, how it regulates plant defence are still unknown.

1.6 Interconnection of tissue specific signals

Under unstressed conditions *UGT76B1* displays the highest expression in the root, mainly in cortex and endodermis, whereas in above ground tissues *UGT76B1* was expressed in very young leaves, hydathodes, sepals, and style (von Saint Paul *et al.*, 2011). Expression pattern of *UGT76B1* in leaves is patchy and reduced in four week-old-plants. Upon pathogen infec-

tion with *Pst* and other stress stimuli *UGT76B1* expression was induced in leaves (von Saint Paul *et al.*, 2011). It is important to state that immune responses are normally measured above ground, notably in leaves (von Saint Paul *et al.*, 2011). Therefore, as *UGT76B1* is mainly expressed in roots, a signal deriving from root to shoot is necessary. To control and coordinate physiological processes in the whole plant, integration of signals of different tissues and the movement of a signal is required (Notaguchi & Okamoto, 2015; Lacombe & Achard, 2016). These signals arise from many different origins, e.g. hydraulic signals, Ca^{2+} or ROS waves, hormones, small peptides/proteins or RNAs (Shabala *et al.*, 2016). In defence signalling the exposure of regulatory processes and defence mechanisms were mainly investigated in above-ground tissues (Coninck *et al.*, 2015). Thereby SA, JA, and ethylene were identified as crucial components in local and systemic defence responses. Many similarities, but also differences of these responses were found in roots (Coninck *et al.*, 2015; Johnson *et al.*, 2016). For example, in maize, SA, JA, and absisic acid levels increased in roots and leaves, after infection with *Colletotrichum graminicola*, but with an even more rapid immune response and higher abundance of hormones in roots (Balmer *et al.*, 2013). Abscisic acid, pH, cytokinins, a precursor of ethylene, malate, and other compounds were related to root to shoot signalling under drought (Schachtman & Goodger, 2008). Root-synthesized cytokinins modified shoot hormonal and ionic status, leading to enhanced growth and fruit yield under salinised conditions (Ghanem *et al.*, 2010). In addition, architecture of root and shoot (Norman *et al.*, 2004) or gene expression (Takei *et al.*, 2002) can be controlled by root-derived signal. Long and short-distance signalling is influenced by different chemical properties. For instance, although uncharged forms of hormones can freely diffuse due to the concentration gradient, the transport of hormones requires active transporters to cross the plasma membrane (Lacombe & Achard, 2016). The major route of root-shoot and shoot-root shift of hormones is the plant vascular system (Notaguchi & Okamoto, 2015). Hydraulic signalling is very fast and could present an important communication path (Christmann *et al.*, 2013).

In addition to root-shoot communication, leaf to leaf communication is studied intensively. For example, the establishment of SAR requires functional SA synthesis, accumulation, and functional SA signalling pathways in the distal leaves (Vernooij *et al.*, 1994; Shah *et al.*, 2014). As mentioned before, methylation of SA increases membrane permeability and vapour pressure and enables long distance transport in plants (Chen *et al.*, 2019). Thus, MeSA was proposed as mobile signal in SAR (Park *et al.*, 2007; Vlot *et al.*, 2009). Other compounds, such as monoterpenes or pipecolic acid were found to induce SAR (Návarová *et al.*, 2012; Singh *et al.*, 2017).

1.7 Pipecolic acid in plant defence

Pipecolic acid (Pip), a compound derived from the amino acid lysine, was also identified as a regulator of plant immunity (Návarová *et al.*, 2012). Following pathogen infection Pip accumulated in local and distal leaves and in petiole exudates from infected leaves, whereas it was hardly detectable in non-inoculated plants. Exogenously applied Pip enhances resistance towards pathogens. In total, Pip was found to influence local plant defence, to be a positive regulation of SA biosynthesis and a priming effect in systemic tissue (Návarová *et al.*, 2012). In addition to the SA accumulation, Pip enhances levels of nitric oxide (NO) and ROS acting upstream of azelaic acid (AzA) and glycerol-3-phosphate (G3P). SA and G3P are required for a SAR response and biosynthesis of Pip in distal leaves. Conversely, plants deficient in NO, ROS, G3P or SA showed reduced Pip accumulation in distal leaves, but did not influence levels of Pip at the local site of infection (Wang *et al.*, 2018a).

Pip is derived from Lysine and two enzymes. The enzymes AGD2-LIKE DEFENCE RESPONSE PROTEIN1 (ALD1) and SAR-DEFICIENT4 (SARD4) were identified as being involved in Pip biosynthesis in plastids (Ding *et al.*, 2016; Hartmann *et al.*, 2017). EDS5 is required for the export of Pip from the plastid to the cytosol (Rekhter *et al.*, 2019). Recently it was demonstrated that N-hydroxy pipecolic acid (N-OH-Pip), which is formed from Pip by FLAVIN CONTAINING MONOOXYGENASE1 (FMO1), is most probably the active, mobile form influencing SAR (Hartmann *et al.*, 2017; Chen *et al.*, 2018). N-OH-Pip was proposed as prime candidate for the mobile defence signal, produced at the infected leaf and establishing defence in distal, uninfected leaves (Hartmann *et al.*, 2018). Application of N-OH-Pip changed defence metabolites, camalexin and SA glucoside next to the expression of pathogenesis-related genes, and thereby enhanced resistance to a bacterial pathogen similar to Pip application (Bernsdorff *et al.*, 2016; Chen *et al.*, 2018). *FMO1*, *ALD1*, and *SARD4* are upregulated during pathogen infection resulting in enhanced Pip, N-OH-Pip levels, and defence activation (Shan & He, 2018). Interestingly, an hexoside of N-OH-Pip was found in infected plant extracts (Chen *et al.*, 2018; Hartmann & Zeier, 2018). Since this hexose form of N-OH-Pip was accumulated during pathogen infection, the activity of N-OH-Pip could be controlled by glucosylation, similar to the mechanism of SA glucosylation (1.3).

1.8 Interaction of SA, ILA, and N-OH-Pip and a potential role of UGTs to control plant defence responses

As stated previously, SA is a central hub for plant defence responses. Its activity is thought to be controlled by conversion to SA glucosides (Vlot *et al.*, 2009; Dempsey *et al.*, 2011; Fu & Dong, 2013). For the deactivation at least three UGTs, UGT74F1, UGT74F2, and UGT76B1

were found to glucosylated SA *in vitro*. Furthermore, other compounds like ILA and N-OH-Pip could potential influence the abundance of free SA and thereby alter plant defence responses. In turn, ILA and N-OH-Pip themselves, seem to be controlled by glucosylation and consequently this could constitute an additional layer of control on the SA-dependent defence pathway (compare Fig. 2).

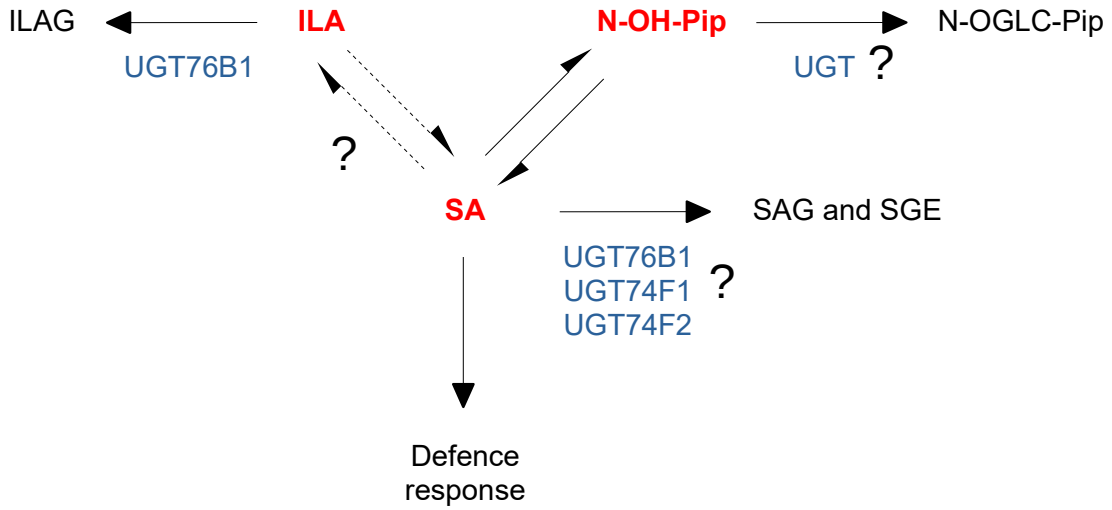

Fig. 2: Potential interplay of SA , ILA, and N-OH-Pip in regulating SA-dependent plant defence responses

SA is a central hub for the activation of plant defence responses. In addition, ILA (von Saint Paul et al.*, 2011) and N-OH-Pip (Hartmann* et al.*, 2018) were shown to have an impact on plant defence. For basal immunity the action of N-OH-Pip (converted from Pip) is mostly dependent on SA (Bernsdorff* et al.*, 2016). For ILA an SA-dependent component was found via inhibition of UGT76B1* in vitro *(Noutoshi* et al.*, 2012). An interaction of N-OH-Pip and ILA is not known so far. Glucosylation of compounds is thought to be a control mechanism to inactivate compounds. The three defence activating compounds, SA , ILA, and N-OH-Pip (red), could be controlled by glucosylation and potential inactivated forms are shown in black. UGT74F1, UGT74F2, and UGT76B1 were shown to glucosylate SA* in vitro. *ILA was glucosyated by UGT76B1* in vitro *and for N-OH-Pip no candidate for glucosylation is known so far. Red active form of compounds, black potential inactivated forms, blue UGTs, converted to (→), potential interaction (⇌).*

1.8.1. Potential interplay of UGTs in SA glucosylation

All three UGTs, UGT74F1, UGT74F2, and UGT76B1, were shown to glucosylate SA *in vitro*. Their role in glucosylating SA *in vivo* and their influence in plant defence is less clear (compare 1.4). Since SAG is found in *ugt74f1-1*, *ugt76b1-1*, and also in ami*ugt74f2,* neither UGT74F1 nor UGT74F2 nor UGT76B1 alone are solely involved in SA glucosylation in *A. thaliana*. How and in which context each of them is involved in SA glucosylation, and how free SA levels are thereby influenced is unclear and controversial. Some studies show up-regulation of SAG after removal of one UGT, whereas others show a slight reduction, but SAG is still present in all single mutants. In our laboratory, side-by-side comparison of ectopic

overexpression of UGT74F1 and UGT74F2 enzymes in transgenic *A. thaliana* resulted in increased SA glucosides, with UGT74F1 being more efficient (Meßner & Schäffner, unpublished). To further test the interaction of UGT74F1 and UGT74F2 in SA glucosylation, a double mutant containing of *ugt74f1-1* knockout and ami*ugt74f2* knockdown in Ws background was generated. Under non-stressed and SA-inducing conditions *ugt74f1-1* ami-*ugt74f2* accumulated wild-type levels of free SA as well as SA glucosides (Yin, 2010). Also the double mutant of *ugt76b1-3* and *ugt74f1-1* (Ws) did not show further reduction of SAG compared to the single mutants and no further increase of free SA (Noutoshi *et al.*, 2012). In these mutants, it is possible that other UGTs take over and glucosylate SA and, thus, SAG production is still present. Either all three UGTs together or even additional UGTs are required for SA glucoside production.

1.8.2. Interaction of SA and ILA via UGT76B1

Next to the interplay of all three UGTs, the interaction between SA and ILA via UGT76B1 could influence SA-dependent defence responses. The turnover of SA by UGT76B1 was inhibited with the amount of present ILA *in vitro*, whereas conversion of SA by UGT74F1 was not influenced by ILA (Noutoshi *et al.*, 2012). No results for an interplay of ILA and SA are known so far *in vivo*. Application of ILA led to enhanced *PR1* expression and increased pathogen resistance (von Saint Paul *et al.*, 2011). If this effect of ILA *in vivo* is dependent on SA and UGT76B1 stayed illusive. In the *ugt76b1* knockout mutant SA as well as ILA levels are enhanced (von Saint Paul *et al.*, 2011; Maksym *et al.*, 2018). Thus, phenotypes of the *ugt76b1* mutant could be due to the increased SA levels, ILA levels or the combination of both. However, induction of SA signalling and observed early senescence of the *ugt76b1* mutant were reverted in SA-deficient *ugt76b1* double mutants (von Saint Paul *et al.*, 2011), illustrating SA-dependency. In conclusion, UGT76B1 was identified as a negatively impacting regulator of SA pathway with glucosylation activity towards SA and ILA, influencing plant defence in a Col background (von Saint Paul *et al.*, 2011). Thus, enhanced ILA levels in *ugt76b1* (Maksym *et al.*, 2018) could lead to enhanced SA levels by the competitive inhibitory effect of ILA towards UGT76B1, and an enhanced plant defence response. ILA might influence free SA pools and plant defence status via UGT76B1.

1.8.3. Interaction of SA and N-OH-Pip

For basal immunity the transcriptional reprogramming via Pip is mostly dependent on SA, but also to some extend independent (Gruner *et al.*, 2013; Bernsdorff *et al.*, 2016). Later on it was found, that Pip is converted to N-OH-Pip by FMO1, which is most probably the active form of Pip (Chen *et al.*, 2018). SA and N-OH-Pip biosynthesis share common regulatory ele-

ments, positively influencing each other during the establishment of SAR (Hartmann & Zeier, 2019). Pip application leads to transcriptional pre-activation of genes involved in pathogen perception, early defence signalling events for establishment of SAR and signalling downstream of pathogen recognition. Synergism of SA and Pip was for example found in *PR1* induction, which was strengthened by a Pip pre-treatment of plants (Bernsdorff *et al.*, 2016).

1.8.4. N-OH-Pip and UGTs

Infection of plants led to an increase of N-OH-Pip, but also an hexoside form of N-OH-Pip was found in infected plant extracts (Chen *et al.*, 2018; Hartmann & Zeier, 2018). This raised the question, if the activity of N-OH-Pip could be controlled by glucosylation. An RNAseq approach revealed that in plants treated exogenously with Pip and during SAR different UGTs were positively regulated. *UGT76B1* was the highest induced UGT in both experiments (Hartmann *et al.*, 2018). *UGT76B1* expression as well as N-OH-Pip and N-OH-Pip hexose are enhanced during plant pathogen defence (von Saint Paul *et al.*, 2011; Chen *et al.*, 2018; Hartmann & Zeier, 2018). Nevertheless, since SA is enhanced in parallel, enhanced *UGT76B1* expression could be related to increased SA levels, rather than increased N-OH-Pip levels.

Next to enhanced SA-marker genes, *FMO1* expression was also induced in the *ugt76b1* knockout (Zhang, unpublished). Enhanced *PR1* and *SAG13* expressions in *ugt76b1* knockout mutant were dependent on SA (ICS1, NPR1, EDS1), but also on FMO1 (von Saint Paul *et al.*, 2011; Zhang, unpublished). This showed that elimination of N-OH-Pip biosynthesis in *ugt76b1* background influenced the expression levels of genes in *ugt76b1*. In addition to enhanced resistance towards biotrophic pathogens, the *ugt76b1* mutant showed an early senescence phenotype dependent on SA (von Saint Paul *et al.*, 2011). Further investigation also revealed that this characteristic of *ugt76b1* was dependent on FMO1 (Zhang, unpublished). This indicates that SA, but also N-OH-Pip play a role in phenotypes occurring in the *ugt76b1* mutant. However, the direct interaction of UGT76B1, Pip and/or Pip-related compounds was yet not tested. Therefore, further investigation in the role of UGT76B1 in N-OH-Pip glucosylation is required.

1.9 Aim of this work

The aim of the present work was to investigate the contribution of UGT76B1, UGT74F1, and UGT74F2 glucosyltransferase enzymes to control the free SA levels and their role during plant defence response. In addition, the possible interplay between all three glucosyltransferases was investigated and differences between UGT76B1, UGT74F1, and UGT74F2 were unveiled. The initial obstacle was the fact that the three *ugt* loss-of-function mutants were not available in the same accession background and thus direct comparisons of the function of the three UGTs was not possible. Comparisons of the single *ugt* mutants among different studies revealed discrepancies and sometimes even contradictory results. Therefore, in order to address these challenges, single, double, and triple mutations were generated in the Col background using a combination of the CRISPR/Cas9-based system for genome editing and crossing. Subsequently, molecular genetic approaches, phenotypic characterization, and chemical analysis of plant compounds were studied.

UGT76B1 was reported to glucosylate both SA and ILA (von Saint Paul *et al.*, 2011; Noutoshi *et al.*, 2012). Interestingly, it was also observed that the presence of ILA inhibited SA glucosylation of UGT76B1 *in vitro* (Noutoshi *et al.*, 2012). Based on these findings, the question arose whether and how this interaction of ILA and SA could influence the plant's resistance towards pathogens *in vivo*. In addition, this interaction was tested in a root growth inhibition assay by the sole or combined application of SA and ILA and by the investigation of SA signalling marker gene expression and induction of superoxide anion production.

A hexose form of N-OH-Pip was identified in infected plants (Chen *et al.*, 2018). N-OH-Pip is an important compound in plant defence and recently claimed as the mobile signal in SAR (Chen *et al.*, 2018; Hartmann *et al.*, 2018). To date, no candidate is known for glucosylation of N-OH-Pip. The interaction of UGT76B1 with Pip and Pip-related compounds was tested *in vitro* and *in vivo* by metabolic analysis. UGT76B1 conjugated N-OH-Pip *in vitro*. Pip and N-OH-Pip were enhanced in the *ugt76b1* mutant, whereas the glucosylated form of N-OH-Pip, which was found in the in vitro assay, was not detectable in the *ugt76b1*, even under exogenous Pip treatment. First steps to understand the interplay of the three pathogen defence activators, SA , ILA, and N-OH-Pip, were made and will be a future aspect for further research.

2 Material and Methods

2.1 Materials

2.1.1. Chemicals

Salicylic acid (SA, 2723.1) from Roth (Germany) and isoleucic acid (ILA, 51576-04-6) from Interchim (France) were used. Isoleucine (Ile, 73-32-5), leucic acid (LA, 498-36-2), and pipecolic acid (Pip, (DL)-Piperidine-2-carboxylic acid; 535-75-1) were obtained from Sigma-Aldrich (Germany). Benzothiadiazole (BTH, BION^{TM}, Syngenta, Germany) was used as SA analogue.

2.1.2. Media

Half Murashige and Skoog medium (½ MS) including vitamins (M0222.0050; Duechefa Biochemie, Netherlands; pH adjusted to 5.7) with 1 % sucrose (4621.2, Roth, Germany) with addition of 0.5 % Gelrite (71010-52-1; Duechefa Biochemie, Netherlands) for solidified media. For grafting ½ MS media without vitamins (M0221.0050; Duechefa Biochemie, Netherlands; pH adjusted to 5.7), sucrose (4621.2, Roth, Germany) concentration as indicated for different plates and 1 % (w/v) Agar (05039; Sigma-Aldrich, Germany) were added.

LB media: 25 g L^{-1} Luria-Bertani (LB) (Duchefa, The Netherlands); 2 ml L^{-1} 1N NaOH; for solidified media 12.5 g L^{-1} Agar (Duchefa, The Netherlands).

Nutrient-yeast extract glycerol (NYGA) agar (pH = 7): 0.3 % (w/v) Bacto yeast extract; 1.8 % (w/v) Bacto Agar; 0.3 %; (w/v) Bacto Peptone. All from BD Bioscience, US; 2 % (v/v) Glyerin (Roth, Germany).

2.1.3. Antibiotics

Kanamycin (working concentration: 50 µg ml^{-1}), rifampicin (100 µg ml^{-1}), and spectinomycin (100 µg ml^{-1}) were obtained from Sigma-Aldrich (Germany), whereas gentamycin (25 µg ml^{-1}) from Roche (Germany). Antibiotic stock solutions were kept at -20 °C dissolved in water except for rifampicin, which was dissolved in methanol.

2.1.4. Primers used for genotyping

Tab. 1: List of primers used for genotyping.

Gene	AGI code	Oligonucleotide (forward)	Oligonucleotide (reverse)	Temp
NahG	-	5′-TCACCTCCCAGAAGGTATCG	5′-GAGATGAAAGCCACCACGTT	55 °C
ICS1	AT1G74710	5′-TGCTTGGCTAGCACAGTTACA	5′-AGCTGATCTGATCCCGACT	55 °C
UGT76B1	AT3G11340	5′-AAGATCCAAGATCAGGGGATAAG	5′-GTCTGATTATGGGAATGCAGATTA	59 °C
UGT76B1	Insertion		5′-TTCATAACCAATCTCGATACAC	55 °C
GFP	-	5′-ACGTAAACGGCCACAAGTTC	5′-TGCTCAGGTAGTGGTTGTCG	60 °C
UGT74F1	AT2G43840	5′-GAGCGACAGAGAGAGATAACGAGA	5′-ACCATCTCAAAGTAAGCAAGGTGT	60 °C
UGT74F2	AT2G43820	5′-TGGGCACTTGACGTTGCTAGAG	5′-TCAAGAAAAGGCAATTCCTCCCACG GAAGTT	58 °C
TRP1	AT5G17990	5′-GCTAAATGATCTTCGTCTGG	5′-CCACTCCTAGTGCCTCTAGTACATC AGCG	55 °C
RBOHD	AT5G47910	5′-TTTGATGCCAAACTCCAAGTC	5′-CGATCTGTTTCACCAATGTCC	55 °C
RBOHF	AT1G64060	5′-CAAAGAGCTCTTCGTGGTTTG	5′-TCTCTATTGTATCTTGTGTCACCG	55 °C
RBOHD, RBOHF	Insertion	5′-ATTTTGCCGATTTCGGAAC		52 °C
TUB9	AT4G20890	5′-GTACCTTGAAGCTTGCTAATCCTA	5′-GTTCTGGACGTTCATCATCTGTTC	55 °C

2.1.5. Primers used for RT-qPCR

Tab. 2: List of primers used for quantitative real-time PCR.

***A. thaliana* genes**				
Gene	**AGI code**	**Oligonucleotide (forward)**	**Oligonucleotide (reverse)**	**Reference**
UBQ5	AT3G62250	5′-GGTGCTAAGAAGAGGAAGAAT	5′-CTCCTTCTTCTGGTAAACGT	von Saint Paul *et al.*, 2011
S16	AT5G18380 AT2G09990	5′-TTTACGCCATCCGTCAGAGTAT	5′-TCTGGTAACGAGAACGAGCAC	von Saint Paul *et al.*, 2011
PR1	AT2G14610	5′-GTGCCAAAGTGAGGTGTAACAA	5′-CGTGTGTATGCATGATCACATC	von Saint Paul *et al.*, 2011
PR2	AT3G57260	5′-TGGTGTCAGATTCCGGTACA	5′-CATCCCTGAACCTTCCTTGA	Maksym (2018)
PR5	AT1G75040	5′-ATCGGGAGATTGCAAATACG	5′-GCGTAGCTATAGGCGTCAGG	Maksym (2018)
SAG13	AT2G29350	5′-TTGCCCACCCATTGTTAAA	5′-GATTCATGGCTCCTTTGGTT	von Saint Paul *et al.*, 2011
CRK7	AT4G23150	5′-ATGTCTTCTCTCTTCCCTTTCATATTCC	5′-ACGAGGATCTAAATCAGACATTG	Yeh *et al.*, 2015
RBOHF	AT1G64060	5′-CTGCGGTTTCGCCATTC	5′-TGTTTCGTCGGCTCTG	Ding *et al.*, 2015
RBOHD	AT5G47910	5′-ATGATCAAGGTGGCTGTTTACCC	5′-ATCCTTGTGGCTTCGTCATGTG	Mehterov *et al.*, 2012
Hybrid		5′-TGGAGAGACTTGGCTGTGAA	5′-GAAAGCAAATTTGGATGTGGA	this study
***Brassica napus* genes**				
Gene	***A. thaliana* ortholog**	**Oligonucleotide (forward)**	**Oligonucleotide (reverse)**	**Reference**
UP1	AT4G33380	5′-AGCCTGAGGAGATATTAGCAGGAA	5′-ATCTCACTGCAGCTCCACCAT	Chen *et al.*, 2010
UBC9	AT4G27960	5′-GCATCTGCCTCGACATCTTGA	5′-GACAGCAGCACCTTGGAAATG	Chen *et al.*, 2010
PR1	AT2G14610	5′-AAAGCTACGCCGACCGACTACGAG	5′-CCAGAAAAGTCGGCGCTACTCCA	Alkooranee *et al.*, 2015

2.2 Plant material and cultivation

2.2.1. List of mutants

Several *A. thaliana* mutants or genetic crossings thereof were used in addition to wild type (accession Col, WT). Mutant lines were obtained from the *Arabidopsis* stock centres (Scholl *et al.*, 2000; Sessions *et al.*, 2002; Alonso *et al.*, 2003) unless otherwise indicated. *ugt76b1-1* knockout mutant (At3g11340; SAIL_1171A11; von Saint Paul *et al.*, 2011), *sid2-1* (AT1G74710; Nawrath & Métraux, 1999), *rbohd* (SALK_070610; AT5G47910; Pogány *et al.*, 2009), *rbohf* (SALK_059888, AT1G64060; Pogány *et al.*, 2009), *abi1-2* (SALK_072009, AT4G26080; Wang *et al.*, 2018b), *aba2-1* (N156; AT1G52340; Christmann *et al.*, 2005), *jar1-1* (N8072, AT2G46370; Staswick *et al.*, 2002), *jin1/myc2* (AT1G32640; Berger *et al.*, 1996), *ein2-1* (N65994, AT5G03280; Guzmán & Ecker, 1990), *fmo1* (AT1G19250; N685510; C. Vlot). In addition, a line constitutively overexpressing line UGT76B1 (von Saint Paul *et al.*, 2011) and a transgenic line expressing the bacterial *nahG* (Gaffney *et al.*, 1993) were employed. The *Brassica napus* PBY0180 Darmor line was obtained from the Genebank at IPK Gatersleben (Gatersleben, Germany).

2.2.2. Liquid culture

Seeds were surface sterilized with 70 % EtOH and after that with commercial bleach diluted 1:1 for 10 min. Afterwards, seeds were washed three times with sterile water. After cold treatment (4 °C) of two to three days, plants were grown under short day conditions in total for 14 days on a shaker with 100 rpm. Six-well dishes contained 5 ml half-strength Murashige and Skoog medium (M1101.0500; Duechefa Biochemie, Netherlands; pH adjusted to 5.7) with 1 % sucrose (4621.2, Roth, Germany). After 12 days, remaining media was exchanged and refilled with appropriate treatment solutions (2 ml): control, 5/25/100 µM salicylic acid (SA, 2723.1, Roth, Germany), same SA concentration with additional 250 µM isoleucic acid (ILA, 51576-04-6, Interchim, France), 500 µM ILA, 500 µM isoleucine (Ile, 73-32-5, Sigma-Aldrich, Germany) or 500 µM leucic acid (LA, 498-36-2, Sigma-Aldrich, Germany). 48 hours after the initiation of the treatment plants were harvested. Deviation from the standard concentration and timing are indicated under the figures. Four mM 4-hydroxy-2,2,6,6-tetramethylpiperidine 1-oxyl (4-OH TEMPO, Sigma-Aldrich, München, Germany) was added to scavenge superoxide radicals (Yokawa *et al.*, 2011). Ten µM diphenyleneiodonium chloride (DPI; Sigma-Aldrich, München, Germany) was used to block the activity of NADPH oxidases (Yokawa *et al.*, 2011). For RNA isolation and metabolic measurements only leaves samples were used, whereas for NBT staining the whole plantlets were stained.

2.2.3. Root growth assay on plates

A. thaliana or *B. napus* (PBY0180 Darmor) seeds were surface sterilized and grown on plates with half-strength Murashige and Skoog medium (M1101.0500; Duechefa Biochemie, Netherlands), 1 % sucrose (4621.2, Roth, Germany) and 0.5 % Gelrite (M0222.0050; Duechefa Biochemie, Netherlands). Seeds were transferred to square petri dishes containing different treatments: Control plates or different concentrations of SA (10 µM), ILA (250 µM or 500 µM), SA and ILA (10 µM and 250 µM), Ile (250 µM), and LA (250 µM). pH of the growth medium was adjusted to 5.7 with sterile potassium hydroxide (0.5 M). After cold treatment (4 °C) for two to three days, plants were grown under short day conditions for nine to ten days for *A. thaliana* and nine days for *B. napus*. Root length was analysed using ImageJ (version 1.51w).

2.2.4. Plant material grown on soil

Plant material was grown in a controlled growth chamber (light/dark regime 10/14 h at 20/16 °C, 80/65 % relative humidity, light at 130 µmol m^{-2} s^{-1}) on a peatmoss-base (Floragard Multiplication substrate, Germany) and quartz sand substrate mixture (8:1) for indicated time. For BTH treatment, three- or four-week-old plants were sprayed with water (containing 0.01 % Silwet L-77) as control or Benzothiadiazole (BTH, BION™, Ciba-Geigy, Germany), a chemical analogue of SA. Spraying mixture contained 0.01 % Silwet L-77 (Lehle Seeds, USA) to support entering BTH into the leaves. Plants were covered with a plastic dome after 1 h. Plant leaves were harvested after 24 or 48 hours. For one biological replicate 25 plants were pooled. In case of chemical treatment, four-week-old plants were watered with different concentrations of SA or ILA (control solution, 10 µM SA (= 0.2 µMol), 250 µM ILA (= 5 µMol), and the combination of ILA and SA (250 µM + 10 µM). Plants were supplied with 20 ml of each solution from above. After three days, plant leaves were inoculated with bacteria. For Pipecolic acid treatment five-week-old plants were either watered with 10 ml control solution or 1 mM Pipecolic acid ((DL)-Piperidine-2-carboxylic acid, Sigma-Aldrich, Germany) solution as described before Návarová *et al.* (2012) and harvested 48 hours after application. Five rosettes were pooled for one biological sample.

2.2.5. Preparation of reciprocal graftings

Grafting protocol was executed as described in Maksym (2018). Seeds were sterilized and sawn on ½ MS medium without vitamins (Duchefa, The Netherlands, 1 % sucrose; 1 % (w/v) Agar). After two days of stratification plants were transferred into growth incubator (MLR 351H, Sanyo, Japan). After three days in constant light (50 µMol m^{-2} s^{-1}) at 22 °C, the light intensity was reduced to 10 µMol m^{-2} s^{-1} for two days in order to stimulate hypocotyl elonga-

tion. Seedlings were cut straight and in the middle of the hypocotyls with a razor blade and rootstocks and scions were combined in intended combinations on ½ MS medium with 0.5 % sucrose. These grafted seedlings were grown under constant light conditions (10 µMol m^{-2} s^{-1}) in 27 °C for one week. For the next week light intensity was enhanced (50 µMol m^{-2} s^{-1}) and short day conditions (10 h light, 22 °C; 14 h dark, 17 °C) were applied. After one week plants were transferred to square Petri dishes (Greiner bio-one, Germany) containing 50 ml ½ MS medium without sucrose. Two weeks later plants were examined for adventitious roots formation and if present removed. If necessary, plants were transferred to the new plates and grown for another two weeks. For gene expression analysis the whole rosettes were harvested.

2.3 Bacterial infection

Pseudomonas syringae pv. tomato DC3000 (*Pst*) was cultivated at 28 °C for two days on selective nutrient-yeast extract glycerol (NYGA) agar (pH = 7; 0.3 % (w/v) Bacto yeast extract; 1.8 % (w/v) Bacto Agar; 0.3 % (w/v) Bacto Peptone, all from BD Bioscience, US; 2 % (v/v) Glyerin, Roth, Germany) supplemented with Rifampicin and Kanamycin (50 µg ml^{-1} each). Plant leaves were inoculated with *Pst* 5 x 10^5 or 5 x 10^6 colony-forming units per ml (cfu ml^{-1}) in 10 mM $MgCl_2$ from their abaxial side using a 1 ml needle-less syringe. Inoculated plants were covered to maintain high humidity. Leaves for bacterial count were harvested 48 h or 72 h after inoculation. For one replicate three leaf discs from three plants were taken and shaken by 600 rpm in 500 µl $MgCl_2$ solution for an hour ($MgCl_2$ 0,01 M + 0,01 % Silwet L-77, Lehle Seeds, USA). Twenty µl of 10-fold dilution series in 10 mM $MgCl_2$ were transferred to selective NYGA agar. After two days of incubation by 28 °C, bacterial colonies were counted and bacterial numbers were calculated. Therefore, spots with 10 to 100 colonies were taken into account. Bacterial titer (cfu cm^{-2}) was calculated as follows: cfu cm^{-2} = colony count * dilution factor * Vol. total/Vol. spotted * 1.18 cm (leaf disc).

2.4 Molecular biology methods

2.4.1. CRISPR/Cas9 approach for mutation of UGT74F1

The *ugt74f2-2* single and *ugt76b1-1 ugt74f2-2* double mutant (called *ugt74f2* and *ugt76b1 ugt74f2* from now on) were obtained by backcrossing with Col wild type and the Col allele *ugt76b1-1* (von Saint Paul *et al.*, 2011). Original line of *ugt74f2-2* contained a point mutations leading to premature stop codon (Q153* mutant; Quiel & Bender, 2003) with additional side mutations (*trp1* and *gl1*), which were eliminated by the backcrossing. Using the CRISPR/Cas9-based system for genome editing in *A. thaliana* (Fauser *et al.*, 2014) a *ugt74f1* allele in

Col background was generated (*ugt74f1-2*; UGT74F1_CRI-1_F: 5'-ATTGTAGCT-TGACACTTCCCATCA-3' and UGT74F1_CRI-1_R: 5'-AAACTGATGGGAAGTGTCAAGCTA-3'; design W. Zhang and A. Schäffner). Wild type and *ugt74f2-2* loss-of-function lines were transformed with a construct targeting the first exon of UGT74F1. The target sequence was located next to a BccI-restriction site three nucleotides upstream of the PAM sequence NGG. A cutting of Cas9 at this position usually leads to mutations by deletion or insertions. This leads to the loss of the restriction site. Thus, a screen for induced mutations could be designed by PCR-amplifying the region flanking the target site and followed by a restriction digest. For the *ugt74f1-2* knockout a deletion of an A in the first exon of UGT74F1 (A at position 466 of the genomic DNA relative to the ATG translation start, called *ugt74f1* from now on) was found, whereas the *ugt74f1-3 ugt74f2-2* double mutant had an Insertion of an A in the first exon of UGT74F1 (inserted A at position 467 of the genomic DNA relative to the ATG translation start, called *ugt74f1 ugt74f2* from now on). Both mutations led to the introduction of a premature stop codon in the first exon of UGT74F1. The *ugt* triple mutant was generated by crossing of *ugt74f1-3 ugt74f2-2* double mutant and *ugt76b1-1* single mutant (called *ugt76b1 ugt74f1 ugt74f2* from now on).

2.4.2. Transformation of plants

Floral dip procedure was applied to transform *A. thaliana* plants (wild type and *ugt74f2-2*). Plants were grown in big round pots (approx. ten per pot) under short day conditions until flowering stage and afterwards transferred to long day conditions. A single colony of transformed *Agrobacterium tumefaciens* was transferred to 2 ml Luria-Bertan media (25 g L^{-1} Luria-Bertani (LB), Duchefa, Netherlands; 2 ml L^{-1} 1N NaOH) with antibiotics (rifampicin (Sigma-Aldrich, Germany; 100 µg ml^{-1}), gentamycin (Roche, Germany; 25 µg ml^{-1}), and spectinomycin (Sigma-Aldrich, Germany; 100 µg ml^{-1}) to form a pre-culture. Bacteria were grown overnight (28 °C, 200 rpm). One ml of the pre-culture was transferred to 250 ml of LB medium including same antibiotics as pre-culture. Bacteria were grown overnight (28 °C, 160 rpm) until stationary growth phase (OD600 1.5-1.6). Bacterial cells were harvested by 10 min centrifugation at 4 °C; 5,500 x g. Pellet was resuspended in 5 % sucrose solution with 0.05 % Silwet L-77 (Lehle Seeds, USA) to OD600 ~0.8. *A. thaliana* plants were dipped into the bacterial suspension and soaked for 45 sec at least twice. Plants were covered with plastic bag to provide high humidity. Plastic bags were removed after 24 h and plants were grown for next 4 to 5 weeks when the first-generation seeds (T0) were harvested and regrown for further selection.

2.4.3. Selection of transgenic plants

Around two-week-old *A. thaliana* seedlings grown on soil were sprayed with BASTA solution (Phosphinothricin; Höchst, Germany) diluted in water (1:800). BASTA-resistant T1 were collected and T2 progeny with a segregation ratio of three resistant to one sensitive plants after BASTA-treatment were selected to guarantee a single insertion. These were resown and again tested for sensitivity T2 plants towards BASTA (leaf test to ensure survival of the sensitive individuals). These sensitive T2 plants may carry a mutation, but have lost the transgene and therefore contain a stable mutation and no further CRISPR/Cas9 activity.

For the hybrid F1 lines selection was carried out by a visible marker, using seed coat expressed GFP (pAlligator2Δ35S vector). T0 was grown and single plants were harvested (T1). Seeds harvested from single plants were counted under microscope for single insertion (3:1) and fluorescent seeds were further cultivated. In the next generation plants, which produced only fluorescent seeds were chosen (T2). For hybrid B1 lines kanamycin (Sigma-Aldrich, Germany; 50 µg ml^{-1}) was used as selection marker. Kanamycin resistant T1 were collected and T2 was tested for its ratio (3:1). In a last steps plants with only resistant progeny were screened and amplified.

2.4.4. Genomic DNA isolation using cetyltrimethylammonium-bromide DNA Miniprep

Young leaf material of one plant was harvested and grinded in a 1.5 ml collection tube with a pistil. Immediately after grinding, 250 µl 2x CTAB buffer (1.4 M NaCl; 100 mM Tris-HCl, pH 8.0; 2 % (w/v) Cetyltrimethylammonium-bromide (CTAB); 20 mM EDTA, pH 8.0) were added and incubated for 20 min in 65 °C. Samples were cooled down for a short moment and 200 µl chloroform/isoamylalcohol (24:1) was added wit intensively mixing for about 1 min. After centrifugation at 14,000 rpm for 2 min, approximately 200 µl of the upper phase was taken to a new 1.5 ml collection tube containing 1 µl of 1 % (w/v) linear polyacrylamide. For precipitation 96 % ethanol was added and samples were put to -20 °C for at least 20 min. Next, samples were centrifuged for 10 min at 14,000 rpm, supernatant was discarded and the pellet was washed with 70 % ethanol. Samples were centrifuged again for 5 min at 14,000 rpm and supernatant was discarded. Finally, ethanol was removed from the samples including drying at 37 °C for about 10 min. One hundred µl water was added to the pellet, which was resolved at room temperature for five minutes.

2.4.5. PCR and gel electrophoresis

Single PCR reaction was conducted in total volume of 10 µl and contained: 1 µl template, 2 µl 5x reaction buffer, 1 µl 2mM dNTPs, 1 µl 50 mM $MgCl_2$, 0.5 µl 10 µM forward primer, 0.5 µl 10 µM reverse primer, 0.1 µl Mango*Taq*™ polymerase (Bioline, USA), 3.9 µl water. PCR was conducted in a T100™ Thermal Cycler (Bio-Rad, USA). The reaction program was as follows: 95 °C for 2 min, followed by 34 cycles of 95 °C for 20 sec, 55-60 °C for 1 min kb^{-1}, 72 °C for 45 sec and final extension 72 °C for 3 min. Primers are indicated in Tab. 1. The amplified products were separated by gel electrophoresis in 1 % or 2 % (w/v) agarose in Tris Acetate-EDTA buffer (TAE; 40 mM Tris, 20 mM acetic acid, 1 mM EDTA) containing 0.5 µg ml^{-1} ethidium bromide. Nucleic acids were visualized with UV light, and documented using Gel Doc2000 system (Bio-Rad, USA).

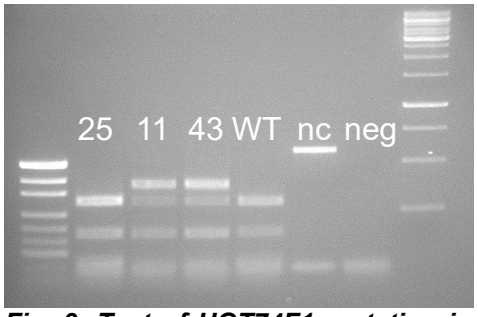

Fig. 3: Test of UGT74F1 mutation in Col background

T2 plants were tested for the CRISPR/ Cas9 activity. Sample number 25 shows WT bands, 11 and 43 are heterozygous for the mutation, WT, WT not cut and negative control.

For genotyping of UGT74F1, UGT74F2, TRP1, and ICS1 mutation, an enzyme digestion was necessary. For UGT74F1 *BccI* mixture (1.8 µl cut smart buffer, 6 µl H_2O, and 0.25 µl *BccI* (2.5 u)), for UGT74F2 *CspCI* (1.8 µl cut smart buffer, 4.4 µl H_2O, 1.2 µl SAM, and 0.6 µl *CspCI* (3 u)), for TRP1 (1.8 µl cut smart buffer, 6 µl H_2O, and 0.25 µl *HaeII* (2.5 u)) and for ICS1 *MfeI* (1.8 µl cut smart buffer, 6 µl H_2O, and 0.25 µl *MfeI* (2.5 u)) were added to the 10 µl PCR reaction and put to 37 °C for 3 h. After this, samples were separated in 2 % (w/v) agarose for around 1 h. In Fig. 3 three different samples are shown. Sample 11 and 43 carrying a wild type and a putative mutation of the UGT74F1 allele. These candidates were resown and screened for homozygous mutants (T3). Sequencing resulted in a deletion of an A in the first exon of UGT74F1 for plant 11 and consequently introducing a premature stop codon.

2.4.6. Extraction of PCR products and DNA sequencing

innuPREP PCRpure *Kit* (Analytik Jena, Germany) for cleaning a PCR reaction or innuPREP *Gel Extraction Kit* (Analytik Jena, Germany) was applied for extracting PCR products from the gel after separation. PCR products of appropriate size were cut from the gel under the UV light and transferred into a 2 ml collection tube. Further steps were performed according to the manufacturer's protocol. Mixture containing the template in an appropriate concentration and forward or reverse primer was added in a sample tube. Sequencing was processed by Eurofins MWG GmbH (Germany).

2.4.7. RNA extraction, cDNA synthesis, and RT-qPCR

Total RNA extraction was carried out with *innuPREP* RNA KIT (Analytik Jena, Germany) according to the manufacturer's instructions. 70-100 mg of plant material was used per sample. RNA integrity and quantity were analysed by measuring the absorption at 260 nm and 280 nm by Nanodrop ND-1000 spectrophotometer (Kisker-biotech, Germany) and 1 % agarose gel electrophoresis. Total RNA (1 µg total RNA) was reverse transcribed for cDNA synthesis using QuantiTect Reverse Transcription Kit (Qiagen, Netherlands) according to the manufacturer's instructions including removal of possible genomic DNA. In order to rule out contamination with the genomic DNA, *TUBULIN9* PCR was performed with primers including an intron at genomic DNA level. Thus genomic DNA contamination could be distinguished by the bigger size of the PCR product. Real-time PCR quantification was performed using a 7500 real-time PCR system (Applied Biosystems) in duplicate assays. Individual PCR reactions were performed in 20 µl total volume according to the manufacturer's instructions (10 µl of 2x SensiMix™ SYBR Low-ROX (Bioline, USA) and 0.25 µM of each sequence-specific primer; see Tab. 2). cDNA was diluted 1:10. The reaction program was as follows: 95 °C for 10 min initial denaturation, followed by 40 cycles of 95 °C for 15 sec, 55 °C for 30 sec, and 72 °C for 45 sec, and a final step of 95 °C for 15 sec. Subsequent melting curve was used to control primer specificity. The housekeeping gene *UBQ5* and *S16* genes were used as an internal control to normalize expression values. Annealing temperature for *CRK7* (Yeh *et al.*, 2015), *RBOHF* (Ding *et al.*, 2015) and *RBOHD* (Mehterov *et al.*, 2012) were 60 °C. For *Brassica napus* samples *UP1* and *UBQ9* were used as reference genes (Chen *et al.*, 2010). *PR1* was measured as described in Alkooranee *et al.* (2015). Cycles values and efficiency of reaction were extracted from the raw data with the qPCR package (Spiess, 2018) and normalized relative quantities (NRQs) were calculated in Excel (Hellemans *et al.*, 2007). Only samples from grafting were analysed differently, but in the same way as described in Maksym (2018), since samples should be joined and compared.

2.4.8. RNA Sequencing

RNA was extracted from three-week-old rosettes of *ugt* mutant set and wild type and *ugt76b1 ugt74f1 ugt74f2* BTH-treated with four biological replicates for each line as described before. Assessment of RNA quality was additional tested by Fragment Analyzer™ including Fragment Analyzer™ Automated CE System (ThermoFischer, Germany). Total RNA was degraded at 90 °C for 5 min and analysed by 2 % agarose gel electrophoresis with the DNF-471 Standard Sensitivity RNA Analysis Kit (15 nt) (SS RNA Kit). With the *PROSize*™ Data Analysis Software (ThermoFischer, Germany) electropherograms and digital gel images

were used for visual inspection, but also ribosomal ratio and assigned RNA Quality Number (RQN) for total RNA were analysed for every sample. All samples had RQN values bigger than 8 and 260/280 nm absorption bigger than 2.0. Samples (RNA concentrations bigger than 84 ng μl^{-1}) were sent to *BGI Tech Solutions Co., Ltd.* (*BGI-Tech*, Hongkong) and quality was rechecked before sequencing. All the samples met the requirements of library construction (BGISEQ-500 Transcriptome) and sequencing. Afterwards, removal of adaptors contamination and low quality reads from raw reads were performed.

RNAseq analysis were conducted by E. Georgii (Institute of Biochemical Plant Pathology, Helmholtz Zentrum München). Alignments of reads were performed with hisat2-2.1.0 (Kim *et al.*, 2015), employing genome assembly from TAIR (TAIR10_chr_all.fas downloaded on 18.02.2019: https://www.arabidopsis.org). For format conversion and sorting of alignments samtools-1.8 (Li *et al.*, 2009) was used. Quantification was performed with stringtie-1.3.4 (Pertea *et al.*, 2015) (Araport11_GFF3_genes_transposons.201606.gff downloaded on 18.02.2019: https://www.arabidopsis.org). For PCA analysis transcripts per million (TPM) gene expression levels were used on log scale (log(TPM+1)) in R version 3.5.0 (R Core Team, 2018) with the prcomp and plot functions (excluding knockout genes). Script provided at http://ccb.jhu.edu/software/stringtie/dl/prepDE.py was applied to prepare count matrices to be used in differential expression analyses. Differential expression analysis was performed with DESeq2 package (version 1.20.0; Love *et al.*, 2014) and Venn diagrams generated with venn package (version 1.7; Dusa, 2018). GO enrichment analysis was executed with fisher-.test, followed by p-value adjustment for multiple testing correction using the false discovery rate method (p.adj.). GO annotation was taken from the org.At.tair.db R package (version 3.6.0; Warnes *et al.*, 2016) using the mappings org.At.tairGO2ALLTAIRS. Heatmap was created with the heatmap.2 function of gplots package (version 3.0.1; Warnes *et al.*, 2016), using TPM data on log scale (log(TPM+1)) selected based on DESeq2 results.

2.5 Metabolic analysis

2.5.1. HPLC-based glucosyltransferase activity assay with recombinant UGTs

UGT76B1, UGT74F1, and UGT74F2 recombinant proteins were produced with the help of B. Geist (Institute of Biochemical Plant Pathology, Helmholtz Zentrum München). Purification of recombinant enzymes and enzyme activity testing was performed as described in Meßner *et al.* (2003) and von Saint Paul *et al.* (2011). For *B. napus* enzymes leaves were sprayed with BTH to obtain cDNA from UGT74F1/UGT74F2 and UGT76B1. Due to the genome triplication there are several related candidate genes. For UGT76B1 only two, while for UGT74F1/ UGT74F2 eleven candidates were predicated (M. Spannagl; MIPS, Helmholtz Zentrum

München). For UGT74F1/UGT74F2 homologous phylogenetic analyses were performed using the whole protein sequence comparing the possible homologs to AthUGT74F1. In addition, information about the domains contributing to the predicted SA binding pocket was used (George Thompson *et al.*, 2017). Four candidates were chosen for further analysis, including the two closest relatives to AthUGT74F1 (27001: BnaA05g03590D/ GSBRNA2T00132627001; 53001: BnaC04g03120D/GSBRNA2T00002253001), one intermediate (54001: BnaC04g03110D/GSBRNA2T00002254001), and the most distant gene (18001: BnaAnng19440D/GSBRNA2T00042418001). All enzymes were tested for glucosylation activity towards SA. In brief, 0.1 M Tris-HCL (pH 7.5), 2.5 mM UDP-glucose, 0.5 µg fusion protein, and different SA or ILA concentrations were added in a final reaction volume of 50 µl. After incubation for 2 h at 30 °C the reaction was stopped by the addition of 15 µl 0.5 M H_3PO_4. Reverse-phase HPLC was performed using an Agilent 1100 HPLC system (Agilent Technologies, Germany) and a Prodigy 5 l ODS (3) column (250 mM long, 4.60 mM i.d.; Phenomenex, Germany). At a flow rate of 1 ml min^{-1} over 23 min the glucose conjugates and the substrates were separated by a linear gradient (8-100 %) acetonitrile against 0.1 % H_3PO_4. Retention times were measured by 302 nm (ILAG: 7.4; SAG 8.2; SGE 9.2; SA 13.0).

2.5.2. LC-MS analyses of SA- and Pip-related compounds

Measurements with LC-MS were performed by B. Lange (Institute of Biochemical Plant Pathology, Helmholtz Zentrum München). Plants were harvested, ground in liquid N2, freeze-dried (Martin Christ) and 20-25 mg plant material re-suspended in 1.5 ml 70 % MeOH. Samples were shaken for 1 h at 1,800 rpm and 4 °C and subsequently centrifuged at 13,000 rpm for 10 min supernatants were dried in Speed Vac (Martin Christ) for 2-2.5 h. 300 µl to 500 µl of the supernatants were freeze-dried overnight (Martin Christ), and the dry matter dissolved in 100 µl 1:1 acetonitrile:H_2O (v:v). The samples were centrifuged for 5 min at 14,000 rpm and 4 °C, 90 µl of supernatants were run over 0.2 µM PVDF Filter and centrifuged, Filtrates were analysed by Ultra Performance Liquid Chromatography (UPLC) Ultra-High Resolution (UHR) tandem quadrupole/Time-Of-Flight (QqToF) mass spectrometry (MS) performed on an Ultimate 3000RS (ThermoFisher, Germany) coupled to Impact II with Apollo II ESI source (Bruker Daltonic, Germany). The chromatographic separation was achieved on a BEH C18 reverse-phase column (150 x 2.1 mM, 1.7 µM particles, Waters Technologies). Eluent A was water with 0.2 % of formic acid and eluent B was acetonitrile 100 %. The gradient elution started with an initial isocratic hold of 5 % B for 5 min, followed by an increase to 20 % B until 7 min, 50 % B until 8 min, 95 % B until 9 min, decreasing to 20 % B until 11 min, 50 % B until 12 min. Finally, the initial conditions of 5 % B were reached after 14 min. The flow rate was 300 µl min^{-1} and the column temperature was maintained at 40 °C. The auto-

sampler temperature was set to 8 °C. Mass calibration was achieved with 50 ml of water, 50 ml isopropanol, 1 ml sodium hydroxide and 200 µl formic acid. To measure SA and SAG 5 µl per sample were injected and two technical replicates were measured in negative ionization mode. The MS was operated as follows: the nebulizer pressure was set to 2 bar, dry gas flow was 10 l min^{-1}, dry gas temperature was 220 °C, capillary voltage was set to 3000 V for the negative mode and the end plate offset was 500 V. Mass spectra were acquired in a mass range of 50-1300 m/z. SA and SAG were identified using an authentic standard (SA, Roth, Germany; SAG, Santa Cruz Biotechnology, USA; p-nitrophenol Fluka Analytical, Germany; camphorsulfonic acid, Sigma-Aldrich, Germany) (retention time in min: SAG 8.0-8.5, SA 10.0-10.2, SGE 9.2-9.5, internal standards p-nitrophenol 10.0-10.1, camphorsulfonic acid 9.0; SA m/z 137.0250, SAG m/z 299.0750, SGE m/z 299.0750, p-nitrophenol m/z 138.0195, camphorsulfonic acid m/z 231.0695) and quantified against an internal standard curve with ten calibration points (SA: R = 0.988, SAG: R = 0.998) and two internal standards with (1 ng $µl^{-1}$). SA and SAG were identified using authentic standards (SA, Sigma-Aldrich, Germany; SAG, Santa Cruz Biotechnology, USA).

To measure Pip, N-OH-Pip, and N-OGLC-Pip, 5 µl per sample were injected and two technical replicates were measured in positive ionization mode. To identify N-OH-Pip and N-OGLC-Pip MS/MS fragmentation pattern was compared with Chen *et al.* (2018). Spiking synthesised N-OH-Pip (Hartmann & Zeier, 2018) confirmed N-OH-Pip peaks. Retention times: Pip: 2.1-2.4 min, N-OH-Pip: 1.6 min, N-OGLC-Pip: 3.3-3.6 min, m/z: Pip: 130.0860, N-OH-Pip: 146.0817, N-OGLC-Pip: 308.1346. Pip was quantified against an external standard curve (DL)-Piperidine-2-carboxylic acid, Sigma-Aldrich, Germany) with six calibration points. No normalization was performed. Later performance of normalization using the total ion chromatogram during the gradient elution led to similar results and no change of major statements.

2.6 Histochemical staining assays

2.6.1. Histochemical localization of gene expression

GUS histochemical staining was performed after Lagarde *et al.* (1996). Plant material is harvested and fixed with a formaldehyde solution (fixation buffer: 0.5 % formaldehyde, 0.05 % (v/v) Triton X-100, 50 mM sodium phosphate, pH 7.0) by vacuum infiltration of the fixation buffer. They are left at room temperature for 30 min. After this samples are washed three times with 50 mM sodium phosphate pH 7.0. Staining buffer (1 mM X-Gluc: 5-bromo-4-chloro-3-indolyl-ß-D-glucuronide (Roth, Germany), 1 mM potassium hexacyanoferrate (II), 1 mM potassium hexacyanoferrate (III), 0.1 % (v/v) Triton X-100, 50 mM sodium phosphate,

pH 7.0) was added and incubated at 37 °C in the dark. Staining was 40 min for UGT76B1, 120 min for UGT74F1, 60 min for UGT74F2. The reaction was stopped by removing the staining solution and after washing 80 % ethanol was added. Removal of chlorophyll was obtained by boiling samples in a water bath (80 °C for 5 min).

2.6.2. NBT and DAB staining

A. thaliana plantlets were vacuum infiltrated with 0.1 % (w/v) nitroblue tetrazolium (NBT; Sigma-Aldrich, Germany) in 50 mM potassium phosphate (pH 6.4), 10 mM NaN_3 and incubated for 2 min for staining of roots and 5 min for staining of leaves in the dark to visualize superoxide production. Chlorophyll was removed by 100 % ethanol treatment at 80 °C. *B. napus* plants were grown nine days on control or 500 µM ILA plates; roots were harvested, vacuum infiltrated and directly destained. Images of single leaves or roots were analysed using ImageJ (version 1.51w). Pixels were determined by using an ImageJ-based macro (PIDIQ) by applying a blue spectrum filter (hue: 140-190; Laflamme *et al.*, 2016).

H_2O_2 formation was assessed by 3,3'-diaminobenzidine (DAB) staining (Daudi & O'Brien, 2012). Roots were vacuum infiltrated with 1 mg ml^{-1} DAB tetrahydrochloride (pH>6.5) (Sigma-Aldrich, Germany) and afterwards incubated for one hour in the dark, whereas leaves were incubated four to eight hours in DAB solution. Chlorophyll was removed with 100 % ethanol at 80 °C. Images were taken using an Olympus BX61 microscope (Olympus, Germany).

2.7 Gene expression analysis by the public database ePlant

Expression patterns of the three UGTs were analysed by public available data in ePlant (Waese *et al.*, 2017). The Heat Map Viewer was used to get an overview over the expression pattern of all three UGTs. Plant eFP Viewer was used for the tissue specific expression pattern. Furthermore, Tissue Specific Root eFP, Chemical eFP and Biotic Stress *Pseudomonas syringae* eFP (section infiltration with virulent pathogen 24 h) were investigated for the expression of the three UGTs. All log2 fold changes were determined by the data mode "relative".

2.8 Statistical analyses

Statistical analyses were performed in R (R 3.5.1 for Windows). For robust statistical analyses, the WRS2 package based on Wilcox' WRS functions was used. Two groups were compared via Welch two sample t-tests. One-way multiple group comparisons were tested in R using the robust one-way ANOVA function *t1way* with lincon post hoc test. p-values were Holm-corrected and adjusted p-values were used for analysis. Two-way ANOVA was performed with the *t2way* function in R (Mair & Wilcox, 2019).

2.9 Modelling of UGT76B1 binding pocket and fitting of SA, ILA, and N-OH-Pip

Modelling of binding pockets was performed by R. Janowski (STB, Helmholtz Zentrum München). To create the homology model of UGT76B1 the amino acid sequence of UGT76B1 was used with the *phyre2* software (http://www.sbg.bio.ic.ac.uk/phyre2; Kelley *et al.*, 2015) including some manual adjustments. The position of UDP-glucose in the structure was deduced by superposition of UGT76B1 model with flavonoid 3-O-glucosyltransferase (PDB ID: 2C1Z; Offen *et al.*, 2006). Next, the 3D model of N-hydroxy Pipecolic acid was created in all possible chiral variants. For placing the compound into the protein the docking program PatchDock (https://bioinfo3d.cs.tau.ac.il/PatchDock/index.html; Schneidman-Duhovny *et al.*, 2005) was used. The ten best docking models for each of stereoismores have been analysed by COOT (Emsley *et al.*, 2010) and the localization near UDP-glucose was used as another exclusion criterion. For comparison of UGT76B1 and UGT74F1/UGT74F2 the amino acid sequence of UGT74F1 was used to create the homology model with the *phyre2* software.

3 Results

3.1 Comparison of the three SA glucosyltransferases UGT76B1, UGT74F1, and UGT74F2

Plant resistance towards biotrophic and hemi-biotrophic pathogens at a local and systemic scale is mediated through the accumulation of endogenous free SA levels (Durrant & Dong, 2004). The increase in endogenous SA subsequently leads to the initiation of SA-mediated defence mechanisms (Pieterse *et al.*, 2009). In addition to the regulation of SA synthesis upon pathogen infection, free SA levels are regulated by downstream modifications that include glucosylation (Rivas-San Vicente & Plasencia, 2011; Chandran *et al.*, 2014; Huot *et al.*, 2014). Glucosylation leads to the inactivation of SA and, thus, attenuates pathogen resistance responses (Vlot *et al.*, 2009). In plants, secondary metabolite UGTs are responsible for the glucosylation of various small molecules including SA, JA, and abscisic acid (Li *et al.*, 2001; Bowles *et al.*, 2005). In *A. thaliana, in vitro* studies have revealed that SA-glucose conjugates can be formed by UGT74F1, UGT74F2, and UGT76B1 (Dean & Delaney, 2008; Maksym *et al.*, 2018). UGT76B1 and UGT74F1 were able to catalyse the conversion of SA to SAG. Although UGT74F2 could form SAG, it primarily catalysed the formation of SGE (Dean & Delaney, 2008).

In contrast to *in vitro* studies, published *in vivo* studies report contradicting data and thus, the function of UGT74F1, UGT74F2, and UGT76B1 *in vivo* is not clear. For instance, Noutoshi *et al.* (2012) reported reduced SAG levels in the leaves of *ugt76b1-3* mutant generated in the Wassilekija (Ws) background. The results in this study indicate that the glucosylation of SA to SAG *in vivo* is partially mediated by UGT76B1. In contrast, similar experiments performed in our laboratory with the same *ugt76b1-3* mutant in the Ws background, failed to confirm reduced SAG levels (Maksym, 2018). In another study, in which *ugt76b1* knockout mutant in the Columbia (Col) background was used, elevated free SA and elevated SAG levels were measured (von Saint Paul *et al.*, 2011). These results indicate that UGT76B1 is not involved in SA glucosylation *in vivo.* Similar discrepancies on the influence of UGT74F1 and UGT74F2 in SA glucosylation were reported (see section 1.4). Additionally, the comparison between the functions of UGT74F1, UGT74F2, and UGT76B1 was challenging as the loss-of- function mutants were only available in different *A. thaliana* accessions.

In this study, the aim was to perform a comprehensive *in silico* and experimental investigation of the roles of UGT74F1, UGT74F2, and UGT76B1 in SAG glucosylation and to what extent they control free SA levels *in planta*. For comparison studies *in vivo*, loss-of-function mutants

for all the three UGTs were generated using CRISPR/Cas9-based technology in the *A. thaliana*, Columbia (Col) background. Additionally, the question if the three UGTs are able to complement each other was addressed.

3.1.1. *In silico* comparison of UGT76B1, UGT74F1, and UGT74F2 binding pocket

In vitro enzymatic studies show that UGT74F1 and UGT74F2 primarily catalyse SA to SAG and SGE, respectively (Lim *et al.*, 2002). A recent study reported that although these two proteins share 77 % of amino acid sequence identity, differences in conformation of the active binding site affected the binding of SA and, thus, resulted in preferential SAG or SGE formation (George Thompson *et al.*, 2017). UGT76B1 glucosylates SA to SAG and is also able to glucosylate ILA *in vitro* (Noutoshi *et al.*, 2012; Maksym *et al.*, 2018). To reveal possible similarities or differences between UGT74F1/UGT74F2 and UGT76B1, protein sequences were compared. In contrast to the high similarity of UGT74F1 and UGT74F2, UGT76B1 shared only 27-29 % of sequence identity with both proteins (Fig. 4A). The fact that UGT76B1 is able to glucosylate ILA strongly indicates that the binding site in UGT76B1 may be significantly different to those of UGT74F1 and UGT74F2. To date the binding site of UGT76B1 has not been studied and therefore, the sites of UGT74F1/UGT74F2 and UGT76B1 were compared.

A multiple amino acid sequence alignment of the three UGTs was generated and the important amino acids for the binding of SA defined by George Thompson *et al.* (2017), were analysed. Of these, His18, Asp111 and Asp366 were conserved in all three UGTs (Fig. 4A, green labelled amino acids). His18 and Asp111 are essential for glucosylation activity of UGT74F1 and UGT74F2 towards SA (George Thompson *et al.*, 2017). To compare the binding pocket structures of the three UGTs, *in silico* structure homology modelling was performed (by R. Janowski, STB, Helmholtz Zentrum München). In UGT74F2 and UGT74F1, hydrophobic and aromatic residues interact with the flat and aromatic SA. The size of potential ligands is thereby substantially restricted. In contrast to UGT74F1 and UGT74F2, the modelled binding pocket residues of UGT76B1 were significantly different. Phe113, Tyr180, Trp364, Thr365 in UGT74F1/UGT74F2 were represented by Leu111, Gly185, Phe367 and Gly368 in UGT76B1 (Fig. 4A, cyan labelled amino acids). Thus, the active site is wider due to the presence of fewer amino acids containing bulky side chains (Fig. 4B). As the aliphatic ILA is a more bulky ligand than SA, it is not able to fit in the binding pockets of UGT74F1 or UGT74F2, but can fit into the binding pocket of UGT76B1 (personal communication Janowski). These findings are compatible with the *in vitro* enzymatic assays mentioned in the beginning of this section.

A

```
UGT76B1    METRETKPVIFLFPFPLQGHLNPMFQLANIFFNRGFSITVIHTEFNS--PNSSNFPHFTF   58
UGT74F1    --MEKMRGHVLAVPFPSQGHITPIRQFCKRLHSKGFKTTHTLTTFIFNTIHLDPSSPISI   58
UGT74F2    --MEHKRGHVLAVPYPTQGHITPFRQFCKRLHFKGLKTTLALTTFVFNSINPDLSGPISI   58

UGT76B1    VSIPDS-----LSEPESYPDVIEILHDLNSKCVAPFGDCLKKLISEEPTAACVIVDALWY   113
UGT74F1    ATISDGYDQGGFSSAGSVPE---YLQNFKTFGSKTVADIIRKHQSTDNPITCIVYDSFMP   115
UGT74F2    ATISDGYDHGGFETADSIDD---YLKDFKTSGSKTIADIIQKHQTSDNPITCIVYDAFLP   115

UGT76B1    FTHDLTEKFNFPRIVLRTVNLSAFVAFSKFHVLREKGYLS-LQETKADSPVPELPYLRMK   172
UGT74F1    WALDLAMDFGLAAAPFFTQ----------SCAVNYINYLSYINNGSLTLPIKDLPLLELQ   165
UGT74F2    WALDVAREFGLVATPFFTQ----------PCAVNYVYYLSYINNGSLQLPIEELPFLELQ   165

UGT76B1    DLPWFQTEDPRSGDKLQIG--VMKSLKSSSGIIFNAIEDLETDQLDEARIEFPVPLFCIG   230
UGT74F1    DLPTFVTPTGSHLAYFEMVLQQFTNFDKADFVLVNSFHDLDLHVK--ELLSKVCPVLTIG   223
UGT74F2    DLPSFFSVSGSYPAYFEMVLQQFINFEKADFVLVNSFQELELHEN--ELWSKACPVLTIG   223

UGT76B1    PFHRYVSAS----------SSSLLAHDMTCLSWLDKQATNSVIYASLGSIASIDESEFL   279
UGT74F1    PTVPSMYLDQQIKSDNDYDLNLFDLKEAALCTDWLDKRPEGSVVYIAFGSMAKLSSEQME   283
UGT74F2    PTIPSIYLDQRIKSDTGYDLNLFESKDDSFCINWLDTRPQGSVVYVAFGSMAQLTNVQME   283

UGT76B1    EIAWGLRNSNQPFLWVVRPGLIHGKEWIEILPKGFIENLEG-RGKIVKWAPQPEVLAHRA   338
UGT74F1    EIASAI--SNFSYLWVVRASE------ESKLPPGFLETVDKDKSLVLKWSPQLQVLSNKA   335
UGT74F2    ELASAV--SNFSFLWVVRSSE------EEKLPSGFLETVNKEKSLVLKWSPQLQVLSNKA   335

UGT76B1    TGGFLTHCGWNSTLEGICEAIPMICRPSFGDQRVNARYINDVWKIGLHLENKVERL----   394
UGT74F1    IGCFMTHCGWNSTMEGLSLGVPMVAMPQWTDQPMNAKYIQDVWKVGVRVKAEKESGICKR   395
UGT74F2    IGCFLTHCGWNSTMEALTFGVPMVAMPQWTDQPMNAKYIQDVWKAGVRVKTEKESGIAKR   395

UGT76B1    -VIENAVRTLMTSSEGEEIRKRIMPMKETVEQCLKLGGSSFRNLENLIAYILSF         447
UGT74F1    EEIEFSIKEVMEGEKSKEMKENAGKWRDLAVKSLSEGGSTDININEFVSKIQIK         449
UGT74F2    EEIEFSIKEVMEGERSKEMKKNVKKWRDLAVKSLNEGGSTDTNIDTFVSRVQSK         449
```

B

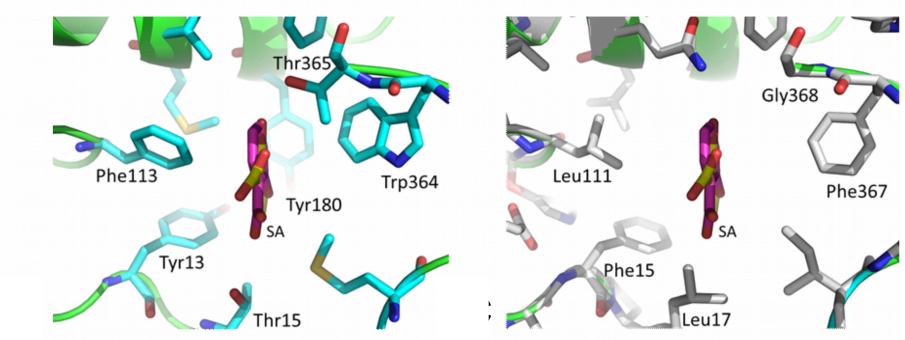

Fig. 4: Comparison of binding pockets of UGTs revealed a wider binding pocket of UGT76B1

A: *Alignment of protein sequence of UGT76B1, UGT74F1, and UGT74F2. Comparison of important amino acids of the binding pocket to glucosylate SA, defined by George Thompson* et al. *(2017). Important residues for glucosylation of SA conserved in all three UGTs are shown in green. Thr15 is important for UGT74F1 vs UGT74F2 specificity to produce SGE. Differences of UGT74F1 and UGT74F2 are shown in red. Cyan amino acids are important differences in binding pocket between UGT74F1/UGT74F2 and UGT76B1 and define the wider binding pocket for ligands of UGT76B1.* ***B:*** *SA modelled into the binding pocket of UGT74F1/UGT74F2 and UGT76B1 (by R. Janowski).*

3.1.2. The generation of SA glucosyltransferase UGT74F1, UGT74F2, and UGT76B1 mutants

A set of all possible single, double, and triple mutant combinations of the three UGTs was generated in *A. thaliana* (Col) by crossing and by using a CRISPR/Cas9-based system (Fauser *et al.*, 2014). Quiel & Bender (2003) had identified a knockout mutant of UGT74F2. The *trp1-100 gl1-1* line in Col background had been mutagenised using ethyl methane sulfonate. Two point mutations led to a premature stop codon in the UGT74F2 gene (*ugt74f2-2* mutation: Q153*). This mutant has not been studied yet, since it also contains two additional mutations (*TRP1* and *GL1*). In order to include a complete loss-of-function mutant in my project, the *ugt74f2-2* mutant was backcrossed into Col wild type. The *ugt74f1-2* allele in Col background was generated using a CRISPR/Cas9-approach. Deletion of a single amino acid in the first exon of UGT74F1 resulted in a premature stop codon. The same CRISPR/Cas9 approach was applied in the *ugt74f2-2* mutant in order to generate a *ugt74f1-3 ugt74f2-2* double mutant, since UGT74F1 and UGT74F2 are positioned next to each other in close proximity on chromosome two. The other double mutant was created by crossing *ugt74f2-2* with the *ugt76b1-1* mutant (Col; von Saint Paul *et al.*, 2011). Finally, the *ugt74f1-3 ugt74f2-2* double mutant was crossed with *ugt76b1-1* to generate a triple *ugt* mutant in Col background.

With the successful construction of the single and various combinatorial mutants of these three enzymes in the Col background, it was possible for the first time to carry out a direct comparison of the three UGTs and their possible interplay in SA glucosylation.

3.1.3. Application of SA and ILA revealed different and similar root growth inhibition in the three *ugt* mutants

As mentioned before, *UGT74F1* and *UGT74F2* glucosylate SA *in vitro* (1.4). The third glucosyltransferase, UGT76B1, glucosylates SA as well as ILA (von Saint Paul *et al.*, 2011; Maksym, 2018). In addition to the role of SA in pathogen stress, it is well known that the presence of high concentrations of SA and ILA inhibit root growth in wild type plants (Wildermuth *et al.*, 2001; von Saint Paul *et al.*, 2011). To examine the role of UGT76B1, UGT74F1, and UGT74F2 *in vivo*, ILA and SA were applied exogenously to *ugt74f1*, *ugt74f2, ugt76b1*, wild type, and a UGT76B1 overexpressing line (OE) and the root growth inhibition was monitored. SA had a negative impact on root growth on all the mutant and wild type relative to the control plants (Fig. 5A). SA application led to a slightly stronger inhibition of root growth in all *ugt* mutants compared to the wild type (Fig. 5B).

Similarly, the application of ILA led to root growth inhibition in all the mutant and wild type genotypes (Fig. 5). Furthermore, the combined application of both of SA and ILA exhibited an even stronger inhibition in all genotypes than the separate applications (Fig. 5A). By contrast, the UGT76B1 OE lines exhibited enhanced root growth relative to wild type on SA treated plates (Fig. 5B and C). In SA treated plants, OE exhibited the longest roots, followed by wild type, while the knockout lines had the shortest roots. These results indicate that all three UGTs may be involved in the detoxification of SA *in vivo* as the mutation of each individual UGT resulted in an enhanced root growth inhibition compared to the wild type. In contrast to these results on ILA plates only the *ugt76b1* mutant was more sensitive towards ILA than the wild. These results indicate that only UGT76B1 may be involved in the detoxification of ILA *in vivo.* Additionally, the enhancement of root growth in UGT76B1 OE lines treated with SA or ILA strongly suggest that the overexpression of UGT76B1 led to the inactivation of both compounds by glucosylation.

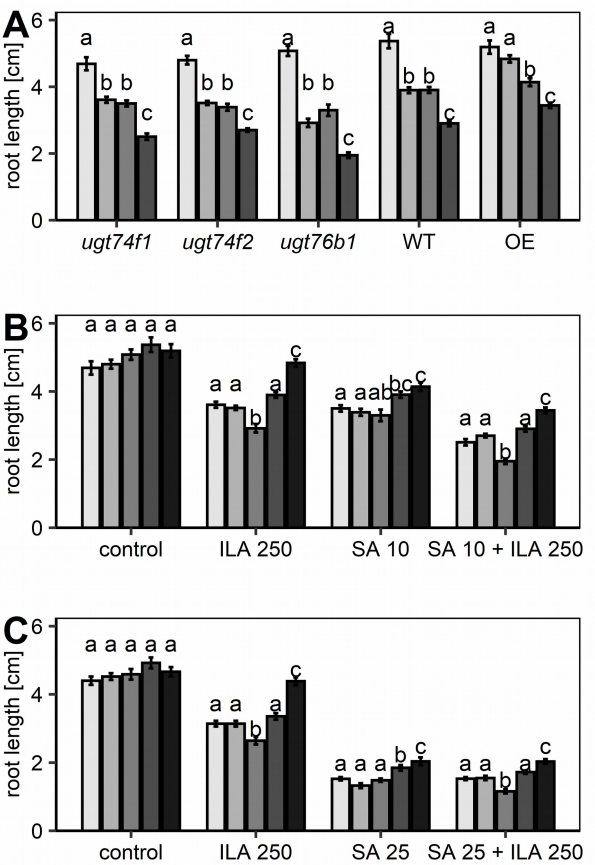

Fig. 5: Root growth inhibition by ILA and SA inversely correlated with* UGT76B1 *expression

A and B: *Plants were grown on control and on media containing 250 µM ILA, 10 µM SA or the combination of both compounds. n = 12 - 16. Genotypes used from left to right:* ugt74f1*,* ugt74f2*,* ugt76b1*, wild type and OE* ***C:*** *Plants were grown on control and on media containing 250 µM ILA, 25 µM SA or the combination of both compounds. n = 10 - 12. Root length was recorded after ten days. means ± SE; Significant differences (adjusted p-value < 0.05) are indicated by letters according to one-way ANOVA. The two experiments were independently repeated three times with similar results.*

3.1.4. SA susceptibility of *ugt* triple mutant

In the next step, SA-mediated root growth inhibition was investigated in UGT double mutants as well as the triple mutant. The double mutants used in this study included *ugt76b1 ugt74f1*, *ugt76b1 ugt74f2*, and *ugt74f1 ugt74f2*. Based on the hypothesis that all three UGTs are necessary for detoxification of SA, the triple mutant should show the highest sensitivity. 10 µM SA revealed that the *ugt76b1* knockout had similar root growth inhibition as *ugt76b1 ugt74f1* and *ugt76b1 ugt74f2* double mutant. Furthermore, the triple mutant was inhibited as strongly as the *ugt76b1* single mutant (Fig. 6A).

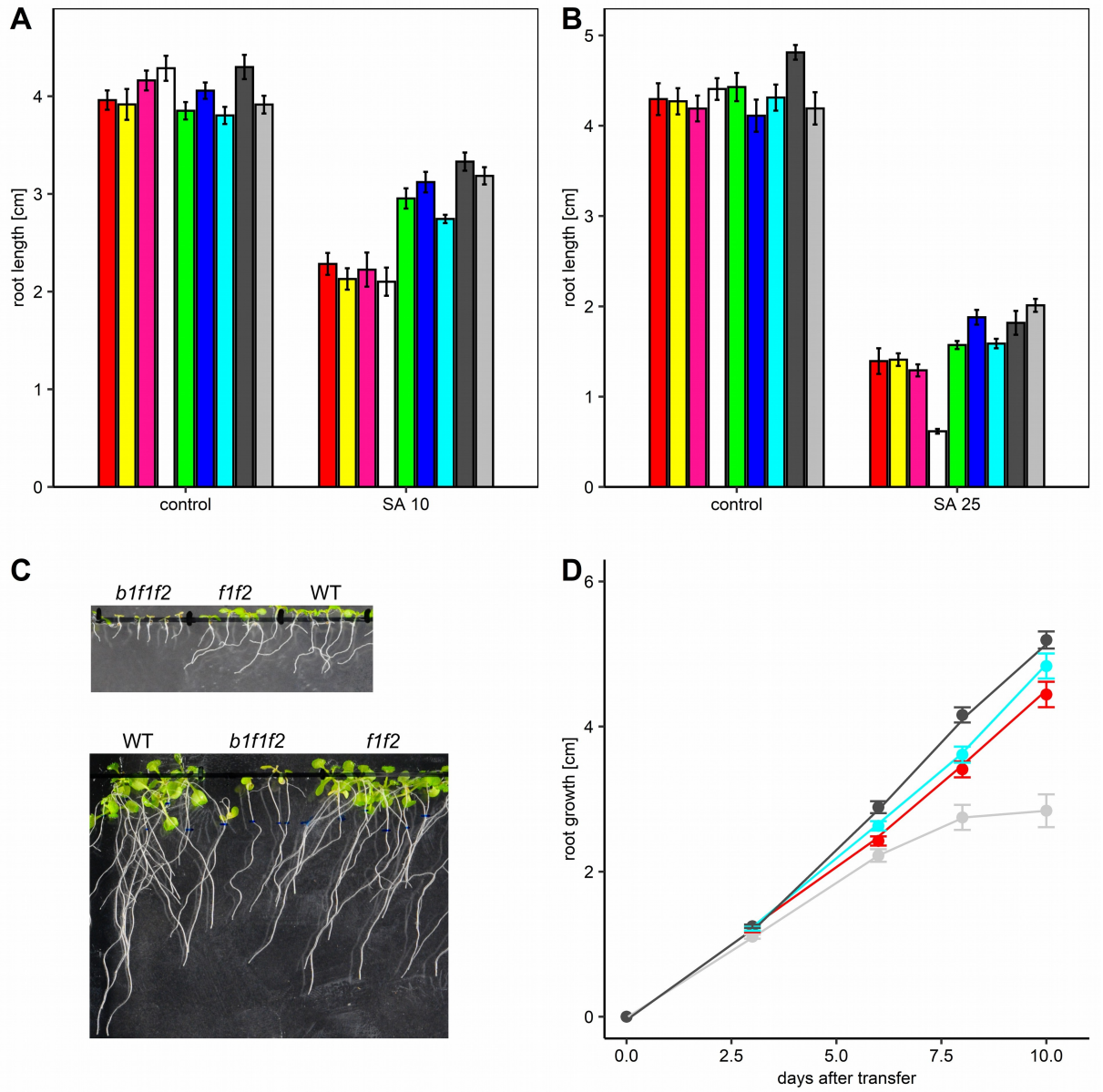

Fig. 6: The* ugt *triple mutant reacted most sensitive to high SA contents

*Plants were grown for ten days on SA plates containing either 10 µM (**A**) or 25 µM SA (**B + C**). From left to right:* ugt76b1 (■), ugt76b1 ugt74f1 (■), ugt76b1 ugt74f2 (■), ugt76b1 ugt74f1 ugt74f2 (□), ugt74f1 (■), ugt74f2 (■), ugt74f1 ugt74f2 (■), *wild type* (■) *and OE* (■). *means ± SE;* ***A:*** *n = 7 - 15.* ***B:*** *9 - 17; Experiments were repeated three times independently with similar results.* ***C:*** *Upper picture: growth of* ugt76b1 ugt74f1 ugt74f2, ugt74f1 ugt74f2 *and wild type after ten days on 25 µM SA. Lower picture: wild type,* ugt76b1 ugt74f1 ugt74f2 and ugt74f1 ugt74f2 *ten days after transfer on SA 10 µM plates.* ***D:*** *Five-day-old seedlings grown on control plates were transferred to 25 µM SA plates. Growth curve of wild type* (■), ugt76b1 ugt74f1 ugt74f2 (■), ugt74f1 ugt74f2 (■) *and* ugt76b1(■). *n = 13 - 18; means ± SE.*

In the presence of a higher concentration (25 µM) of SA, double mutant plants had similar root growth inhibition to the single mutant plants (Fig. 6B). By contrast, the *ugt* triple mutant had by far the most sensitive root growth inhibition phenotype. To exclude differential impacts on germination, the experiment was repeated where wild type, *ugt76b1 ugt74f1 ugt74f2*,

ugt74f1 ugt74f2, and *ugt76b1* plants were sown on control plates and transferred to plates containing 25 µM SA five days after germination. Again *ugt76b1 ugt74f1 ugt74f2* exhibited slower root growth rate. The roots stopped growing altogether between eight and ten days. In addition to growth inhibition, the triple mutant showed smaller, yellowing rosettes (Fig. 6C and D).

Furthermore, the effects of SA-mediated growth inhibition between the *ugt* triple mutant and wild type was investigated in older plants. Soil grown plants were treated with BTH, a chemical analogue of SA. Two weeks after application, plants were photographed, and rosettes were harvested to determine their dry weight. In control plants, there were no significant differences in total leaf area, the yellow leaf area or dry weight between the wild type and triple mutant (Fig. 7). In contrast, the BTH-treated triple mutant showed smaller rosettes with lower dry weight (Fig. 7A and C) and enhanced yellow leaf area (Fig. 7B). In summary, the *ugt* triple mutant showed enhanced sensitivity towards SA in both seedlings and older plants.

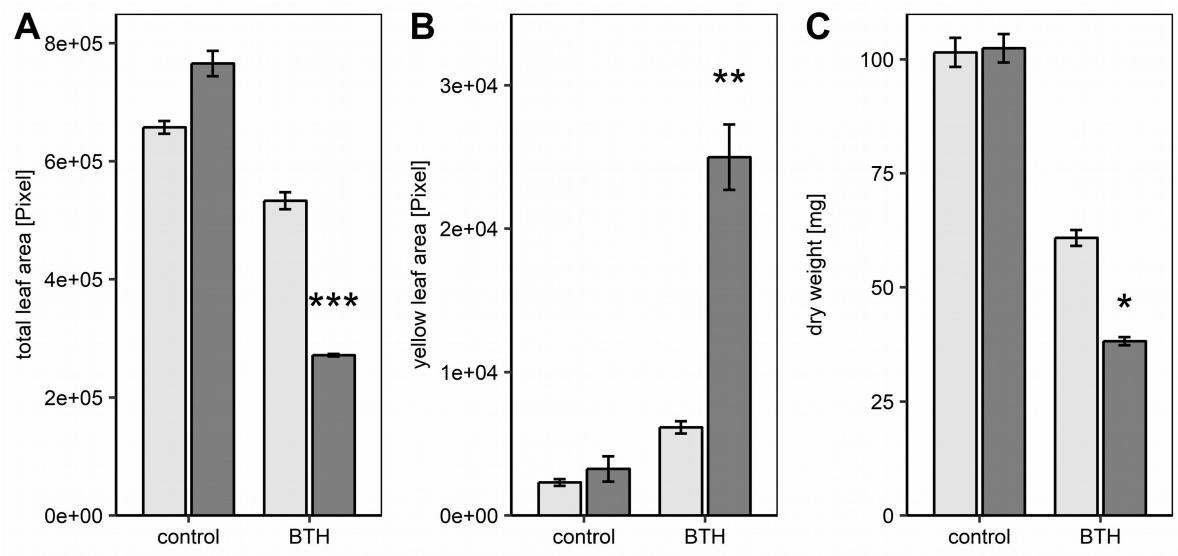

Fig. 7: The* ugt *triple revealed hypersensitivity towards SA-inducing treatment

Twenty-four-days-old plants were sprayed with BTH [1mM] or control solution and analysed two weeks after treatment. Light grey bars resemble wild type, whereas dark grey bars resemble ugt76b1 ugt74f1 ugt74f2*. Bars represent means ± SE; n = 5.* ***A:*** *total leaf area* ***B:*** *yellow leaf area* ***C:*** *dry weight of the whole rosette. Experiment was repeated two times. Differences between wild type and* ugt *triple mutant were analysed by Welch two sample t-test; * = p < 0.05, ** = p < 0.01 and *** = p < 0.001.*

3.1.5. Comparison of *UGT76B1*, *UGT74F1*, and *UGT74F2* gene expression

Expression patterns of the three UGTs were analysed using gene expression data from a publicly available database, ePlant (Waese *et al.*, 2017). The three UGTs showed different gene expression patterns during the course of plant development. The *UGT74F1* gene was highly expressed in freshly germinated seeds, during early flowering stages, in cotyledons, in

young leaves and roots. *UGT74F2* expression was observed in the pods of the first silique, in dry seeds and roots. Finally, *UGT76B1* was induced in late flowering stages and in roots. In roots *UGT76B1* was highest expressed (log2 fold change 4.27), compared to *UGT74F1* (2.94) and *UGT74F2* (1.37). The spatial expression pattern in roots also differed, *UGT74F1* was observed in the endodermis. *UGT74F2* was expressed in epidermis, cortex and pericycle. *UGT76B1* displays expression in the root mainly in epidermis, cortex and pericycle. In addition, the expression patterns of the three UGTs under different treatments were analysed. In plants exposed to various hormone treatments, *UGT76B1* was observed to be highly induced by SA treatment (log2 fold change 4.73). *UGT74F2* was also induced by SA treatment (2.33), but to a lower extend than *UGT76B1*, whereas *UGT74F1* showed no induction (-0.41). *UGT74F1* was induced by 2,3,5-triiodobenzoic acid treatment, an inhibitor of auxin transport (log2 fold change 1.56). Additionally, *UGT74F2* (1.53) and *UGT76B1* (1.26) were induced by this compound as well. In plants infected with pathogens, *Pst* infiltration lead to the enhanced expression of all three UGTs. The fold change post infection was 4.46, 3.13, and 1.31 for *UGT76B1*, *UGT74F2*, and *UGT74F1*, respectively. Taken together, there is an overlap in expression profiles of the three UGTs in plants treated with SA, *Pst*, and 2,3,5-triiodobenzoic acid, although with varying intensities.

Following the analysis of expression data by using public available database, further comparative expression patterns of the three UGTs were analysed by using transgenic lines harbouring promoter GFP-GUS reporter fusions that have been described in von Saint Paul *et al.* (2011) and Meßner & Schäffner (unpublished). In leaves *UGT74F1* and *UGT74F2* were expressed in the vascular tissue. In contrast, *UGT76B1* was expressed in a more irregular way, spread across the leaf tissue (Fig. 8). In roots it was conspicuous that *UGT76B1* showed strong expression in the root tips, whereas no signal was detected for *UGT74F1* and *UGT74F2* (Fig. 8). This results coincide with the results of public available data described above.

To further investigate a possible interaction and compensation of one UGT by another, GUS expression was monitored in single *ugt* knockouts. The aim was to examine if the deactivation of one UGT could provoke an up-regulation or altered expression pattern of the other UGTs and thus compensate for the loss. However, the expression pattern did not change when one UGT was missing compared to the expression in the wild-type background (Fig. 8). There was however a slight induction of *UGT76B1* when one of the other UGTs was missing.

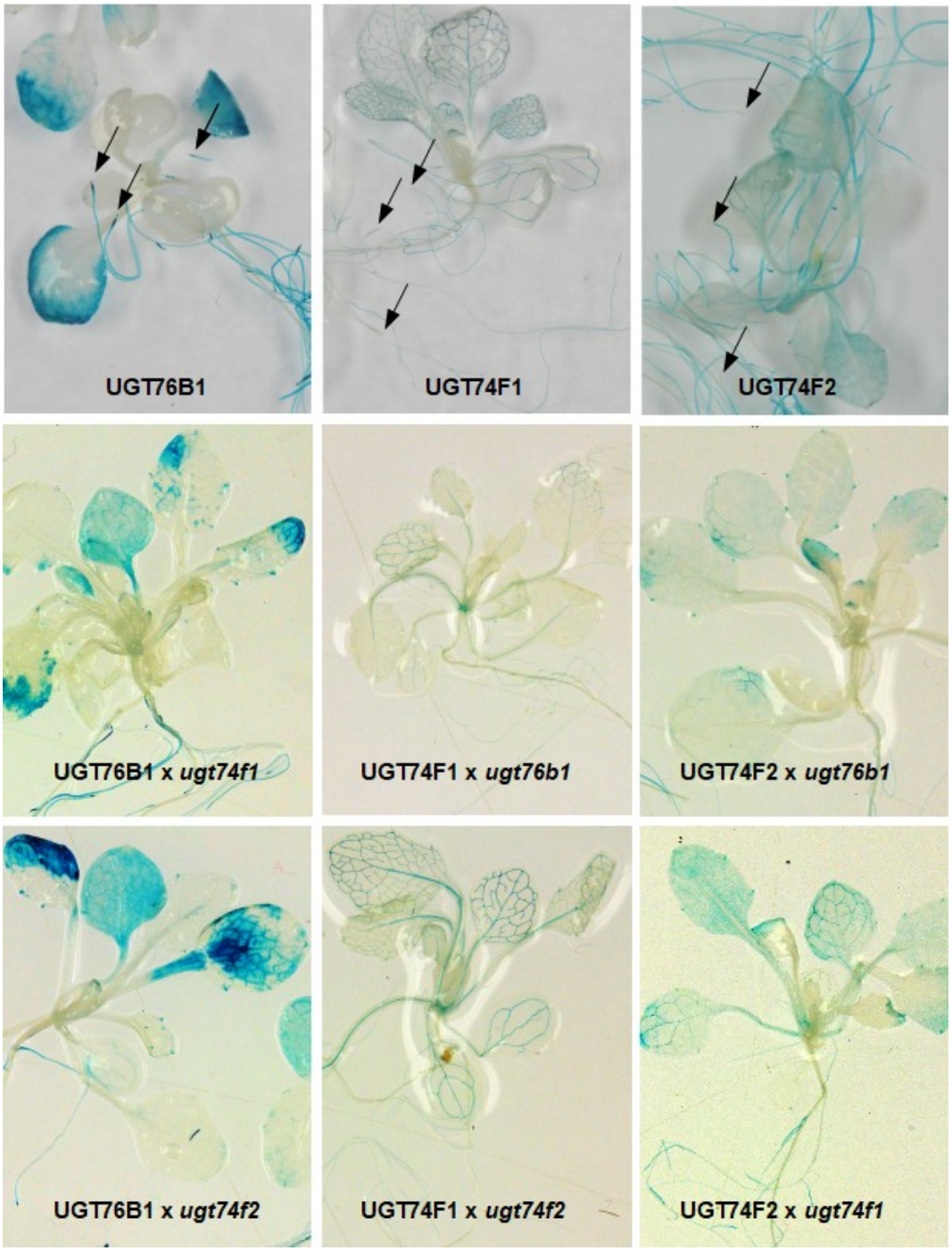

***Fig. 8: Different expression of* UGT76B1, UGT74F1*, and* UGT74F2**

Three-week-old plants were stained for GUS expression for two hours and pictures were taken for comparisons of the expression patterns (n = 5). First line is showing expression of UGT76B1, UGT74F1*, and* UGT74F2 *in wild-type background. The following two lines show expression of different* UGT*s in the absence of one other respective* UGT*.*

3.1.6. Comparison of pathogen defence and early senescence in *ugt* knockouts

Mutation of *UGT76B1* has been reported to enhance pathogen resistance and an early senescence phenotype, relative to wild type (von Saint Paul *et al.*, 2011). To investigate whether *ugt74f1* and *ugt74f2* mutants share similar characteristics, a comparison of wild type, ugt76b1, *ugt74f1*, and *ugt74f2* mutant genotypes infected with *Pst* was conducted. *ugt74f1* and *ugt74f2* were more susceptible to pathogens than *ugt76b1* (Fig. 9A). Neither *PR1* induction nor early senescence phenotype were observed in both *ugt74fs* (Fig. 9B + C). These results indicated that next to the different expression pattern of the three UGTs (3.1.5), the mutations of UGTs had different impacts on plant resistance and leaf senescence.

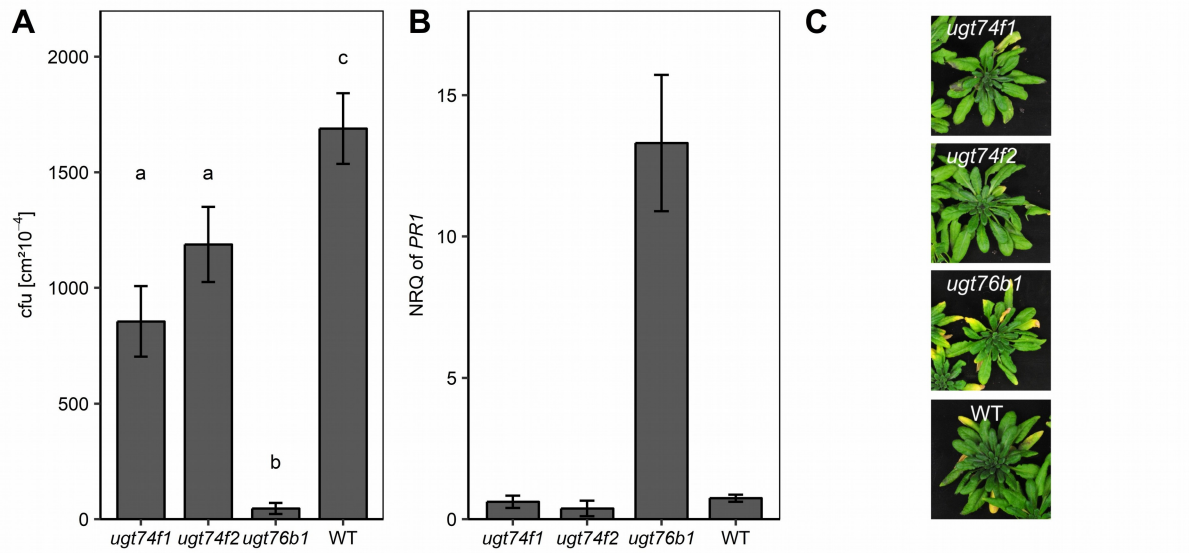

***Fig. 9: Mutation of UGT74F1 or UGT74F2 did not influence pathogen defence as in* ugt76b1**

A: *Four-week-old* ugt74f1*,* ugt74f2*,* ugt76b1 *mutants and wild-type plants were inoculated with* Pst *(5 x 10^6 cfu).* Pst *titres were determined at two days dpi. Bars represent the average of four replicates. means ± SE; Significant differences (adjusted p-value < 0.05) are indicated by letters according to one-way ANOVA. The experiment was independently repeated three times with similar results.* ***B:*** PR1 *expression in four-week-old plants. Gene expression was assessed by RT-qPCR and normalized to* S16 *and* UBQ5*. means ± SE; n = 3.* ***C:*** *Senescence phenotype of rosettes of eight-week old Arabidopsis plants.*

3.1.7. Comparison of SA, SAG, and SGE content

To find out whether all three UGTs are involved in SA glucosylation *in planta*, LC-MS analysis was performed to measure the content of SA and its glucosylated derivatives. Three-week-old plants were harvested under normal and stress conditions (BTH treatment). All mutants, single, double, and the triple mutant, of the three UGTs were included.

Under control conditions *ugt74f1*, *ugt74f2*, and *ugt74f1 ugt74f2* double mutant showed SA levels similar to wild type. All mutants containing UGT76B1 mutation showed enhanced SA levels (Fig. 10A). In *ugt76b1* SAG levels were enhanced, whereas *ugt74f1*, *ugt74f2*, and

double mutant did not show a similar increase (Fig. 10B). Conversely, *ugt74f1* knockout had reduced SAG levels. The introgression of *ugt74f1* in *ugt76b1* background led to a strong reduction of SAG content in *ugt76b1 ugt74f1* double mutant, whereas introgression of *ugt74f2* in *ugt76b1* enhanced SAG levels. To abolish total SAG production all three UGTs had to be mutated (Fig. 10B). SGE levels were completely dependent on UGT74F2, since in the *ugt74f2* no SGE was detectable. Furthermore, in *ugt76b1* and *ugt76b1 ugt74f1* SGE was enhanced. In summary, in the *ugt76b1* knockout all three compounds were significantly different from wild type and only the mutation of UGT76B1 influenced free SA levels. SAG production was mainly dependent on UGT74F1 and SGE production completely dependent on UGT74F2.

Under stress treatment SA, SAG, and SGE production was induced in wild type, showing an induced stress response to BTH treatment (Fig. 10). Similar enhancement of all three compounds was also found in *ugt76b1* under control conditions. After BTH treatment no differences in the levels of all three compounds were found in *ugt76b1* compared to the wild type. For *ugt74f1*, *ugt74f2*, and *ugt74f1 ugt74f2* free SA levels were increased in the same manner as in wild type (Fig. 10A). Highest SAG levels were found in *ugt74f2*, which could be reduced to wild-type-like levels by introgression of *ugt74f1* mutation in the *ugt74f2* background. In *ugt76b1 ugt74f1* no enhancement of SAG due to BTH treatment was observed, whereas *ugt76b1* and *ugt76b1 ugt74f2* showed wild-type-like levels (Fig. 10B). Nevertheless, in *ugt74f1* induced SAG levels were similar to wild type. In the triple mutant production of SAG was abolished. Mutants containing *ugt74f2* mutation did not show detectable levels of SGE (Fig. 10C). Next to wild type, SGE was most prominently changed in *ugt74f1* and to a lesser extent in *ugt76b1* or *ugt76b1 ugt74f1* compared to untreated plants. Taken together, under BTH treatment SA levels in all possible combinations of *ugt* mutants were not significantly different from wild type, even though SAG and SGE levels differed among the *ugt* mutants. Only overexpression of UGT76B1 led to reduced free SA levels (Fig. 10A).

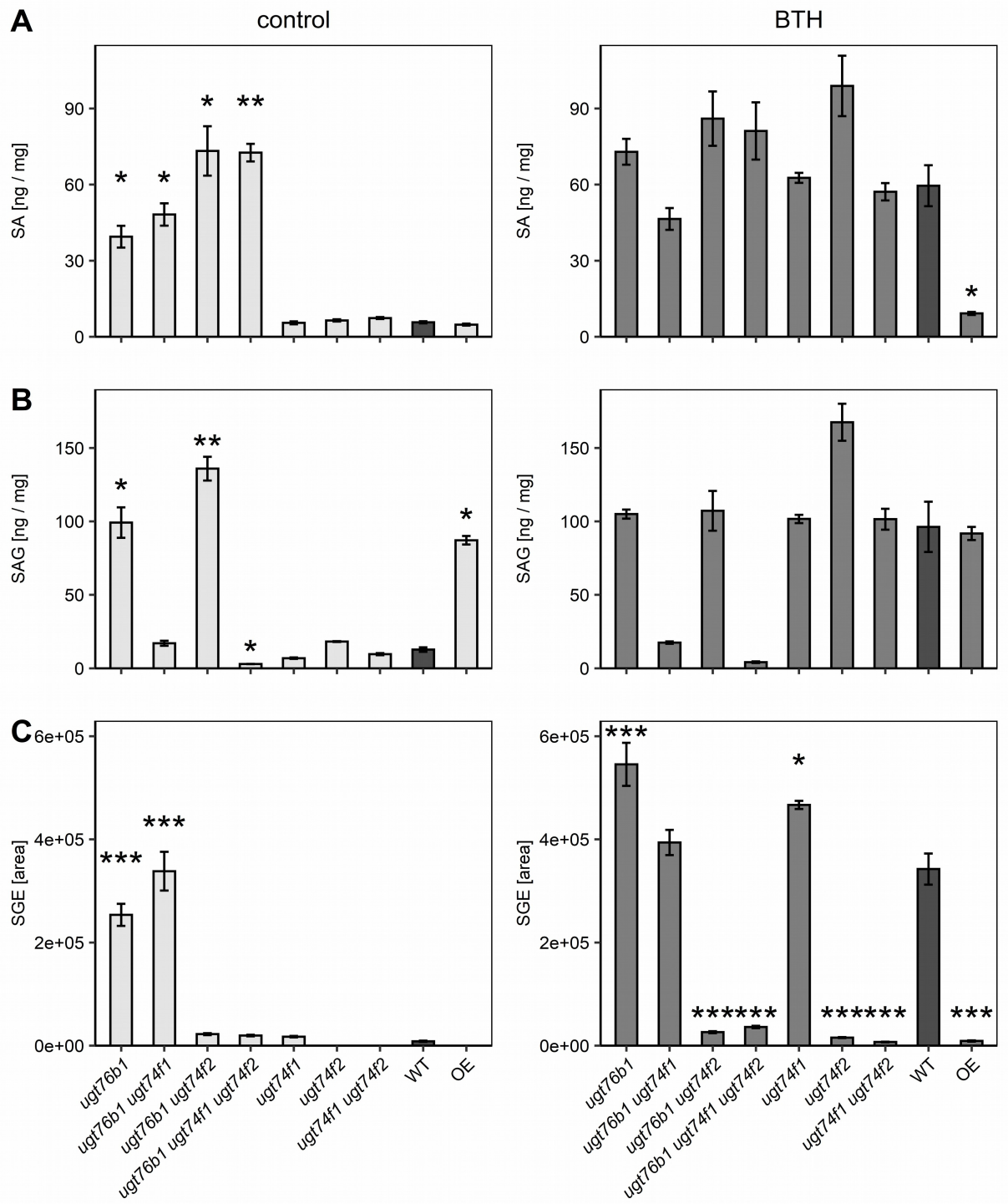

Fig. 10: Measurements of SA, SAG, and SGE in the* ugt *mutant set under control and under SA-inducing conditions

Three-week-old plants of the complete ugt *mutant set, wild type and OE were sprayed with control solution or BTH and harvested 48 h later. The same material was used for RNA-seq analysis (Fig. 11A and B).* ***A:*** *SA.* ***B:*** *SAG.* ***C:*** *SGE contents. Bars represent the average of four replicates. WT is filled with dark grey colour. means ± SE. Authentic standards were used to quantify SA and SAG, while SGE was relatively quantified according to the m/z peak of LC-MS measurement. Significant differences between mutants and WT (p.adj. values) were analysed by t1way ANOVA. * = p < 0.05, ** = p < 0.01 and *** = p < 0.001.*

3.1.8. Comparison of gene expression in different *ugt* mutants by RNA-sequencing

To get a deeper insight into how the mutation of one, UGT76B1, UGT74F1, or UGT74F2, or multiple UGTs may influence expression levels of genes, an RNA-sequencing approach was conducted. Samples of the same material as in Fig. 10 were used with the aim of analysing all different *ugt* mutant combinations under control conditions. For the stress treatment only wild type and the *ugt* triple mutant (*ugt76b1 ugt74f1 ugt74f2*) were chosen, since SA levels were enhanced, but SA glucosylation was abolished (Fig. 10).

To get an overview of the data, expression profiles from all genotypes and treatments were subjected to a principal component analysis (PCA, Fig. 11A and B). The projection on the first two principal components showed a good clustering of biological replicates. The first component describes 34 % of variance in the dataset, with the highest difference in untreated wild type compared to BTH-treated samples. Part of this shift goes in parallel with the loss of UGT76B1, since all mutants with the mutation in UGT76B1 (*ugt76b1*, *ugt76b1 ugt74f2*, *ugt76b1 ugt74f1*, and *ugt76b1 ugt74f1 ugt74f2*) formed a cluster that is separated from the remaining genotypes by the first component. The loss of UGT76B1 shifted the global expression pattern from the wild type in the same direction as the BTH treatment, with BTH having a more pronounced effect than loss of UGT76B1. In addition, *ugt76b1 ugt74f1 ugt74f2* compared with and without treatment could point out genes, that were induced by BTH independently of these three UGTs. Since *ugt76b1 ugt74f1* and *ugt76b1 ugt74f1 ugt74f2* formed a common cluster, *ugt74f2* was not strongly contributing to gene expression on top of *ugt76b1 ugt74f1*.

Along the second component, the differences were mostly related to the presence of UGT74F1. The biological replicates of all mutant lines with the knockout of UGT74F1 (*ugt74f1*, *ugt74f1 ugt74f2*, *ugt76b1 ugt74f1*, *ugt76b1 ugt74f1, ugt74f2*) could be distinguished by this component from all other genotypes. The double mutation of UGT74F1 and UGT74F2 led to a strong shift along the second component, whereas the single gene mutants were located closer to wild type, *ugt74f2* being the opposite extreme to *ugt74f1 ugt74f2*. *ugt76b1 ugt74f1* seems to be a combination between genes expressed in *ugt76b1* and *ugt74f1* along both components. Taken together, the expression analysis showed a major impact of *UGT76B1* and *UGT74F1* presence on the transcriptome, culminating in *ugt76b1 ugt74f1* with combined gene expression effects from both principal components.

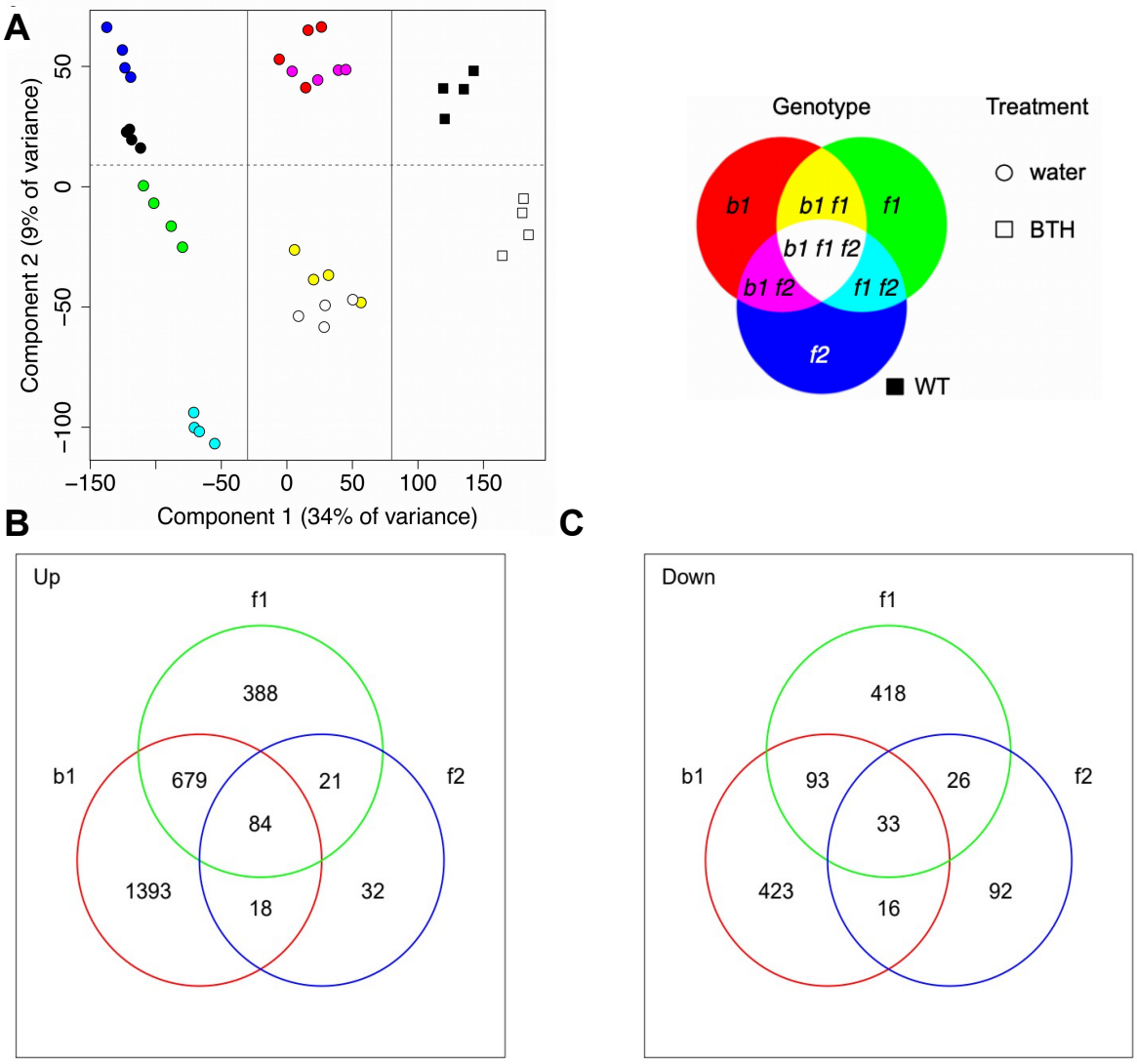

Fig. 11: RNA-seq data overview and comparison of single knockout mutants of UGTs

A**:** *Principal Component Analysis (PCA) of gene expression profiles (excluding the three knockout genes) from all samples, with two components explaining 43 % of the whole variance in the dataset. Along the first component the loss of UGT76B1 shifted the global expression pattern from the wild type in the same direction as the BTH treatment. Along the second component, the differences were mostly related to the presence of UGT74F1. Venn diagrams of* ***B:*** *up-regulated and* ***C:*** *down-regulated genes of* ugt *single mutants in comparison with the wild type. In the* ugt74f2 *mutant least genes were regulated, whereas in the* ugt76b1 *mutant highest number of regulated genes was found. The knockout mutants* ugt74f1 *and* ugt76b1 *share common genes, but also different genes were regulated in each mutant. Only significantly regulated genes (adjusted p-values < 0.05) with a log2 fold change bigger than one were considered.*

3.1.8.1 Comparison of gene expression in single *ugt* mutants

3.1.8.1.1 Gene expression in single *ugt* knockouts

After the overview revealed major impact of *UGT76B1* and *UGT74F1* in changes of transcriptome, with UGT76B1 showing a shift in the same direction as stress response triggered by BTH treatment, the three single knockouts, *ugt76b1*, *ugt74f1*, and *ugt74f2* were analysed

in more detail to understand how all three mutants are involved in stress responses. Differences in the genes regulated by the knockout mutation of one UGT compared to another can hint to differently controlled processes. This can highlight the influence of one gene in the regulation of the whole transcriptome. In addition, common genes could reveal in which processes all three UGTs are involved. Genes with adjusted p-values of < 0.05 and more than twofold changes were used for further analyses (Venn diagrams; Fig. 11C and D). According to these criteria, 2,738 genes were regulated in *ugt76b1* with 2,174 up- and 565 down-regulated in comparison to wild type. For *ugt74f1* 1,740 genes were regulated, 1,170 up and 570 down, and for *ugt74f2* 322 genes were regulated, 155 up and 167 down. These numbers show that in *ugt76b1* more genes are regulated than in *ugt74f1* (37 % less regulated compared to *ugt76b1*) and *ugt74f2* (85 %). All three mutants shared 117 regulated genes (84 up and 33 down). Among the commonly up-regulated genes, various transcription factors were found. Among these transcription factors four were found to be regulated by chitooctaose treatment, an elicitor of plant defence responses against pathogens (AT5G51190, AT3G44350, AT1G71520 and AT5G56960; Libault *et al.*, 2007). Furthermore, WRKY transcription factors were found. WRKY58 was induced by BTH treatment (AT3G01080; Wang *et al.*, 2006) and WRKY30 was induced after oxidative stress treatment (AT5G24110; Scarpeci *et al.*, 2013). In addition, genes that could be involved in ROS scavenging, *GSTU24* (AT1G17170), inducible by H_2O_2, SA, and pathogens (Queval *et al.*, 2009) and *PER4* (AT1G14540), enhanced by pathogen inoculation (Thilmony *et al.*, 2006; González-Pérez *et al.*, 2011), were found. Furthermore, genes involved in plant pathogen defence signalling, (AT3G11010; Galon *et al.*, 2008; AT1G01560; Bethke *et al.*, 2012) were present. The overlap of *ugt74f1* and *ugt76b1* contained 772 genes (679 up and 93 down). The mutants *ugt74f1* and *ugt74f2* shared 47 genes (21 up and 26 down), whereas *ugt76b1* and *ugt74f2* shared 34 genes (18 up and 16 down).

To get an overview of the expression controlled by the three UGTs, a heatmap showing gene expression of the same genes in the *ugt* mutants, wild type and wild type BTH-treated samples was generated. Because a huge amount of genes were regulated by UGT76B1 and UGT74F1, genes regulated with a log2 fold change greater or equal to four (p.adj. ≤ 0.001 for *ugt74f1* or *ugt74f2*; p.adj. ≤ $1E^{-60}$ for *ugt76b1*) were compared. The analysis revealed a general pattern of gene regulation. Most genes had lowest expression level in *ugt74f2* and wild type, slightly higher expression in *ugt74f1*, an even higher in *ugt76b1.* Highest level was found with treatment of BTH (compare Fig. S1A). Many of these genes were also involved in defence response (genes with gene ontology (GO) annotations to defence are labelled with a black bar). Only few genes had highest expression in *ugt74f1* (compare Fig. S1B). Only four

genes were found to be highest regulated in the four biological replicates of *ugt74f1*, with AT3G28915 not highly induced by BTH and AT1G69920, AT1G43160, and AT1G68050 also highly induced by BTH treatment. All of them were not annotated to the defence GO term.

3.1.8.1.2 Gene ontology enrichment analysis to reveal gene expression similarities and differences in *ugt* single mutants

Gene Ontology (GO) enrichment analysis was performed to interpret sets of genes with respect to their functional characteristics and identify, which processes are affected in the different single *ugt* mutants. Significantly enriched GO terms that are shared between mutants reveal commonly activated or repressed processes, whereas GO terms only enriched for a specific mutant can give hints about uniquely regulated processes. In *ugt74f2* no enriched GO terms were found. In *ugt76b1* 398 and in *ugt74f1* 358 GO terms were significantly enriched among the up-regulated genes (Tab. S1). From the 398 overrepresented GO terms of *ugt76b1* 295 were also found in *ugt74f1*. Thus, a big overlap of GO terms regulated in both mutants was revealed (64 %). 103 GO terms were exclusively regulated in *ugt76b1* and 63 exclusively in *ugt74f1.*

To compare the *ugt76b1* and *ugt74f1* mutants in more detail, the 30 most overrepresented GO terms were analysed (see Tab. 3). It has to be mentioned that the adjusted p-values (p.adj.) for *ugt76b1* for the first 30 GO terms were much lower ($1.60E^{-191}$-$5.29E^{-88}$) than for *ugt74f1* ($4.66E^{-124}$-$1.31E^{-63}$). This indicated higher degrees of enrichment for *ugt76b1*. The first 13 overrepresented GO terms of the *ugt76b1* knockout were also found in the first 30 overrepresented GO terms for the *ugt74f1* knockout. Many GO terms according defence response and immune system were found in both mutants. For example, the most enriched GO term among the up-regulated genes was defence response (GO:0006952) for both, *ugt76b1* (p.adj. $1.60E^{-191}$) and *ugt74f1* (p.adj. $4.66E^{-124}$). The number of genes annotated to this GO term were compared for *ugt76b1* and *ugt74f1*. In *ugt76b1*, 502 defence response genes were up-regulated. In *ugt74f1* 305. Among these 305, 242 were also regulated in *ugt76b1*.

In contrast to the common enriched GO terms under the first 30 overrepresented GO terms, also differences between *ugt76b1* and *ugt74f1* were found. SA biosynthetic and metabolic process or response to SA stimulus appeared under the top 30 enriched GO terms in *ugt76b1*, which were not found in *ugt74f1* (Tab. 3; marked in red). These GO terms appeared later in the ranking of *ugt74f1*, with less significant enrichment scores. For example, GO:0009697 (SA biosynthetic process) was found on position 14 with p.adj. $1.47E^{-105}$ in the *ugt76b1* mutant (141 significantly up-regulated genes), but only on position 66 with p.adj. $1.12E^{-47}$ in the *ugt74f1* mutant (74 genes, 67 shared with *ugt76b1*).

Tab. 3 Gene Ontology (GO) enrichment analysis of genes up-regulated in* ugt *single mutants

Thirty most enriched GO terms in ugt76b1 *(p.adj. $1.60E^{-191}$-$5.29E^{-88}$) and* ugt74f1 *(p.adj. $4.66E^{-124}$-$1.31E^{-63}$). GO terms of SA biosynthetic and metabolic processes, which were only enriched in* ugt76b1*, are marked in red.*

ugt76b1	IDs	*ugt74f1*	IDs
GO:0006952	defence response	**GO:0006952**	defence response
GO:0002376	immune system process	**GO:0009607**	response to biotic stimulus
GO:0045087	innate immune response	**GO:0006950**	response to stress
GO:0006955	immune response	**GO:0043207**	response to external biotic stimulus
GO:0009814	defence response, incompatible interaction	**GO:0051707**	response to other organism
GO:0009627	systemic acquired resistance	**GO:0002376**	immune system process
GO:0009607	response to biotic stimulus	**GO:0050896**	response to stimulus
GO:0043207	response to external biotic stimulus	**GO:1901700**	response to oxygen-containing compound
GO:0051707	response to other organism	**GO:0010033**	response to organic substance
GO:0042493	response to drug	**GO:0042221**	response to chemical
GO:0098542	defence response to other organism	**GO:0009605**	response to external stimulus
GO:0006950	response to stress	**GO:0009620**	response to fungus
GO:0009605	response to external stimulus	**GO:0001101**	response to acid chemical
GO:0009697	salicylic acid biosynthetic process	**GO:0042493**	response to drug
GO:0031347	regulation of defence response	**GO:0098542**	defence response to other organism
GO:0034976	response to ER stress	**GO:0045087**	innate immune response
GO:0009696	salicylic acid metabolic process	**GO:0006955**	immune response
GO:0080134	regulation of response to stress	**GO:0010200**	response to chitin
GO:0046677	response to antibiotic	**GO:0050832**	defence response to fungus
GO:0046189	phenol-containing compound biosynthetic process	**GO:0051704**	multi-organism process
GO:0051704	multi-organism process	**GO:0010243**	response to organonitrogen compound
GO:0018958	phenol-containing compound metabolic process	**GO:0009814**	defence response, incompatible interaction
GO:0050896	response to stimulus	**GO:0042446**	hormone biosynthetic process
GO:0033554	cellular response to stress	**GO:0009725**	response to hormone
GO:0042537	benzene-containing compound metabolic process	**GO:0009719**	response to endogenous stimulus
GO:0009751	response to salicylic acid	**GO:0031347**	regulation of defence response
GO:0071236	cellular response to antibiotic	**GO:0080134**	regulation of response to stress
GO:1901700	response to oxygen-containing compound	**GO:0042445**	hormone metabolic process
GO:0071446	cellular response to SA stimulus	**GO:0071229**	cellular response to acid chemical
GO:0010200	response to chitin	**GO:0009627**	systemic acquired resistance

To get a deeper insight in SA-related processes, genes involved in SA biosynthesis and SA signalling were compared between the different single mutants. SA biosynthetic and SA signalling genes are highly induced in *ugt76b1* relative to *ugt74f1*, whereas in *ugt74f2* genes were mostly not significantly regulated (Tab. 4). For example, *ICS1*, involved in SA biosynthesis during pathogen infection, revealed a log2 fold change of more than two in *ugt76b1*, but not in *ugt74f1*. *NPR1*, a master regulator of SA downstream signalling, was regulated with a log2 fold change of 1.21 in *ugt76b1*, whereas in *ugt74f1* the change was lower than two times (0.76) and not significantly regulated in *ugt74f2* (compare Tab. 4). Thus, in contrast to UGT74F1 and UGT74F2, UGT76B1 was involved in regulation of SA downstream signalling leading to pathogen defence responses (Fig. 9). Also other SA signalling genes were more than two fold up-regulated in *ugt76b1* (compare expression of *PR1*, *PR2, PR3*, and *PR5*) and less or not regulated in *ugt74f1*.

***Tab. 4: Expression of genes involved in SA biosynthesis or signalling in* ugt76b1*,* ugt74f1*, and* ugt74f2**

Genes expression from the RNAseq approach. Values are shown for ugt76b1*,* ugt74f1*, and* ugt74f2 *as log2 fold changes with adjusted p-values smaller than 0.05.*

ATG	annotation	*ugt76b1*	*ugt74f1*	*ugt74f2*
AT3G48090	*EDS1*	2.18	0.77	0.65
AT3G52430	*PAD4*	2.97	0.90	
AT5G14930	*SAG101*	1.94	1.00	0.37
AT1G74710	*ICS1*	2.30	0.27	
AT1G73805	*SARD1*	3.85	0.99	0.98
AT5G26920	*CBP60g*	2.46	0.79	
AT5G65210	*TGA1*	0.78		
AT5G10030	*TGA4*		0.46	
AT3G20770	*EIN3*	0.48	0.40	
AT2G27050	*EIL1*	-0.15	0.20	
AT4G39030	*EDS5*	2.66	1.04	
AT1G64280	*NPR1*	1.21	0.76	
AT5G45110	*NPR3*	1.51		
AT4G19660	*NPR4*	1.26	0.18	0.28
AT2G14610	*PR1*	6.10	1.24	
AT3G57260	*PR2*	6.40		
AT3G12500	*PR3*	1.06		
AT1G75040	*PR5*	5.35	1.05	
AT2G29350	*SAG13*	5.24	0.97	

3.1.8.2 The *ugt* triple mutation had an effect on stress responsive gene expression

To perceive how the transcriptome changes when all three UGTs are mutated, a comparison between *ugt76b1 ugt74f1 ugt74f2* and wild type under control conditions was performed. In the triple mutant, 3,379 genes were regulated (2,309 up, 1,070 down), including many genes related to stress response in plants (compare Tab. S2). The stress induced genes identified include 19 peroxidases, which are stress indicators in plants (Pandey *et al.*, 2017), 16 glutathione S-transferases, which have been shown to be induced by stress and pathogen infection (Gullner *et al.*, 2018) and 32 cytochrome P450 monooxygenases, which *inter alia* play critical roles in the biosynthesis of defence compounds, hormones or signalling molecules (Schuler & Werck-Reichhart, 2003).

Furthermore, ten leucine-rich repeat (LRR) receptor kinases, among them FLS2, which activate defence response against pathogens, were enhanced (Belkhadir *et al.*, 2014). NACs (Nuruzzaman *et al.*, 2013) and WRKYs (Rushton *et al.*, 2010) transcription factors are known to play a role in initiation and control of plant immunity. 22 NACs and 31 WRKYs were found to be induced. Interestingly, seven other UDP glucosyltransferases were positively regulated, among them *UGT76D1*, which was recently shown to influences SA homeostasis and immune responses (Huang *et al.*, 2018). In general eight hits for pathogen and 52 hits for resistance were found. This shows that many stress responsive genes were controlled and suppressed by UGT76B1, UGT74F1, and UGT74F2.

3.1.8.2.1 The comparisons of differences in the gene expression profile between the *ugt* triple, the *ugt76b1*, and the *ugt74f1 ugt74f2* mutant

Since many genes were regulated in the *ugt* triple mutant, the question arose whether certain genes are only regulated in the absence of all three genes, which could give hints to the interaction of the three UGTs. Therefore, the *ugt* triple mutant was compared to *ugt76b1* and *ugt74f1 ugt74f2*. A big overlap in gene expression between of the triple mutant, *ugt76b1* single mutant and *ugt74f1 ugt74f2* double mutant was found. Only 229 genes were exclusively up- and 550 down-regulated in the triple mutant and thus representing around 23 % of genes significantly regulated only in the triple mutant. Among the exclusively up-regulated genes, genes involved in abiotic stress signalling like cold stress and abscisic acid pathway (AT2G38390; Kim & Kang, 2018), drought or freezing stress (AT5G17460; Ren *et al.*, 2018) were found. In addition, genes involved in diverse defence reaction were also identified. For the latter, examples are AT1G17860 (Arnaiz *et al.*, 2018), which is induced after spider mite feeding, AT4G13510, which is an ammonium transporter activated during pathogen attack as sensor of nitrogen content (Liu *et al.*, 2010) and AT5G03210, which is a response to different viruses (Castelló *et al.*, 2011).

3.1.8.2.2 Similarities between BTH treated wild type and *ugt* triple mutant

The PCA showed that with the mutation of all three UGTs expression level of genes were shifted towards the same direction as wild type with stress treatment (Fig. 11A). Therefore, it could be assumed that similar genes, which are regulated by BTH treatment are also regulated in a similar manner as in the absence of the three UGTs. By the application of SA analogue BTH 5,805 genes were changed in wild type (3,318 up; 2,487 down), whereas 3,379 genes (2,309 up, 1,070 down) were regulated in *ugt76b1 ugt74f1 ugt74f2* without any treatment. 1,344 genes were not up-regulated in the triple mutant and 1,693 genes not down-regulated compared to BTH-treated wild type. Among the 3,379 genes regulated in the *ugt* triple mutant 82 % were regulated in the same way as in BTH-treated wild type (2,762:1,974 up; 788 down). Taken these results together it was shown that 48 % of genes, which are regulated by BTH in wild type, were repressed UGT76B1, UGT74F1, and UGT74F2 under non-stressed condition. It has to be mentioned that genes were regulated by the application of BTH also in the triple mutant (2,049:799 up; 1,350 down). Among them 68 % (1,401:588 up; 813 down) were responsive in wild type treated with BTH in the same manner. These group of genes resemble genes which may be independent of the three UGTs.

3.1.8.3 SA responsive genes in *ugt* triple mutant

For SA inducible genes 217 marker genes were described (Blanco *et al.*, 2009). In control conditions, SA responsive genes were screened and compared between wild type, *ugt76b1 ugt74f1 ugt74f2*, *ugt76b1*, and *ugt74f1 ugt74f2*. This could give hints about how SA responses are controlled by the three UGTs. From these 217 SA marker genes 178 genes were induced by BTH treatment, an SA analogue (Tab. S3). Without any treatment 155 genes were induced in the *ugt* triple mutant with an overlap of 152 genes also induced by BTH treatment in wild type (Tab. S3). Thus, this SA responsive genes were repressed by the three UGTs under control conditions. It has to be mentioned that most of these genes were regulated by *UGT76B1*, since in *ugt76b1* single mutant 164 genes were induced. In contrast, in the *ugt74f1 ugt74f2* double mutant only 37 genes were up-regulated (Tab. S3).

3.1.8.4 ROS responsive genes in *ugt* triple mutant

One of the first steps during perception of bacterial pathogens is the formation of reactive oxygen species (ROS), as well as, the biosynthesis of SA. Since ROS signalling plays an important role in plant stress defence, genes induced in *ugt* mutants were compared to a microarray study published (Gadjev *et al.*, 2006). They compared eight different datasets with exogenous application of oxidative stress-causing agents and mutants with altered activity of enzymes influencing ROS. With this approach, 32 transcripts were identified as markers for general oxidative stress. Remarkably, *UGT76B1* was differentially expressed in at least six of

the eight ROS-related microarrays and, therefore, categorised as an indicator for the general oxidative stress response. To see if genes related to ROS are affected in *ugt76b1 ugt74f1 ugt74f2*, the expression of the 32 marker genes was checked (Tab. S4). Among these 32 genes, 27 were induced by BTH application in the wild type. For the mutants without any treatment *ugt76b1* exhibited 24 genes, the triple mutant 21, whereas *ugt74f1 ugt74f2* exhibited only eight. This study suggests that UGT76B1 and to lesser extend UGT74F1 and UGT74F2 affected the regulating of ROS-related processes. To get a better knowledge about how genes involved in ROS may be regulated by the expression of *UGT*s, another study with 42 marker genes for ROS production in plant defence was compared to the *ugt* mutant datasets (Vaahtera *et al.*, 2014). From 42 genes 22 were also regulated by BTH treatment in wild-type plants (Tab. S5). For the mutants without any treatment 20, 13, and three genes were identified in *ugt76b1*, the triple mutant, and *ugt74f1 ugt74f2*, respectively. The comparison of these two studies showed that genes identified as ROS marker genes were regulated by UGT76B1 and UGT74F1/UGT74F2.

To directly test for ROS formation in the *ugt* mutants, seedlings were stained with NBT (nitroblue tetrazolium) for the detection of O_2^- radicals (Fig. 12A and B). In *ugt76b1* and in the triple mutant a significant enhancement of staining was revealed. *ugt74f1 ugt74f2* showed a tendency of increased O_2^- radicals, which was not significantly different from wild type. These results matched the observed marker gene expression patterns described above.

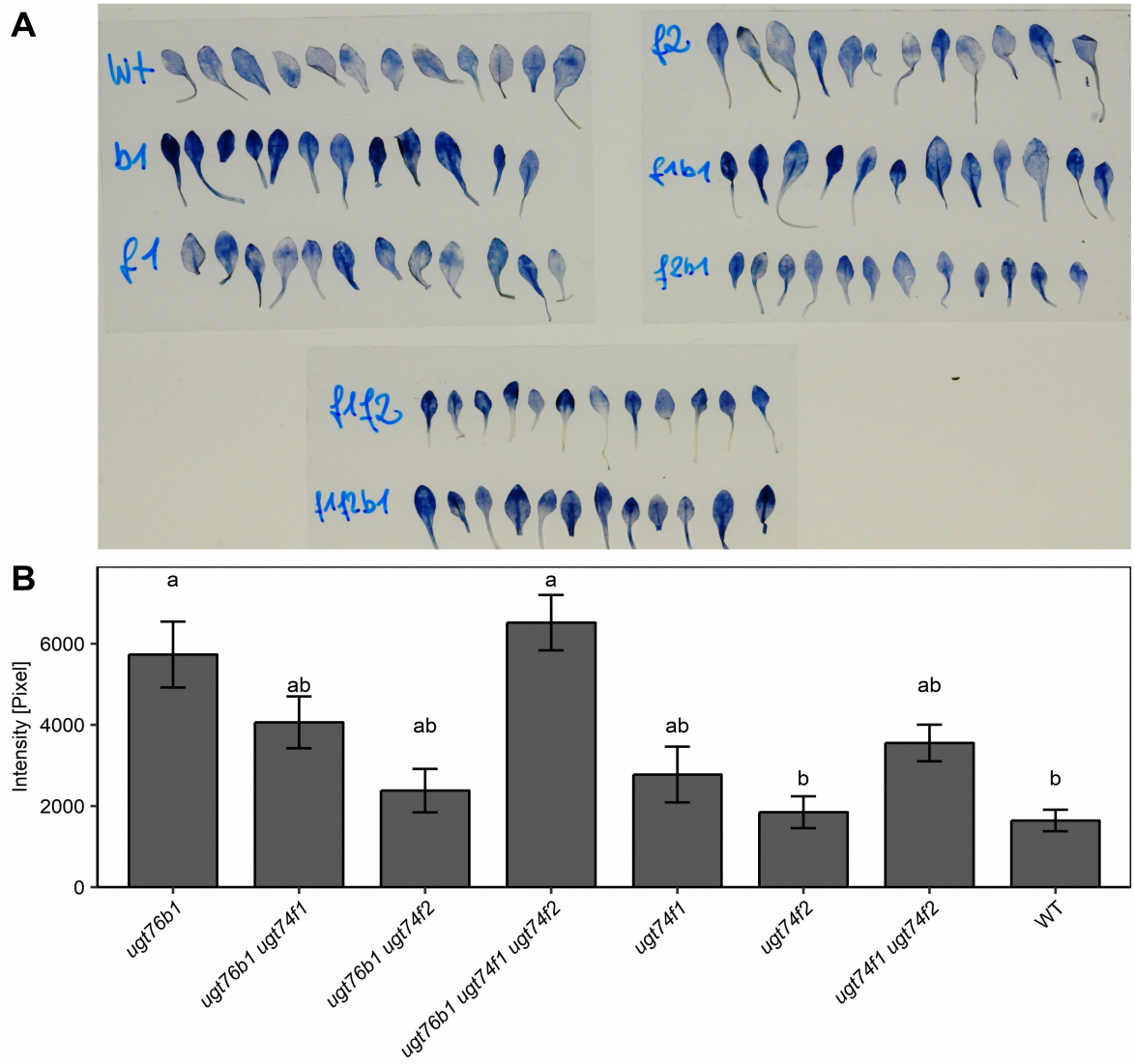

Fig. 12: O_2^- radicals were differently regulated in the* ugt *mutants

Fourteen-day-old wild-type seedlings were harvested and stained with NBT for superoxide readical detection. Blue indicates O_2^- radicals. A: Picture of staining of the different genotypes. B: Quantified intensity of pixel of the image; means ± SE; n = 12. Significant differences (p.adj. < 0.05) are indicated by letters according to one-way ANOVA.

3.1.9. Expression of UGTs in different *ugt* mutation background

The expression levels of the three *UGT*s were checked in the different *ugt* knockout mutants in the RNAseq approach data. Neither the expression of *UGT74F1* nor the expression of *UGT74F2* were changed in *ugt76b1* with a log2 fold change higher than one, whereas UGT76B1 expression was enhanced in the *ugt74f1*, *ugt74f2*, and *ugt74f1 ugt74f2* mutants (Tab. 5).

Tab. 5: Expression levels of* UGT76B1*,* UGT74F1*, and* UGT74F2 *in different* ugt *mutant combinations

Expression levels of the three UGT*s were analysed from the RNAseq approach in different mutant combinations of UGTs. Values are shown as log2 fold changes with adjusted p-values smaller than 0.05.*

mutant	gene of interest	log2 fold change
ugt76b1	*UGT74F1*	
	UGT74F2	0.43
ugt74f1	*UGT76B1*	1.55
	UGT74F2	0.67
ugt74f2	*UGT76B1*	1.27
	UGT74F1	
ugt76b1 ugt74f1	*UGT74F2*	0.53
ugt76b1 ugt74f2	*UGT74F1*	
ugt74f1 ugt74f2	*UGT76B1*	1.57

3.1.10. Oxidation of SA as another SA modification in *ugt* triple mutant

As mentioned in the introduction, processes other than glucosylation can modify SA and thus, are also involved in controlling levels of free SA (1.3). Out of these possible modifications, genes involved in oxidation of SA and further processing, *S3H*, *S5H*, and *UGT76D1*, were strongly enhanced by BTH treatment (Tab. 6). The same genes were up-regulated in the *ugt* triple mutant under control conditions as well.

Tab. 6: Expression levels of SA modifying enzymes

Genes expression from the RNAseq approach were analysed for SA modifying enzymes next to the three UGTs. Values are shown as log2 fold changes with adjusted p-values smaller than 0.05.

ATG	annotation	WT BTH vs WT control	Triple *ugt* control vs WT control	Triple *ugt* BTH vs triple *ugt* control
AT3G11480	*BSMT1*			
AT1G07260	*UGT71C3*			-0.85
AT2G03760	*SOT12*	0.52	0.39	-0.55
AT4G27260	*GH3.5*			0.79
AT5G24530	*S5H*	5.03	4.06	1.06
AT4G10500	*S3H*	7.21	5.32	2.13
AT2G26480	*UGT76D1*	5.82	3.66	2.02
AT5G03490	*UGT89A2*	0.45		

Under normal condition SA was induced significantly in the *ugt* triple mutant, whereas with the additional treatment no further, significant increase of SA was observed compared to the

wild type. Thus, the *ugt* triple mutant was insensitive to further stimulation. Other processes involved in controlling free SA levels might further be enhanced in this mutant under BTH treatment. This was confirmed by enhanced expression levels of *GH3.5*, *S3H*, *S5H*, and *UGT76D1*. These genes were even further enhanced in *ugt* triple mutant treated with BTH compared to the untreated *ugt* triple mutant (Tab. 6). This would suggest that upon stress induction, mutant plants lacking SA glucosylation enzymes activated the SA-oxidation pathway to regulate endogenous SA levels.

Since levels of SA, SAG, and SGE were measured with LC-MS, profiles of wild type and *ugt* triple mutant were checked for the possible occurrence of DHBA xyloside (DHBAX) and glucoside (DHBAG). For DHBAX (m/z 285.0605; mass at 285.0605 is the [M+H]+ ion of DHBAG ion of DHBA), three different peaks were found with the correct mass (retention times: 5.3, 7.8 + 8.0, and 8.6). These could be due to the possibility of hydrolysis at different position (2,3-DHBA and 2,5-DHBA). From the chromatograms no differentiation between the three peaks was possible. Nevertheless, in wild type, all three peaks were enhanced after BTH treatment. Additionally, in *ugt76b1 ugt74f1 ugt74f2*, all three peaks increased confirming observed gene expression pattern with higher levels of DHBAX as result (Fig. 13A). For DHBA glucoside (DHBAG; m/z 315.0711) five different peaks were found. Of these five, one was not induced by BTH treatment in wild type and hence excluded. Three of them showed elevated levels (retention times: 1.6, 4.1, 6.1) in *ugt* triple mutant, whereas one showed similar levels as wild type (retention time: 8.4; Fig. 13B). Without the real identification of the individual peaks, only the trend of the peaks enhanced by BTH can be analysed in the *ugt* triple mutant. The majority, six out of seven, were elevated in *ugt* triple mutant. Together with the increased gene regulation of *S3H*, *S5H*, and *UGT76D1*, it can be speculated that oxidation of SA was increased if glucosylation by all three UGTs was missing. Nevertheless, SA levels were still enhanced in *ugt76b1 ugt74f1 ugt74f2* compared to the wild type (Fig. 10).

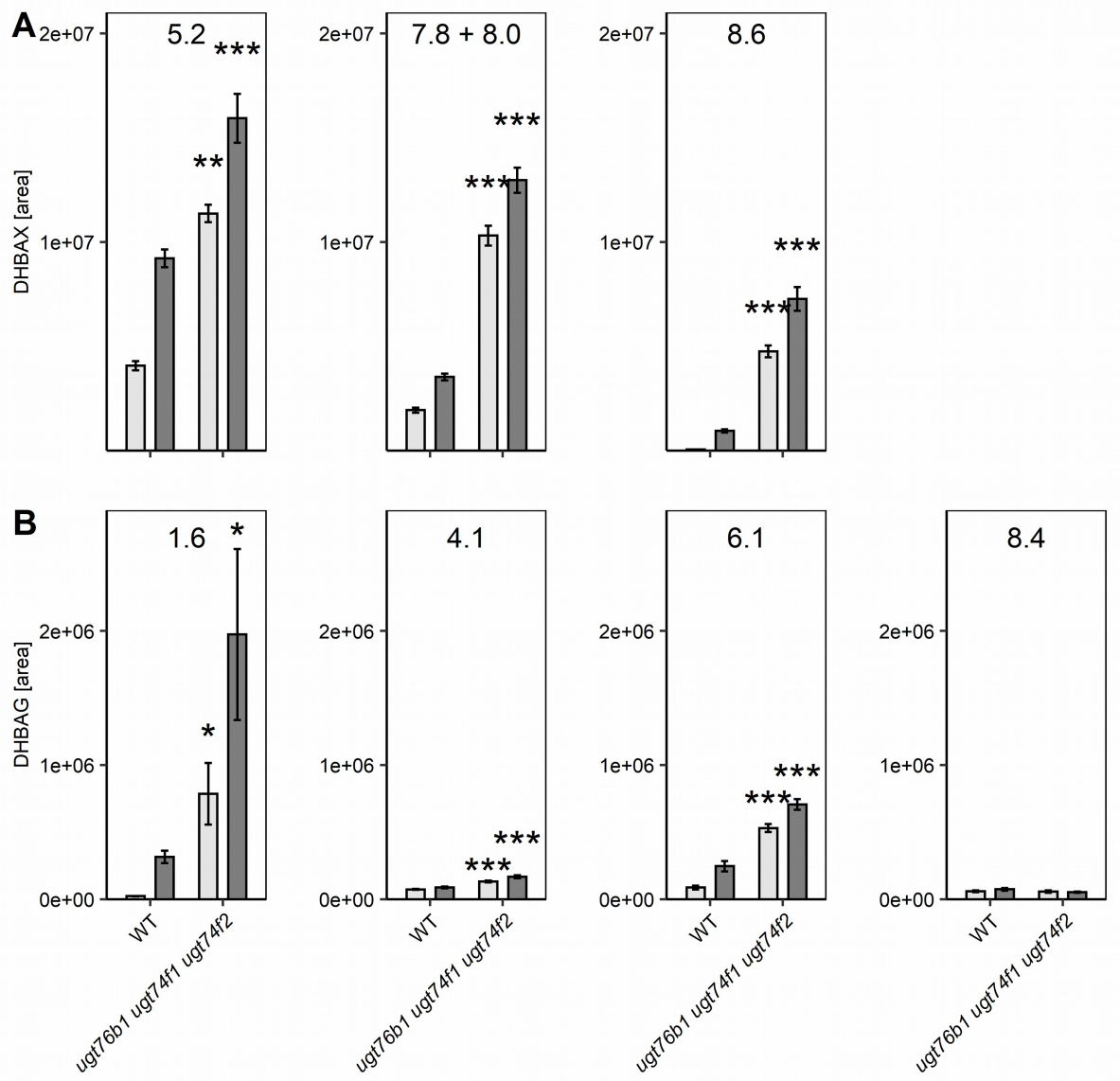

Fig. 13: SA conversion to DHBA and DHBA conjugates as another mechanism of controlling free SA levels in* ugt *triple mutant

Possible peaks of DHBA sugars were analysed in three-week-old plants of wild type and ugt76b1 ugt74f1 ugt74f2 *without (light grey) and with BTH treatment (dark grey).* ***A:*** *Three possible DHBAX peaks.* ***B:*** *Four possible DHBAG peaks. Different retention times are indicated at the corresponding plots. means ± SE; n = 4. Differences between triple mutant and wild type were analysed by Welch two sample t-test; * = p < 0.05, ** = p < 0.01 and *** = p < 0.001.*

3.1.11. The glucosyltransferase UGT74F1 was unable to compensate for the loss of UGT76B1

UGT76B1 and UGT74F1 were shown to both act as SA glucosyltransferase *in vitro.* However, LC-MS analyses of *ugt* mutant combinations showed that UGT76B1 and UGT74F1 had various influence on the free SA levels and SAG production (Fig. 10). One known difference

of the two enzymes is the glucosylation of ILA. UGT76B1 was able to glucosylate ILA, whereas UGT74F1 could not (3.1.1).

To test the redundancy of the two UGTs and to see if phenotypes found in *ugt76b1* can be rescued by UGT74F1, UGT74F1 was introgressed in the *ugt76b1* knockout mutant. AS the expression patterns of UGT76B1 and UGT74F1 were different (Fig. 8), a hybrid construct was designed by Maksym (2018). This construct was composed of *UGT74F1* CDS fused with *UGT76B1* 5' and 3' regulatory regions. Single insertion transgenic lines were established (hybrid F1 1-7). In all hybrid F1 lines *PR1* induction was still up-regulated compared to the wild type (Fig. 14A). The hybrid construct was expressed with different levels among those hybrid lines, but was not correlated with the expression level of *PR1* (Fig. 14B).

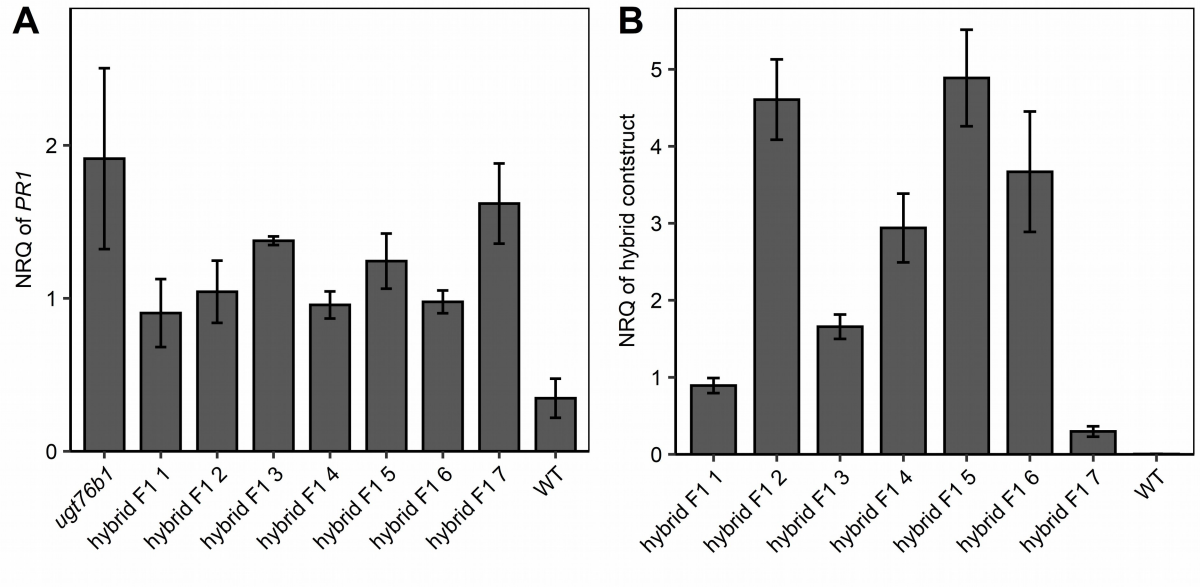

Fig. 14: Induced expression levels of* PR1 *in* ugt76b1 *was not complemented by UGT74F1 CDS

***A:** NRQ of* PR1 *expression in* ugt76b1*,* ugt76b1 *complemented with* UGT74F1 *(hybrid F1 1-7), and WT. n = 3; means ± SE.* ***B:** NRQ of hybrid construct expression in* ugt76b1 *complemented with CDS of* UGT74F1 *(hybrid F1 1-7) and WT. In WT the artificial construct was not detected. Gene expression was assessed by RT-qPCR and normalized to* S16 *and* UBQ5*. n = 3; means ± SE.*

To further investigate the influence of UGT74F1 complementation in *ugt76b1* two different hybrid lines with low (hybrid F1 1) and high (hybrid F1 2) hybrid construct expression levels were chosen. As a positive control *ugt76b1* was complemented with *UGT76B1* (comp. B1 1 and 2; design and transformation by R. Maksym). For this set of lines, including *ugt76b1* and wild type as control, *PR1* expression, dry weight of rosettes, early senescence phenotype, superoxide anion content and bacterial growth were tested. In all these treatments hybrid F1 lines showed similar results comparable to *ugt76b1*, whereas comp. B1 lines showed complementation of *ugt76b1* phenotypes (Fig. 15). Even though both enzymes are SA glucosyl-

transferases, it was demonstrated that *UGT74F1* under the promoter of UGT76B1 could not rescue the phenotype present in *ugt76b1*.

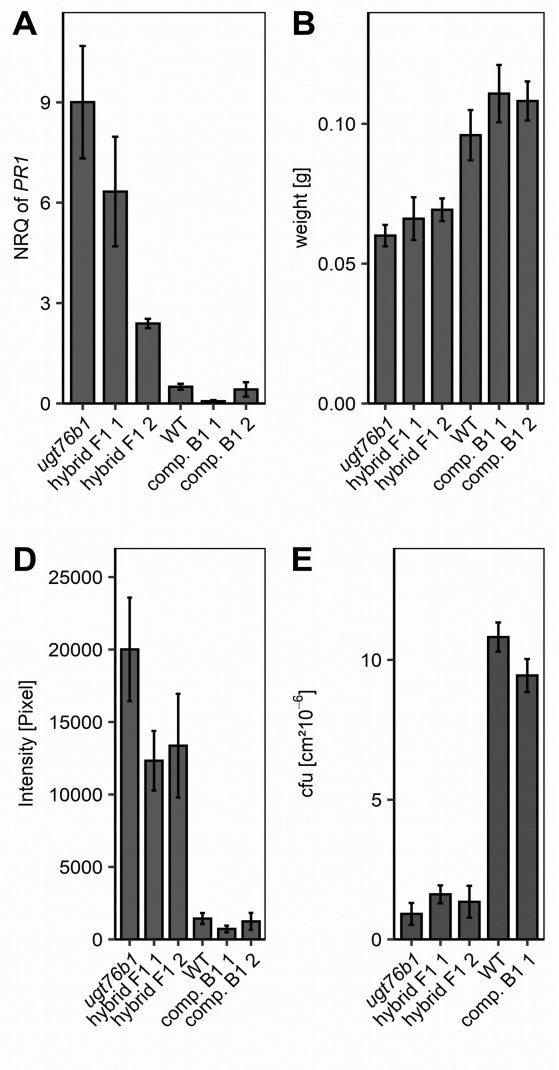

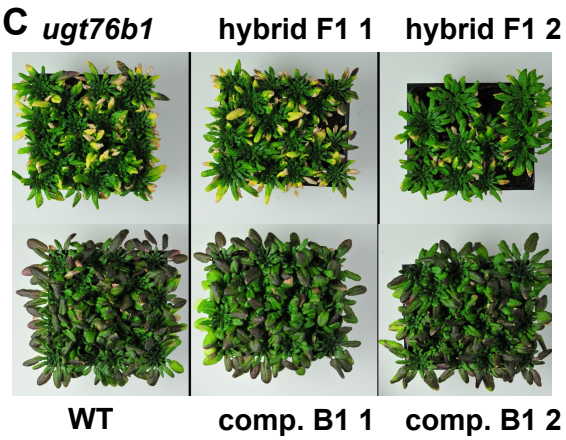

Fig. 15:* ugt76b1 *phenotypes were compensated by UGT76B1, but not with UGT74F1 hybrid construct

Phenotypes of ugt76b1, ugt76b1 *complemented with CDS of* UGT74F1 (*hybrid F1 1; hybrid F1 2), WT and* ugt76b1 *complemented with CDS of* UGT76B1 (*comp. B1 1; comp. B1 2) were compared.* **A:** *NRQ of* PR1 *expression in four-week-old plants. n = 3; means ± SE.* ***B:*** *Dry weight of rosettes. n = 10; means ± SE.* ***C:*** *Senescence phenotype of 60-days-old plants.* ***D:*** *NBT staining of two-week-old seedlings. n = 9; means ± SE.* **E:** *Infection study. Four-week-old plants were inoculated with* Pst *(5 x 10^5 cfu), and the resulting* Pst *titres* in planta *were determined at 3 dpi. Bars represent the average of three replicates. means ± SE.*

3.1.12. Homologs of UGTs in *Brassica napus*

In addition to *A. thaliana*, ILA and SA have been reported to be present in various plants, including *Brassica napus* (rape seed) (Ratzinger *et al.*, 2009; Dempsey & Klessig, 2017; Maksym *et al.*, 2018). Since both compounds are found in diverse plant species, the aim was to identify homologues of UGT76B1 and UGT74F1/UGT74F2 in *B. napus* and to determine if they are similarly involved in SA and/or ILA glucosylation. In collaboration with M. Spannagl (MIPS, Helmholtz Zentrum München), homologues of AthUGT76B1 and AthUGT74F1/ AthUGT74F2 were identified from the *B. napus* genome. Due to the genome triplication in *B. napus* several related candidate genes were found. For UGT76B1 only two, while for UGT74F1/UGT74F2 eleven candidates were predicated.

Out of the eleven candidates, four were chosen for further analysis, including the two closest relatives to AthUGT74F1 (27001; 53001), one intermediate (54001) and the most distant gene (18001). Full gene names are given in 2.5.1. The position 15 was checked for the four candidates. 27001 and 53001 revealed a serine at this position, which is typical for AthUGT74F1, whereas in 18001 and 54001 a threonine was present, which is typical for AthUGT74F2. In order to test and analyse their function in SA glucosylation, the selected genes were amplified to enable their recombinant expression in *E. coli.* The recombinant proteins of UGT76B1 and UGT74F1/UGT74F2 were tested for glucosylation activity towards SA. For the two UGT76B1-related enzymes only 14001 showed glucosylation activity towards SA. All four UGT74F1/UGT74F2 candidates produced SAG (Fig. 16A). Only for the two UGT74F2-like enzymes was SGE also detectable. The active UGT76B1 candidate 14001 glucosylated ILA as well as SA *in vitro* (Fig. 16B).

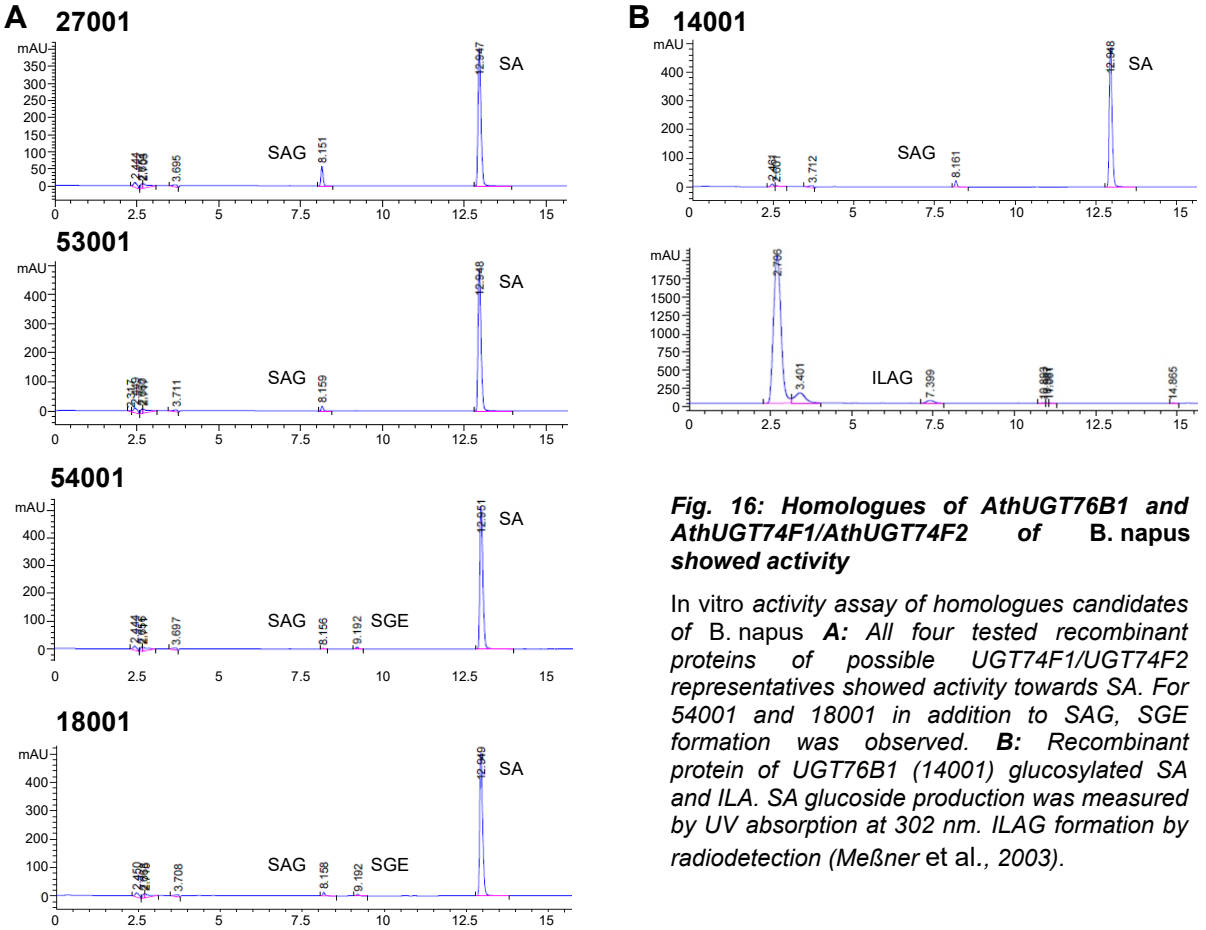

Fig. 16: Homologues of AthUGT76B1 and AthUGT74F1/AthUGT74F2 of* B. napus *showed activity

In vitro *activity assay of homologues candidates of* B. napus ***A:*** *All four tested recombinant proteins of possible UGT74F1/UGT74F2 representatives showed activity towards SA. For 54001 and 18001 in addition to SAG, SGE formation was observed.* ***B:*** *Recombinant protein of UGT76B1 (14001) glucosylated SA and ILA. SA glucoside production was measured by UV absorption at 302 nm. ILAG formation by radiodetection (Meßner* et al.*, 2003).*

3.2 The isoleucic acid - distinct impacts on plant defence, root growth, and formation of reactive oxygen species

3.2.1. Exogenous ILA enhances SA-related plant defence mechanism to biotrophic pathogen

The inhibitory effect of ILA on SA glucosylation by UGT76B1 *in vitro* and the induction of plant defence by the exogenous application of ILA raised the question of whether ILA interferes with SA signalling *in vivo* (von Saint Paul *et al.*, 2011; Noutoshi *et al.*, 2012). To address the interaction of SA and ILA during plant defence, soil-grown wild-type plants were pretreated with 10 µM SA, 250 µM ILA and a combination of both compounds. Three days after this treatment, plants were infected with *Pst*. The application of the low concentration of 10 µM SA solution alone did not induce plant defence responses (Fig. 17). In contrast, treatment with 250 µM ILA led to a slight reduction of bacterial growth, while the combination of 10 µM SA and 250 µM ILA provoked an enhanced resistance and repressed bacterial growth by more than one log10-scale relative to control or SA treated plants (Fig. 17).

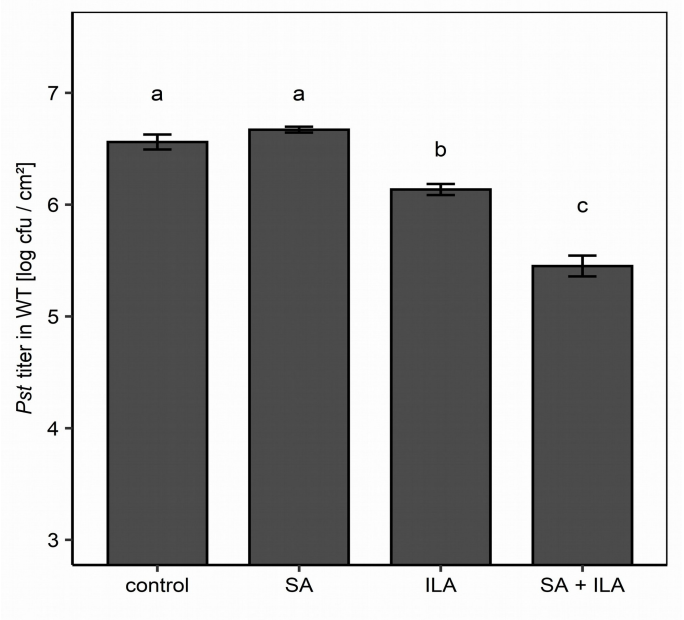

Fig. 17: Repression of bacterial pathogens upon SA and ILA application

Four-week-old soil grown plants were watered with control solution, 10 µM SA, 250 µM ILA or the combination of 10 µM SA and 250 µM ILA. After three days the plants were inoculated with Pst *(5 x 10^5 cfu), and the resulting* Pst *titers were determined at three days after infection (dpi). Bars represent the means ± SE of four biological replicates. Significant differences (p.adj. values) are indicated by letters according to one-way ANOVA. The experiment was independently repeated three times with similar results.*

3.2.2. The exogenous application of ILA enhances endogenous free SA levels and SA-dependent gene expression

To test responses induced by ILA application, a liquid culture system with young seedlings were used. After the application of 250 µM and 500 µM ILA, only the higher ILA concentration enhanced *PR1* expression significantly in the liquid culture system with young seedlings (Fig. 18A). Consequently, 500 µM of ILA was used in the following experiments. Endogenous free

SA levels were measured 24 h and 48 h after ILA application. No difference in SA content was observed after 24 h relative to control plants. However, after 48 h of ILA treatment, SA levels increased significantly in wild type compared to non-treated plants (Fig. 18B). In addition, ILA induced *PR1* expression was shown to be SA-dependent. In the SA-depleted mutant NahG *sid2*, no up-regulation of *PR1* expression was observed 48 h after ILA treatment (Fig. 18C).

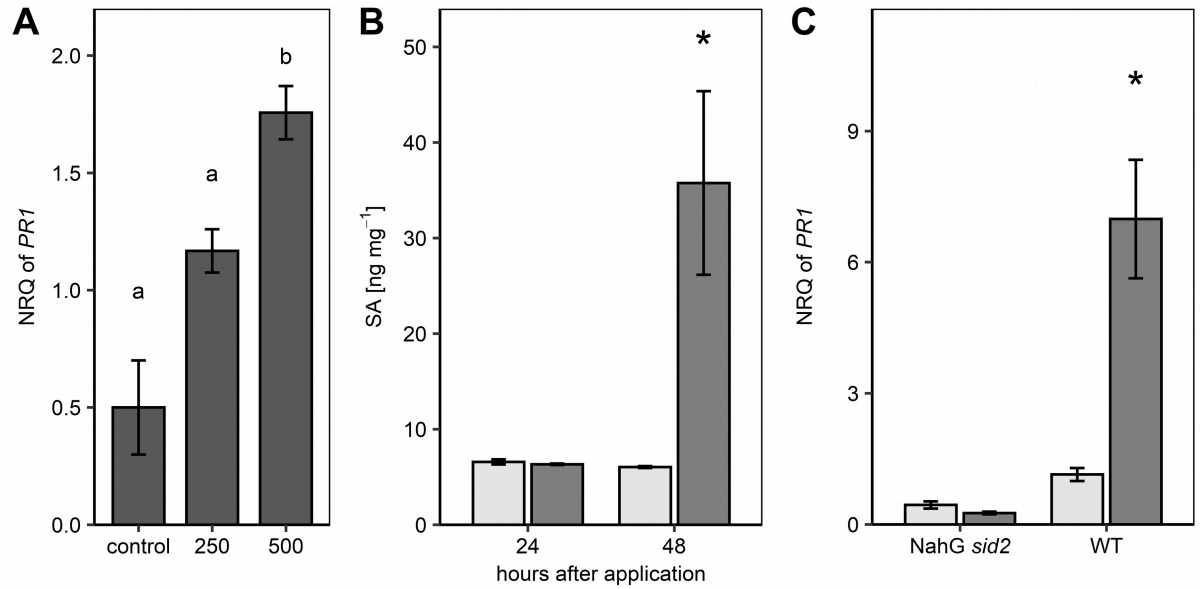

Fig. 18: ILA induced endogenous level of SA and SA-dependent* PR1 *expression

A:*Transcript abundance of SA marker gene* PR1 *in leaves of 14-day-old plantlets grown in liquid culture were measured by RT-qPCR 48 h after application of control, 250 µM or 500 µM ILA solution. Gene expression was normalized to* S16 *and* UBQ5*. means ± SE; n = 3-4. Significant differences (p.adj. values) are indicated by letters according to one-way ANOVA.* ***B:*** *Free SA levels in leaves of 12-day-old wild-type seedlings treated 24 h or 48 h with medium containing 500 µM ILA (dark grey bars) or control medium (light grey bars). means ± SE; n = 4.* ***C:*** PR1 *expression in leaves of 14-day-old plantlets grown in liquid culture were measured by RT-qPCR 48 h after application of 500 µM ILA to wild type (WT) or SA-depleted NahG sid2 plants; control medium (light grey bars) or ILA-containing medium (dark grey bars). Gene expression was normalized to* S16 *and* UBQ5*; means ± SE; n = 4. For B and C differences between treated or untreated plants were analysed by Welch two sample t-test; * = p < 0.05.*

Based on the results that showed that the combined treatment of SA and ILA led to an enhanced pathogen resistance in soil grown wild type plants (Fig. 17), *PR1* expression was measured after the combined treatment of SA and ILA in wild type and *ugt76b1* seedlings. Similar to the pathogen experiments (Fig. 17), the seedlings were treated with the lower concentration of 250 µM ILA in combination with rising concentrations of SA (Fig. 19A). In wild type, a higher *PR1* expression in plants treated with both ILA and SA was observed compared to plant treated only with SA (Fig. 19). A two-way between-groups analysis of variance revealed a significant impact of SA and ILA on *PR1* expression and a significant

interaction term indicative of a non-additive, positive interaction ($p < 0.005$ for both factors and for the interaction term).

In *ugt76b1*, an increased *PR1* expression upon the exogenous application of SA was observed. However, in contrast to the wild type, the enhancement of PR1 expression by the additional application of 250 µM ILA was not observed (Fig. 19B). Two-way between-groups analysis of variance showed only an influence of the SA concentration on *PR1* ($p < 0.01$), while the effect of ILA ($p = 0.269$) and the interaction ($p = 0.137$) were not significant.

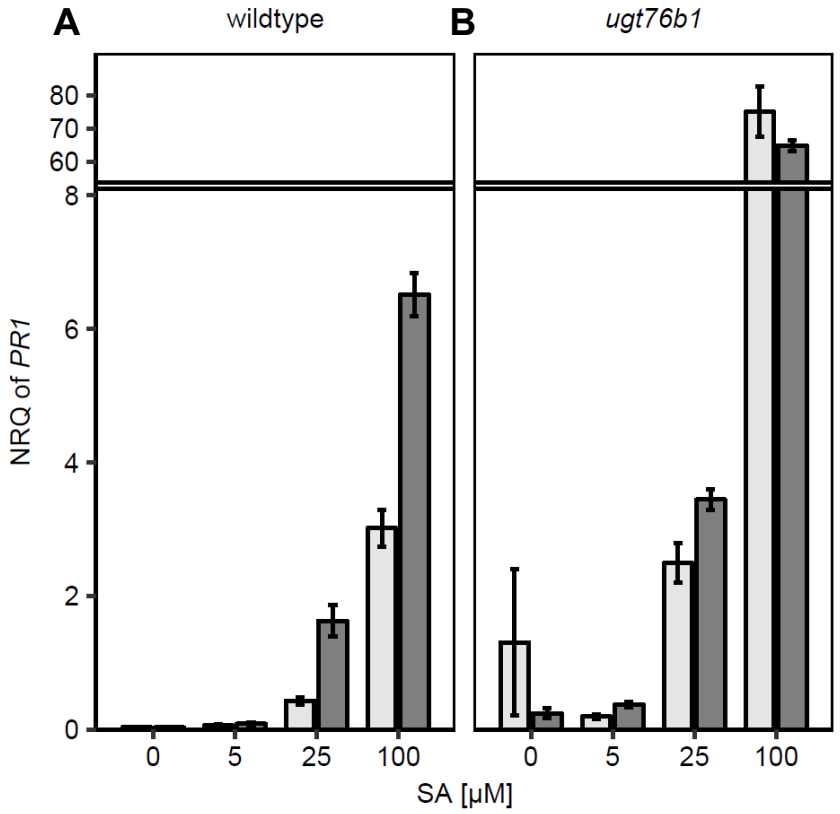

Fig. 19: Interaction of SA and ILA* in planta *were dependent on UGT76B1

A: PR1 *expression in wild type and* ***B:*** PR1 *expression in the* ugt76b1 *mutant was investigated in leaves of 14-day-old seedlings that had been incubated 48 h with increasing concentrations of SA (0, 5, 25, 100 µM) in the absence (light-grey bars) and presence of 250 µM ILA (dark grey bars). Expression values are normalized to* S16 *and* UBQ5*; means ± SE; n = 3-4.*

In addition to the SA signalling marker gene *PR1*, senescence associated marker genes *SAG13* and *SAG21* were induced by ILA (Fig. 20A). To see if the interaction of ILA and SA is also working with higher SA levels and to exclude a plateau of *PR1* expression, 500 and 750 µM SA were applied to wild type. The interaction effect of ILA and SA was still observed for higher concentrations of SA up to 750 µM (Fig. 20B). As *PR1* is already induced in *ugt76b1*

without exogenous SA, and 100 µM SA lead to a very strong *PR1* induction, it was confirmed that the marker gene was further inducible with higher SA concentrations. This demonstrated that the *PR1* induction did not plateau upon 100 µM SA application in combination with 250 µM ILA (Fig. 20C). Thus, the additional effect of ILA was attenuated in the *ugt76b1* mutant.

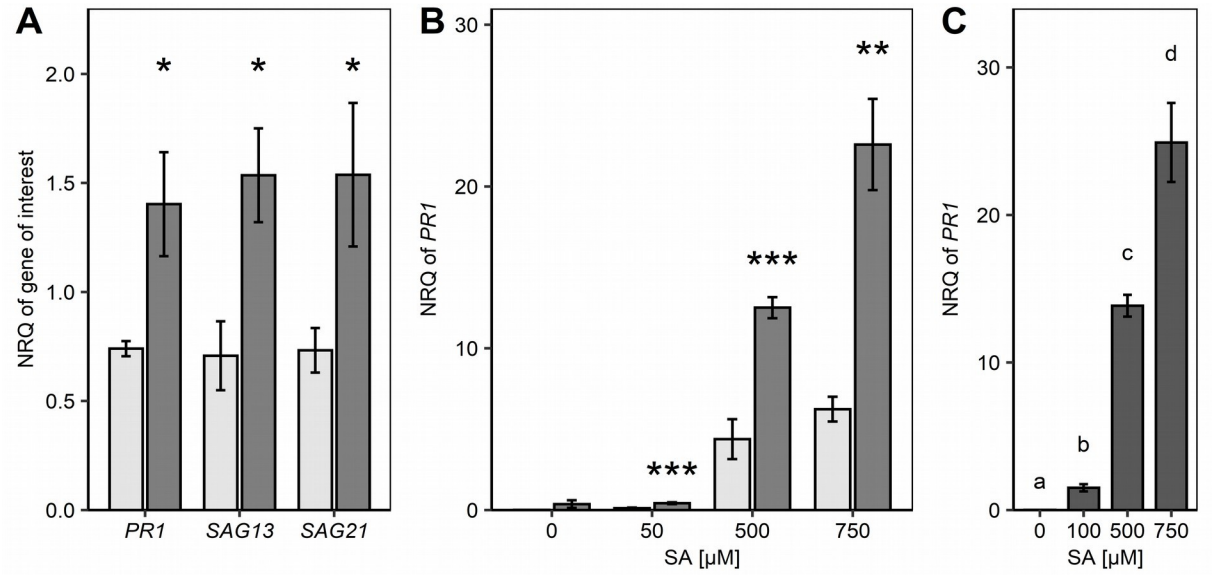

Fig. 20: ILA effect on SA signalling and interaction with high SA concentrations

A: *Transcript levels of SA marker gene* PR1 *and senescence marker genes* SAG13 *and* SAG21 *were measured by RT-qPCR 48 h after application of 500 µM ILA. Leaves were harvested from 14-day-old plantlets grown in liquid culture. A similar up-regulation of* PR1 *and* SAG13 *was shown by von Saint Paul* et al. *(2011) after ILA spraying onto soil-grown plants. means ± SE.; n = 4.* ***B:*** *Interaction of SA and ILA in wild type with higher SA concentrations.* PR1 *expression in leaves of 14-day-old wild-type seedlings 48 h after addition of media with increasing concentrations of SA (µM) without (light grey bars) and with ILA (250 µM; dark grey bars). means ± SE.; n = 3. Differences between ILA treated or untreated plants were analysed by Welch two sample t-test; *** = p < 0.001; ** = p < 0.01; * = p < 0.05.* ***C:*** *SA-dependent induction of* PR1 *in* ugt76b1. PR1 *expression in leaves of 14-day-old* ugt76b1 *seedlings 48 h after addition of media with increasing concentrations of SA as indicated. means ± SE; n = 4. Significant differences (p.adj. < 0.05) are indicated by letters according to one-way ANOVA. Marker gene expression was normalized to* S16 *and* UBQ5 *in all cases.*

3.2.3. ILA induces superoxide anion formation

ROS are intrinsically involved in SA-dependent defence reactions, which can be also induced by exogenously applied SA (Torres *et al.*, 2006; Vlot *et al.*, 2009; Khokon *et al.*, 2011; Herrera-Vásquez *et al.*, 2015). As ILA potentiates SA-related responses (Fig. 17, 18, and 19), the impact of ILA on ROS production was examined. *A. thaliana* seedlings were treated with ILA, SA and a combination of both compounds and stained for the O_2^- radicals using NBT. ILA, at a concentration of 500 µM, induced superoxide levels to a similar extent as 500 µM of SA (Fig. 21A). To test for a potential interaction between SA and ILA in ROS induction, 100 µM SA, 250 µM ILA and the combination of SA and ILA were used. 100 µM SA did not evoke a detectable effect, while 250 µM ILA resulted in an enhanced superoxide production (Fig.

21B). Interestingly, the combined application of 100 µM SA and 250 µM ILA did not show any further enhancement. In contrast to *PR1* gene expression (Fig. 19A), 100 µM SA did not evoke a detectable effect, while 250 µM ILA resulted in an enhanced superoxide production. The combined application of SA and ILA did not show any further enhancement. Thus, ILA might induce superoxide in an SA-independent manner.

To test that hypothesis, the induction of superoxide anions in NahG *sid2* and wild-type plants treated with 500 µM ILA was compared. ILA induced superoxide formation in both lines supporting an SA-independent O_2^- induction by ILA (Fig. 21C). To further investigate a possible link between ILA and superoxide production, *ugt76b1*, wild type and OE were analysed. Intriguingly, the *ugt76b1* knockout mutant containing the highest endogenous ILA level (Maksym *et al.*, 2018), exhibited enhanced constitutive O_2^- production compared to the wild type and the OE (Fig. 21D).

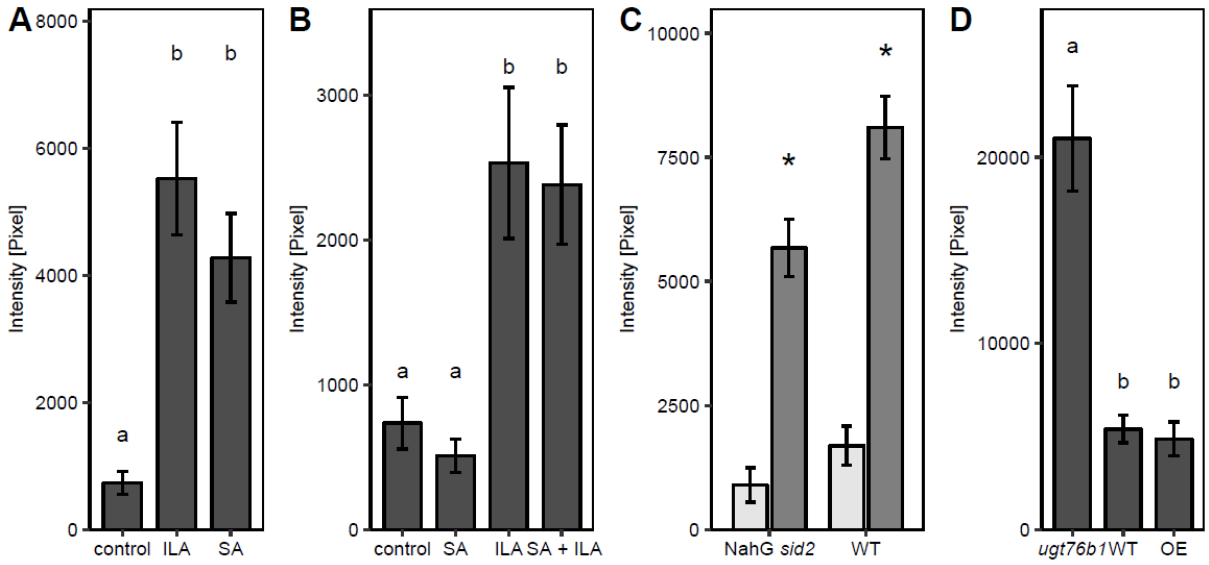

Fig. 21: ILA enhances superoxide radicals in leaves

O_2^- radical detected by NBT staining in leaves of two-week-old seedlings. ***A:*** *Twelve-day-old wild-type seedlings were treated with 500 µM ILA or 500 µM SA and stained with NBT after 48 h. Staining of leaves was quantified; means ± SE; n = 9.* ***B:*** *Superoxide detection 48 h after treatment with 100 µM SA, 250 µM ILA and a combination of both compounds. means ± SE; n = 9.* ***C:*** *O_2^- radicals in leaves stained by NBT staining in two-week-old NahG* sid2 *(n = 21) and wild-type (WT; n = 15) seedlings 48 h after treatment with 500 µM ILA. means ± SE; differences between treated or untreated plants were analysed by Welch two sample t-test. * = p < 0.05.* ***D:*** *O_2^- radicals detected in leaves of* ugt76b1*, wild type (WT) and UGT76B1 overexpressor (OE). means ± SE; n = 20-23.* ***A****,* ***B*** *and* ***D****: Significant differences (p.adj. < 0.05) are indicated by letters according to one-way ANOVA. The experiments were independently repeated three times with similar results.*

Furthermore, SA-depleted *ugt76b1* was tested for superoxide production. In the *ugt76b1* NahG *sid2* triple mutant superoxide was enhanced (Fig. 22A). Thus the application of ILA, but maybe also the internal content of ILA could influence superoxide production independent of SA. Since ROS induction is one of the earliest cellular responses following pathogen

recognition (Torres *et al.*, 2006), earlier time points after ILA application (3 h, 24 h, and 48 h) were examined. Enhancement of O_2^- radicals due to the application of ILA was a rapid and sustainable response (Fig. 22B). ILA induced O_2^- radicals already after 3 h, whereas SA was induced only after 48 h (Fig. 18A).

Superoxide radicals can be converted to H_2O_2, which is a signalling molecule *in planta* (Sabater & Martín, 2013). Thus, in a next step H_2O_2 content was investigated after ILA application. Interestingly, 3,3'-diaminobenzidine (DAB) staining of wild-type plants grown in the presence of 500 µM ILA did not reveal enhanced H_2O_2 content. In contrast, ILA tended to reduced the staining intensity in comparison to control plants (Fig. 22C).

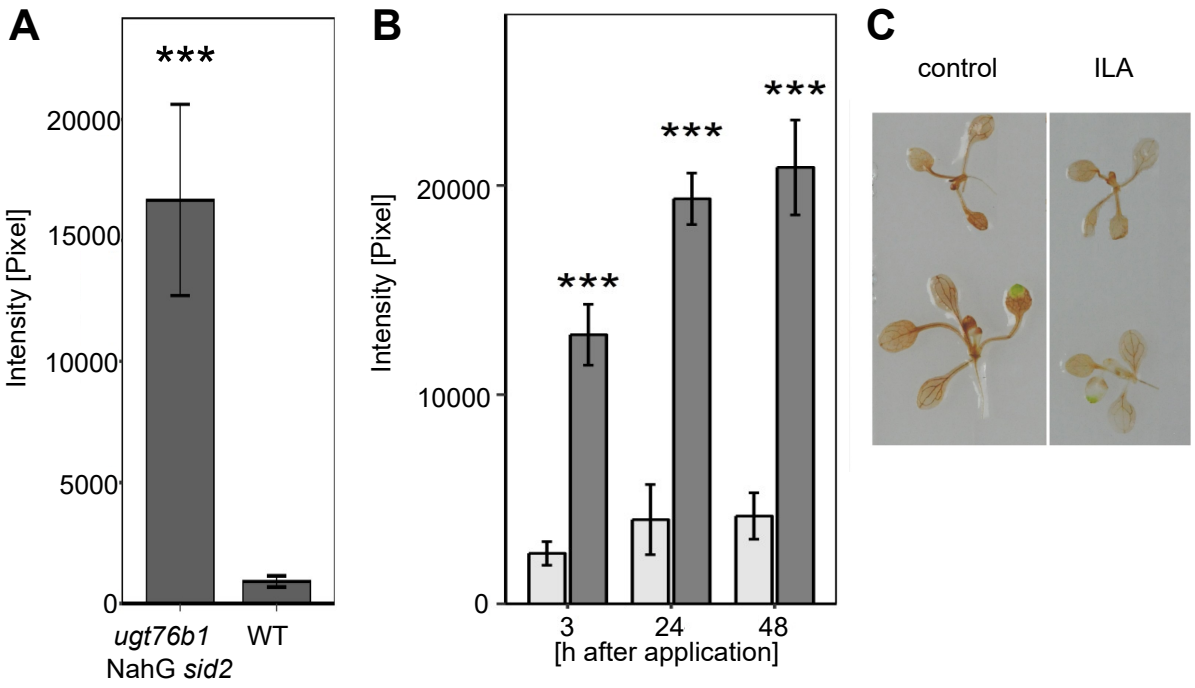

Fig. 22: Internal induction of O_2^- radicals in* ugt76b1 *was SA-independent and O_2^- radicals, but not H_2O_2 content, were induced rapidly after ILA application

A: *O_2^- radicals detected in leaves of two-week-old wild-type (WT) and* ugt76b1 *NahG* sid2 *seedlings by NBT staining. means ± SE; n = 9. Differences between wild type and SA-deficient* ugt76b1 *were analysed by Welch two sample t-test; *** = p < 0.001.* ***B:*** *Twelve-day-old plants were treated with 500 µM ILA (dark grey bars) and harvested at different time points after addition of ILA application. O_2^- radicals were detected by NBT staining and quantified. means ± SE; n = 12. Differences between treated or untreated plants were analysed by Welch two sample t-test; *** = p < 0.001.* ***C:*** *Hydrogen peroxide detection in ten-day-old wild-type plants grown on control or ILA (500 µM) plates. Plants were stained for 8 h with DAB.*

Since NBT may not be specific for the detection of superoxide anions, the superoxide scavenger 4-OH TEMPO, a superoxide scavenger, was employed (Yokawa *et al.*, 2011; Noctor *et al.*, 2016). Indeed, 4-OH TEMPO suppressed the NBT signal supporting the formation of superoxide (Fig. 23A). When DPI, an inhibitor of flavin-containing enzymes and general

NAPDH oxidase inhibitor was applied together with ILA, there was still a significant induction of NBT staining indicating the independence of ROS induction by ILA (Fig. 23A).

The NADPH D and F are key components and crucial for apoplastic ROS production in response to pathogens (Morales *et al.*, 2016). To address their involvement in ILA-induced superoxide formation, *RBOHD* and *RBOHF* transcripts and the ability of the double knockout mutant *rbohd rbohf* to produce O_2^- radicals were monitored after application of 500 µM ILA. ILA still was able to induce O_2^- radicals in the *rbohd rbohf* mutant, however to a lesser extent than in wild type (Fig. 23B). The expression of *RBOHD* was induced threefold, while *RBOHF* was only slightly up-regulated (Fig. 23C). Furthermore, the expression of *CRK7*, a known mediator of oxidative signalling induced by extracellular ROS (Idänheimo *et al.*, 2014), was induced (Fig. 23C). Thus, plasma membrane NADPH oxidases might participate in ILA-stimulated ROS production.

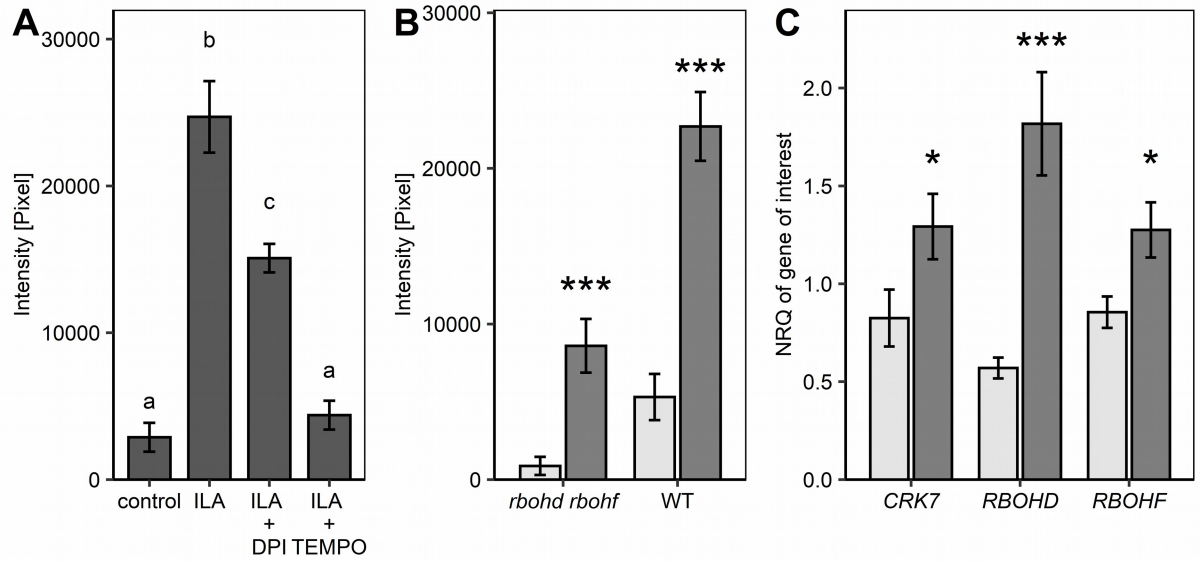

Fig. 23: NADPH oxidases contribute only partially to ILA-induced superoxide formation

A: *NBT staining was sensitive to superoxide scavenger 4-OH-TEMPO (TEMPO) and reduced by addition of DPI. Twelve-day-old seedlings were treated with 500 µM ILA, with ILA and 4-OH-TEMPO or with ILA and DPI for 3.5 h. NBT staining of the leaves was determined as a semi-quantitative measurement. means ± SE; n = 9. Significant differences (p.adj. < 0.05) are indicated by letters according to one-way ANOVA.* ***B:*** *O_2^- radical detected by NBT staining in 14-day-old wild-type and* rbohd rbohf *seedlings treated for 48 h either with control medium (light grey bars) or with medium containing 500 µM ILA (dark grey bars). means ± SE; n = 9.* ***C:*** *ROS-related genes (*CRK7, RBOHD *and* RBOHF*) were induced by exogenous ILA application in wild type. Gene expression was assessed by RT-qPCR and normalized to* S16 *and* UBQ5*. means ± SE; n = 4; differences between treated or untreated plants were analysed by Welch two sample t-test. *** = p < 0.001; * = p < 0.05.*

3.2.4. Root growth inhibition by ILA was independent of SA and ROS

In addition to the impact on pathogen defence, exogenously applied ILA represses root growth in a UGT76B1-dependent manner (Fig. 5). The SA-deficient NahG *sid2* was employed to explore whether the ILA-related root growth inhibition was dependent on SA as

observed in the ILA-enhanced pathogen response. In this experiment NahG *sid2* and wild type, as well as, *ugt76b1* NahG *sid2* and *ugt76b1* showed similar growth responses (Fig. 24A), indicating that root growth inhibition by ILA was independent of SA.

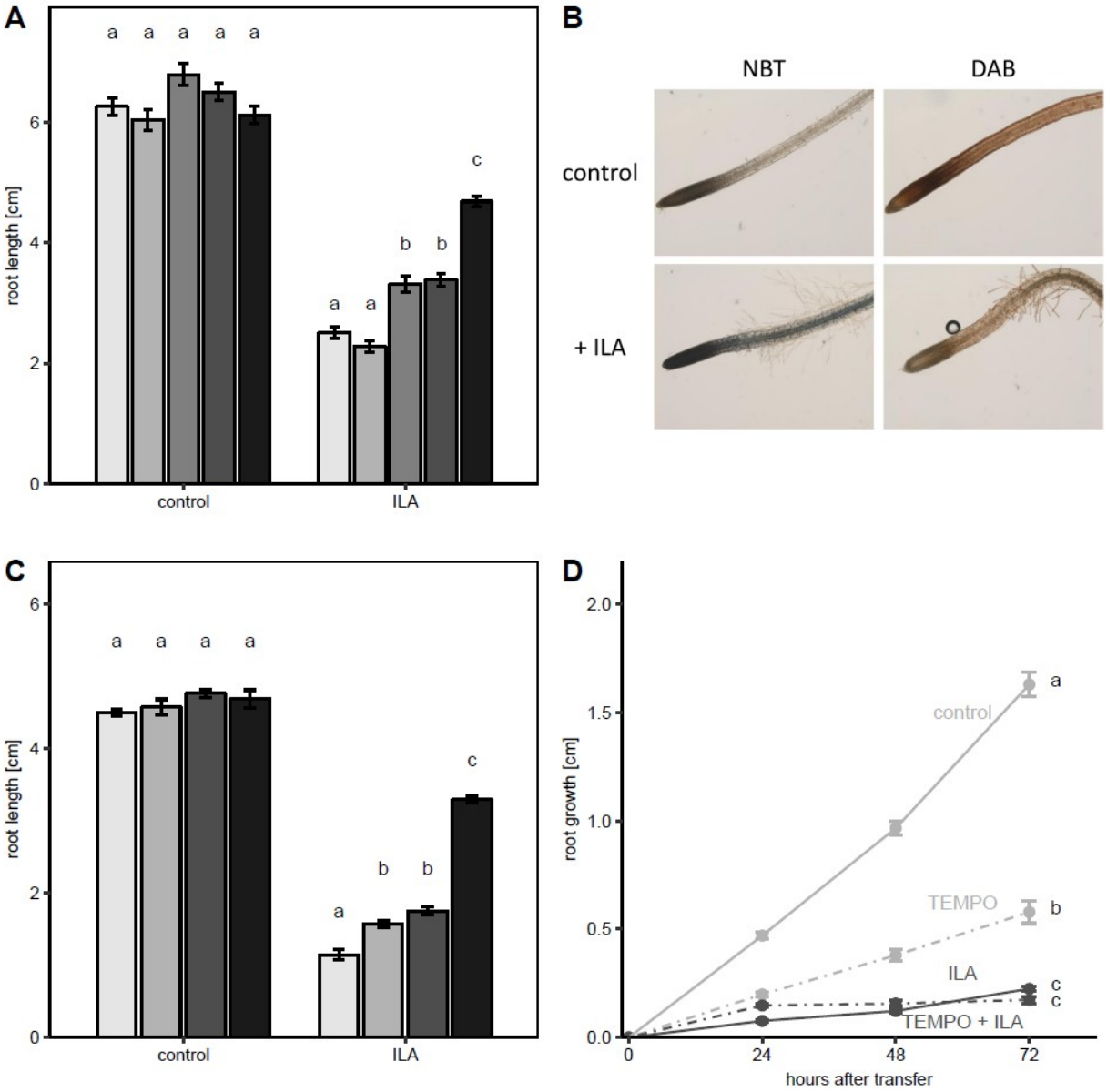

Fig. 24: SA- and superoxide-independent root growth inhibition by ILA

A: *Root growth inhibition on media without (control) or with 500 µM ILA for* ugt76b1, ugt76b1 *NahG* sid2, *wild type, NahG* sid2 *and UGT76B1 OE (from left to right) after ten days.* ***B:*** *NBT and DAB staining of primary root tips of wild-type plants after growth on control or 500 µM ILA plates after ten days.* ***C:*** *Root length of nine-day-old* ugt76b1, *wild-type,* rbohd rbohf *and UGT76B1 OE plants (from left to right) on media without (control) or with 500 µM ILA. Significant differences among the genotypes of each group in (A) and (C) (p.adj. < 0.05) are indicated by letters according to one-way ANOVA. means ± SE; n = 13-18.* ***D:*** *ILA-induced root growth inhibition in the presence of the* O_2^- *scavenger 4-OH-TEMPO (TEMPO 4mM). means ± SE; n = 10-32. Different letters indicate a significant difference according to a two-way ANOVA with treatment and time as discrete factors (p.adj. < 0.05; Methods). The experiment was independently repeated two times.*

It is well established that ROS are involved in regulation of root growth (Dunand *et al.*, 2007; Tsukagoshi, 2016). Therefore, the formation of O_2^- and H_2O_2 in roots in response to exogenous ILA was assessed. While DAB staining indicated H_2O_2 was lower after ILA treatment than in control roots, NBT visualized an ILA-dependent enhanced superoxide content in the elongation zone and in the meristem (Fig. 24B). When the *rbohd rbohf* mutant was challenged with 500 µM ILA, a wild-type-like repression of root growth was observed (Fig. 24C). In the presence of the superoxide scavenger 4-OH-TEMPO, ILA still triggered root growth inhibition (Fig. 24D). These results may indicate that increased superoxide anion contents were not involved in ILA-induced root growth inhibition.

As UGT76B1 is a mediator of SA and JA signalling (von Saint Paul *et al.*, 2011), two mutants involved in JA signalling and perception, *jar1* and *jin1*, were tested for their root growth phenotype on ILA plates. On ILA plates the *jar1* and *jin1* mutants showed similar root growth inhibition as wild-type plants and the *jar1 ugt76b1* and *jin1 ugt76b1* double mutants were comparable to the *ugt76b1* single mutant. Neither the mutation of *jar1* (Fig. 25A) nor of *jin1* (Fig. 25B) had influence on the UGT76B1-dependent root growth pattern on ILA. Similarly, mutants affecting abscisic acid biosynthesis and perception or ethylene signalling did not abolish the root growth inhibition caused by the application of ILA (Fig. 25C).

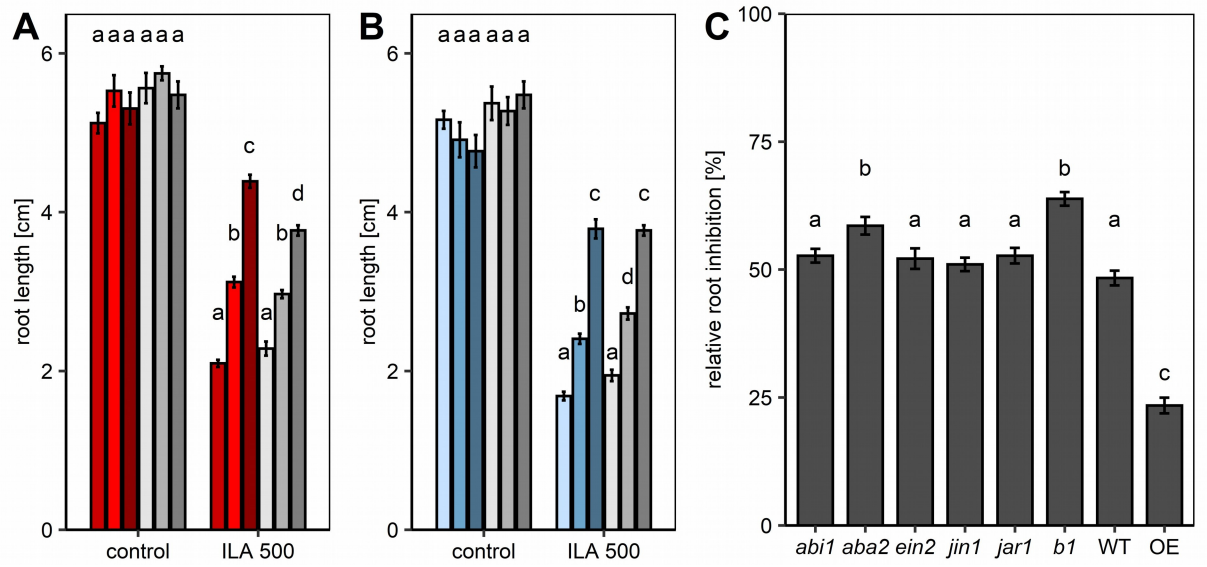

Fig. 25: Root growth inhibition by ILA was independent of different hormone pathways

Ten-day-old A. thaliana *seedlings were grown on control or ILA 500 µM plates. JA signalling mutants in combination with* ugt76b1 *or OE with* ***A:*** jar1 ugt76b1*,* jar1*,* jar *OE (n = 13-15) or* ***B:*** jin1 ugt76b1*,* jin1*,* jin1 *OE (n = 4-15) were tested for root growth inhibition on ILA plates.* ***C:*** *Root growth inhibition by ILA of different hormone-related mutants. Root growth inhibition after growth for ten days on 500 µM ILA-containing medium is shown relative to root growth on control medium of the respective line. Plant lines related to abscisic acid biosynthesis and perception:* aba2*,* abi1*; to ethylene signalling:* ein2*; and to JA signalling and perception:* jin1*,* jar1 *were used. Control and reference lines:* ugt76b1*, wild type (WT) and UGT76B1 overexpressor (OE). n = 11-24. Significant differences among the genotypes for each treatment (p.adj. < 0.05) are indicated by letters according to one-way ANOVA. means ± SE.*

In addition to root growth inhibition, roots of ILA-treated plants looked more hairy compared to the roots grown on control plates (Fig. 24B). Therefore, roots of plants grown on ILA plates were investigated more further. From the root tip to the origin of the first root hairs the distance was reduced and the length of root hairs was induced by ILA application (Fig. 26).

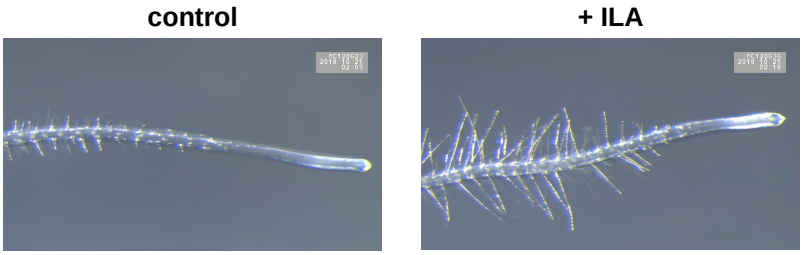

Fig. 26: ILA led to shorter root tips and longer root hairs

Ten-day-old plants grown on control or ILA (500 µM) plates were investigated. At this time-point ILA clearly led to root growth inhibition, but in addition also to a shorter distance of root tip to the first visible root hair and enhanced root hair length. n = 10. Experiment was repeated 3 times.

3.2.5. Although structurally related to ILA, leucic acid and isoleucine induce different effects in *A. thaliana*

To test whether compounds structurally related to ILA could provoke similar effects, two closely related compounds, leucic acid (LA) and isoleucine (Ile) were examined. Both compounds occur naturally in *A. thaliana* and other plant species (Maksym *et al.*, 2018). *A. thaliana* wild-type seedlings were treated with LA or Ile alone and in combination with SA. *PR1* expression was not significantly affected by 500 µM of Ile or LA (Fig. 27A). Furthermore, no differences in *PR1* expression between SA only, Ile and SA or LA and SA combination treatments were found (Fig. 27A). Similarly, O_2^- was not up-regulated by the application of LA or Ile (Fig. 27B). In contrast, all compounds reduced root growth with Ile being the least effective and LA having the strongest impact. Interestingly, Ile-related growth repression was independent from the UGT76B1 expression level, while both ILA and LA showed a UGT76B1-dependent pattern. Wild type or constitutive *UGT76B1* expression mitigated the root growth inhibition (Fig. 27C), which may be attributed to the ability of UGT76B1 shown *in vitro* to glucosylate ILA as well as LA (Maksym *et al.*, 2018).

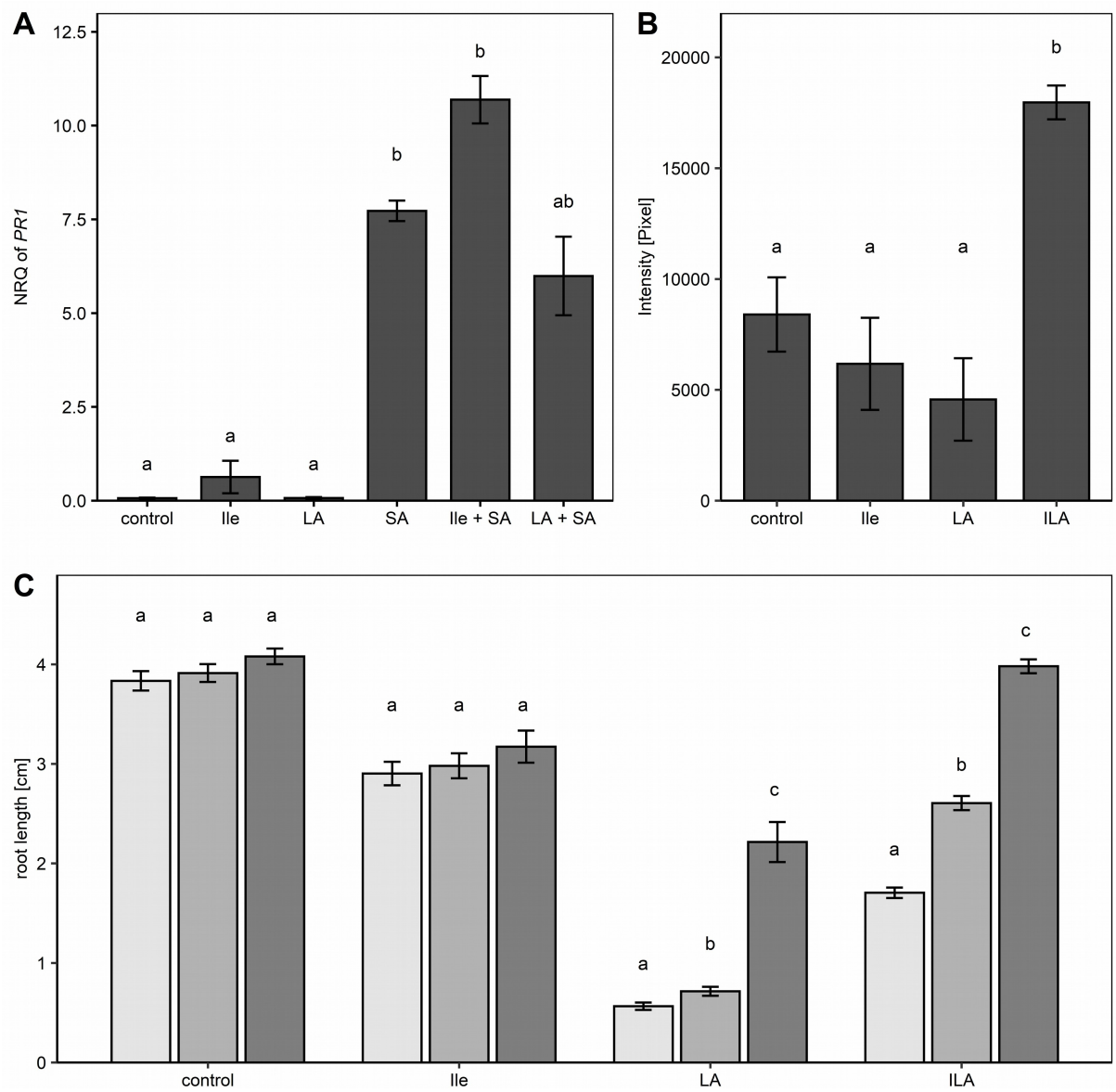

Fig. 27: Investigating the effect of ILA and its two closely related compounds Ile and LA on SA signalling, ROS induction and root growth inhibition

A: PR1 *expression in 14-day-old seedlings in response to 500 µM Ile or 500 µM LA or 100 µM SA, 250 µM Ile and 100 µM SA, 250 µM LA and 100 µM SA after 48 h of treatment.* PR1 *expression was determined by RT-qPCR and normalized to* S16 *and* UBQ5. *means ± SE; n = 3 - 4.* ***B:*** *Superoxide radical induction assessed by NBT staining 48 h after application of 500 µM Ile, LA or ILA to two-week-old seedlings. means ± SE; n = 12.* ***C:*** *Root growth inhibition on ILA-, Ile- and LA-containing media (250 µM each). Root lengths were recorded after nine days. Root length of* ugt76b1 *(light grey), wild type (grey) and UGT76B1 overexpressor (dark grey) were compared within the treatments. means ± SE; n = 19-23. Significant differences (p.adj. < 0.05) are indicated by letters according to one-way ANOVA. Experiments were independently repeated two times with similar results.*

3.2.6. ILA responses are conserved in *Brassica napus*

To assess whether ILA functions in a similar manner in *B. napus* as in *A. thaliana*, *B. napus* seedlings were tested for ILA-induced *PR* gene expression, superoxide induction, and root growth inhibition. *BnPR1* was induced in leaves when seedlings were grown on 500 µM ILA-containing plates (Fig. 28A). In roots of these plants, O_2^- radicals were strongly enhanced in comparison to control plants (Fig. 28B). ILA was also effective in reducing root growth in *B. napus* (Fig. 28C). Thus, ILA-induced responses were similar in *B. napus* and *A. thaliana.*

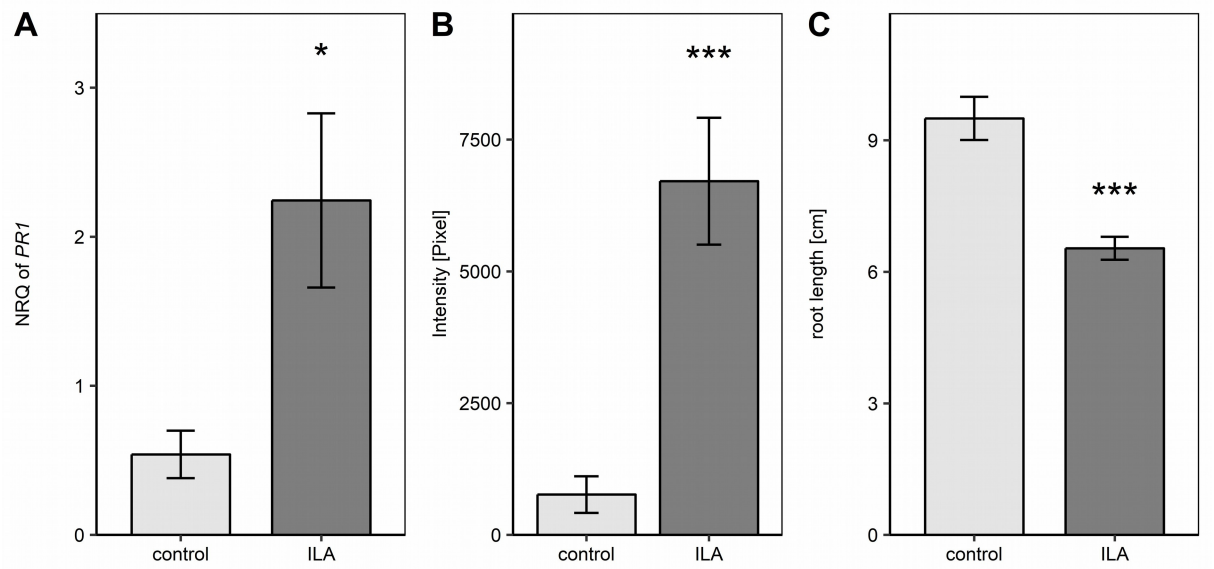

***Fig. 28: ILA induced* PR1 *expression and superoxide radicals and led to root growth inhibition in* B. napus**

Seedlings were grown for nine days on either control medium (light grey bars) or medium containing 500 µM ILA (dark grey bars). ***A:*** BnPR1 *expression level in* B. napus *leaves was assessed by RT-qPCR and normalized to* BnUP1 *and* BnUBQ9*. means ± SE, n = 3.* ***B:*** *NBT staining of* B. napus *roots. means ± SE, n = 15.* ***C:*** *Root length of* B. napus *plants. means ± SE, n = 10-11. Welch two sample t-test was performed to test differences between untreated and treated plants; *** = p < 0.001; * = p < 0.05.*

3.3 UGT76B1 influences pipecolic acid content by glucosylation

Pipecolic acid (Pip), a small molecule derived from lysine, plays an important role in plant defence. The production of Pip is induced after pathogen infection in local and distal leaves. In contrast, Pip was hardly detectable in non-inoculated plants (Návarová *et al.*, 2012). It is speculated that N-hydroxy pipecolic acid (N-OH-Pip), which is formed from Pip by FMO1, is most probably the active compound inducing SAR (Chen *et al.*, 2018; Hartmann *et al.*, 2018). In addition a glucosylated N-OH-Pip, N-OGLC-Pip, was also found in infected plant extracts (Chen *et al.*, 2018). To show that SA and Pip and their corresponding derivatives are up-regulated by *Pst* infection in parallel, three-week-old wild-type *A. thaliana* plants were sprayed with bacterial or control solution. Rosettes were harvested 48 h post infection and the con-

tents of SA, SAG, SGE, Pip, N-OH-Pip, and N-OGLC-Pip were measured by LC-MS. SA, SAG, SGE, Pip, and N-OGLC-Pip were all induced after infection (Fig. 29). In contrast to the other compounds, N-OH-Pip was detectable only after infection (Chen *et al.*, 2018). For the mass 308.1346 (N-OGLC-Pip) different peaks were found, but only one was induced by *Pst* treatment. MS/MS fragmentation confirmed this peak as a hexose form of N-OH-Pip and this peak had same fragmentation pattern as the N-OGLC-Pip peak identified and measured by Chen *et al.* (2018). Thus, only this peak, induced by *Pst*, was defined as N-OGLC-Pip and evaluated.

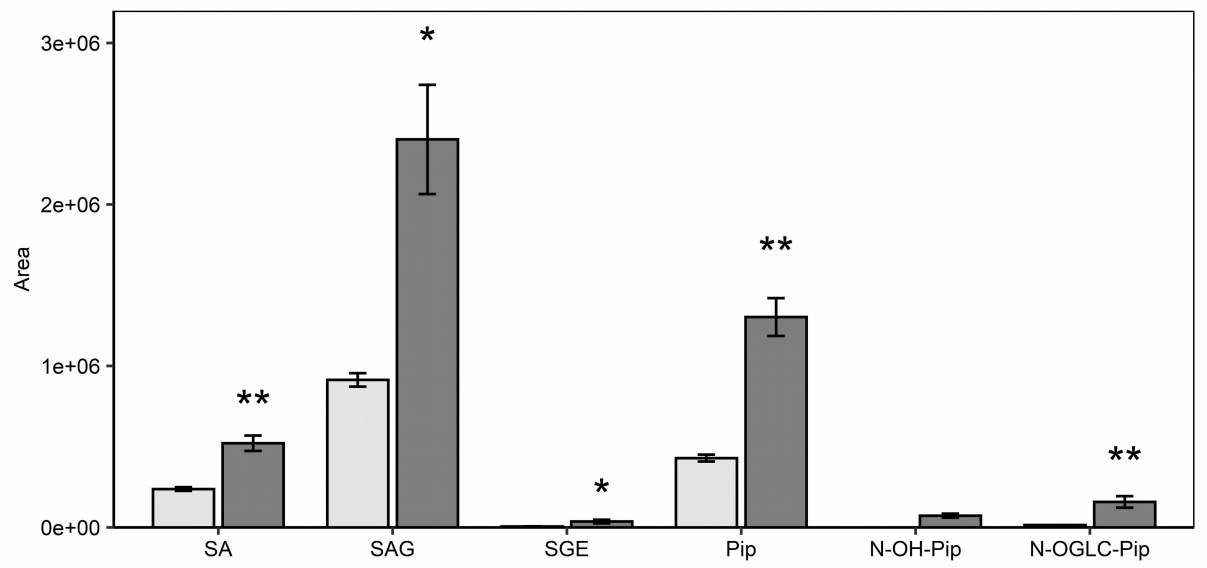

Fig. 29: SA and Pip derivatives were induced by infection

Three-week-old plants were sprayed with a control solution or Pst *(5 x 10^8 cfu). Whole rosettes leaves were harvested after 48 h and four biological replicates, pooled from 25 plants each, were measured by LC-MS. SA, SAG, and SGE and Pip, N-OH-Pip, and N-OGLC-Pip content were analysed. Bars represent the average of four replicates. means ± SE; Welch two sample t-test was performed to test differences between untreated and* Pst *treated plants; ** = p < 0.01; * = p < 0.05.*

3.3.1. In the *ugt76b1* knockout, systemic acquired resistance and pipecolic acid biosynthesis related genes are enhanced

In our lab it was shown that early senescence in *ugt76b1* was dependent on *NPR1*, *EDS1*, and *FMO1* and *FMO1* expression is highly induced in *ugt76b1* background (Zhang, unpublished). In addition, *UGT76B1* was highly induced after Pip treatment and during SAR (Hartmann *et al.*, 2018). In the GO enrichment analysis of genes up-regulated in *ugt76b1* background, the GO term for SAR (GO:0009627) was significantly overrepresented (Tab. 4). All three known biosynthetic genes for Pip and N-OH-Pip, *ALD1*, *SARD4*, and *FMO1*, were enhanced in *ugt76b1* (Tab. 7). Additionally, *EDS5*, proposed as transporter of Pip, was also induced. Due to these findings, the question about a connection between Pip/FMO1 and UGT76B1 arose.

***Tab. 7: Expression of SAR related genes in* ugt76b1**
Gene expression from the RNAseq approach regarding SAR biosynthetic genes. Values are shown for ugt76b1 *and wild type treated with BTH as log2 fold changes with according adjusted p-values.*

ATG	annotation	*ugt76b1*
AT1G19250	*FMO1*	5.20
AT2G13810	*ALD1*	4.64
AT5G52810	*SARD4*	2.94
AT4G39030	*EDS5*	2.66

3.3.2. Pip was regulated in a UGT76B1-dependent manner

Since biosynthetic genes of Pip and N-OH-Pip were up-regulated in *ugt76b1*, it was investigated whether the expression of *UGT76B1* would influence the level of Pip and the other Pip derivates. Pip, N-OH-Pip, and N-OGLC-Pip derivatives were analysed in *ugt76b1* knockout, wild type, and a UGT76B1 OE by LC-MS under control conditions. Pip was detected in the *ugt76b1* line but hardly detectable in wild type and OE Pip (Fig. 30A and 31A). N-OH-Pip was only detectable in *ugt76b1*, whereas N-OGLC-Pip was present in wild type and OE lines (Fig. 31B and C). To further confirm the identity and the enhancement of the N-OH-Pip peak in *ugt76b1*, the elution of the N-OH-Pip standard compared to *ugt76b1* plant extract and spiking of N-OH-Pip to *ugt76b1* plant extract were performed (Fig. 30E). N-OH-Pip identified from *ugt76b1* plant extract was confirmed as it eluted at the same time point as the of N-OH-Pip standard.

The content of Pip and its Pip derivates were also measured after stress induced conditions (BTH treatment). Pip was enhanced in all three genotypes after BTH treatment. Still the *ugt76b1* knockout exhibited highest amounts of Pip levels compared to the wild type and OE (Fig. 30B and 31A). BTH treatment led to a further accumulation of N-OH-Pip in the *ugt76b1* knockout mutant, whereas N-OGLC-Pip was still not detectable (Fig. 30C and 31B). In wild type and OE N-OH-Pip was detectable after the treatment, but in lower amounts than in *ugt76b1* untreated (Fig. 29, Fig. 31). N-OGLC-Pip was enhanced in wild type and OE (Fig. 30D and 31C).

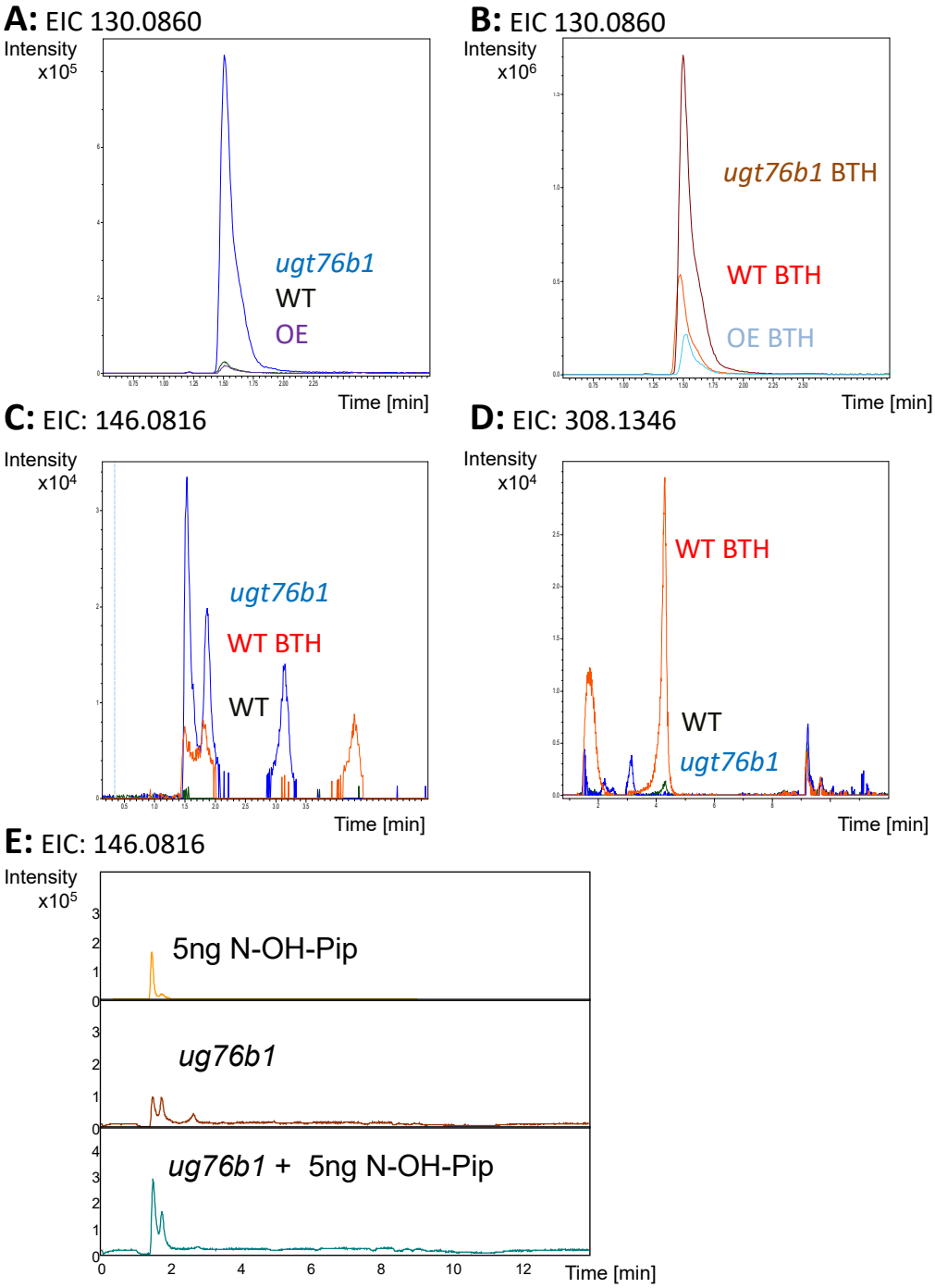

Fig. 30: LC-MS profiles of Pip and Pip derivatives and spiking of plant extract with N-OH-Pip

A-D: *Three-week-old plants were sprayed with control solution or BTH. Whole rosettes leaves were harvested after 48 h and four biological replicates, pooled from 25 plants each, were measured by LC-MS.* ***A:*** *LC-MS chromatograms of Pip of* ugt76b1*, WT and OE.* ***B:*** *Chromatograms of Pip after BTH treatment.* ***C:*** *N-OH-Pip chromatograms of WT with and without BTH treatment compared to* ugt76b1*.* ***D:*** *N-OGLC-Pip.* ***E:*** *Comparison of the elution profile of N-OH-Pip standard and plant extract of* ugt76b1*. In addition, spiking of* ugt76b1 *plant extract with N-OH-Pip standard further confirmed the N-OH-Pip identification next to MS/MS profile compared to Chen* et al. *(2018).*

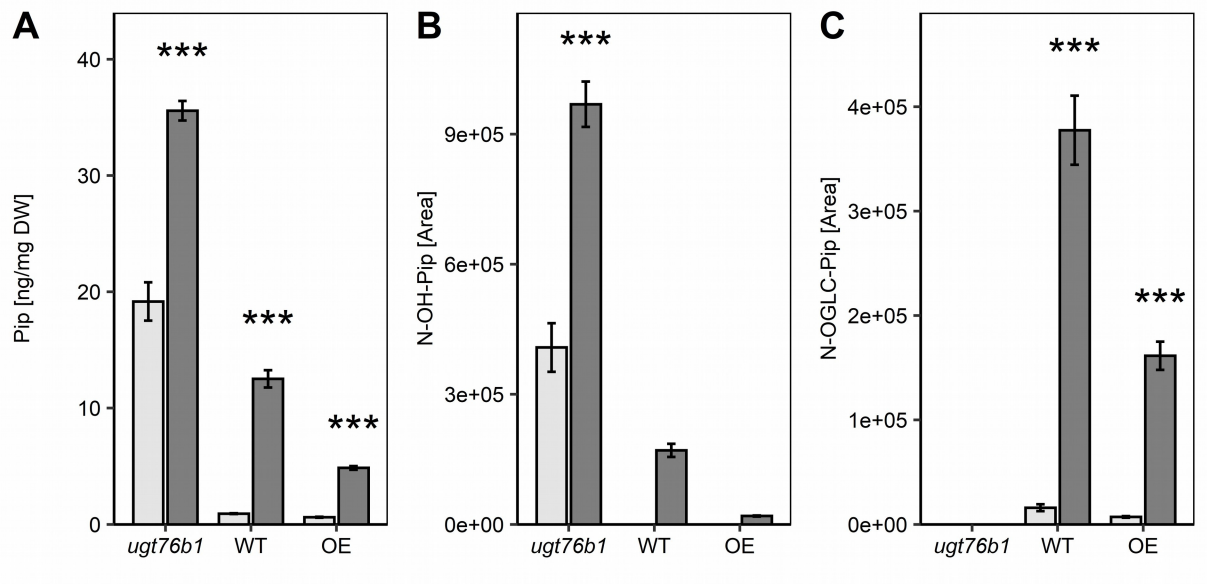

Fig. 31: Pip and Pip derivatives were dependent on* UGT76B1 *expression

Quantified levels of Pip, N-OH-Pip, and N-OGLC-Pip content of ugt76b1*, wild type and OE. Chromatograms are partially shown in Fig. 30. Bars represent the average of four replicates. means ± SE; Welch two sample t-test was performed to test differences between untreated and BTH treated plants; *** = p < 0.001.*

3.3.3. Watering of Pip still showed no induction of N-OGLC-Pip in *ugt76b1*

As mentioned before, *UGT76B1* transcripts were strongly enhanced upon exogenous Pip application along with transcripts of SA- and SAR-related genes (Hartmann & Zeier, 2018). To address the role of UGT76B1-dependent glucosylation, plants exhibiting different *UGT76B1* expression levels were either treated with water or Pip. Additionally NahG *sid2* and *ugt76b1 ugt74f1 ugt74f2* were included. In the control samples, Pip was only detected in the *ugt76b1* single and combined *ugt* triple mutant, confirming previous results of induced Pip levels in *ugt76b1* (Fig. 31 and 32). N-OH-Pip was hardly detectable in wild type, but significantly enhanced in *ugt76b1* background. The hexose form of N-OH-Pip was not detected in mutants with *ugt76b1* mutation, but in all other lines (Fig. 32).

After the application of Pip, all lines showed high enhancement of Pip content compared to untreated conditions (Fig. 32). However, in the SA-deficient mutant, Pip was notably decreased. N-OH-Pip was hardly detectable in wild type, but significantly enhanced in the *ugt76b1* background. With the application of Pip, the level of N-OH-Pip was still enhanced in the *ugt76b1* mutant compared to the wild type (~8.5 times), while the OE exhibited lowest contents. Strikingly, even with exogenous addition of Pip neither in *ugt76b1* single mutant nor in the *ugt* triple mutant was N-OGLC-Pip detectable, but present in the other lines including wild type. Furthermore, for all treatments the addition of *ugt74f1 ugt74f2* to *ugt76b1*, did not further influence Pip, N-OH-Pip, or N-OGLC-Pip levels.

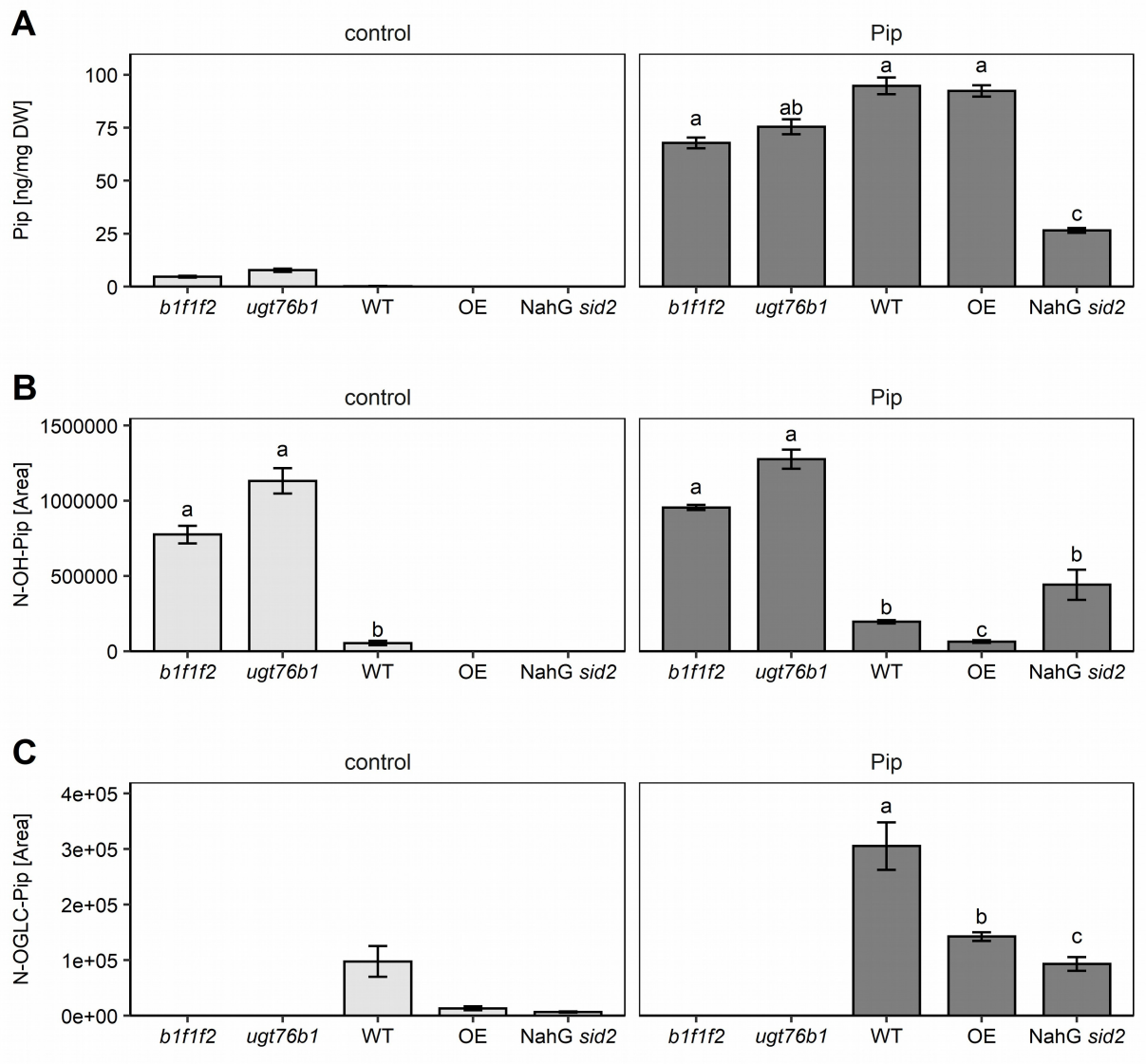

***Fig. 32: Watering of Pip did not lead to N-OGLC-Pip production in* ugt76b1**

Five-week-old plants were watered with control solution or 1 mM DL-Pip. Whole rosettes leaves were harvested after 48 h and four biological replicates, pooled from 25 plants each, were measured by LC-MS. Pip, N-OH-Pip, and N-OGLC-Pip content of ugt76b1 ugt74f1 ugt74f2 *(*b1f1f2*),* ugt76b1*, wild type, OE and NahG* sid2 *were analysed. Bars represent the average of four replicates. No bar was plotted, when the signal was under the detection limit. Significant differences between lines in the control or Pip-watered treatment (p.adj. values) are indicated by letters according to one-way ANOVA.*

3.3.4. N-OH-Pip fits in the active site of the UGT76B1 binding pocket and UGT76B1 converts N-OH-Pip *in vitro*

In the *ugt76b1* mutant neither BTH treatment (Fig. 31) nor Pip watering (Fig. 32) induced the formation of N-OGLC-Pip. As a result, a direct influence of UGT76B1 on N-OGLC-Pip was taken in consideration. To test this hypothesis analysis of the binding pocket of UGT76B1 was performed. This was modelled by R. Janowski in collaboration with our research group. It was shown that there was enough space in the UGT76B1 active site to accommodate N-

OH-Pip. Several different orientations of N-OH-Pip would be conceivable (Fig. 33A). To confirm the model, N-OH-Pip was synthesized from piperidine (Hartmann & Zeier, 2018) and an *in vitro* test was performed. UGT76B1 was able to catalyse the production of N-OGLC-Pip from N-OH-Pip (Fig. 33B). These *in vitro* results were compared to previous *in vivo* chromatograms. MS/MS of the mass 308.1346 (N-OGLC-Pip) revealed same fragmentation peaks as found before and by Chen *et al.* (2018) (Fig. 33C).

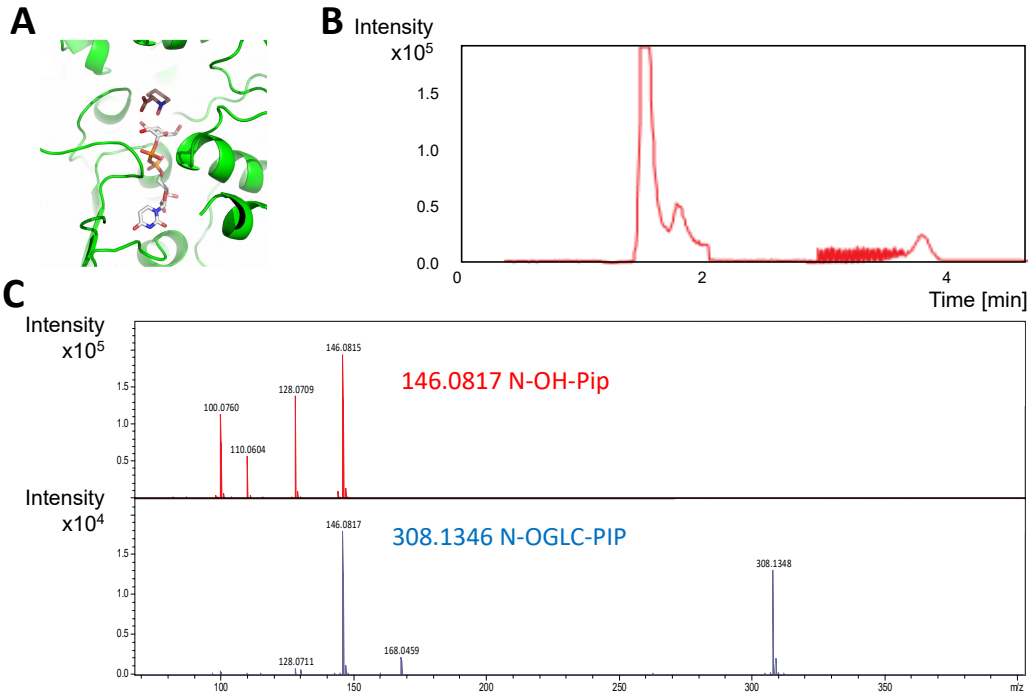

Fig. 33: N-OH-Pip as substrate of UGT76B1

A: *Modelling of N-OH-Pip into the binding pocket of UGT76B1. One possible scenario representing most probable orientation of the N-OH-Pip with its N-OH hydroxyl group oriented to the UDP-glucose moiety (by R. Janowski).* ***B:*** *Enzyme assay of UGT76B1 showing N-OH-Pip is converted to N-OGLC-Pip (conducted by B. Lange).* ***C:*** *MS/MS of N-OH-Pip (m/z: 146.0817) and N-OGLC-Pip (m/z: 308.1346).*

3.3.5. Influence of ILA on Pip content

In addition to SA and ILA, UGT76B1 was shown to glucosylate N-OH-Pip. ILA was able to enhance internal SA levels (Fig. 19) and consequently the influence of ILA on Pip levels was investigated. If the exogenous application of ILA would block UGT76B1 activity, Pip and N- OH-Pip levels could be enhanced by the reduction of N-OH-Pip glucosylation. ILA application led to an induction of SA (Fig. 18) and in parallel to an induction of Pip after 48 hours (Fig. 34A). Furthermore, N-OH-Pip was only detectable after ILA application (Fig. 34B). In contrast to those, N-OGLC-Pip showed a trend, but no significant change after ILA treatment (Fig. 34C). It has to be mentioned, that this effect could also originate from the high variation of the biological samples. Furthermore, expression of the biosynthetic gene of N-OH-Pip,

FMO1, was induced by ILA (Fig. 34D). Thus, the boost of N-OH-Pip by ILA could firstly be due to a weakened glucosylation and secondly to the enhanced biosynthesis of N- OH-Pip.

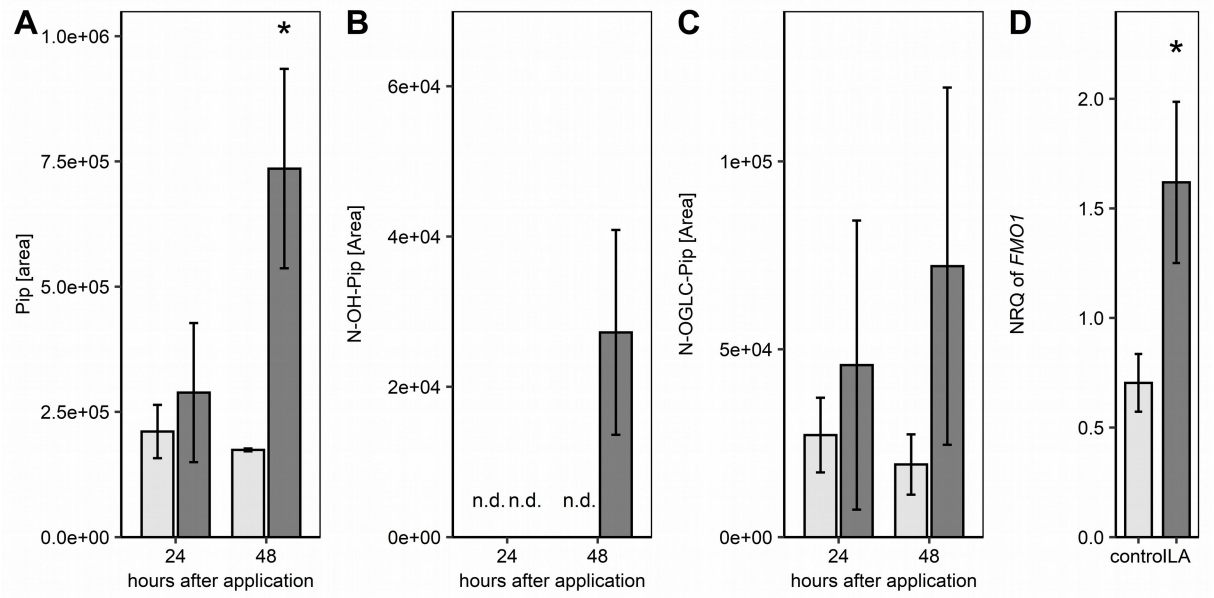

Fig. 34: Effect of ILA on endogenous levels of Pip, Pip derivatives and* FMO1 *expression

A: *Pip levels in leaves of 14-day-old wild-type seedlings 24 h and 48 h after incubation in medium containing 500 µM ILA (dark grey bars) or in control medium (light grey bars). means ± SE; n = 3-4. Same material was used as for SA measurement (Fig. 18).* ***B:*** *N-OH-Pip levels.* ***C:*** *N-OGLC-Pip levels.* ***D:*** *Transcript abundance of* FMO1 was *measured by RT-qPCR 48 h after application of 500 µM ILA. Gene expression was normalized to* S16 *and* UBQ5*; means ± SE; n = 4. Differences between treated or untreated plants were analysed by Welch two sample t-test; * = p < 0.05.*

3.3.6. FMO1 acts up-stream of UGT76B1

It is known that FMO1 can synthesize N-OH-Pip from Pip and *fmo1* knockout mutants lack N-OH-Pip and N-OGLC-Pip (Chen *et al.*, 2018; Hartmann *et al.*, 2018). If UGT76B1 converts N-OH-Pip to N-OGLC-Pip downstream of FMO1, N-OH-Pip should accumulate and N-OGLC-Pip should not be present in *ugt76b1.* Therefore, in the *ugt76b1 fmo1* and the *fmo1* single mutant, neither N-OGLC-Pip nor N-OH-Pip would be expected. Pip and Pip-derivatives were measured in wild type, *fmo1*, *ugt76b1*, and *fmo1 ugt76b1* after BTH treatment. In the *fmo1* mutant no N-OH-Pip or N-OGLC-Pip was found as expected, whereas in *ugt76b1*, N-OH-Pip was enriched and N-OGLC-Pip was not detectable (Fig. 35). In the *fmo1 ugt76b1* double mutant, no N-OH-Pip or N-OGLC-Pip was found, exhibiting same Pip and Pip derivatives pattern as the *fmo1* single mutant (Fig. 35). Thus, in *fmo1 ugt76b1* double mutant enhanced Pip and N-OH-Pip levels as found in *ugt76b1* single mutant were abolished.

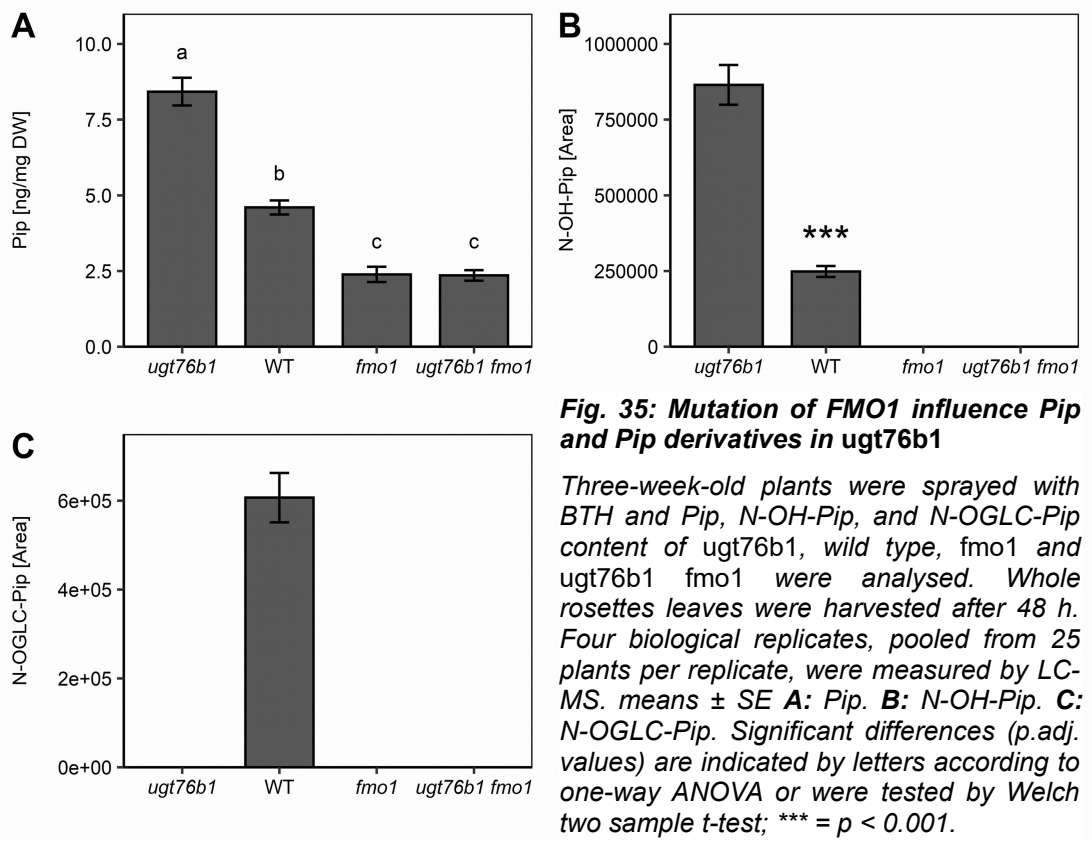

***Fig. 35: Mutation of FMO1 influence Pip and Pip derivatives in* ugt76b1**

Three-week-old plants were sprayed with BTH and Pip, N-OH-Pip, and N-OGLC-Pip content of ugt76b1*, wild type,* fmo1 *and* ugt76b1 fmo1 *were analysed. Whole rosettes leaves were harvested after 48 h. Four biological replicates, pooled from 25 plants per replicate, were measured by LC-MS. means ± SE* ***A:*** *Pip.* ***B:*** *N-OH-Pip.* ***C:*** *N-OGLC-Pip. Significant differences (p.adj. values) are indicated by letters according to one-way ANOVA or were tested by Welch two sample t-test; *** = p < 0.001.*

3.3.7. Root growth inhibition and ROS induction induced by ILA were Pip-independent

The exogenously application of Pip was shown to inhibit root growth (Wang *et al.*, 2018a). Since ILA enhanced Pip and N-OH-Pip levels *in planta* (Fig. 34), root growth inhibition by ILA could be influenced by N-OH-Pip levels in roots. If ILA-induced enhancement of N-OH-Pip levels would led to enhanced root growth inhibition, *fmo1* plants, lacking N-OH-Pip, should exhibit enhanced root growth on ILA plates similar to the OE. However, *fmo1* plants grown on ILA-containing plates revealed even higher sensitivity towards ILA as wild type (Fig. 36A). As the absence of N-OH-Pip did not attenuate the root growth inhibition by ILA, an FMO1- and thereby N-OH-Pip-independent mechanism would be conceivable.

Furthermore, it was tested, if the SA-independent superoxide radical production by ILA is dependent on Pip. Therefore, the *ald1* mutant was treated with ILA superoxide radical formation was monitored. The intensity of NBT staining of the Pip-depleted *ald1* mutant was still enhanced compared to untreated *ald1* mutant plants. Thus, it seems that this induction is independent of Pip (Fig. 36B). Taken all these results together it was shown that ILA induced superoxide anion formation seemed to be independent of Pip.

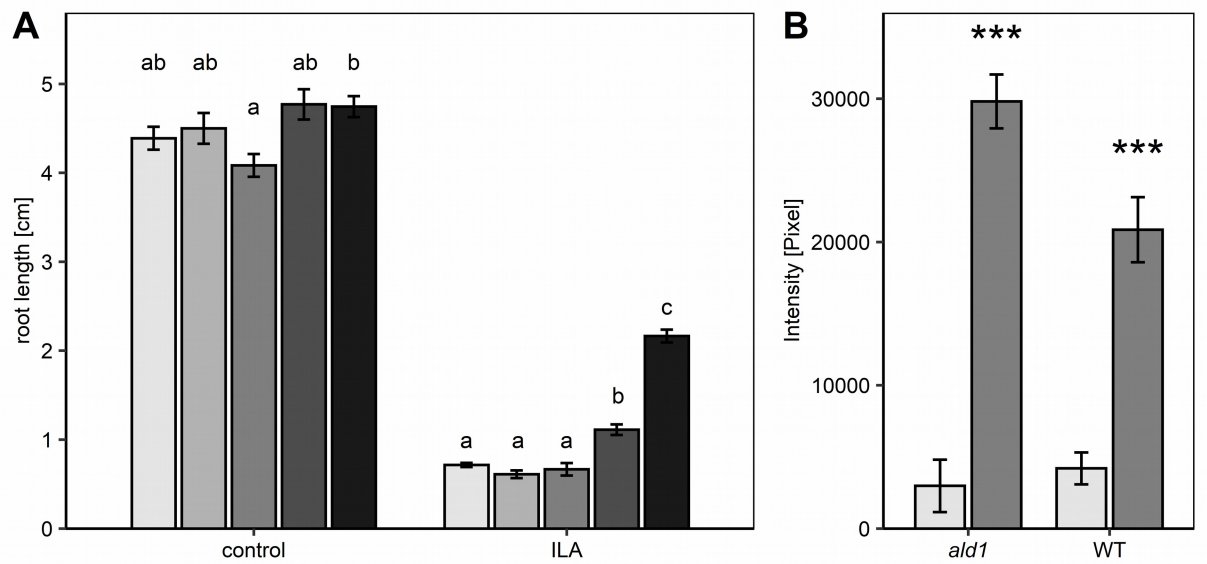

Fig. 36: Root growth inhibition and superoxide radical production by ILA were not dependent on Pip

A: *Root growth on media without (control) or with 500 µM ILA for* ugt76b1*,* ugt76b1 fmo1*,* fmo1*, wild type,* fmo1 *UGT76B1 OE (from left to right, light grey to black bar) after ten days. means ± SE. n = 7 - 10. Significant differences among the genotypes for each treatment (p.adj. < 0.05) are indicated by letters according to one-way ANOVA.* ***B:*** *O_2^- radical detected by NBT staining in leaves of two-week-old seedlings. 12-day-old* ald1 *or wild-type seedlings were treated with 500 µM ILA and stained with NBT after 48 h. Staining of leaves was quantified; means ± SE; n = 12. differences between treated or untreated plants were analysed by Welch two sample t-test. *** = p < 0.001.*

3.4 SA and Pip derivates were not compensated by UGT74F1 introgression in *ugt76b1*

As shown before introgression of UGT74F1 in the *ugt76b1* background, UGT74F1 could not rescue the phenotypes of *ugt76b1*, whereas the complementation with UGT76B1 led to the mutant reverting to wild type (Fig. 15). Since N-OH-Pip was found as another substrate of UGT76B1, Pip and Pip derivates were measured in these lines (names of the lines are explained in 3.1.11) together with SA and SA derivates (Fig. 37). It has to be mentioned that levels of free SA and Pip were two to three times lower, compared to former experiments. Nevertheless, in hybrid F1 lines, SA and Pip showed a tendency of enhanced levels (Fig. 37A and D) and were more similar to *ugt76b1* than to wild type. For SAG/SGE and N-OH-Pip/N-OGLC-Pip the situation was even more clear. Most interestingly, SAG, SGE, and N-OH-Pip levels were highly induced in hybrid F1 lines, but like wild type in comp. B1 lines (Fig. 37B, C and E). N-OGLC-Pip was not detectable in *ugt76b1* or hybrid F1 1 line, and only in two samples of hybrid F1 2 very low levels were measured (Fig. 37F). To sum up, Pip and SA levels of hybrid F1 lines were more similar to *ugt76b1*, whereas of comp. B1 lines the levels were more similar to wild type.

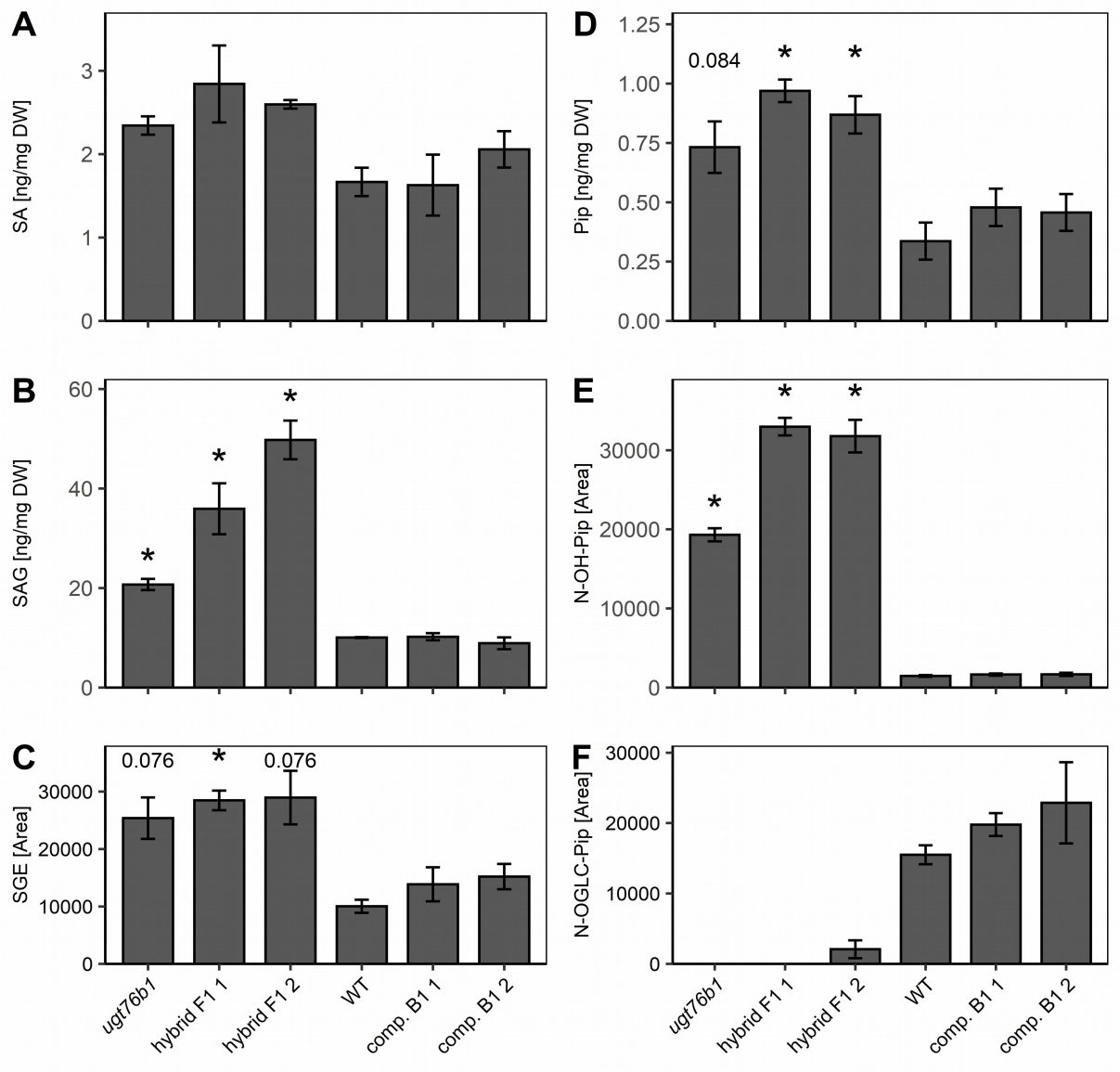

Fig. 37: SA and Pip derivates of* ugt76b1 *were not changed by introgression of UGT74F1

Four-week old plants of ugt76b1, ugt76b1 *complemented with CDS of* UGT74F1 (*hybrid F1 1; hybrid F1 2), WT and* ugt76b1 *complemented with CDS of* UGT76B1 (*comp. B1 1; comp. B1 2) were compared for SA (**A**), SAG (**B**), SGE (**C**), Pip (**D**), N-OH-Pip (**E**) and N-OGLC-Pip (**F**) levels against wild type. Bars represent the average of four replicates. means ± SE. Authentic standards were used to quantify SA, SAG and Pip while SGE, N-OH-Pip and N-OGLC-Pip were relatively quantified according to the m/z peak of LC-MS measurement. Significant differences between mutants and WT (p.adj. values) were analysed by one-way ANOVA. * = p < 0.05. For N-OGLC-Pip in hybrid F1 2 line only two samples showed very low levels, whereas the other two were not applicable and set to a value of zero.*

3.5 The *UGT76B1* expression in root influenced *PR* gene expression in shoot

Physiological processes in the whole plant need to be controlled and coordinated by the integration of signals of different tissues (Notaguchi & Okamoto, 2015; Lacombe & Achard, 2016). Signals originated in roots can influence processes in leaves and *vice versa* (Dodd, 2005; Schachtman & Goodger, 2008). Although *UGT76B1* is highly expressed in the root endodermal cells and to lesser extent in older leaves, regulation of defence marker genes and pathogen resistance was tested in leaves (von Saint Paul *et al.*, 2011). Therefore, this means that the high expression of *UGT76B1* in roots could lead to a signal influencing shoot reaction. To test if the knockout mutation of *ugt76b1* in root can influence expression of defence marker genes in leaves of wild type, chimeric plants had to been produced. Hetero-grafts composed of *ugt76b1* scion and wild-type rootstock as well as the opposite combination was applied. In addition, homo-grafts of *ugt76b1* and wild type were fused together.

Previous experiment of Maksym (2018) pointed out that wild-type roots lead to down-regulation of *PR1*, *PR2*, and *PR5* in shoot of *ugt76b1*. In addition *ugt76b1 s*howed slight up-regulation of *PR* genes in wild-type rosettes. The grafting procedure, cutting of very young plants and wounding-induced formation of adventitious roots, has low efficiency. Due to small amount of plants and in order to confirm former results, grafting experiments were extended to join former and new data. Five-day-old plants were cut and rosettes of *ugt76b1* plants were transferred to roots of wild type (ko/wt) and *vice versa* (wt/ko). As control wild type (wt/wt) and *ugt76b1* (ko/ko) plants were generated. Wild-type root led to wild-type expression of *PR1*, *PR2*, and *PR5* also in *ugt76b1* rosette, whereas *ugt76b1* root enhanced these marker genes in wild-type shoot (Fig. 38). This further examination showed that the genotype of the root had influence on the *PR* gene expression of shoot independent of the shoots genotype (Fig. 38A). The defence status of the rosette leaves is controlled by *UGT76B1* expression in roots and largely independent from the presence of UGT76B1 in the leaves.

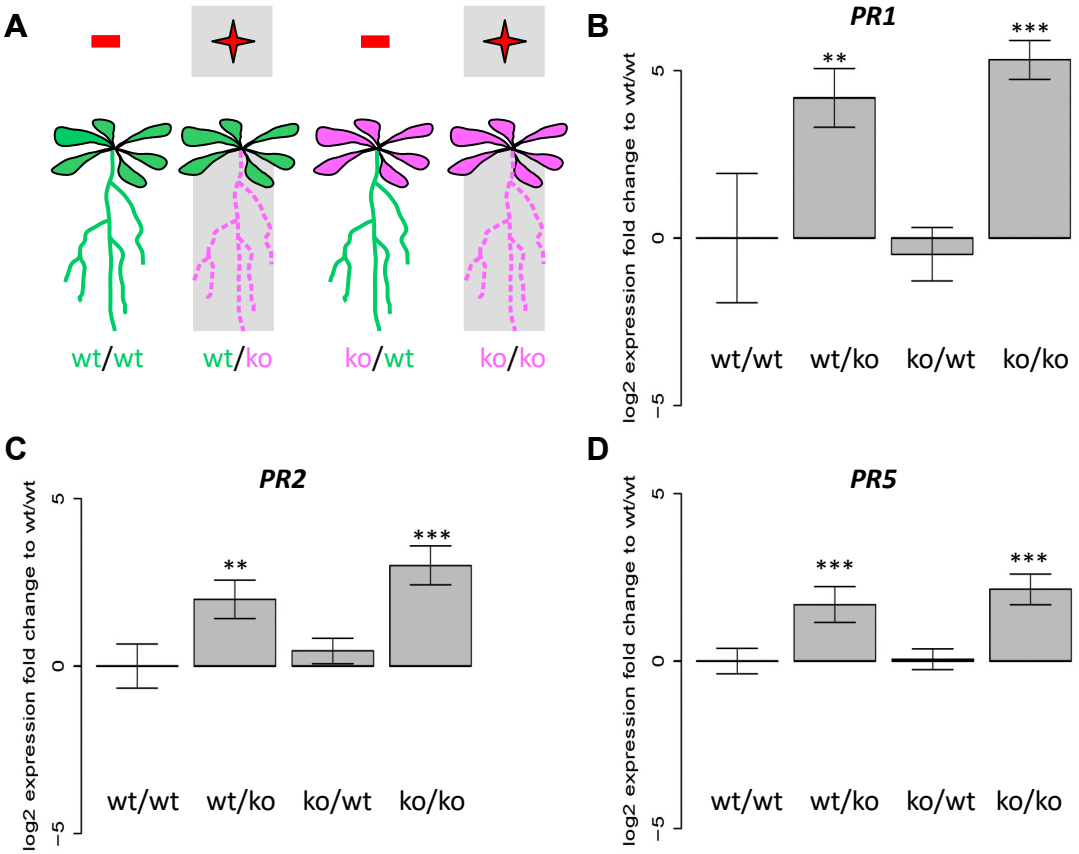

Fig. 38: Expression of* PR1, PR2, *and* PR5 *marker genes in grafted plants

***A**: Scheme and summary of grafting results of* ugt76b1 *and wild type. Gene expression of* PR1 *(**B**),* PR2 *(**C**),* PR5 *(**D**) in homo- and heterografts of* ugt76b1 *and wild type. wt = wild type, ko =* ugt76b1*. Plants were grown after grafting for six weeks. Gene expression was assessed by RT-qPCR and normalized to* S16 *and* UBQ5*. Arithmetic means and standard errors from log2 transformed data from five independent experiments. n = 11-16. Around 50 % of samples were grafted by R. Maksym. Asterisks above the bars indicate significance of the difference to the wt/wt homo-grafts, ** = p < 0.01, *** = p < 0.001 (paired ANOVA equal variance).*

The identity of the mobile signal released by *ugt76b1* roots is still unknown. One of the proposed candidate is ILA, since its levels are changed in *ugt76b1* mutant (Maksym *et al.*, 2018). The pathway for ILA biosynthesis *in planta* is not known yet and grafting of *ugt76b1* and a mutant impaired in ILA synthesis would be required. On the other hand SA levels are increased in *ugt76b1.* Therefore SA-dependency of this root to shoot signal was examined. In *ugt76b1* NahG *sid2* plants no up-regulation of *PR1* in shoots was observed any more showing that local SA is needed for the gene expression pattern of *ugt76b1*. To test if the signal of the root is dependent on SA, SA-depleted mutant combined with *ugt76b1* roots were grafted with wild-type shoot. If the signal transported from root to shoot is dependent on SA no induction of SA marker genes in shoot should be observed. Comparison between wt / SA-

free *ugt76b1* with wt/wt revealed a significant induction due to SA-free *ugt76b1* roots in wild-type rosettes (Fig. 39).

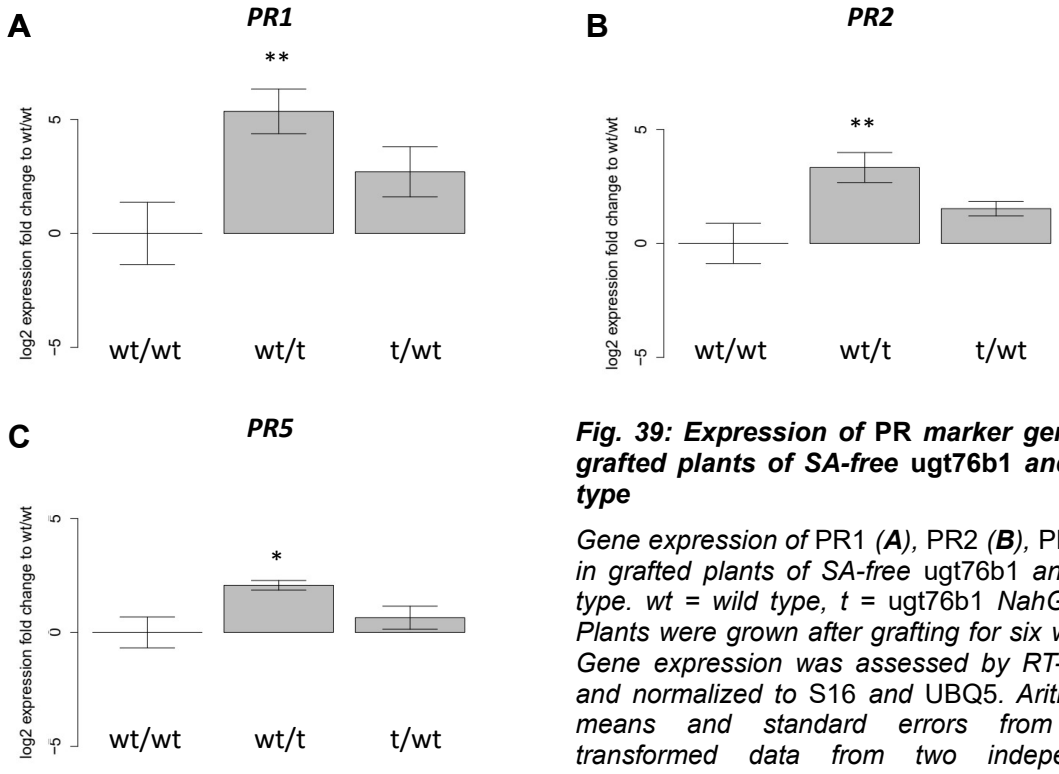

Fig. 39: Expression of* PR *marker genes in grafted plants of SA-free* ugt76b1 *and wild type

Gene expression of PR1 *(**A**),* PR2 *(**B**),* PR5 *(**C**) in grafted plants of SA-free* ugt76b1 *and wild type. wt = wild type, t =* ugt76b1 *NahG* sid2*. Plants were grown after grafting for six weeks. Gene expression was assessed by RT-qPCR and normalized to* S16 *and* UBQ5*. Arithmetic means and standard errors from log2 transformed data from two independent experiments. n = 5 - 8 for* PR1 *and* PR2*. n = 3-6 for* PR5*. Asterisks above the bars indicate significance of the difference to the wt/wt homo-grafts, ** = p < 0.01, * = p < 0.05 (paired ANOVA equal variance).*

4 Discussion

SA-related defence is triggered by the recognition of pathogens leading to the induction of ICS1 and EDS1/PAD4-dependent SA biosynthesis and production. To control and attenuate free SA concentrations, SA is glucosylated and thereby thought to be inactivated. The glucosyltransferases UGT76B1, UGT74F1, and UGT74F2 were shown to form SA glucosides *in vitro* and thus could be possible candidates involved in the regulation of endogenous free SA levels (Dean *et al.*, 2005; Song *et al.*, 2008; Noutoshi *et al.*, 2012; George Thompson *et al.*, 2017; Maksym *et al.*, 2018). Nevertheless, their impact on plant defence *in vivo* was inconclusive and no side-by-side comparison of mutants was possible due to the lack of mutant alleles in the same genetic background. The aim of this thesis was to investigate the role of the three UGTs in SA glucosylation and the subsequent regulation of free SA levels upon pathogen infection.

4.1 All three UGTs contribute to SA glucosylation

A set of all possible single, double, and triple mutant combinations of the three UGTs was generated in *A. thaliana* (Col) by crossing and by using a CRISPR/Cas9-based system. Mutations of all three UGTs were necessary to completely abolish SA glucosides. In accordance with these results, the sensitivity of the *ugt* triple mutant in an SA root growth inhibition assay was enhanced relative to the sensitivity of the *ugt74f1 ugt74f2* or the *ugt76b1 ugt74f1* double mutants in the presence of high SA levels (Fig. 6). In addition, a hypersensitivity of the *ugt* triple mutant compared to the wild type was observed under BTH treatment. The total leaf area and total rosette weight were reduced in the *ugt* triple mutant after BTH treatment compared to the wild type. Furthermore, the yellow leaf area representing leaf chlorosis was enhanced in the *ugt* triple mutant treated with BTH (Fig. 7). Collectively, these results underlined the role of all three UGTs in SA tolerance. Even though all three UGTs contributed to the production of SAG, only the *ugt76b1* mutant exhibited enhanced free SA level under control conditions (Fig. 10A, compare section 4.2.3). This would indicate that only UGT76B1 controls free SA levels in the absence of stress. In a previous study of our laboratory, a triple mutant in Ws background, *ugt76b1 ugt74f1* ami*ugt74f2*, was generated with residual activity of amiRNA-silenced UGT74F2 (Maksym, 2018). SA was slightly enhanced in this triple mutant, whereas SAG levels were significantly reduced. However, SGE levels were only slightly reduced. Nevertheless, in the Ws background, all three UGTs were contributing to SAG production, even though it was not completely abolished as in the *ugt* triple mutant in Col background. This could be explained by the residual activity of amiRNA-silenced

UGT74F2. In the Ws *ugt* triple mutant SGE was still present, whereas it was abolished in the Col *ugt* triple mutant (Fig. 10C). Furthermore, root growth inhibition assays with high SA also revealed hypersensitivity of the Ws *ugt* triple mutant. Taken together, these results indicated that all three UGTs were able to glucosylate SA and thereby participated in SAG production *in planta.*

4.2 Differences of UGT76B1, UGT74F1, and UGT74F2

4.2.1. Differences in the transcript expression profiles of *UGT76B1*, *UGT74F1*, and *UGT74F2*

The question whether UGT74F1, UGT74F2, and UGT76B1 might interact or would be able to compensate each other was addressed. In this thesis BTH, an SA analogue, was used for stress treatment. The expression level of *UGT76B1* was highly induced by BTH (log2 fold change 6.91), whereas the level of *UGT74F2* was only slightly induced (0.55) and *UGT74F1* not significantly regulated (-0.98). Data acquired from a public database ePlant (3.1.5) showed that *UGT76B1* was also highly induced by SA and *Pst* treatment. UGT74F2 was also induced by both, but to a lower extend than *UGT76B1,* whereas *UGT74F1* showed no induction by SA treatment and lowest induction after pathogen infection. In our laboratory UGT74F1 and UGT74F2 transcripts were not induced by both treatments (Meßner & Schäffner, unpublished).

Public available expression data showed, that the three UGT differed in their expression during plant development and in different plant tissues (ePlant, 3.1.5). This was confirmed by promoter-reporter expression analysis in this thesis. For example, *UGT74F1* and *UGT74F2* were expressed in the vascular tissue of leaves, whereas *UGT76B1* was expressed in a more irregular way, spread across the leaf tissue (Fig. 8). Furthermore, the expression pattern of UGT74F1 or UGT74F2 did not changed when UGT76B1 was missing. Only a slight induction of *UGT76B1* was observed, when one of the other UGT was missing (Fig. 8). This was also confirmed by RNAseq expression data. Neither the expression of *UGT74F1* nor the expression of *UGT74F2* were changed in the *ugt76b1* mutant with a log2 fold change higher than one (Tab. 5). In contrast to UGT74F1 and UGT74F2, UGT76B1 was induced in *ugt74f1*, *ugt74f2,* and *ugt74f1 ugt74f2* (Tab. 5). Nevertheless, due to their different spatial expression and due to the findings that in the knockout mutant of one UGT, the two others were not induced, an interplay of the three UGTs is rather unlikely on the transcriptome level.

4.2.2. UGT74F2 does not influence the level of free SA

Chemical analysis revealed that SGE was induced after stress in wild type, but was abolished in *ugt74f2* under control and BTH treatment (Fig. 10). Thus, SGE *in planta* was exclusively formed by UGT74F2. This was also shown by Dean & Delaney (2008), who used a knockdown mutant of UGT74F2. However, the abolition of UGT74F2 showed significant changes in free SA nor in SAG contents (Fig. 10). SAG levels in *ugt74f2* were slightly enhanced only after stress treatment, but not significantly different compared to the wild type. This increased SAG level could be produced through UGT76B1 activity, which was induced in *ugt74f2* and by BTH treatment (Tab. 5). In contrast to *UGT76B1* expression, *UGT74F2* was only slightly induced when plants were treated with BTH (0.55). In literature, *UGT74F2* was shown to be enhanced after pathogen infection (Song, 2006). Furthermore, a *UGT74F2* overexpression line was more susceptible towards pathogens (Song *et al.*, 2008). In accordance with these results, the *ugt74f2* knockout mutants showed slightly higher resistance after infection (Fig. 9). However, the observed resistant phenotype was independent of SA as no changes in free SA content or SA signalling were found when compared to the wild type (Fig. 9 and 10). In consistency with these findings, Boachon *et al.* (2014) found a higher resistance of *ugt74f2* knockdown after 48 h, but neither increased *PR1* expression nor enhanced free SA levels. Still, the constitutive overexpression of UGT74F2 negatively affected SA levels (Song, 2006). As mentioned before, other substrates of UGT74F2 with higher affinity compared to SA were found (Li *et al.*, 2015). Thus, the observed slightly increased resistance of *ugt74f2* could also result from changes in other compounds. For example, a role of nicotine, a nicotinate derivate, in plant defence was demonstrated in tobacco (Li *et al.*, 2015). Indeed, a higher activity of UGT74F2 towards nicotinate compared to SA and decreased levels of nicotinate O-glucoside were found in the *ugt74f2* knockdown mutant. Furthermore, contents of nicotinate were enhanced in *ugt74f2* after infection (Li *et al.*, 2015). Therefore, the nicotinate O-glucosylation activity of UGT74F2 provides an alternative role for UGT74F2, independent of SA and SA derivates.

4.2.3. UGT76B1, but not UGT74F1, controls free SA levels

Enhanced SAG contents in the *ugt76b1* mutant first led to the conclusion that UGT76B1 was not an SA glucosyltransferase (von Saint Paul *et al.*, 2011). However, in later publications and in this thesis, it was shown that UGT76B1 plays a role in SAG production (Noutoshi *et al.*, 2012; Maksym *et al.*, 2018, Fig. 10). UGT74F1 also contributes to SAG production (Dean & Delaney, 2008; Fig. 10). SAG levels were influenced by both enzymes. Hence, in the fol-

lowing subsections, UGT76B1 and UGT74F1 will be compared in order to identify common and different properties of these two enzymes and their role in plant defence.

4.2.3.1 Common genes controlled by UGT76B1 and UGT74F1

Under non-stressed conditions, a big overlap of genes regulated by UGT76B1 and UGT74F1 was found (Fig. 11C and D). Processes, that were enriched in the *ugt76b1* mutant were also enriched in the *ugt74f1* mutant (Tab. 3). Nevertheless, the expression levels of commonly regulated genes were induced more strongly in *ugt76b1* compared to *ugt74f1* (e.g. Tab. 4). In total, more genes were regulated in the *ugt76b1* mutant than in the *ugt74f1* mutant (Fig. 11C and D). Furthermore, distinct spatial expression patterns of both UGTs were shown (Fig. 8). From this finding, it was unclear, how these two enzymes might interact to control gene expression and SAG production.

4.2.3.2 UGT74F1 plays a role in SAG production not influencing free SA levels

While SAG content was reduced in the *ugt74f1* knockout, it was enhanced in the *ugt76b1* mutant under control conditions. Enhanced SAG levels of *ugt76b1* were reduced to wild-type level by the introgression of *ugt74f1*. Highest SAG contents were found in *ugt76b1 ugt74f2* (Fig. 10B). Thus, UGT74F1 had a negative effect on the production of SAG. UGT74F1 was shown to be involved in SAG production by exogenous SA feeding of *ugt74f1* WS mutant. After the application of SA less SAG was produced in *ugt74f1* Ws mutant (Dean & Delaney, 2008). All these findings showed that UGT74F1 was involved in SAG production under non-stressed conditions.

SAG level was up-regulated in *ugt74f1* and *ugt76b1* comparable to wild type by BTH treatment (Fig. 10B). This was also the case for the *ugt76b1 ugt74f2* double mutant. SAG content was only reduced in the *ugt76b1 ugt74f1* double. This suggested that under BTH treatment, UGT76B1 produced major proportion of SAG and *vice versa* in the *ugt74f1* knockout. Thus, UGT76B1 and UGT74F1 seemed to influence SAG level production under stress conditions, even though their expression patterns were distinct (Fig. 8) and *UGT74F1* was not induced in the *ugt76b1* knockout under control conditions (Tab. 5). It cannot be excluded that another glucosyltransferase was interacting with UGT74F1 or UGT74F2 under BTH treatment and in the absence of UGT76B1, and thus influencing SAG levels. Nevertheless, an influence of another glucosyltransferase can be excluded when all three UGTs were mutated, since SAG was almost completely abolished in the triple *ugt* mutant (Fig. 10B). To address this question, RNAseq data of the single and double mutant of the UGTs after BTH treatment would be necessary. Nevertheless, the reduction of SAG due to UGT74F1 mutation did not influence free SA contents of *ugt74f1*, *ugt74f1 ugt74f2* or *ugt76b1 ugt74f1*. Thus, neither SA signalling

nor stress response was influenced by the mutation of UGT74F1 (Fig. 9). In summary, UGT74F1 did not influence the pool of free SA, but was producing major proportions of SAG.

4.2.3.3 UGT76B1 is controlling free SA levels

Besides GO terms for pathogen defence and immune response, SA biosynthetic and metabolic process were enriched among the up-regulated GO terms in *ugt76b1* (Tab. 4). This is in line with the findings of enhanced SA levels of the *ugt76b1* knockout, whereas in the *ugt74f1* mutant SA levels stayed unchanged (Fig. 10A). Therefore, SA biosynthesis seemed to be controlled by UGT76B1 or influenced by a feedback loop enhanced in *ugt76b1*. In the *ugt76b1* mutant SA, SAG, and SGE levels were enhanced under non-stressed conditions to a level comparable to wild type after BTH application. Therefore, it is not surprising that *ugt76b1* revealed a higher resistance phenotype towards pathogen infection than *ugt74f1* (Fig. 9). In conclusion, *ugt76b1* revealed a primed defence status without any stress treatment, resulting in enhanced pathogen resistance. This was also reflected by the induction of similar genes in *ugt76b1* and in wild-type BTH-treated plants (same shift of genes at the first axis of the PCA analysis; Fig. 11A). It has to be mentioned that Noutoshi *et al.* (2012), who used Ws instead of Col background, found enhanced SA and reduced SAG levels in *ugt76b1* and *ugt74f1* with and without infection. Free SA levels did not differ in both mutants. Nevertheless, infection studies showed only slight reduction of pathogen growth in *ugt74f1*, but a higher resistant phenotype of *ugt76b1.* This could argue against the same levels of free SA in these two Ws mutants. A slight reduction of bacterial growth in *ugt74f1* was also found for the mutant in Col background. The reduced bacterial growth of the *ugt74f1* mutant was minor in comparison to the *ugt76b1* mutant (Fig. 9).

After BTH treatment free SA and SAG levels of *ugt74f1* were induced to wild-type levels, whereas in *ugt76b1*, no further induction compared to *ugt76b1* under control conditions was found (Fig. 10A and B). Free SA levels of wild type and *ugt76b1* after BTH treatment did not differ significantly. *UGT76B1*, but not *UGT74F1* was up-regulated after BTH treatment (6.91 vs not significantly regulated). In addition, *UGT76B1* was shown to be up-regulated in response to pathogens (von Saint Paul *et al.*, 2011), whereas no regulation of *UGT74F1* was observed (Song, 2006; Song *et al.*, 2008; Okamoto *et al.*, 2009). With BTH treatment free SA levels were only reduced in UGT76B1 OE (Fig. 10A). These findings confirmed a role of UGT76B1 in attenuation of SA levels after pathogen attack. In summary, these results suggest a role of UGT76B1 in regulation of SA levels. UGT76B1 seemed to suppress SA up-regulation under control conditions. The overexpression of UGT76B1 played a role in attenuation of free SA under stress inducing conditions.

By regulation of free SA levels, UGT76B1 might play a role in balancing plant response and growth. One hint for this role was found by the smaller rosette size of *ugt76b1* compared to the wild type (Fig. 15B). Furthermore, the early senescence (Fig. 15C) and the early flowering phenotype of *ugt76b1*, maybe related to enhanced SA levels, hint to a control mechanism of UGT76B1 regarding senescence and flowering (von Saint Paul *et al.*, 2011).

4.2.4. Possible reasons for different SA levels in *ugt76b1* and *ugt74f1*

4.2.4.1 Local differentiation according to UGT expression patterns

The question arose how this specific free SA regulation by UGT76B1 was possible, since UGT76B1 and UGT74F1 were both involved in SAG production, but only in *ugt76b1* free SA levels were induced. Different pools of SA and SAG, which have different tasks, might be conceivable. These pools could be discriminated by the localisation in the plant tissue. Different expression patterns of the UGTs were observed. UGT74F1 was mostly expressed in the vascular tissue, whereas UGT76B1 was expressed in a more patchy way (Fig. 8). UGT74F1 would only glucosylate SA in the vascular tissue, whereas the expression of *UGT76B1* seemed to be more widely spread reaching free SA in several different tissues. Thus, SA and SAG pools in vascular tissue would not lead to enhanced free SA and SA downstream events, whereas the second pool would trigger plant defence responses. Under BTH treatment both UGTs were involved in SAG production. Only when both enzymes were abolished SAG production was reduced (Fig. 10B). This finding demonstrated an interplay of two enzymes. For this a transport or re-localisation of free SA would be necessary, so that in the absence of one UGT the other could glucosylate the free SA of the other location. On the other hand the introgression of the CDS of *UGT74F1* expressed under the promoter of *UGT76B1* could not compensate the phenotypes of *ugt76b1*. SA signalling and SA derivates were still induced (Fig. 14, Fig. 37). Since *UGT74F1* was expressed under the promoter of UGT76B1, local differentiation by the dissimilar expression pattern in the plant tissues of both glucosyltransferase may be excluded.

Importantly, it has to be considered that only SAG levels, but not free SA levels were influenced by the mutation of UGT74F1, whereas in the *ugt76b1* mutant free SA and SAG were enhanced. Next to the fact that SA is converted to SAG, the role of SAG in plant defence is not so clear as often thought. SAG is assumed to be the storage form of SA and could be hydrolysed to free SA (Vlot *et al.*, 2009). Radiolabelled SAG was shown to be taken up into the vacuoles (Vaca *et al.*, 2017). Nevertheless, up to date, there is no study showing that vacuolar SAG is released and converted to free SA upon pathogen attack in *A. thaliana* (Maruri-López *et al.*, 2019). This could indicate that the ability of both enzymes to produce

SAG is not the only cause to inhibit SA-related plant defence. UGT76B1 was able to use also other plant defence activating substrates, which could not be converted by UGT74F1. The possible interplay of different substrates of UGT76B1 and their influence on free SA will be discussed later on (4.2.5).

4.2.4.2 UGT76B1 might regulate transporters for SAG sequestration into vacuoles

SAG is thought to be stored in the vacuole (Vlot *et al.*, 2009; Fu & Dong, 2013), but might be easily converted back to free SA (Vidhyasekaran, 2015). Vacuolar sequestration of SAG seems to be a protection mechanisms and ensures that there is no end-product inhibition of SA glucosylation in the cytosol (Vaca *et al.*, 2017). Thus, a transport mechanism for SAG from cytosol to vacuole is presumable. This uptake of SAG to the vacuole might involve ABC transporters and H^+ antiporters (Vaca *et al.*, 2017). Blockage of the transport of SAG to the vacuole could result in enhanced SAG and SA levels in the cytosol, and consequently activation of NPR1, downstream SA signalling and plant immune response (Fu & Dong, 2013; Seyfferth & Tsuda, 2014). If UGT76B1 is involved in controlling the activation of the import of SAG to the vacuole, the elimination of UGT76B1 could lead to enhanced SA and SAG levels in the cytosol. This enhanced SA in the cytosol could serve as a stress signal in plants and amplify SA biosynthesis and SA signalling. Indeed, SA biosynthetic and SA signalling genes were enhanced in the in *ugt76b1* mutant (Tab. 4). If UGT74F1 would not influence this activation and in the *ugt74f1* mutant SAG would be transported to the vacuole, free SA in the cytosol would not be influenced. On the other hand, if UGT76B1 is involved in controlling the export of SAG from the vacuole to the cytoplasm, the elimination of UGT76B1 leads to an export of SAG from the vacuole to the cytosol, which could be converted to SA, resulting in enhanced free SA levels.

To find candidates involved in SAG transport to the vacuole, genes that were significantly down-regulated in the *ugt76b1* mutant, but differently or not regulated in the *ugt74f1* mutant, were screened for transporters. Ten transporters were down-regulated in the *ugt76b1* mutant and not/or up-regulated in *ugt74f1* (Tab. 8). Two ABC transporter AT3G13640 and AT3G53480 were found, but both are not localised to the vacuole membrane. Three genes out of the ten are thought to be localised to the vacuole according to TAIR database (AT1G72140, AT3G54830, AT4G00910). The function of AT3G54830 and AT4G00910 in leaves are not known so far. AT4G00910 was shown to be up-regulated in roots during the early stages of drought stress (Rasheed *et al.*, 2016). Also AT1G72140 was predominately expressed in roots and identified as nitrate efflux transporter (He *et al.*, 2017). Later on, it was shown that AT1G72140 is a transporter for indole-3-butyric acid, a precursor of auxin, influencing lateral root formation (Michniewicz *et al.*, 2019).

Tab. 8: Possible candidates of SAG transporters

Candidate genes of transporters negatively regulated in ugt76b1 and *not regulated in* ugt74f1. *Localisation was determined according toTAIR database.*

ATG	*ugt76b1*	annotation	located in
AT1G67640	-2.60	Lysine histidine transporter-like 2	plasma membrane
AT4G00910	-1.70	aluminum activated malate transporter family protein	plant-type vacuole membrane
AT3G13640	-1.59	ABC transporter E family member 1	eukaryotic translation initiation factor 3 complex, membrane
AT1G72140	-1.37	putative peptide / nitrate transporter	integral component of membrane, nucleus, plant-type vacuole membrane, vacuolar membrane
AT2G36590	-1.25	proline transporter 3	cytoplasm, plasma membrane
AT3G54830	-1.24	transmembrane amino acid transporter family protein	nucleus, plasma membrane, vacuolar membrane
AT3G53480	-1.17	ABC transporter G family member 37	mitochondrion, plasma membrane, plasmodesma
AT1G60030	-1.13	nucleobase-ascorbate transporter 7	plasma membrane, plasmodesma
AT1G33440	-1.12	putative peptide/nitrate transporter	integral component of membrane, plasma membrane
AT5G04770	-1,11	cationic amino acid transporter 6	chloroplast, chloroplast membrane, integral component of membrane, plasma membrane

As the export of SAG from the vacuole to the cytosol and its conversion to SA could influence free SA levels, transporters activated in *ugt76b1* and not or differently regulated in *ugt74f1* were analysed. Twenty-seven enhanced transporters were found (Tab. S6). Only few examples of transporters involved in the export of secondary compounds from the vacuole are known (Martinoia, 2018). One example is the nitrate/peptide family (NPF) transporter NPF2.9 from *Catharanthus roseus* which exports strictosidine from the vacuole to the cytosol (Payne *et al.*, 2017). Two NPF transporters (NPF5.13 and NPF3.1) were enhanced in *ugt76b1*. NPF5.13 has unknown function. NPF3.1 was up-regulated in the leaves of infected *A. thaliana* (Pike *et al.*, 2013) and was shown to transport gibberellins and abscisic acid (Tal *et al.*, 2016). Eleven ABC transporter, with eight ABC transporters to localise to the vacuolar membrane (ABCI: AT1G67940; ABCC: AT1G30410, AT1G30420, AT2G47800, AT3G13080, AT3G13090, AT3G60160, AT3G60970), were found. Seven belong to the ABC subfamily C (ABCC). ABCC transporters were shown to be involved in different processes including the transport of plant hormones. Furthermore, ABCC members revealed enhanced expression after pathogen infection and after SA application (Wanke & Kolukisaoglu, 2010).

In summary, possible first candidates for transporters located to the vacuole exclusively regulated by UGT76B1 were found. The scenario of UGT76B1 influencing the transport of SAG would help to understand how UGT76B1 could influence free SA levels, whereas UGT74F1

was involved in SAG production, but not in controlling free SA levels. If and how UGT76B1 influence the export or import of SAG to the vacuole would need further studies in future.

4.2.5. Interplay of the three defence activating compounds, SA, ILA, and N-OH-Pip via UGT76B1

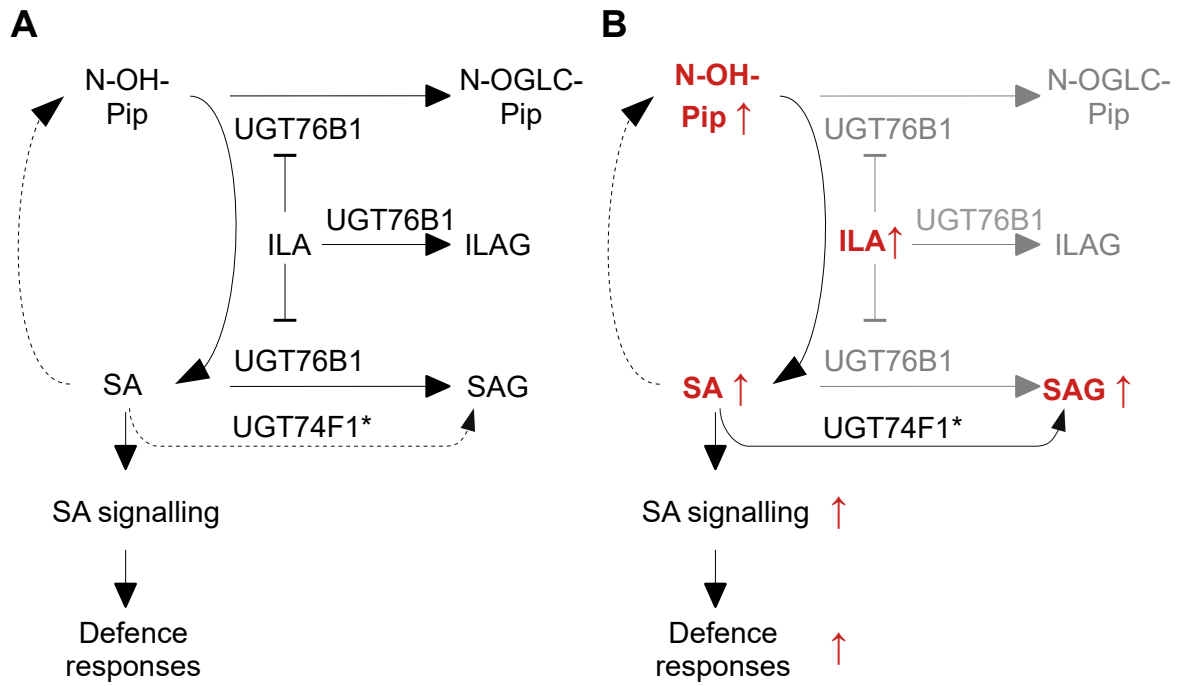

Fig. 40: UGT76B1 suppresses defence responses by controlling ILA, N-OH-Pip, and free SA levels

A: *In wild type UGT76B1 was shown to negatively influence free SA levels and downstream SA signalling. This was achieved by glucosylation of free SA. Furthermore, UGT76B1 was shown to also glucosylate ILA and N-OH-Pip. Enhanced N-OH-Pip increased free SA levels via UGT76B1 dependent and independent pathways. Exogenously added ILA was shown to inhibit SA as well as N-OH-Pip glucosylation. In addition to UGT76B1, UGT74F1 was influencing SAG production.* ***B:*** *In* ugt76b1 *SA levels and SA signalling were enhanced due to the abolishment of glucosylation. Furthermore, ILA and N-OH-Pip were enhanced. Increased N-OH-Pip levels could also result in enhanced SA levels. SAG levels were enhanced due to the conversion by UGT74F1*. SAG production by UGT74F1 did not influence free SA levels in the* ugt76b1 *background (see Fig. 10). converted to (→), increase (↑), repression (┤).*

Besides SA , ILA, and N-OH-Pip were converted by UGT76B1. A model of UGT76B1 and the possible interplay of SA , ILA, and N-OH-Pip is shown in Fig. 40. ILA interferes with SA glucosylation via UGT76B1 by competitive inhibition *in vitro* (Bauer *et al.*, 2020) and *in vivo* (Fig. 5 and 19). Furthermore, exogenous application of ILA led to enhanced SA and N-OH-Pip levels (Fig. 18 and 34). N-OH-Pip was found to be another substrate of UGT76B1 (Fig. 33) and levels of N-OH-Pip were dependent on *UGT76B1* expression (Fig. 31). The levels of N-OH-Pip in turn influence SA signalling and *UGT76B1* expression (Hartmann & Zeier, 2019). The importance of UGT76B1 in controlling ILA, N-OH-Pip, and free SA to suppress

defence responses under control conditions is further highlighted by the consequences due to *ugt76b1* mutation (Fig. 40B). In the absence of UGT76B1 all three compounds were up-regulated, leading to enhanced SA signalling (Tab. 4) and plant defence (Fig. 9). Since neither UGT74F1 nor UGT74F2 influenced ILA or N-OH-Pip levels, the ability of UGT76B1 to convert and control these two compounds represents an additional layer to control SA-dependent defence pathway. The interplay of SA , ILA, and N-OH-Pip is discussed in more detail in the following sections.

4.2.5.1 Interplay of SA and ILA

The modelling of the binding pocket of the three UGTs revealed that the binding pocket of UGT76B1 is rather wide compared to UGT74F1/UGT74F2. Hence, ILA only fits to the UGT76B1 binding pocket (Fig. 4). Furthermore, the root growth inhibition tests showed that the *ugt76b1* single mutant was hypersensitive to the ILA application, whereas the *ugt74f1* and the *ugt74f2* mutant were not different from wild type. In addition, UGT76B1 OE had longer roots than wild type (Fig. 5). For SA all three *ugt* showed the same root growth inhibition, which was stronger than in wild-type seedlings (Fig. 5). All three UGTs were involved in SA inactivation *in vivo*, whereas the inactivation of ILA was solely due to UGT76B1 activity.

Application of ILA led to a rise in free SA (Fig. 18). This was attributed to the inhibition of SA glucosylation of UGT76B1 by ILA, resulting in enhanced defence response and pathogen resistance (Fig. 17, 18, 19, and 20). Already a slight shift in SA homeostasis could be enough to induce a positive feedback on SA biosynthesis (Shah, 2003). The combination of SA and ILA led to a higher *PR1* up-regulation than SA alone. This effect was lost in *ugt76b1* mutants (Fig. 19). Therefore, the enhanced ILA concentrations enforced free SA via UGT76B1. Regardless of the mechanistic implementation, the positive impact of ILA on SA responses constitutes an additional layer of control on the SA-dependent defence pathway. ILA declines after infection by *Pst*, while *UGT76B1* is transcriptionally induced (von Saint Paul *et al.*, 2011; Maksym *et al.*, 2018). Thus, both incidents would cooperate to enhance UGT76B1-dependent SA conjugation in order to attenuate and control SA levels and defence response.

4.2.5.2 Interplay of N-OH-Pip and ILA

As mentioned before, ILA might only be used by UGT76B1 as substrate, but not by UGT74F1 and UGT74F2, since their binding pocket was shown to be to narrow. Consequently, an interplay of ILA and N-OH-Pip was only possible via UGT76B1 and not UGT74F1 or UGT74F2. Exogenously applied increasing ILA levels led to reduced glucosylation of N-OH-Pip by UGT76B1 *in vitro* (Bauer *et al.*, 2020). In addition, exogenous application of ILA led to an increase of N-OH-Pip and *FMO1* expression *in vivo* (Fig. 34). In contrast to

ILA, Pip, N-OH-Pip, and N-OGLC-Pip were increased after pathogen attack (Fig. 29). Hence, the same interplay between ILA and N-OH-Pip as described above for ILA and SA is conceivable. The combination of *UGT76B1* expression and ILA levels could attenuate and control N-OH-Pip levels after pathogen attack.

4.2.5.3 Interplay of N-OH-Pip and SA

N-OH-Pip was found as a third substrate of UGT76B1 (Fig. 31 and 33). *FMO1* expression was enhanced in the *ugt76b1* mutant (Zhang, unpublished). The levels of N-OH-Pip were negatively correlated to *UGT76B1* expression, but were not further increased due to the introgression of *ugt74f1 ugt74f2* in *ugt76b1* background (Fig. 32). Lines of *ugt76b1* complemented with the CDS of UGT74F1 were more similar to *ugt76b1* than wild type (Fig. 37). This may indicate, that neither UGT74F1 nor UGT74F2 control levels of N-OH-Pip. N-OGLC-Pip production was not observed in *ugt76b1* under control conditions and after Pip feeding (Fig. 32). Thus, the glucosylation of N-OH-Pip to this hexoside from was totally dependent on UBT76B1. Enhanced N-OH-Pip levels could interfere with SA glucosylation via UGT76B1 and *vice versa.* Rising N-OH-Pip levels inhibited UGT76B1 glucosylation activity towards SA, however less effectively than ILA (Bauer *et al.*, 2020). Free SA and N-OH-Pip could reinforce each other by mutually blocking their glucosylation in the wild-type background.

Different results for the activation of Pip biosynthesis and Pip accumulation by SA in local leaves were found, whereas in distal leaves the effect was positive (Hartmann & Zeier, 2019). This different results in local leaves could originate from different treatment periods. The missing interaction of N-OH-Pip and SA in local leaves was explained by different kinetics of SA and N-OH-Pip accumulation. In infected, local leaves SA levels rose earlier than N-OH-Pip levels, whereas in distal leaves an opposite pattern was found. After 36 hours both compounds were present in leaves and thus could enable a positive interaction (Hartmann & Zeier, 2019). A negative influence of SA on Pip biosynthesis or Pip levels was described after 24 hours (Hartmann *et al.*, 2018). Since treatments used in this thesis were 48 hours, both compounds were able to interact. Pip biosynthetic genes were up-regulated after BTH treatment (SA analogue) after 48 hours (Tab. 7). In addition, N-OH-Pip and N-OGLC-Pip levels were reduced or not detected in the SA-depleted NahG *sid2* mutant compared to the wild type (Fig. 32). These results would hint to an influence of SA towards N-OH-Pip production. Furthermore, SA application led to induced Pip levels in local leaves after 48 hours (Wang *et al.*, 2018a). Thus, a positive interaction of SA and N-OH-Pip at this time-point would be conceivable.

4.2.6. SA and Pip biosynthesis regulatory elements were influenced in *ugt76b1*

In addition to the direct impact of UGT76B1 by glucosylation of the three compounds, interactions on the transcriptional level for SA and N-OH-Pip biosynthesis were shown. SA and Pip biosynthesis share common regulatory elements. SARD1 and CBP60g target *ICS1*, but also the promoters of *ALD1* and *FMO1.* Thus, the transcription factors promoted SA and N-OH-Pip biosynthesis in parallel (Sun *et al.*, 2015). In *tga1-1 tga4-1* double mutant, SA and Pip accumulation were dramatically reduced upon pathogen infection in accordance with the reduced expression levels of *SARD1* and *CBP60g* (Sun *et al.*, 2018). Furthermore, the SA-biosynthesis activating module of EDS1 and PAD4 was shown to also activated *ALD1* and *FMO1* and led to the accumulation of Pip and N-OH-Pip (Bernsdorff *et al.*, 2016). N-OH-Pip application led to activation of SA biosynthesis by induction of *ICS1* and SA signalling was enhanced (Chen *et al.*, 2018). This indicates a complex amplification loop including positive co-regulation of SA and N-OH-Pip biosynthesis (summarized in Hartmann & Zeier, 2019). In the *ugt76b1* knockout SA as well as N-OH-Pip biosynthetic genes were up-regulated (Tab 4 and 7). In addition, EDS1/PAD4 and *SARD1/CBP60g* were enhanced. Thus, in the *ugt76b1* mutant the common regulatory elements of SA and N-OH-Pip biosynthesis were also enhanced at the transcriptional level.

In our lab the *ugt76b1 fmo1* double mutant exhibited lower levels of Pip and no N-OH-Pip. Whereas SA levels in the *ugt76b1* single mutant were significantly enhanced compared to the wild type, in the *ugt76b1 fmo1* double mutant SA levels were reduced (Bauer *et al.*, 2020). Thus, the removal of N-OH-Pip led to reduced SA levels in the *ugt76b1* background. N-OH-Pip influenced SA levels also independently of UGT76B1, maybe via the transcriptional amplification loop of positive co-regulation of SA and N-OH-Pip biosynthesis at the transcriptional level.

4.2.7. SA-independent effects of UGT76B1 may also contribute to plant defence

In contrast to *ugt74f1* and *ugt74f2*, the induction of superoxide radicals was found in *ugt76b1* (Fig. 12). These constitutively increased superoxide levels were shown to be independent of SA as SA-free *ugt76b1* still revealed enhanced superoxide (Fig. 22). Besides SA, ILA levels are induced in *ugt76b1* (Maksym *et al.*, 2018). Thus, external application of ILA (Fig. 21), but maybe also internal levels, influenced superoxide formation independently of SA. In addition to SA-dependent regulation of plant defence, SA-independent pathways exist (Pieterse & van Loon, 1999). In defence responses initial apoplastic generation of superoxide by the NADPH oxidases RBOHD and RBOHF is thought to be the first step after pathogen recogni-

tion (Morales *et al.*, 2016). Superoxide anions were shown themselves to act antimicrobially (Fang, 2011). Furthermore, they can activate defence genes and defence compound synthesis (Jabs *et al.*, 1997). In addition, O_2^- radicals can modify amino acids. Especially cysteines are known to be sensitive to superoxide radicals. Thus, oxidation of proteins by superoxide radicals could lead to a signal at the production side of O_2^- radicals (Sabater & Martín, 2013). Another possibility by which superoxide radicals could induce defence signalling is the reaction of superoxide radicals with nitric oxide radicals resulting in enhanced peroxynitrite levels. Peroxynitrite is also known as signalling compound, *inter alia* in plant defence (Gaupels *et al.*, 2011; Vandelle & Delledonne, 2011).

Since UGT74F1 and UGT74F2 could not regulate the levels of ILA, the regulation of superoxide production induced by ILA could be another characteristic of UGT76B1. It was shown that systemic defence has an SA-independent component. In the *sid2* mutant a certain level of priming of plants was still observed and the *sid2 ald1* double mutant was more susceptible to bacterial infection than the single mutants (Bernsdorff *et al.*, 2016). In a microarray approach of *ugt76b1* compared to the wild type, SA-responsive, SA-related, but also SA-independent changes in gene expression were revealed (Zhang, unpublished). Resistance of *ugt76b1* towards *Pst* infection was to a small part independent of *ICS1* and *NPR1* (Zhang, unpublished). This hints to an SA-independent branch regulated by UGT76B1. One example could be the enhanced regulation of gene expression of *ETHYLENE RESPONSIVE TRANSCRIPTION FACTOR1* (*ERF1;* Zhang, unpublished). In general, it is known that ERFs are enhanced during pathogen infection. They play a pivotal role in adaptation to biotic and abiotic stresses (Singh *et al.*, 2002). In the *ugt76b1* mutant four ERFs were significantly down-, whereas 14 were up-regulated (including *ERF1*) (Tab. S9). These could influence pathogen defence response controlled by UGT76B1 in an SA-independent manner.

4.3 Influences of ILA on plant growth

In addition to the involvement of ILA in plant defence in *A. thaliana*, ILA was present in different plant species including monocotyledonous and dicotyledonous plants, herbaceous and woody plants (Maksym *et al.*, 2018). This suggests a universal and important role of ILA within the plant kingdom. However the chemically closely related, isomeric LA and the related VA were only sporadically found in the different plant species (Maksym *et al.*, 2018). Still the functions of ILA are sparsely known.

4.3.1. ILA might be involved in early senescence phenotype

It was shown that the interplay of SA and ROS induced accelerated leaf senescence involved the WRKY75 transcription factor (Guo *et al.*, 2017). Overexpression of *WRKY75* promoted

SA production, suppressed ROS scavenging and led to an early leaf senescence phenotype (Guo *et al.*, 2017). In the *ugt76b1* mutant *WRKY75* was highly induced (log2 fold change 5.75). Since superoxide anions and SA were induced by ILA, ILA might be involved in the early senescence phenotype of the *ugt76b1* knockout (Fig. 9C).

The initiation of programmed cell death in response to photooxidative stress was shown to be induced by chloroplast-derived predominance of superoxide radicals over H_2O_2 (Straus *et al.*, 2010). Changes in the ratio between singlet oxygen and superoxide radicals *versus* H_2O_2 could provoke a switch from defence response to programmed leaf senescence (Sabater & Martín, 2013). Higher levels of O_2^- radicals were found in *ugt76b1* mutant (Fig. 12 and 21D). It can be speculated that the high superoxide radical content might have led to this phenotype. ILA induced superoxide anion formation SA-independently (Fig. 21), whereas H_2O_2 formation was not affected (Fig. 22B). Thus, superoxide anions were distinctly regulated by ILA. The shift of the ratio between O_2^- radicals and H_2O_2 could play an important role in to initiate the early leave senescence phenotype in *ugt76b1*.

Furthermore, SA is known to regulate developmental leaf senescence and induces the expression of senescence-associated genes (*SAG*s) (Jibran *et al.*, 2013). ILA enhanced the expression *SAG13* and *SAG21* (Fig. 20A). *SAG13* and *SAG21* are up-regulated during early senescence (Bhat *et al.*, 2019). Since exogenous application of ILA led to elevated SA levels, the ILA-enhanced expression of *SAG*s could be dependent on SA (Fig. 18).

4.3.2. Role of ILA during root growth inhibition

It is known that exogenously applied SA, as well as other plant hormones like abscisic acid (Rodrigues *et al.*, 2009), auxin (Okumura *et al.*, 2013) or methyl-jasmonate (Staswick *et al.*, 1992) reduce primary root growth. In addition to plant hormones, amino acids like proline or glutamic acid were able to negatively influence root growth of *A. thaliana* seedlings via SA signalling and calcium-mediated oxidative burst (Chen *et al.*, 2011a). In contrast, the action of ILA on root growth inhibition was independent of SA (Fig. 24A) and independent of changes in other hormone pathways (Fig. 25). Other compounds, like naringenin (Hernández & Munné-Bosch, 2012) or 3,4-(methylenedioxy) cinnamic acid (Steenackers *et al.*, 2016), showed SA-independent root growth inhibition. In addition, ROS formation is correlated and linked to root elongation via controlling root meristem size and the transition from cell division to elongation (Tsukagoshi, 2016). Hence, the question arose, if the enhanced superoxide anion content induced by ILA might play a role in root growth inhibition. O_2^- and H_2O_2 are found in the root tip with a higher O_2^- level in the root meristem, while H_2O_2 is enhanced in the differentiation zone. The balance of superoxide and hydrogen peroxide controls the transition

zone and thereby determines the size of the meristem vs the positioning of the elongation zone (Dunand *et al.*, 2007; Tsukagoshi, 2016). A strong change in superoxide content, distribution and thus a shift in O_2^- to H_2O_2 ratio could be the reason why ILA represses root growth instead of promoting it. However, several findings argue against an involvement of the ILA-induced O_2^- in inhibiting root growth. Kwak *et al.* (2003) had revealed that RBOHD and RBOHF were involved in abscisic acid-induced root growth inhibition. Neither in *rbohd rbohf* double mutant nor in abscisic acid-pathway mutants the root growth inhibition by ILA could be rescued (Fig. 24C and 25). Second, the inhibition was still observed in the presence of the O_2^- radical scavenger 4-OH-TEMPO (Fig. 24D). Third, the application of Ile and LA also enhance root growth inhibition in wild-type plants, but did not influence the superoxide radical levels (Fig. 27C). This indicated a different and possibly common mechanism of ILA, LA and Ile.

Furthermore, it was shown that FMO1 can influence root growth inhibition by *de novo* synthesis of H_2O_2 downstream of SOG1 and influencing root meristem size in response to DNA damage (Chen & Umeda, 2015). ILA did not enhance H_2O_2 levels in roots (Fig. 24B) and the mutation of FMO1 did not mitigate the root growth inhibition induced by ILA (Fig. 36A). Taken together, the inhibition of root growth by ILA was shown as an SA-, Pip-, and maybe superoxide radical-independent impact. The mechanism of the ILA effect remains elusive.

As mentioned before, SA also inhibits root growth, but the underlying mechanisms are still vague. Chromatin modification were shown to influence root development upon SA treatment in pearl millet. SA treatment decreased the methylation, which was positively correlated with the root growth, suggesting SA regulated root growth by the methylome (Ngom *et al.*, 2017). SA inhibited root cell elongation by abolishing specific ROS maxima ($\cdot OH$ and H_2O_2), whereas superoxide anion levels were not changed in *A. thaliana* (Jones, 2009). Superoxide was induced upon ILA application, whereas H_2O_2 seemed to be reduced (Fig. 22). Thus, maybe the action of ILA could be similar as SA in abolishing H_2O_2 maxima.

The plant hormone auxin was shown to play a central role in primary root growth (Rahman *et al.*, 2007). For example, the primary root growth inhibition by JA reduces root meristem activity by auxin regulation (Chen *et al.*, 2011b). The auxin-reporter DR5::GFP was not altered after the application of SA (75 µM), thus indicating no involvement of auxin in root growth inhibition triggered by exogenous SA (Jones, 2009). In contrast to this, it was shown that low concentrations of SA mediated auxin distribution in the root apical meristem. Activation of PIN1 and TAA1 influenced cell division activity of the meristem, whereas PIN2 and PIN7 were repressed. Application of low concentrations of SA (30 µM) led to an increase of auxin (DR5:GFP reporter line). In contrast high concentrations of SA (150 µM) led to a decrease of

auxin in the root tip (Pasternak *et al.*, 2019). Root growth inhibition was exhibited for both concentrations, whereby a concentration ≥ 50 µM stopped primary root growth. They concluded that depending on the concentration, SA has a role as a developmental regulator (SA < 50 µM) or as a stress hormone (SA > 50 µM) (Pasternak *et al.*, 2019). For ILA first tests of application of 500 µM ILA to DR5:GFP reporter line did not reveal changes in auxin accumulation compared to control. Since low and high levels of SA evoked different response towards auxin, lower levels of ILA should be tested in future. Also the use of Auxin-deficient mutant on ILA plates could answer this question. Thus, auxin could still play a role in root growth inhibition by ILA in dose-dependent manner.

4.3.3. Specificity of ILA perception and action in comparison to LA and Ile

All three 2-hydroxy carboxylic acid were conjugated by UGT76B1 *in vitro*, but only ILA and LA were detectable in *A. thaliana* (von Saint Paul *et al.*, 2011; Maksym *et al.*, 2018). The regulation of ILA and LA seemed to be independent of each other (Maksym *et al.*, 2018). It was shown that ILA and LA accumulated differently during plant development and during defence responses. ILA declined in four-week-old compared to two-week-old plants, whereas LA increased. Upon pathogen infection LA stayed unchanged and ILA decreased (Maksym *et al.*, 2018). Due to their chemical structure, it is most likely the 2-hydroxy carboxylic acid originate from the BCAAs. However, the ILA levels *in planta* declined, whereas its potential precursor, the related BCAA Ile, remained unchanged during plant growth (Maksym *et al.*, 2018). Thus, ILA was specifically regulated *in planta* differently from LA and Ile, and not only a side-product of repressed BCAA degradation. In addition to their differential accumulation, in this thesis the effects of ILA on plant defence responses were shown to be specific and distinct from those of LA and Ile. LA and Ile did neither provoke an induction of *PR1* nor of superoxide production (Fig. 27A and B). However, all three compounds led to root growth inhibition in wild-type plants (Fig. 27C). This indicated a possibly common mechanism of ILA, LA, and Ile in root growth inhibition. Nevertheless, using the same concentration of LA, Ile, and ILA led to a dramatical reduction of root by LA, whereas ILA and in particular Ile exhibited a less pronounced inhibition. Furthermore, the inhibition provoked by Ile was independent of UGT76B1. Thus, even though all three compounds led to root growth inhibition the extent of each compound was different. How ILA is detected and how the perception of ILA is differentiated from such closely related compounds stays elusive. The perception of ILA may occur at different levels. UGT76B1 seems to be the target in relation to SA-dependent defence responses enhanced by ILA (Fig. 18 and 19). The perception mechanisms for induction of superoxide, partially involving RBOHD and RBOHF (Fig. 23), and the provoked root growth

inhibition by ILA are unclear. However, such unknown mechanisms have to specifically differentiate ILA from the closely related isomeric LA and from the amino acid Ile.

4.4 Root to shoot communication

Changed levels of SA, ILA, and N-OH-Pip were found in *ugt76b1* knockout mutant leaves. All can potentially influencing plant defence. However, *UGT76B1* is mainly expressed in roots (von Saint Paul *et al.*, 2011). Furthermore, roots displayed higher levels of ILA compared to leaves (Maksym *et al.*, 2018). Hence, the question arose, if a signal derived from the root can influence the defence status of the leaf. This signal would be repressed by the presence of UGT76B1 in the root. It was shown that *PR1*, *PR2,* and *PR5* expression in leaves was dependent on the genotype of the root (Fig. 38). Changed SA levels in *ugt76b1* could lead to an SA-dependent signal from root to shoot. For cucumber, SA was found in phloem sap, and therefore postulated as a potential mobile signal (Métraux *et al.*, 1990). It was demonstrated that in the *ugt76b1* mutant SA is not the translocated signal for root-shoot communication. *PR1* was sill induced in wild-type shoot grafted to an SA-deficient *ugt76b1* root stock (Fig. 39). Nevertheless, SA is still necessary for the local induction of *PR* genes in the leaf of *ugt76b1* (von Saint Paul *et al.*, 2011). A similar result was found in tobacco plants. It was revealed that in systemic leaves of NahG transgenic tobacco plants no SAR response was induced due to infection (Gaffney *et al.*, 1993). Nevertheless, when SA was tested as mobile signal by grafting experiments, plants grafted from root stocks unable to accumulate SA, were fully capable of inducing resistance in leaves (Vernooij *et al.*, 1994). It can be concluded that an SA-independent signal was emitted from *ugt76b1* root influencing gene expression in wild-type shoot.

The next candidate for a signal controlled by UGT76B1 would be ILA. Levels of ILA were higher in belowground tissue compared to leaf tissue (Maksym, 2018). A signal derived from roots with enhanced ILA levels may influence a signal delivered to shoot. In addition, soil watering of ILA solution enhanced resistance of plants towards *Pst* infection in leaves (Fig. 17). As the pathway for ILA biosynthesis *in planta* is not known yet, this assumption could not be verified with grafting experiments. For this, a combination of a double mutant of *ugt76b1* and the mutation impairing ILA synthesis together with wild-type rosettes would be necessary.

Furthermore, the third substrate of UGT76B1, N-OH-Pip, could be the mobile signal. N-OH-Pip was already proposed as mobile signal in leaf to leaf communication during SAR (Chen *et al.*, 2018). The precursor of N-OH-Pip, Pip, was enriched in phloem exudates collected from infected leaves (Bernsdorff *et al.*, 2016). N-OH-Pip is produced from Pip by FMO1,

which also played a role in regulating of H_2O_2 in root tips (Chen & Umeda, 2015). Expression of *FMO1* was shown in the vascular tissue of elongation and differentiation zone. Application of zeocin, a double strand break inducer, increased the accumulation of H_2O_2 in root tips. Furthermore, higher *FMO1* expression in the epidermis and vasculature of the meristematic zone and the lateral root cap were found after zeocin treatment (Chen & Umeda, 2015). Since *FMO1* is also expressed in roots, N-OH-Pip can not be excluded as a candidate for root-shoot communication. To test dependency of UGT76B1 derived-root signal on FMO1, *PR* expression in wild-type leaves grafted with *fmo1 ugt76b1* root stock should be tested in the future.

In addition to these three compounds also different, currently unknown genes or compounds that could play a role in the root-to-shoot signalling of *ugt76b1*. Thieme *et al.* (2015) identified 2006 genes producing mobile RNAs in *A. thaliana*. Comparison of these 2,006 genes to significantly, at least two fold changed genes in the *ugt76b1* mutant resulted in 22 genes with negative and 273 with positive regulation (Tab. S7). Among the 273 enhanced RNAs, 129 were classified as shoot to root signals, 108 with bidirectional and 36 exclusively transported from root to shoot. In another study, phloem-derived RNAs were identified as mobile, potential long-distance signals of leaves (Deeken *et al.*, 2008). Among these genes, 18 were positively regulated in *ugt76b1* (Tab. S8). These numbers show that many possible mobile signals could be regulated by UGT76B1 in the root, which may influence the plant defence status also in the leaf tissue.

4.5 Outlook

This study established that UGT76B1, in contrast to UGT74F1 or UGT74F2, has the function to repress SA-related defence responses during non-stressed conditions. The role of UGT76B1 to control plant pathogen defence responses was clearly shown, while UGT74F1 plays a minor role in plant pathogen defence responses. It is probable that UGT76B1 and UGT74F1 are not redundant, and maybe other functions of UGT74F1 can be identified in the future. UGT74F1 was not able to compensate for the loss of UGT76B1 regarding pathogen defence. A further step could be to test the opposite situation: is UGT76B1 able to compensate for the loss of UGT74F1. Therefore, UGT76B1 should be introgressed under the UGT74F1 promoter into the *ugt74f1* mutant.

As also shown in this thesis, all three UGTs had to be mutated to abolish SAG levels with UGT74F1 having major impact on SAG production under non-stressed conditions. SAG levels were enhanced in the *ugt76b1* mutant, but reduced by the introgression of the UGT74F1 mutation in the *ugt76b1* background. This indicates an interplay of the UGTs in

SAG production. How this interaction takes place remains unclear, especially because both enzymes had distinct cellular expression patterns. Furthermore, UGT74F1 did not compensate for the loss of UGT76B1, although UGT74F1 was expressed under the UGT76B1 promoter. This would contradict the interplay of UGT76B1 and UGT74F1. In order to complete the picture in the future, UGT76B1 could be expressed with the 5' and 3' regulatory regions of UGT74F1, and introgressed in the *ugt76b1* mutant. This would answer the question, if UGT76B1 under the expression pattern of UGT74F1 is still able to revert phenotypes of the *ugt76b1* mutant.

Importantly, it has to be considered that the role of SAG in plant defence is not as clear as presumed. In fact, the ability of UGT76B1 and UGT74F1 to glucosylate SA did not influence SA-related plant defence in the same manner in both loss of function mutants. The loss of UGT74F1 did not influence free SA levels in the *ugt74f1* mutant and in the *ugt76b1 ugt74f1* double mutant SA levels were not different than in the *ugt76b1* single mutant. Therefore, maybe also other triggers next to SAG production were needed as well to induce free SA. UGT76B1 accepts at least two more plant defence response-activating substrates (ILA and N-OH-Pip). Hence, further investigations should focus on the interplay of SA, ILA, N-OH-Pip, and possibly other compounds as triggers inducing SA-dependent responses. An untargeted metabolomic approach could be employed in order to compare the *ugt76b1* and the *ugt74f1* knockout. In this way, more differences between the both glucosyltransferases and their roles in regulating specific processes *in planta* could be identified. Furthermore, using a yeast two-hybrid approach might enable the identification of interaction partners of UGT76B1 and UGT74F1 and thus, could lead to further identification of differences between the two enzymes.

In addition to the role of ILA in plant defence, SA-independent effects of ILA were discovered. It still remains unclear whether links between the three separable responses, pathogen defence, root growth inhibition, and superoxide radical production, exist. Moreover, the molecular and cellular targets of ILA-induced repression of root growth are not yet know. To make a first step towards answering these questions and to test SA-independent effects of ILA, transcriptome analyses of wild type and NahG *sid2* after ILA treatment are necessary.

Besides the responses of ILA in *A. thaliana*, similar responses were found in the dicot crop *B. napus.* Furthermore, it was shown that the defence gene expression was activated by the application of ILA in barley (Zhang, unpublished). So far ILA was found in all analysed plant species (Maksym *et al.*, 2018). In summary, further investigation of the action of ILA-related mechanisms could acquire a broader knowledge about plant defence strategies and investigations of these processes in other plant species could be useful for agriculture.

5 References

Alkooranee JT, Yin Y, Aledan TR, Jiang Y, Lu G, Wu J, Li M. 2015. Systemic Resistance to Powdery Mildew in *Brassica napus* (AACC) and *Raphanus alboglabra* (RRCC) by *Trichoderma harzianum* TH12. *PLOS ONE* **10**: 1-20.

Alonso JM, Stepanova AN, Leisse TJ, Kim CJ, Chen H, Shinn P, Stevenson DK, Zimmerman J, Barajas P, Cheuk R *et al.* **2003.** Genome-Wide Insertional Mutagenesis of *Arabidopsis thaliana*. *Science* **301**: 653-657.

Arnaiz A, Talavera-Mateo L, Gonzalez-Melendi P, Martinez M, Diaz I, Santamaria ME. 2018. *Arabidopsis* Kunitz Trypsin Inhibitors in Defense Against Spider Mites. *Frontiers in Plant Science* **9**: 986.

Ashraf M, Akram N, Arteca R, Foolad M. 2010. The physiological, biochemical and molecular roles of brassinosteroids and salicylic acid in plant processes and salt tolerance. *Critical Reviews in Plant Sciences* **29**: 162-190.

Baek D, Pathange P, CHUNG J-S, Jiang J, Gao L, Oikawa A, Hirai MY, Saito K, Pare PW, Shi H. 2010. A stress-inducible sulphotransferase sulphonates salicylic acid and confers pathogen resistance in *Arabidopsis*. *Plant, Cell & Environment* **33**: 1383-1392.

Balmer D, Papajewski DV, Planchamp C, Glauser G, Mauch-Mani B. 2013. Induced resistance in maize is based on organ-specific defence responses. *The Plant Journal* **74**: 213-225.

Bauer S, Mekonnen DW, Geist B, Lange B, Zhang W, Schäffner AR. 2020. The isoleucic acid triad: distinct impacts on plant defense, root growth and formation of reactive oxygen species, *Journal of Experimental Botany* (accepted).

Belkhadir Y, Yang L, Hetzel J, Dangl JL, Chory J. 2014. The growth-defense pivot: crisis management in plants mediated by LRR-RK surface receptors. *Trends in Biochemical Sciences* **39**: 447-456.

Berger S, Bell E, Mullet JE. 1996. Two Methyl Jasmonate-Insensitive Mutants Show Altered Expression of AtVsp in Response to Methyl Jasmonate and Wounding. *Plant Physiology* **111**: 525-531.

Bernsdorff F, Döring A-C, Gruner K, Schuck S, Bräutigam A, Zeier J. 2016. Pipecolic Acid Orchestrates Plant Systemic Acquired Resistance and Defense Priming via Salicylic Acid-Dependent and -Independent Pathways. *The Plant Cell* **28**: 102-129.

Bethke G, Pecher P, Eschen-Lippold L, Tsuda K, Katagiri F, Glazebrook J, Scheel D, Lee J. 2012. Activation of the *Arabidopsis thaliana* Mitogen-Activated Protein Kinase MPK11 by the Flagellin-Derived Elicitor Peptide, flg22. *Molecular Plant-Microbe Interactions* **25**: 471-480.

Bhat MA, Lone HA, Mehraj SS. 2019. Chapter 14 - Nutrient Remobilization During Senescence. In: Sarwat, M. & Tuteja, N., eds. *Senescence Signalling and Control in Plants*. Academic Press, 227- 237.

Blanco F, Salinas P, Cecchini NM, Jordana X, Van Hummelen P, Alvarez ME, Holuigue L. 2009. Early genomic responses to salicylic acid in *Arabidopsis*. *Plant Molecular Biology* **70**: 79-102.

Boachon B, Gamir J, Pastor V, Erb M, Dean JV, Flors V, Mauch-Mani B. 2014. Role of two UDP-Glycosyltransferases from the L group of *Arabidopsis* in resistance against *Pseudomonas syringae*. *European Journal of Plant Pathology* **139**: 707-720.

Bowles D, Isayenkova J, Lim E-K, Poppenberger B. 2005. Glycosyltransferases: managers of small molecules. *Current Opinion in Plant Biology* **8**: 254-263.

Bowles D, Lim E-K, Poppenberger B, Vaistij FE. 2006. Glycosyltransferases of lipophilic small molecules. *Annu. Rev. Plant Biol.* **57**: 567-597.

Caputi L, Malnoy M, Goremykin V, Nikiforova S, Martens S. 2012. A genome-wide phylogenetic reconstruction of family 1 UDP-glycosyltransferases revealed the expansion of the family during the adaptation of plants to life on land. *The Plant Journal* **69**: 1030-1042.

Cartwright AM, Lim E-K, Kleanthous C, Bowles DJ. 2008. A kinetic analysis of regiospecific glucosylation by two glycosyltransferases of *Arabidopsis thaliana*: domain swapping to introduce new activities. *Journal of Biological Chemistry* **283**: 15724-15731.

Castelló MJ, Carrasco JL, Navarrete-Gómez M, Daniel J, Granot D, Vera P. 2011. A Plant Small Polypeptide Is a Novel Component of DNA-Binding Protein Phosphatase 1-Mediated Resistance to *Plum pox virus* in *Arabidopsis*. *Plant Physiology* **157**: 2206-2215.

Chandran D, Rickert J, Huang Y, Steinwand M, Marr S, Wildermuth M. 2014. Atypical E2F Transcriptional Repressor DEL1 Acts at the Intersection of Plant Growth and Immunity by Controlling the Hormone Salicylic Acid. *Cell Host & Microbe* **15**: 506-513.

Chen F, D'Auria JC, Tholl D, Ross JR, Gershenzon J, Noel JP, Pichersky E. 2003. An *Arabidopsis thaliana* gene for methylsalicylate biosynthesis, identified by a biochemical genomics approach, has a role in defense. *The Plant Journal* **36**: 577-588.

Chen H, Xue L, Chintamanani S, Germain H, Lin H, Cui H, Cai R, Zuo J, Tang X, Li X *et al.* **2009.** ETHYLENE INSENSITIVE3 and ETHYLENE INSENSITIVE3-LIKE1 Repress *SALICYLIC ACID INDUCTION DEFICIENT2* Expression to Negatively Regulate Plant Innate Immunity in *Arabidopsis*. *The Plant Cell* **21**: 2527-2540.

Chen J, Zhang Y, Wang C, Lü W, Jin JB, Hua X. 2011a. Proline induces calcium-mediated oxidative burst and salicylic acid signaling. *Amino Acids* **40**: 1473-1484.

Chen L, Wang W-S, Wang T, Meng X-F, Chen T-t, Huang X-X, Li Y-j, Hou B-K. 2019. Methyl Salicylate Glucosylation Regulates Plant Defense Signaling and Systemic Acquired Resistance. *Plant Physiology* **180**: 2167-2181.

Chen P, Umeda M. 2015. DNA double-strand breaks induce the expression of flavin-containing monooxygenase and reduce root meristem size in *Arabidopsis thaliana*. *Genes to Cells* **20**: 636-646.

Chen Q, Sun J, Zhai Q, Zhou W, Qi L, Xu L, Wang B, Chen R, Jiang H, Qi J *et al.* **2011b.** The Basic Helix-Loop-Helix Transcription Factor MYC2 Directly Represses *PLETHORA* Expression during Jasmonate-Mediated Modulation of the Root Stem Cell Niche in *Arabidopsis*. *The Plant Cell* **23**: 3335-3352.

Chen X, Truksa M, Shah S, Weselake RJ. 2010. A survey of quantitative real-time polymerase chain reaction internal reference genes for expression studies in *Brassica napus*. *Analytical Biochemistry* **405**: 138-140.

Chen Y-C, Holmes EC, Rajniak J, Kim J-G, Tang S, Fischer CR, Mudgett MB, Sattely ES. 2018. N-hydroxy-pipecolic acid is a mobile metabolite that induces systemic disease resistance in *Arabidopsis*. *Proceedings of the National Academy of Sciences* **115**: E4920-E4929.

Christmann A, Grill E, Huang J. 2013. Hydraulic signals in long-distance signaling. *Current Opinion in Plant Biology* **16**: 293-300.

Christmann A, Hoffmann T, Teplova I, Grill E, Müller A. 2005. Generation of Active Pools of Abscisic Acid Revealed by *In Vivo* Imaging of Water-Stressed *Arabidopsis*. *Plant Physiology* **137**: 209-219.

Coninck BD, Timmermans P, Vos C, Cammue BP, Kazan K. 2015. What lies beneath: belowground defense strategies in plants. *Trends in Plant Science* **20**: 91-101.

Daudi A, O'Brien JA. 2012. Detection of Hydrogen Peroxide by DAB Staining in *Arabidopsis* Leaves. *Bio-protocol* **2**: e263.

Dean JV, Delaney SP. 2008. Metabolism of salicylic acid in wild-type, *ugt74f1* and *ugt74f2* glucosyltransferase mutants of *Arabidopsis thaliana*. *Physiologia Plantarum* **132**: 417-425.

Dean JV, Mohammed LA, Fitzpatrick T. 2005. The formation, vacuolar localization, and tonoplast transport of salicylic acid glucose conjugates in tobacco cell suspension cultures. *Planta* **221**: 287-296.

Deeken R, Ache P, Kajahn I, Klinkenberg J, Bringmann G, Hedrich R. 2008. Identification of *Arabidopsis thaliana* phloem RNAs provides a search criterion for phloem-based transcripts hidden in complex datasets of microarray experiments. *The Plant Journal* **55**: 746-759.

Dempsey DA, Klessig DF. 2017. How does the multifaceted plant hormone salicylic acid combat disease in plants and are similar mechanisms utilized in humans? *BMC Biology* **15**: 23.

Dempsey DA, Vlot AC, Wildermuth MC, Klessig DF. 2011. Salicylic Acid Biosynthesis and Metabolism. *The Arabidopsis Book* **2011**: e0156.

Ding P, Rekhter D, Ding Y, Feussner K, Busta L, Haroth S, Xu S, Li X, Jetter R, Feussner I *et al.* 2016. Characterization of a Pipecolic Acid Biosynthesis Pathway Required for Systemic Acquired Resistance. *The Plant Cell* **28**: 2603-2615.

Ding S, Zhang B, Qin F. 2015. *Arabidopsis* RZFP34/CHYR1, a Ubiquitin E3 Ligase, Regulates Stomatal Movement and Drought Tolerance via SnRK2.6-Mediated Phosphorylation. *The Plant Cell* **27**: 3228-3244.

Dodd IC. 2005. Root-to-shoot signalling: Assessing the roles of 'up' in the up and down world of long-distance signalling *in planta*. *Plant and Soil* **274**: 251-270.

Dubiella U, Seybold H, Durian G, Komander E, Lassig R, Witte C-P, Schulze WX, Romeis T. 2013. Calcium-dependent protein kinase/NADPH oxidase activation circuit is required for rapid defense signal propagation. *Proceedings of the National Academy of Sciences* **110**: 8744-8749.

Dunand C, Crèvecoeur M, Penel C. 2007. Distribution of superoxide and hydrogen peroxide in *Arabidopsis* root and their influence on root development: possible interaction with peroxidases. *New Phytologist* **174**: 332-341.

Durner J, Klessig DF. 1996. Salicylic Acid Is a Modulator of Tobacco and Mammalian Catalases. *Journal of Biological Chemistry* **271**: 28492-28501.

Durrant W, Dong X. 2004. Systemic Acquired Resistance. *Annual Review of Phytopathology* **42**: 185-209.

Dusa A. 2018. venn: Draw Venn Diagrams. *https://cran.r-project. org/web/packages/venn/index.html (accessed 08/28/2018)*.

Emsley P, Lohkamp B, Scott WG, Cowtan K. 2010. Features and development of *Coot*. *Acta Crystallographica Section D* **66**: 486-501.

Fang FC. 2011. Antimicrobial Actions of Reactive Oxygen Species. *mBio* **2**: e00141-11.

Fauser F, Schiml S, Puchta H. 2014. Both CRISPR/Cas-based nucleases and nickases can be used efficiently for genome engineering in *Arabidopsis thaliana*. *The Plant Journal* **79**: 348-359.

Fu ZQ, Dong X. 2013. Systemic Acquired Resistance: Turning Local Infection into Global Defense. *Annual Review of Plant Biology* **64**: 839-863.

Gachon CM, Langlois-Meurinne M, Saindrenan P. 2005. Plant secondary metabolism glycosyltransferases: the emerging functional analysis. *Trends in Plant Science* **10**: 542-549.

Gadjev I, Vanderauwera S, Gechev TS, Laloi C, Minkov IN, Shulaev V, Apel K, Inzé D, Mittler R, Van Breusegem F. 2006. Transcriptomic Footprints Disclose Specificity of Reactive Oxygen Species Signaling in *Arabidopsis*. *Plant Physiology* **141**: 436-445.

Gaffney T, Friedrich L, Vernooij B, Negrotto D, Nye G, Uknes S, Ward E, Kessmann H, Ryals J. 1993. Requirement of Salicylic Acid for the Induction of Systemic Acquired Resistance. *Science* **261**: 754-756.

Galon Y, Nave R, Boyce JM, Nachmias D, Knight MR, Fromm H. 2008. Calmodulin-binding transcription activator (CAMTA) 3 mediates biotic defense responses in *Arabidopsis*. *FEBS Letters* **582**: 943-948.

Gaupels F, Spiazzi-Vandelle E, Yang D, Delledonne M. 2011. Detection of peroxynitrite accumulation in *Arabidopsis thaliana* during the hypersensitive defense response. *Nitric Oxide* **25**: 222-228.

George Thompson AM, Iancu CV, Neet KE, Dean JV, Choe J-y. 2017. Differences in salicylic acid glucose conjugations by UGT74F1 and UGT74F2 from *Arabidopsis thaliana*. *Scientific Reports* **7**: 46629.

Ghanem ME, Albacete A, Smigocki AC, Frébort I, Pospišilová H, Martinez-Andújar C, Acosta M, Sánchez-Bravo J, Lutts S, Dodd IC *et al.* **2010.** Root-synthesized cytokinins improve shoot growth and fruit yield in salinized tomato (*Solanum lycopersicum* L.) plants. *Journal of Experimental Botany* **62**: 125-140.

González-Pérez S, Gutiérrez J, García-García F, Osuna D, Dopazo J, Lorenzo O`, Revuelta JL, Arellano JB. 2011. Early Transcriptional Defense Responses in *Arabidopsis* Cell Suspension Culture under High-Light Conditions. *Plant Physiology* **156**: 1439-1456.

Grant JJ, Loake GJ. 2000. Role of reactive oxygen intermediates and cognate redox signaling in disease resistance. *Plant Physiology* **124**: 21-30.

Grubb CD, Zipp BJ, Kopycki J, Schubert M, Quint M, Lim E-K, Bowles DJ, Pedras MSC, Abel S. 2014. Comparative analysis of *Arabidopsis* UGT74 glucosyltransferases reveals a special role of UGT74C1 in glucosinolate biosynthesis. *The Plant Journal* **79**: 92-105.

Gruner K, Griebel T, Návarová H, Attaran E, Zeier J. 2013. Reprogramming of plants during systemic acquired resistance. *Frontiers in Plant Science* **4**: 252.

Gullner G, Komives T, Király L, Schröder P. 2018. Glutathione S-Transferase Enzymes in Plant-Pathogen Interactions. *Frontiers in Plant Science* **9**: 1836.

Guo P, Li Z, Huang P, Li B, Fang S, Chu J, Guo H. 2017. A Tripartite Amplification Loop Involving the Transcription Factor WRKY75, Salicylic Acid, and Reactive Oxygen Species Accelerates Leaf Senescence. *The Plant Cell* **29**: 2854-2870.

Guzmán P, Ecker JR. 1990. Exploiting the triple response of *Arabidopsis* to identify ethylene-related mutants. *The Plant Cell* **2**: 513-523.

Hartmann M, Kim D, Bernsdorff F, Ajami-Rashidi Z, Scholten N, Schreiber S, Zeier T, Schuck S, Reichel-Deland V, Zeier J. 2017. Biochemical Principles and Functional Aspects of Pipecolic Acid Biosynthesis in Plant Immunity. *Plant Physiology* **174**: 124-153.

Hartmann M, Zeier J. 2018. l-lysine metabolism to N-hydroxypipecolic acid: an integral immune-activating pathway in plants. *The Plant Journal* **96**: 5-21.

Hartmann M, Zeier J. 2019. N-hydroxypipecolic acid and salicylic acid: a metabolic duo for systemic acquired resistance. *Current Opinion in Plant Biology* **50**: 44-57.

Hartmann M, Zeier T, Bernsdorff F, Reichel-Deland V, Kim D, Hohmann M, Scholten N, Schuck S, Bräutigam A, Hölzel T *et al.* **2018.** Flavin Monooxygenase-Generated N-Hydroxypipecolic Acid Is a Critical Element of Plant Systemic Immunity. *Cell* **173**: 456-469.e16.

He Y-N, Peng J-S, Cai Y, Liu D-F, Guan Y, Yi H-Y, Gong J-M. 2017. Tonoplast-localized nitrate uptake transporters involved in vacuolar nitrate efflux and reallocation in *Arabidopsis*. *Scientific Reports* **7**: 6417.

Hellemans J, Mortier G, De Paepe A, Speleman F, Vandesompele J. 2007. qBase relative quantification framework and software for management and automated analysis of real-time quantitative PCR data. *Genome Biology* **8**: R19.

Hernández I, Munné-Bosch S. 2012. Naringenin inhibits seed germination and seedling root growth through a salicylic acid-independent mechanism in *Arabidopsis thaliana*. *Plant Physiology and Biochemistry* **61**: 24-28.

Herrera-Vásquez A, Salinas P, Holuigue L. 2015. Salicylic acid and reactive oxygen species interplay in the transcriptional control of defense genes expression. *Frontiers in Plant Science* **6**: 171.

Huang J, Gu M, Lai Z, Fan B, Shi K, Zhou Y-H, Yu J-Q, Chen Z. 2010. Functional Analysis of the *Arabidopsis PAL* Gene Family in Plant Growth, Development, and Response to Environmental Stress. *Plant Physiology* **153**: 1526-1538.

Huang T, Jander G, de Vos M. 2011. Non-protein amino acids in plant defense against insect herbivores: Representative cases and opportunities for further functional analysis. *Phytochemistry* **72**: 1531-1537.

Huang X-x, Zhu G-q, Liu Q, Chen L, Li Y-j, Hou B-k. 2018. Modulation of Plant Salicylic Acid-Associated Immune Responses via Glycosylation of Dihydroxybenzoic Acids. *Plant Physiology* **176**: 3103-3119.

Huot B, Yao J, Montgomery BL, He SY. 2014. Growth-Defense Tradeoffs in Plants: A Balancing Act to Optimize Fitness. *Molecular Plant* **7**: 1267-1287.

Idänheimo N, Gauthier A, Salojärvi J, Siligato R, Brosché M, Kollist H, Mähönen AP, Kangasjärvi J, Wrzaczek M. 2014. The *Arabidopsis thaliana* cysteine-rich receptor-like kinases CRK6 and CRK7 protect against apoplastic oxidative stress. *Biochemical and Biophysical Research Communications* **445**: 457-462.

Jabs T, Tschöpe M, Colling C, Hahlbrock K, Scheel D. 1997. Elicitor-stimulated ion fluxes and O_2^- from the oxidative burst are essential components in triggering defense gene activation and phytoalexin synthesis in parsley. *Proceedings of the National Academy of Sciences* **94**: 4800-4805.

Jibran R, Hunter DA, Dijkwel PP. 2013. Hormonal regulation of leaf senescence through integration of developmental and stress signals. *Plant Molecular Biology* **82**: 547-561.

Johnson SN, Erb M, Hartley SE. 2016. Roots under attack: contrasting plant responses to below- and aboveground insect herbivory. *New Phytologist* **210**: 413-418.

Jones, A. M. (2009). Plant-pathogen interactions: microbial pathogenesis, plant immunity and plant-pathogen crosstalk, Doctoral dissertation, UC Berkeley.

Kadota Y, Sklenar J, Derbyshire P, Stransfeld L, Asai S, Ntoukakis V, Jones JD, Shirasu K, Menke F, Jones A *et al.* **2014.** Direct Regulation of the NADPH Oxidase RBOHD by the PRR-Associated Kinase BIK1 during Plant Immunity. *Molecular Cell* **54**: 43-55.

Kelley LA, Mezulis S, Yates CM, Wass MN, Sternberg MJ. 2015. The Phyre2 web portal for protein modeling, prediction and analysis. *Nature Protocols* **10**: 845-858.

Khokon M, Okuma E, Hossain MA, Munemasa S, Uraji M, Nakamura Y, Mori IC, Murata Y. 2011. Involvement of extracellular oxidative burst in salicylic acid-induced stomatal closure in *Arabidopsis*. *Plant, Cell and Environment* **34**: 434-443.

Kim D, Langmead B, Salzberg SL. 2015. HISAT: a fast spliced aligner with low memory requirements. *Nature methods* **12**: 357-360.

Kim Y-O, Kang H. 2018. Comparative expression analysis of genes encoding metallothioneins in response to heavy metals and abiotic stresses in rice (*Oryza sativa*) and *Arabidopsis thaliana*. *Bioscience, Biotechnology, and Biochemistry* **82**: 1656-1665.

Kimura S, Hunter K, Vaahtera L, Tran C, Vaattovaara A, Rokka A, Christina Stolze S, Harzen A, Meißner L, Wilkens M *et al.* **2019.** CRK2-mediated control of ROS production by phosphorylation of the RBOHD C-terminus in *Arabidopsis*. *BioRxiv*.

Krinke O, Ruelland E, Valentová O, Vergnolle C, Renou J-P, Taconnat L, Flemr M, Burketová L, Zachowski A. 2007. Phosphatidylinositol 4-Kinase Activation Is an Early Response to Salicylic Acid in *Arabidopsis* Suspension Cells. *Plant Physiology* **144**: 1347-1359.

Kwak JM, Mori IC, Pei Z-M, Leonhardt N, Torres MA, Dangl JL, Bloom RE, Bodde S, Jones JD, Schroeder JI. 2003. NADPH oxidase AtrbohD and AtrbohF genes function in ROS-dependent ABA signaling in *Arabidopsis*. *The EMBO Journal* **22**: 2623-2633.

Lacombe B, Achard P. 2016. Long-distance transport of phytohormones through the plant vascular system. *Current Opinion in Plant Biology* **34**: 1-8.

Laflamme B, Middleton M, Lo T, Desveaux D, Guttman DS. 2016. Image-Based Quantification of Plant Immunity and Disease. *Molecular Plant-Microbe Interactions* **29**: 919-924.

Lagarde D, Basset M, Lepetit M, Conejero G, Gaymard F, Astruc S, Grignon C. 1996. Tissue-specific expression of *Arabidopsis* AKT1 gene is consistent with a role in K^+ nutrition. *The Plant Journal* **9**: 195-203.

Lairson L, Henrissat B, Davies G, Withers S. 2008. Glycosyltransferases: structures, functions, and mechanisms. *Annu. Rev. Biochem.* **77**: 521-555.

Larqué-Saavedra A, Martin-Mex R (2007) In: Hayat S, Ahmad A (ed), Effects of Salicylic Acid on the Bioproductivity of Plants, Springer Netherlands.

Li H, Handsaker B, Wysoker A, Fennell T, Ruan J, Homer N, Marth G, Abecasis G, Durbin R, Subgroup 1000GPDP. 2009. The Sequence Alignment/Map format and SAMtools. *Bioinformatics* **25**: 2078-2079.

Li W, Zhang F, Chang Y, Zhao T, Schranz ME, Wang G. 2015. Nicotinate O-Glucosylation Is an Evolutionarily Metabolic Trait Important for Seed Germination under Stress Conditions in *Arabidopsis thaliana*. *The Plant Cell* **27**: 1907-1924.

Li X, Svedin E, Mo H, Atwell S, Dilkes BP, Chapple C. 2014. Exploiting Natural Variation of Secondary Metabolism Identifies a Gene Controlling the Glycosylation Diversity of Dihydroxybenzoic Acids in *Arabidopsis thaliana*. *Genetics* **198**: 1267-1276.

Li Y, Baldauf S, Lim E-K, Bowles DJ. 2001. Phylogenetic Analysis of the UDP-glycosyltransferase Multigene Family of *Arabidopsis thaliana*. *Journal of Biological Chemistry* **276**: 4338-4343.

Libault M, Wan J, Czechowski T, Udvardi M, Stacey G. 2007. Identification of 118 *Arabidopsis* Transcription Factor and 30 Ubiquitin-Ligase Genes Responding to Chitin, a Plant-Defense Elicitor. *Molecular Plant-Microbe Interactions* **20**: 900-911.

Lim E-K, Bowles DJ. 2004. A class of plant glycosyltransferases involved in cellular homeostasis. *The EMBO Journal* **23**: 2915-2922.

Lim E-K, Doucet CJ, Li Y, Elias L, Worrall D, Spencer SP, Ross J, Bowles DJ. 2002. The Activity of *Arabidopsis* Glycosyltransferases toward Salicylic Acid, 4-Hydroxybenzoic Acid, and Other Benzoates. *Journal of Biological Chemistry* **277**: 586-592.

Liu G, Ji Y, Bhuiyan NH, Pilot G, Selvaraj G, Zou J, Wei Y. 2010. Amino acid homeostasis modulates salicylic acid-associated redox status and defense responses in *Arabidopsis*. *The Plant Cell* **22**: 3845-3863.

Liu X, Rockett KS, Kørner CJ, Pajerowska-Mukhtar KM. 2015. Salicylic acid signalling: new insights and prospects at a quarter-century milestone. *Essays in Biochemistry* **58**: 101-113.

Love MI, Huber W, Anders S. 2014. Moderated estimation of fold change and dispersion for RNA-seq data with DESeq2. *Genome Biology* **15**: 550.

Lu H, Greenberg JT, Holuigue L. 2016. Editorial: Salicylic Acid Signaling Networks. *Frontiers in Plant Science* **7**: 238.

Mackelprang R, Okrent RA, Wildermuth MC. 2017. Preference of *Arabidopsis thaliana* GH3.5 acyl amido synthetase for growth versus defense hormone acyl substrates is dictated by concentration of amino acid substrate aspartate. *Phytochemistry* **143**: 19-28.

Mair P, Wilcox RR. 2019. Robust statistical methods in R using the WRS2 package. *Behavior Research Methods*: 1-25.

Maksym, R. P. (2018). Arabidopsis small molecule glucosyltransferase UGT76B1 conjugates both ILA and SA and is essential for the root-driven control of defense marker genes in leaves, Doctoral dissertation, Ludwig-Maximilians-Universität München.

Maksym RP, Ghirardo A, Zhang W, von Saint Paul V, Lange B, Geist B, Hajirezaei M-R, Schnitzler J-P, Schäffner AR. 2018. The defense-related isoleucic acid differentially accumulates in *Arabidopsis* among branched-chain amino acid-related 2-hydroxy carboxylic acids. *Frontiers in Plant Science* **9**: 766.

Mamer OA, Reimer ML. 1992. On the mechanisms of the formation of L-alloisoleucine and the 2-hydroxy-3-methylvaleric acid stereoisomers from L-isoleucine in maple syrup urine disease patients and in normal humans. *Journal of Biological Chemistry* **267**: 22141-21477.

Martinoia E. 2018. Vacuolar Transporters - Companions on a Longtime Journey. *Plant Physiology* **176**: 1384-1407.

Maruri-López I, Aviles-Baltazar NY, Buchala A, Serrano M. 2019. Intra and Extracellular Journey of the Phytohormone Salicylic Acid. *Frontiers in Plant Science* **10**: 423.

Mehterov N, Balazadeh S, Hille J, Toneva V, Mueller-Roeber B, Gechev T. 2012. Oxidative stress provokes distinct transcriptional responses in the stress-tolerant *atr7* and stress-sensitive *loh2 Arabidopsis thaliana* mutants as revealed by multi-parallel quantitative real-time PCR analysis of ROS marker and antioxidant genes. *Plant Physiology and Biochemistry* **59**: 20-29.

Meßner B, Thulke O, Schäffner AR. 2003. *Arabidopsis* glucosyltransferases with activities toward both endogenous and xenobiotic substrates. *Planta* **217**: 138-146.

Métraux JP, Signer H, Ryals J, Ward E, Wyss-Benz M, Gaudin J, Raschdorf K, Schmid E, Blum W, Inverardi B. 1990. Increase in Salicylic Acid at the Onset of Systemic Acquired Resistance in Cucumber. *Science* **250**: 1004-1006.

Michniewicz M, Ho C-H, Enders TA, Floro E, Damodaran S, Gunther LK, Powers SK, Frick EM, Topp CN, Frommer WB *et al.* **2019.** TRANSPORTER OF IBA1 Links Auxin and Cytokinin to Influence Root Architecture. *Developmental Cell* **50**: 599-609.e4.

Miura K, Okamoto H, Okuma E, Shiba H, Kamada H, Hasegawa PM, Murata Y. 2013. SIZ1 deficiency causes reduced stomatal aperture and enhanced drought tolerance via controlling salicylic acid-induced accumulation of reactive oxygen species in *Arabidopsis*. *The Plant Journal* **73**: 91-104.

Morales J, Kadota Y, Zipfel C, Molina A, Torres M-A. 2016. The *Arabidopsis* NADPH oxidases RbohD and RbohF display differential expression patterns and contributions during plant immunity. *Journal of Experimental Botany* **67**: 1663-1676.

Morris K, Mackerness SAH, Page T, John CF, Murphy AM, Carr JP, Buchanan-Wollaston V. 2000. Salicylic acid has a role in regulating gene expression during leaf senescence. *The Plant Journal* **23**: 677-685.

Mur LA, Kenton P, Atzorn R, Miersch O, Wasternack C. 2006. The outcomes of concentration-specific interactions between salicylate and jasmonate signaling include synergy, antagonism, and oxidative stress leading to cell death. *Plant physiology* **140**: 249-262.

Návarová H, Bernsdorff F, Döring A-C, Zeier J. 2012. Pipecolic Acid, an Endogenous Mediator of Defense Amplification and Priming, Is a Critical Regulator of Inducible Plant Immunity. *The Plant cell* **24**: 5123-5141.

Nawrath C, Métraux J-P. 1999. Salicylic Acid Induction - Deficient Mutants of *Arabidopsis* Express *PR2* and *PR5* and Accumulate High Levels of Camalexin after Pathogen Inoculation. *The Plant Cell* **11**: 1393-1404.

Ngom B, Sarr I, Kimatu J, Mamati E, Kane NA. 2017. Genome-wide analysis of cytosine DNA methylation revealed salicylic acid promotes defense pathways over seedling development in pearl millet. *Plant Signaling & Behavior* **12**: e1356967.

Noctor G, Mhamdi A, Foyer CH. 2016. Oxidative stress and antioxidative systems: recipes for successful data collection and interpretation. *Plant, Cell & Environment* **39**: 1140-1160.

Norman JMV, Frederick RL, Sieburth LE. 2004. BYPASS1 Negatively Regulates a Root-Derived Signal that Controls Plant Architecture. *Current Biology* **14**: 1739-1746.

Notaguchi M, Okamoto S. 2015. Dynamics of long-distance signaling via plant vascular tissues. *Frontiers in Plant Science* **6**: 161.

Noutoshi Y, Okazaki M, Kida T, Nishina Y, Morishita Y, Ogawa T, Suzuki H, Shibata D, Jikumaru Y, Hanada A *et al.* **2012.** Novel Plant Immune-Priming Compounds Identified via High-Throughput Chemical Screening Target Salicylic Acid Glucosyltransferases in *Arabidopsis*. *The Plant Cell* **24**: 3795-3804.

Nuruzzaman M, Sharoni AM, Kikuchi S. 2013. Roles of NAC transcription factors in the regulation of biotic and abiotic stress responses in plants. *Frontiers in Microbiology* **4**: 248.

Offen W, Martinez-Fleites C, Yang M, Kiat-Lim E, Davis BG, Tarling CA, Ford CM, Bowles DJ, Davies GJ. 2006. Structure of a flavonoid glucosyltransferase reveals the basis for plant natural product modification. *The EMBO Journal* **25**: 1396-1405.

Okamoto M, Tsuboi Y, Chikayama E, Kikuchi J, Hirayama T. 2009. Metabolic movement upon abscisic acid and salicylic acid combined treatments. *Plant Biotechnology* **26**: 551-560.

Okumura K-i, Goh T, Toyokura K, Kasahara H, Takebayashi Y, Mimura T, Kamiya Y, Fukaki H. 2013. GNOM/FEWER ROOTS is Required for the Establishment of an Auxin Response Maximum for *Arabidopsis* Lateral Root Initiation. *Plant and Cell Physiology* **54**: 406-417.

Orman-Ligeza B, Parizot B, de Rycke R, Fernandez A, Himschoot E, Van Breusegem F, Bennett MJ, Périlleux C, Beeckman T, Draye X. 2016. RBOH-mediated ROS production facilitates lateral root emergence in *Arabidopsis*. *Development* **143**: 3328-3339.

Overmyer K, Brosch M, Kangasjärvi J. 2003. Reactive oxygen species and hormonal control of cell death. *Trends in Plant Science* **8**: 335-342.

Pandey V, Awasthi M, Singh S, Tiwari S, Dwivedi U. 2017. A Comprehensive Review on Function and Application of Plant Peroxidases. *Biochemistry & Analytical Biochemistry* **6**: 308.

Park S-W, Kaimoyo E, Kumar D, Mosher S, Klessig DF. 2007. Methyl Salicylate Is a Critical Mobile Signal for Plant Systemic Acquired Resistance. *Science* **318**: 113-116.

Pasternak T, Groot EP, Kazantsev FV, Teale W, Omelyanchuk N, Kovrizhnykh V, Palme K, Mironova VV. 2019. Salicylic Acid Affects Root Meristem Patterning via Auxin Distribution in a Concentration-Dependent Manner. *Plant Physiology* **180**: 1725-1739.

Payne RM, Xu D, Foureau E, Carqueijeiro MIST, Oudin A, de Bernonville TD, Novak V, Burow M, Olsen C-E, Jones DM *et al.* **2017.** An NPF transporter exports a central monoterpene indole alkaloid intermediate from the vacuole. *Nature Plants* **3**: 16208.

Pertea M, Pertea GM, Antonescu CM, Chang T-C, Mendell JT, Salzberg SL. 2015. StringTie enables improved reconstruction of a transcriptome from RNA-seq reads. *Nature Biotechnology* **33**: 290-295.

Pieterse CM, Leon-Reyes A, Van der Ent S, Van Wees SC. 2009. Networking by small-molecule hormones in plant immunity. *Nature Chemical Biology* **5**: 308.

Pieterse CM, van Loon LC. 1999. Salicylic acid-independent plant defence pathways. *Trends in Plant Science* **4**: 52-58.

Pike S, Gao F, Kim MJ, Kim SH, Schachtman DP, Gassmann W. 2013. Members of the NPF3 Transporter Subfamily Encode Pathogen-Inducible Nitrate/Nitrite Transporters in Grapevine and *Arabidopsis*. *Plant and Cell Physiology* **55**: 162-170.

Podebrad F, Heil M, Leib S, Geier B, Beck T, Mosandl A, Sewell AC, Böhles H. 1997. Analytical approach in diagnosis of inherited metabolic diseases: Maple syrup urine disease (MSUD) - simultaneous analysis of metabolites in urine by enantioselective multidimensional capillary gas chromatography-mass spectrometry (enantio-MDGC-MS). *Journal of High Resolution Chromatography* **20**: 355-362.

Pogány M, von Rad U, Grün S, Dongó A, Pintye A, Simoneau P, Bahnweg G, Kiss L, Barna B, Durner J. 2009. Dual Roles of Reactive Oxygen Species and NADPH Oxidase RBOHD in an *Arabidopsis*-Alternaria Pathosystem. *Plant Physiology* **151**: 1459-1475.

Qi J, Wang J, Gong Z, Zhou J-M. 2017. Apoplastic ROS signaling in plant immunity. *Current Opinion in Plant Biology* **38**: 92-100.

Queval G, Thominet D, Vanacker H, Miginiac-Maslow M, Gakière B, Noctor G. 2009. H_2O_2-Activated Up-Regulation of Glutathione in *Arabidopsis* Involves Induction of Genes Encoding Enzymes Involved in Cysteine Synthesis in the Chloroplast. *Molecular Plant* **2**: 344-356.

Quiel JA, Bender J. 2003. Glucose Conjugation of Anthranilate by the *Arabidopsis* UGT74F2 Glucosyltransferase Is Required for Tryptophan Mutant Blue Fluorescence. *Journal of Biological Chemistry* **278**: 6275-6281.

Rahman A, Bannigan A, Sulaman W, Pechter P, Blancaflor EB, Baskin TI. 2007. Auxin, actin and growth of the *Arabidopsis thaliana* primary root. *The Plant Journal* **50**: 514-528.

Rajjou L, Belghazi M, Huguet R, Robin C, Moreau A, Job C, Job D. 2006. Proteomic Investigation of the Effect of Salicylic Acid on *Arabidopsis* Seed Germination and Establishment of Early Defense Mechanisms. *Plant Physiology* **141**: 910-923.

Rasheed S, Bashir K, Matsui A, Tanaka M, Seki M. 2016. Transcriptomic Analysis of Soil-Grown *Arabidopsis thaliana* Roots and Shoots in Response to a Drought Stress. *Frontiers in Plant Science* **7**: 180.

Ratzinger A, Riediger N, von Tiedemann A, Karlovsky P. 2009. Salicylic acid and salicylic acid glucoside in xylem sap of *Brassica napus* infected with *Verticillium longisporum*. *Journal of Plant Research* **122**: 571-579.

Rekhter D, Lüdke D, Ding Y, Feussner K, Zienkiewicz K, Lipka V, Wiermer M, Zhang Y, Feussner I. 2019. Isochorismate-derived biosynthesis of the plant stress hormone salicylic acid. *Science* **365**: 498-502.

Ren Y, Miao M, Meng Y, Cao J, Fan T, Yue J, Xiao F, Liu Y, Cao S. 2018. DFR1-Mediated Inhibition of Proline Degradation Pathway Regulates Drought and Freezing Tolerance in *Arabidopsis*. *Cell Reports* **23**: 3960-3974.

Rivas-San Vicente M, Plasencia J. 2011. Salicylic acid beyond defence: its role in plant growth and development. *Journal of Experimental Botany* **62**: 3321-3338.

Rodrigues A, Santiago J, Rubio S, Saez A, Osmont KS, Gadea J, Hardtke CS, Rodriguez PL. 2009. The Short-Rooted Phenotype of the brevis radix Mutant Partly Reflects Root Abscisic Acid Hypersensitivity. *Plant Physiology* **149**: 1917-1928.

Ross J, Li Y, Lim E-K, Bowles DJ. 2001. Higher plant glycosyltransferases. *Genome Biology* **2**: reviews3004.1.

Rushton PJ, Somssich IE, Ringler P, Shen QJ. 2010. WRKY transcription factors. *Trends in Plant Science* **15**: 247-258.

Sabater B, Martín M. 2013. Hypothesis: increase of the ratio singlet oxygen plus superoxide radical to hydrogen peroxide changes stress defense response to programmed leaf death. *Frontiers in Plant Science* **4**: 479.

Saema S, Rahman Lu, Singh R, Niranjan A, Ahmad IZ, Misra P. 2016. Ectopic overexpression of WsSGTL1, a sterol glucosyltransferase gene in *Withania somnifera*, promotes growth, enhances glycowithanolide and provides tolerance to abiotic and biotic stresses. *Plant Cell Reports* **35**: 195-211.

von Saint Paul V, Zhang W, Kanawati B, Geist B, Faus-Keßler T, Schmitt-Kopplin P, Schäffner AR. 2011. The *Arabidopsis* Glucosyltransferase UGT76B1 Conjugates Isoleucic Acid and Modulates Plant Defense and Senescence. *The Plant Cell* **23**: 4124-4145.

Scarpeci TE, Zanor MI, Mueller-Roeber B, Valle EM. 2013. Overexpression of *AtWRKY30* enhances abiotic stress tolerance during early growth stages in *Arabidopsis thaliana*. *Plant Molecular Biology* **83**: 265-277.

Schachtman DP, Goodger JQ. 2008. Chemical root to shoot signaling under drought. *Trends in Plant Science* **13**: 281-287.

Schneidman-Duhovny D, Inbar Y, Nussinov R, Wolfson HJ. 2005. PatchDock and SymmDock: servers for rigid and symmetric docking. *Nucleic Acids Research* **33**: W363-W367.

Scholl RL, May ST, Ware DH. 2000. Seed and Molecular Resources for *Arabidopsis*. *Plant Physiology* **124**: 1477-1480.

Schuler MA, Werck-Reichhart D. 2003. Functional Genomics of P450S. *Annual Review of Plant Biology* **54**: 629-667.

Sessions A, Burke E, Presting G, Aux G, McElver J, Patton D, Dietrich B, Ho P, Bacwaden J, Ko C *et al.* 2002. A High-Throughput *Arabidopsis* Reverse Genetics System. *The Plant Cell* **14**: 2985-2994.

Seyfferth C, Tsuda K. 2014. Salicylic acid signal transduction: the initiation of biosynthesis, perception and transcriptional reprogramming. *Frontiers in Plant Science* **5**: 697.

Shabala S, White RG, Djordjevic MA, Ruan Y-L, Mathesius U. 2016. Root-to-shoot signalling: integration of diverse molecules, pathways and functions. *Functional Plant Biology* **43**: 87-104.

Shah J. 2003. The salicylic acid loop in plant defense. *Current Opinion in Plant Biology* **6**: 365-371.

Shah J, Chaturvedi R, Chowdhury Z, Venables B, Petros RA. 2014. Signaling by small metabolites in systemic acquired resistance. *The Plant Journal* **79**: 645-658.

Shan L, He P. 2018. Pipped at the Post: Pipecolic Acid Derivative Identified as SAR Regulator. *Cell* **173**: 286-287.

Singh A, Lim G-H, Kachroo P. 2017. Transport of chemical signals in systemic acquired resistance. *Journal of Integrative Plant Biology* **59**: 336-344.

Singh KB, Foley RC, Oñate-Sánchez L. 2002. Transcription factors in plant defense and stress responses. *Current Opinion in Plant Biology* **5**: 430-436.

Singh R, Singh S, Parihar P, Mishra RK, Tripathi DK, Singh VP, Chauhan DK, Prasad SM. 2016. Reactive Oxygen Species (ROS): Beneficial Companions of Plants' Developmental Processes. *Frontiers in Plant Science* **7**: 1299.

Song JT. 2006. Induction of a salicylic acid glucosyltransferase, AtSGT1, is an early disease response in *Arabidopsis thaliana*. *Molecules and Cells (Springer Science and Business Media BV)* **22**: 233-238.

Song JT, Koo YJ, Seo HS, Kim MC, Choi YD, Kim JH. 2008. Overexpression of *AtSGT1*, an *Arabidopsis* salicylic acid glucosyltransferase, leads to increased susceptibility to *Pseudomonas syringae*. *Phytochemistry* **69**: 1128-1134.

Spiess A. 2018. qpcR: Modelling and analysis of real-time PCR data. *R package version 1.4-1. https://CRAN.R-project.org/package=qpcR*.

Staswick PE, Su W, Howell SH. 1992. Methyl jasmonate inhibition of root growth and induction of a leaf protein are decreased in an *Arabidopsis thaliana* mutant. *Proceedings of the National Academy of Sciences* **89**: 6837-6840.

Staswick PE, Tiryaki I, Rowe ML. 2002. Jasmonate Response Locus JAR1 and Several Related *Arabidopsis* Genes Encode Enzymes of the Firefly Luciferase Superfamily That Show Activity on Jasmonic, Salicylic, and Indole-3-Acetic Acids in an Assay for Adenylation. *The Plant Cell* **14**: 1405-1415.

Steenackers W, Cesarino I, Klima P, Quareshy M, Vanholme R, Corneillie S, Kumpf RP, Van de Wouwer D, Ljung K, Goeminne G *et al.* **2016.** The Allelochemical MDCA Inhibits Lignification and Affects Auxin Homeostasis. *Plant Physiology* **172**: 874-888.

Straus MR, Rietz S, Ver Loren van Themaat E, Bartsch M, Parker JE. 2010. Salicylic acid antagonism of EDS1-driven cell death is important for immune and oxidative stress responses in *Arabidopsis*. *The Plant Journal* **62**: 628-640.

Sun T, Busta L, Zhang Q, Ding P, Jetter R, Zhang Y. 2018. TGACG-BINDING FACTOR 1 (TGA1) and TGA4 regulate salicylic acid and pipecolic acid biosynthesis by modulating the expression of *SYSTEMIC ACQUIRED RESISTANCE DEFICIENT1* (*SARD1*) and *CALMODULIN-BINDING PROTEIN60g* (*CBP60g*). *New Phytologist* **217**: 344-354.

Sun T, Zhang Y, Li Y, Zhang Q, Ding Y, Zhang Y. 2015. ChIP-seq reveals broad roles of SARD1 and CBP60g in regulating plant immunity. *Nature Communications* **6**: 10159.

Takei K, Takahashi T, Sugiyama T, Yamaya T, Sakakibara H. 2002. Multiple routes communicating nitrogen availability from roots to shoots: a signal transduction pathway mediated by cytokinin. *Journal of Experimental Botany* **53**: 971-977.

Tal I, Zhang Y, Jørgensen ME, Pisanty O, Barbosa IC, Zourelidou M, Regnault T, Crocoll C, Olsen CE, Weinstain R *et al.* **2016.** The *Arabidopsis* NPF3 protein is a GA transporter. *Nature Communications* **7**: 11486.

Thieme CJ, Rojas-Triana M, Stecyk E, Schudoma C, Zhang W, Yang L, Miñambres M, Walther D, Schulze WX, Paz-Ares J *et al.* **2015.** Endogenous *Arabidopsis* messenger RNAs transported to distant tissues. *Nature Plants* **1**: 15025.

Thilmony R, Underwood W, He SY. 2006. Genome-wide transcriptional analysis of the *Arabidopsis thaliana* interaction with the plant pathogen *Pseudomonas syringae pv. tomato* DC3000 and the human pathogen *Escherichia coli* O157:H7. *The Plant Journal* **46**: 34-53.

Tiwari P, Sangwan RS, Sangwan NS. 2016. Plant secondary metabolism linked glycosyltransferases: An update on expanding knowledge and scopes. *Biotechnology Advances* **34**: 714-739.

Torres MA, Jones JD, Dangl JL. 2005. Pathogen-induced, NADPH oxidase-derived reactive oxygen intermediates suppress spread of cell death in *Arabidopsis thaliana*. *Nature Genetics* **37**: 1130-1134.

Torres MA, Jones JD, Dangl JL. 2006. Reactive oxygen species signaling in response to pathogens. *Plant Physiology* **141**: 373-378.

Tsukagoshi H. 2016. Control of root growth and development by reactive oxygen species. *Current Opinion in Plant Biology* **29**: 57-63.

Vaahtera L, Brosché M, Wrzaczek M, Kangasjärvi J. 2014. Specificity in ROS signaling and transcript signatures. *Antioxidants and Redox Signaling* **21**: 1422-1441.

Vaca E, Behrens C, Theccanat T, Choe J-Y, Dean JV. 2017. Mechanistic differences in the uptake of salicylic acid glucose conjugates by vacuolar membrane-enriched vesicles isolated from *Arabidopsis thaliana*. *Physiologia Plantarum* **161**: 322-338.

Vandelle E, Delledonne M. 2011. Peroxynitrite formation and function in plants. *Plant Science* **181**: 534-539.

Vernooij B, Friedrich L, Morse A, Reist R, Kolditz-Jawhar R, Ward E, Uknes S, Kessmann H, Ryals J. 1994. Salicylic Acid Is Not the Translocated Signal Responsible for Inducing Systemic Acquired Resistance but Is Required in Signal Transduction. *The Plant Cell* **6**: 959-965.

Vidhyasekaran P (2015) Salicylic acid signaling in plant innate immunity. In P Vidhyasekaran (ed), Plant Hormone Signaling Systems in Plant Innate Immunity. Signaling and Communication in Plant Series, 2, Springer, Dordrecht, The Netherlands, 27-122

Vlot AC, Dempsey DA, Klessig DF. 2009. Salicylic Acid, a Multifaceted Hormone to Combat Disease. *Annual Review of Phytopathology* **47**: 177-206.

Vogt T, Jones P. 2000. Glycosyltransferases in plant natural product synthesis: characterization of a supergene family. *Trends in Plant Science* **5**: 380-386.

Waese J, Fan J, Pasha A, Yu H, Fucile G, Shi R, Cumming M, Kelley LA, Sternberg MJ, Krishnakumar V *et al.* **2017.** ePlant: Visualizing and Exploring Multiple Levels of Data for Hypothesis Generation in Plant Biology. *The Plant Cell* **29**: 1806-1821.

Wang C, Liu R, Lim G-H, de Lorenzo L, Yu K, Zhang K, Hunt AG, Kachroo A, Kachroo P. 2018a. Pipecolic acid confers systemic immunity by regulating free radicals. *Science Advances* **4**: eaar4509.

Wang D, Amornsiripanitch N, Dong X. 2006. A Genomic Approach to Identify Regulatory Nodes in the Transcriptional Network of Systemic Acquired Resistance in Plants. *PLOS Pathogens* **2**: 1-9.

Wang J, Hou B. 2009. Glycosyltransferases: key players involved in the modification of plant secondary metabolites. *Frontiers of Biology in China* **4**: 39-46.

Wang K, He J, Zhao Y, Wu T, Zhou X, Ding Y, Kong L, Wang X, Wang Y, Li J *et al.* **2018b.** EAR1 Negatively Regulates ABA Signaling by Enhancing 2C Protein Phosphatase Activity. *The Plant Cell* **30**: 815-834.

Wanke D, Kolukisaoglu H. 2010. An update on the ABCC transporter family in plants: many genes, many proteins, but how many functions? *Plant Biology* **12**: 15-25.

Warnes GR, Bolker B, Bonebakker L, Gentleman R, Liaw WHA, Lumley T, Maechler M, Magnusson A, Moeller S, Schwartz M *et al.* **2016.** Various R Programming Tools for Plotting Data. *https://cran.r-project.org/web/packages/gplots/index.html (accessed 06/08/2018)*.

Westfall CS, Sherp AM, Zubieta C, Alvarez S, Schraft E, Marcellin R, Ramirez L, Jez JM. 2016. *Arabidopsis thaliana* GH3.5 acyl acid amido synthetase mediates metabolic crosstalk in auxin and salicylic acid homeostasis. *Proceedings of the National Academy of Sciences* **113**: 13917-13922.

Wildermuth MC, Dewdney J, Wu G, Ausubel FM. 2001. Isochorismate synthase is required to synthesize salicylic acid for plant defence. *Nature* **414**: 562-565.

Yan S, Dong X. 2014. Perception of the plant immune signal salicylic acid. *Current Opinion in Plant Biology* **20**: 64-68.

Yeh Y-H, Chang Y-H, Huang P-Y, Huang J-B, Zimmerli L. 2015. Enhanced *Arabidopsis* pattern-triggered immunity by overexpression of cysteine-rich receptor-like kinases. *Frontiers in Plant Science* **6**: 322.

Yin, R. (2010). *Arabidopsis* flavonoid glycosylation impacts on phenylpropanoid biosynthesis and plant growth, Doctoral dissertation, Ludwig-Maximilian-Universität München.

Yokawa K, Kagenishi T, Kawano T, Mancuso S, Baluška F. 2011. Illumination of *Arabidopsis* roots induces immediate burst of ROS production. *Plant Signaling & Behavior* **6**: 1460-1464.

Yonekura-Sakakibara K, Hanada K. 2011. An evolutionary view of functional diversity in family 1 glycosyltransferases. *The Plant Journal* **66**: 182-193.

Zeier J. 2013. New insights into the regulation of plant immunity by amino acid metabolic pathways. *Plant, Cell & Environment* **36**: 2085-2103.

Zhang K, Halitschke R, Yin C, Liu C-J, Gan S-S. 2013. Salicylic acid 3-hydroxylase regulates *Arabidopsis* leaf longevity by mediating salicylic acid catabolism. *Proceedings of the National Academy of Sciences* **110**: 14807-14812.

Zhang Y, Fan W, Kinkema M, Li X, Dong X. 1999. Interaction of NPR1 with basic leucine zipper protein transcription factors that bind sequences required for salicylic acid induction of the *PR1* gene. *Proceedings of the National Academy of Sciences* **96**: 6523-6528.

Zhang Y, Li X. 2019. Salicylic acid: biosynthesis, perception, and contributions to plant immunity. *Current Opinion in Plant Biology* **50**: 29-36.

Zhang Y, Xu S, Ding P, Wang D, Cheng YT, He J, Gao M, Xu F, Li Y, Zhu Z *et al.* **2010.** Control of salicylic acid synthesis and systemic acquired resistance by two members of a plant-specific family of transcription factors. *Proceedings of the National Academy of Sciences* **107**: 18220-18225.

Zhang Y, Zhao L, Zhao J, Li Y, Wang J, Guo R, Gan S, Liu C-J, Zhang K. 2017. S5H/DMR6 encodes a salicylic acid 5-hydroxylase that fine-tunes salicylic acid homeostasis. *Plant Physiology* **175**: 1082-1093.

Zhang Z, Li Q, Li Z, Staswick PE, Wang M, Zhu Y, He Z. 2007. Dual Regulation Role of GH3.5 in Salicylic Acid and Auxin Signaling during *Arabidopsis-Pseudomonas syringae* Interaction. *Plant Physiology* **145**: 450-464.

6 Supplementary data

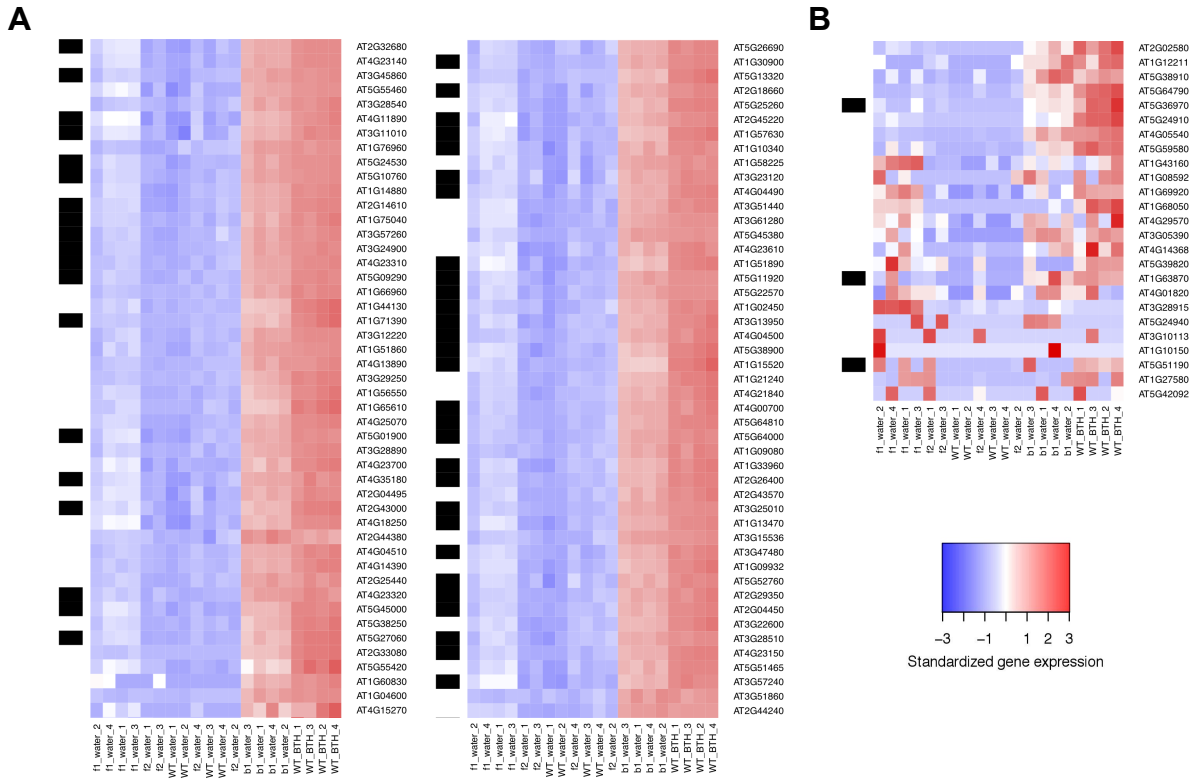

Fig. S1: Heatmap of gene regulation of* ugt *mutants

Induced genes of the ugt *single mutants and wild-type BTH-treated samples were compared in their gene expression. Therefore, genes with a log2 fold change greater or equal to four (p.adj. ≤ 0.001 for* ugt74f1 *or* ugt74f2*; p.adj. ≤ 1e-60 for* ugt76b1*) were chosen. The colour code from blue to red shows lowest to high intensity of standardized gene induction in corresponding sample. Genes labelled with a black bars are annotated to GO term annotations "defence". **A:** Genes showing general observed pattern with highest expression of genes in* ugt76b1 *and BTH-treated wild type. **B:** Genes starting to diverge from this general pattern.*

Tab. S1: Enriched GO terms of genes up-regulated in the* ugt76b1 (*b1*) *and* ugt74f1 (*f1*) *mutant

b1	IDs	p.adj.	*f1*	IDs	p.adj.
GO:0006952	defense response	1.60E-191	GO:0006952	defense response	4.66E-124
GO:0002376	immune system process	1.30E-163	GO:0009607	response to biotic stimulus	4.33E-105
GO:0045087	innate immune response	1.13E-150	GO:0006950	response to stress	5.65E-105
GO:0006955	immune response	1.57E-149	GO:0043207	response to external biotic stimulus	1.02E-104
GO:0009814	defense response, incompatible interaction	2.69E-149	GO:0051707	response to other organism	1.02E-104
GO:0009627	systemic acquired resistance	6.44E-145	GO:0002376	immune system process	2.26E-95
GO:0009607	response to biotic stimulus	3.38E-139	GO:0050896	response to stimulus	3.78E-91
GO:0043207	response to external biotic stimulus	1.22E-138	GO:1901700	response to oxygen-containing compound	3.78E-91
GO:0051707	response to other organism	1.22E-138	GO:0010033	response to organic substance	3.42E-86
GO:0042493	response to drug	1.58E-133	GO:0042221	response to chemical	4.67E-86
GO:0098542	defense response to other organism	6.95E-133	GO:0009605	response to external stimulus	8.24E-86
GO:0006950	response to stress	5.82E-123	GO:0009620	response to fungus	1.70E-84
GO:0009605	response to external stimulus	1.70E-109	GO:0001101	response to acid chemical	1.78E-84
GO:0009697	salicylic acid biosynthetic process	1.47E-105	GO:0042493	response to drug	1.78E-84
GO:0031347	regulation of defense response	1.50E-105	GO:0098542	defense response to other organism	3.11E-84
GO:0034976	response to endoplasmic reticulum stress	9.73E-103	GO:0045087	innate immune response	6.91E-79
GO:0009696	salicylic acid metabolic process	3.14E-102	GO:0006955	immune response	2.69E-78
GO:0080134	regulation of response to stress	3.71E-102	GO:0010200	response to chitin	6.53E-74
GO:0046677	response to antibiotic	4.73E-101	GO:0050832	defense response to fungus	1.41E-73
GO:0046189	phenol-containing compound biosynthetic process	6.45E-101	GO:0051704	multi-organism process	2.25E-72
GO:0051704	multi-organism process	2.87E-100	GO:0010243	response to organonitrogen compound	5.38E-72
GO:0018958	phenol-containing compound metabolic process	1.02E-97	GO:0009814	defense response, incompatible interaction	2.30E-69
GO:0050896	response to stimulus	3.01E-97	GO:0042446	hormone biosynthetic process	2.02E-66
GO:0033554	cellular response to stress	5.17E-97	GO:0009725	response to hormone	1.04E-65
GO:0042537	benzene-containing compound metabolic process	1.23E-95	GO:0009719	response to endogenous stimulus	1.76E-65
GO:0009751	response to salicylic acid	3.26E-89	GO:0031347	regulation of defense response	3.64E-65
GO:0071236	cellular response to antibiotic	3.83E-89	GO:0080134	regulation of response to stress	4.95E-65
GO:1901700	response to oxygen-containing compound	4.53E-89	GO:0042445	hormone metabolic process	6.57E-65
GO:0071446	cellular response to SA stimulus	3.91E-88	GO:0071229	cellular response to acid chemical	7.08E-65
GO:0010200	response to chitin	5.29E-88	GO:0009627	systemic acquired resistance	1.31E-63
GO:0009863	SA mediated signaling pathway	1.41E-87	GO:1901698	response to nitrogen compound	1.58E-59
GO:0035690	cellular response to drug	1.30E-86	GO:0048583	regulation of response to stimulus	1.68E-58

b1	IDs	p.adj.	*f1*	IDs	p.adj.
GO:0010243	response to organonitrogen compound	1.69E-86	GO:0009753	response to jasmonic acid	2.37E-58
GO:0051716	cellular response to stimulus	2.13E-86	GO:0010817	regulation of hormone levels	1.63E-57
GO:0017000	antibiotic biosynthetic process	1.11E-85	GO:0007165	signal transduction	3.40E-56
GO:0031348	negative regulation of defense response	2.34E-85	GO:0009751	response to salicylic acid	8.84E-56
GO:0002682	regulation of immune system process	1.70E-84	GO:0002682	regulation of immune system process	1.52E-54
GO:0048583	regulation of response to stimulus	2.59E-84	GO:0045088	regulation of innate immune response	3.66E-54
GO:0050776	regulation of immune response	3.82E-84	GO:1901701	cellular response to oxygen-containing compound	4.92E-54
GO:0045088	regulation of innate immune response	1.40E-83	GO:0050776	regulation of immune response	5.86E-54
GO:0071229	cellular response to acid chemical	1.71E-83	GO:0071236	cellular response to antibiotic	9.14E-54
GO:0050832	defense response to fungus	4.39E-82	GO:0009863	SA mediated signaling pathway	3.75E-53
GO:0010941	regulation of cell death	1.53E-81	GO:0071446	cellular response to SA stimulus	6.56E-53
GO:0008219	cell death	1.97E-81	GO:0023052	signaling	8.02E-53
GO:0012501	programmed cell death	1.15E-80	GO:0032870	cellular response to hormone stimulus	2.12E-52
GO:0042221	response to chemical	1.89E-79	GO:0071495	cellular response to endogenous stimulus	4.44E-52
GO:0009626	plant-type hypersensitive response	3.04E-79	GO:0010941	regulation of cell death	5.26E-52
GO:0034050	host programmed cell death induced by symbiont	4.72E-79	GO:0012501	programmed cell death	6.28E-52
GO:0010363	regulation of plant-type hypersensitive response	2.54E-78	GO:0008219	cell death	9.79E-52
GO:0009620	response to fungus	2.66E-78	GO:0007154	cell communication	2.76E-51
GO:0006612	protein targeting to membrane	1.04E-77	GO:0070887	cellular response to chemical stimulus	4.87E-51
GO:0080135	regulation of cellular response to stress	2.00E-77	GO:0051716	cellular response to stimulus	5.57E-51
GO:0043067	regulation of programmed cell death	2.26E-77	GO:0035690	cellular response to drug	6.94E-51
GO:0072657	protein localization to membrane	4.05E-77	GO:0080135	regulation of cellular response to stress	2.83E-50
GO:0090150	establishment of protein localization to membrane	4.05E-77	GO:0043067	regulation of programmed cell death	4.14E-50
GO:0042446	hormone biosynthetic process	1.10E-76	GO:0010363	regulation of plant-type hypersensitive response	5.63E-50
GO:0010033	response to organic substance	1.55E-72	GO:0006612	protein targeting to membrane	1.23E-49
GO:0001101	response to acid chemical	1.92E-72	GO:0009626	plant-type hypersensitive response	1.41E-49
GO:0016999	antibiotic metabolic process	2.03E-72	GO:0034050	host programmed cell death induced by symbiont	1.78E-49
GO:0042445	hormone metabolic process	9.68E-72	GO:0072657	protein localization to membrane	2.55E-49
GO:0007165	signal transduction	4.20E-70	GO:0090150	establishment of protein localization to membrane	2.55E-49
GO:0009617	response to bacterium	7.22E-70	GO:0014070	response to organic cyclic compound	5.64E-49

b1	IDs	p.adj.	*f1*	IDs	p.adj.
GO:0048585	negative regulation of response to stimulus	1.21E-69	GO:0035556	intracellular signal transduction	7.28E-49
GO:0014070	response to organic cyclic compound	4.92E-69	GO:0009617	response to bacterium	4.43E-48
GO:1901701	cellular response to oxygen-containing compound	2.45E-68	GO:0046677	response to antibiotic	7.95E-48
GO:0060548	negative regulation of cell death	1.91E-66	GO:0009697	salicylic acid biosynthetic process	1.12E-47
GO:1901698	response to nitrogen compound	6.63E-66	GO:0072330	monocarboxylic acid biosynthetic process	2.01E-46
GO:0023052	signaling	1.83E-65	GO:0009696	salicylic acid metabolic process	7.53E-46
GO:0070887	cellular response to chemical stimulus	3.32E-65	GO:0046189	phenol-containing compound biosynthetic process	7.53E-46
GO:0043069	negative regulation of programmed cell death	4.48E-64	GO:0009867	jasmonic acid mediated signaling pathway	1.09E-45
GO:0071495	cellular response to endogenous stimulus	6.23E-64	GO:0071395	cellular response to jasmonic acid stimulus	1.09E-45
GO:0007154	cell communication	2.02E-63	GO:0042537	benzene-containing compound metabolic process	2.22E-45
GO:0032870	cellular response to hormone stimulus	4.35E-63	GO:0031348	negative regulation of defense response	5.53E-45
GO:0035556	intracellular signal transduction	1.50E-62	GO:0071705	nitrogen compound transport	6.77E-44
GO:0009862	systemic acquired resistance, salicylic acid mediated signaling pathway	1.59E-62	GO:0018958	phenol-containing compound metabolic process	1.46E-43
GO:0010817	regulation of hormone levels	1.25E-61	GO:0071310	cellular response to organic substance	2.51E-43
GO:0000165	MAPK cascade	2.46E-60	GO:0009723	response to ethylene	6.02E-43
GO:0023014	signal transduction by protein phosphorylation	2.46E-60	GO:0060548	negative regulation of cell death	1.43E-42
GO:0071407	cellular response to organic cyclic compound	5.73E-58	GO:0043069	negative regulation of programmed cell death	3.86E-42
GO:0009867	jasmonic acid mediated signaling pathway	1.18E-56	GO:0033554	cellular response to stress	4.66E-41
GO:0071395	cellular response to jasmonic acid stimulus	1.18E-56	GO:0002679	respiratory burst involved in defense response	7.42E-41
GO:0071310	cellular response to organic substance	1.93E-56	GO:0045730	respiratory burst	7.42E-41
GO:0009753	response to jasmonic acid	3.67E-54	GO:0065008	regulation of biological quality	1.34E-40
GO:0071705	nitrogen compound transport	7.58E-54	GO:0048585	negative regulation of response to stimulus	1.76E-39
GO:0009719	response to endogenous stimulus	6.32E-52	GO:0071702	organic substance transport	2.63E-39
GO:0072330	monocarboxylic acid biosynthetic process	2.46E-51	GO:0000165	MAPK cascade	2.77E-39
GO:0009725	response to hormone	3.02E-51	GO:0023014	signal transduction by protein phosphorylation	2.77E-39
GO:0042742	defense response to bacterium	1.26E-49	GO:0009755	hormone-mediated signaling pathway	7.23E-38
GO:0071702	organic substance transport	2.08E-48	GO:0017000	antibiotic biosynthetic process	9.43E-38
GO:1901617	organic hydroxy compound biosynthetic process	4.69E-47	GO:0009862	systemic acquired resistance, salicylic acid mediated signaling pathway	2.55E-37

b1	IDs	p.adj.	*f1*	IDs	p.adj.
GO:0010310	regulation of hydrogen peroxide metabolic process	9.20E-47	GO:0071407	cellular response to organic cyclic compound	5.86E-37
GO:0006986	response to unfolded protein	3.35E-46	GO:0009611	response to wounding	7.79E-36
GO:0034620	cellular response to unfolded protein	3.35E-46	GO:0016999	antibiotic metabolic process	3.37E-35
GO:0035967	cellular response to topologically incorrect protein	3.35E-46	GO:0009414	response to water deprivation	2.68E-34
GO:0030968	endoplasmic reticulum unfolded protein response	1.24E-45	GO:0009415	response to water	9.98E-34
GO:0002679	respiratory burst involved in defense response	2.71E-45	GO:0042742	defense response to bacterium	2.42E-33
GO:0045730	respiratory burst	2.71E-45	GO:0006865	amino acid transport	3.27E-33
GO:0009595	detection of biotic stimulus	9.65E-44	GO:0065007	biological regulation	4.79E-33
GO:2000377	regulation of reactive oxygen species metabolic process	1.76E-43	GO:0006820	anion transport	4.79E-33
GO:0051193	regulation of cofactor metabolic process	4.63E-43	GO:0015849	organic acid transport	2.39E-32
GO:0006605	protein targeting	8.34E-42	GO:0046942	carboxylic acid transport	2.39E-32
GO:0065008	regulation of biological quality	2.88E-41	GO:0009737	response to abscisic acid	3.94E-31
GO:0009755	hormone-mediated signaling pathway	1.35E-39	GO:0097305	response to alcohol	3.94E-31
GO:1901615	organic hydroxy compound metabolic process	7.05E-38	GO:0015711	organic anion transport	4.91E-31
GO:0017144	drug metabolic process	9.45E-38	GO:0009738	abscisic acid-activated signaling pathway	3.79E-30
GO:0006810	transport	2.43E-37	GO:0016053	organic acid biosynthetic process	7.53E-30
GO:0015833	peptide transport	5.76E-35	GO:0046394	carboxylic acid biosynthetic process	7.53E-30
GO:0051179	localization	6.63E-35	GO:0010310	regulation of hydrogen peroxide metabolic process	8.03E-29
GO:0051234	establishment of localization	1.16E-34	GO:0071215	cellular response to abscisic acid stimulus	1.08E-28
GO:0042886	amide transport	1.48E-34	GO:0097306	cellular response to alcohol	1.08E-28
GO:0046907	intracellular transport	2.07E-33	GO:0032787	monocarboxylic acid metabolic process	3.50E-28
GO:0051606	detection of stimulus	2.59E-33	GO:0015833	peptide transport	2.58E-27
GO:0006468	protein phosphorylation	3.68E-33	GO:0010035	response to inorganic substance	4.47E-27
GO:0016301	kinase activity	2.27E-32	GO:0042886	amide transport	4.74E-27
GO:0006886	intracellular protein transport	2.00E-31	GO:0006605	protein targeting	5.26E-27
GO:0009636	response to toxic substance	3.05E-31	GO:2000377	regulation of reactive oxygen species metabolic process	1.56E-26
GO:0070727	cellular macromolecule localization	3.38E-31	GO:0051193	regulation of cofactor metabolic process	2.60E-26
GO:0009723	response to ethylene	4.53E-31	GO:0009595	detection of biotic stimulus	5.61E-26
GO:0015031	protein transport	6.10E-31	GO:0034976	response to endoplasmic reticulum stress	1.07E-25
GO:0045184	establishment of protein localization	6.10E-31	GO:0006810	transport	1.13E-25
GO:0034613	cellular protein localization	8.73E-31	GO:0044283	small molecule biosynthetic process	2.28E-25

b1	IDs	p.adj.	*f1*	IDs	p.adj.
GO:0042743	hydrogen peroxide metabolic process	2.16E-30	GO:0042538	hyperosmotic salinity response	5.91E-25
GO:0051641	cellular localization	3.80E-29	GO:0051179	localization	1.57E-24
GO:0009738	abscisic acid-activated signaling pathway	5.01E-29	GO:0033993	response to lipid	2.94E-24
GO:0032787	monocarboxylic acid metabolic process	8.49E-29	GO:0009695	jasmonic acid biosynthetic process	3.95E-24
GO:0010035	response to inorganic substance	1.49E-28	GO:0009694	jasmonic acid metabolic process	4.25E-24
GO:0051649	establishment of localization in cell	2.05E-28	GO:0051234	establishment of localization	4.44E-24
GO:0008104	protein localization	2.64E-28	GO:0050794	regulation of cellular process	5.53E-24
GO:0072593	reactive oxygen species metabolic process	3.03E-28	GO:0002252	immune effector process	7.85E-23
GO:0006865	amino acid transport	3.12E-28	GO:0051606	detection of stimulus	4.84E-22
GO:0005886	plasma membrane	3.20E-28	GO:0071396	cellular response to lipid	2.99E-21
GO:0006820	anion transport	4.49E-28	GO:0002237	response to molecule of bacterial origin	7.44E-21
GO:0033036	macromolecule localization	4.82E-28	GO:0050789	regulation of biological process	7.64E-21
GO:0071944	cell periphery	7.58E-28	GO:0006468	protein phosphorylation	8.52E-21
GO:0035966	response to topologically incorrect protein	1.24E-27	GO:0070727	cellular macromolecule localization	9.73E-21
GO:0043900	regulation of multi-organism process	1.64E-27	GO:0009692	ethylene metabolic process	1.29E-20
GO:0071215	cellular response to abscisic acid stimulus	3.24E-27	GO:0009693	ethylene biosynthetic process	1.29E-20
GO:0097306	cellular response to alcohol	3.24E-27	GO:0043449	cellular alkene metabolic process	1.29E-20
GO:0016772	transferase activity, transferring phosphorus-containing groups	5.46E-27	GO:0043450	alkene biosynthetic process	1.29E-20
GO:0016053	organic acid biosynthetic process	6.54E-27	GO:1900673	olefin metabolic process	1.29E-20
GO:0046394	carboxylic acid biosynthetic process	6.54E-27	GO:1900674	olefin biosynthetic process	1.29E-20
GO:0048519	negative regulation of biological process	8.38E-27	GO:0006886	intracellular protein transport	1.40E-20
GO:0015849	organic acid transport	1.26E-26	GO:0006972	hyperosmotic response	2.12E-20
GO:0046942	carboxylic acid transport	1.26E-26	GO:1901617	organic hydroxy compound biosynthetic process	2.42E-20
GO:0003824	catalytic activity	8.06E-26	GO:0046907	intracellular transport	3.09E-20
GO:0065007	biological regulation	1.13E-25	GO:0034613	cellular protein localization	6.43E-20
GO:0015711	organic anion transport	1.54E-25	GO:0071944	cell periphery	1.14E-19
GO:0006979	response to oxidative stress	1.23E-23	GO:0006970	response to osmotic stress	1.41E-19
GO:0016740	transferase activity	1.74E-23	GO:0006811	ion transport	1.72E-19
GO:0016310	phosphorylation	2.02E-23	GO:0017144	drug metabolic process	1.98E-19
GO:0009408	response to heat	1.24E-22	GO:0043436	oxoacid metabolic process	2.06E-19
GO:0008150	biological_process	1.46E-22	GO:0019752	carboxylic acid metabolic process	2.11E-19
GO:0002252	immune effector process	2.83E-22	GO:0006082	organic acid metabolic process	2.14E-19

b1	IDs	p.adj.	*f1*	IDs	p.adj.
GO:0002237	response to molecule of bacterial origin	9.07E-22	GO:0015031	protein transport	3.44E-19
GO:0009737	response to abscisic acid	6.53E-21	GO:0045184	establishment of protein localization	3.44E-19
GO:0097305	response to alcohol	6.53E-21	GO:0042743	hydrogen peroxide metabolic process	5.05E-19
GO:0050794	regulation of cellular process	6.59E-21	GO:0009628	response to abiotic stimulus	1.11E-18
GO:0044283	small molecule biosynthetic process	1.27E-20	GO:0033036	macromolecule localization	1.29E-18
GO:0042538	hyperosmotic salinity response	1.99E-20	GO:0008150	biological_process	1.84E-18
GO:0006811	ion transport	2.23E-20	GO:0048519	negative regulation of biological process	1.99E-18
GO:0009404	toxin metabolic process	5.93E-20	GO:0072593	reactive oxygen species metabolic process	5.02E-18
GO:0009692	ethylene metabolic process	9.78E-19	GO:0008104	protein localization	6.53E-18
GO:0009693	ethylene biosynthetic process	9.78E-19	GO:0005886	plasma membrane	7.37E-18
GO:0043449	cellular alkene metabolic process	9.78E-19	GO:0051641	cellular localization	9.54E-18
GO:0043450	alkene biosynthetic process	9.78E-19	GO:0051649	establishment of localization in cell	1.82E-17
GO:1900673	olefin metabolic process	9.78E-19	GO:0009651	response to salt stress	2.04E-17
GO:1900674	olefin biosynthetic process	9.78E-19	GO:0030968	endoplasmic reticulum unfolded protein response	2.54E-17
GO:0003674	molecular_function	1.42E-18	GO:0006986	response to unfolded protein	3.81E-17
GO:0000302	response to reactive oxygen species	1.28E-17	GO:0034620	cellular response to unfolded protein	3.81E-17
GO:0009415	response to water	2.30E-17	GO:0035967	cellular response to topologically incorrect protein	3.81E-17
GO:0009414	response to water deprivation	2.54E-17	GO:0043900	regulation of multi-organism process	5.54E-17
GO:0009407	toxin catabolic process	4.21E-17	GO:0016301	kinase activity	8.87E-17
GO:0050789	regulation of biological process	4.55E-17	GO:0009404	toxin metabolic process	3.44E-16
GO:0071396	cellular response to lipid	5.20E-17	GO:0016310	phosphorylation	3.66E-16
GO:0009611	response to wounding	7.80E-17	GO:0003674	molecular_function	1.11E-15
GO:0042542	response to hydrogen peroxide	1.04E-15	GO:1901615	organic hydroxy compound metabolic process	1.78E-14
GO:0098754	detoxification	1.09E-15	GO:0009266	response to temperature stimulus	3.32E-14
GO:0016020	membrane	1.68E-15	GO:0003824	catalytic activity	4.16E-14
GO:0019752	carboxylic acid metabolic process	9.64E-15	GO:0009407	toxin catabolic process	4.98E-14
GO:0005575	cellular_component	2.53E-14	GO:0098754	detoxification	4.53E-13
GO:0006972	hyperosmotic response	3.81E-14	GO:0016772	transferase activity, transferring phosphorus-containing groups	5.86E-13
GO:0005576	extracellular region	5.78E-14	GO:0010286	heat acclimation	6.19E-13
GO:0048523	negative regulation of cellular process	1.59E-13	GO:0016740	transferase activity	1.67E-12
GO:0071456	cellular response to hypoxia	1.62E-13	GO:0042430	indole-containing compound metabolic process	2.91E-12
GO:0043436	oxoacid metabolic process	1.88E-13	GO:0005575	cellular_component	7.81E-12

b1	IDs	p.adj.	*f1*	IDs	p.adj.
GO:0006082	organic acid metabolic process	1.98E-13	GO:0009636	response to toxic substance	1.23E-11
GO:0009266	response to temperature stimulus	2.43E-13	GO:0006857	oligopeptide transport	3.29E-11
GO:0007568	aging	3.74E-13	GO:0010583	response to cyclopentenone	3.85E-11
GO:0052542	defense response by callose deposition	3.96E-13	GO:0009409	response to cold	3.90E-11
GO:0033993	response to lipid	4.84E-13	GO:0019748	secondary metabolic process	3.90E-11
GO:0006984	ER-nucleus signaling pathway	6.16E-13	GO:0015706	nitrate transport	1.67E-10
GO:0010286	heat acclimation	6.21E-13	GO:0044281	small molecule metabolic process	1.95E-10
GO:0043090	amino acid import	6.88E-13	GO:0009625	response to insect	3.35E-10
GO:0009642	response to light intensity	8.58E-13	GO:0071456	cellular response to hypoxia	5.61E-10
GO:0001666	response to hypoxia	9.58E-13	GO:0048523	negative regulation of cellular process	7.26E-10
GO:0036294	cellular response to decreased oxygen levels	1.41E-12	GO:0035966	response to topologically incorrect protein	8.20E-10
GO:0071453	cellular response to oxygen levels	1.41E-12	GO:0015698	inorganic anion transport	8.41E-10
GO:0006498	N-terminal protein lipidation	1.93E-12	GO:0052542	defense response by callose deposition	1.11E-09
GO:0006499	N-terminal protein myristoylation	1.93E-12	GO:0036294	cellular response to decreased oxygen levels	1.94E-09
GO:0010583	response to cyclopentenone	2.48E-12	GO:0071453	cellular response to oxygen levels	1.94E-09
GO:0036293	response to decreased oxygen levels	2.55E-12	GO:0009987	cellular process	1.96E-09
GO:0098581	detection of external biotic stimulus	3.07E-12	GO:0042435	indole-containing compound biosynthetic process	1.96E-09
GO:0018377	protein myristoylation	3.13E-12	GO:0043090	amino acid import	2.40E-09
GO:0070482	response to oxygen levels	3.49E-12	GO:0007568	aging	2.72E-09
GO:0009625	response to insect	3.73E-12	GO:0019438	aromatic compound biosynthetic process	3.57E-09
GO:0031365	N-terminal protein amino acid modification	5.06E-12	GO:0010167	response to nitrate	5.05E-09
GO:0006497	protein lipidation	2.07E-11	GO:0005576	extracellular region	5.09E-09
GO:0042157	lipoprotein metabolic process	2.07E-11	GO:0001666	response to hypoxia	6.15E-09
GO:0042158	lipoprotein biosynthetic process	2.07E-11	GO:0016020	membrane	7.21E-09
GO:0016045	detection of bacterium	3.28E-11	GO:0036293	response to decreased oxygen levels	1.12E-08
GO:0098543	detection of other organism	3.28E-11	GO:0070482	response to oxygen levels	1.36E-08
GO:0009628	response to abiotic stimulus	1.29E-10	GO:0042436	indole-containing compound catabolic process	3.83E-08
GO:0052545	callose localization	2.14E-10	GO:1901362	organic cyclic compound biosynthetic process	8.43E-08
GO:0006464	cellular protein modification process	4.65E-10	GO:0006568	tryptophan metabolic process	1.22E-07
GO:0036211	protein modification process	4.65E-10	GO:0006586	indolalkylamine metabolic process	1.22E-07
GO:0043543	protein acylation	4.91E-10	GO:0009581	detection of external stimulus	1.38E-07
GO:0033037	polysaccharide localization	5.06E-10	GO:0009684	indoleacetic acid biosynthetic process	2.07E-07

b1	IDs	p.adj.	*f1*	IDs	p.adj.
GO:0006888	ER to Golgi vesicle-mediated transport	5.04E-09	GO:0009683	indoleacetic acid metabolic process	2.45E-07
GO:0015706	nitrate transport	5.81E-09	GO:0009850	auxin metabolic process	2.62E-07
GO:0010150	leaf senescence	5.82E-09	GO:0009817	defense response to fungus, incompatible interaction	3.56E-07
GO:0090693	plant organ senescence	5.82E-09	GO:0009851	auxin biosynthetic process	4.16E-07
GO:0009644	response to high light intensity	5.94E-09	GO:0008152	metabolic process	6.63E-07
GO:0010167	response to nitrate	1.57E-08	GO:0006569	tryptophan catabolic process	1.23E-06
GO:0015698	inorganic anion transport	2.37E-08	GO:0046218	indolalkylamine catabolic process	1.23E-06
GO:0030246	carbohydrate binding	6.83E-08	GO:0052545	callose localization	1.47E-06
GO:0006970	response to osmotic stress	7.43E-08	GO:0016045	detection of bacterium	2.06E-06
GO:0005783	endoplasmic reticulum	1.76E-07	GO:0098543	detection of other organism	2.06E-06
GO:0009817	defense response to fungus, incompatible interaction	1.96E-07	GO:0033037	polysaccharide localization	2.37E-06
GO:0043562	cellular response to nitrogen levels	2.29E-07	GO:0030246	carbohydrate binding	2.37E-06
GO:0009987	cellular process	2.99E-07	GO:0009074	aromatic amino acid family catabolic process	2.60E-06
GO:0004672	protein kinase activity	3.06E-07	GO:0098581	detection of external biotic stimulus	3.69E-06
GO:0006457	protein folding	3.29E-07	GO:0006979	response to oxidative stress	3.97E-06
GO:0009651	response to salt stress	4.25E-07	GO:0010150	leaf senescence	4.36E-06
GO:0012505	endomembrane system	4.25E-07	GO:0090693	plant organ senescence	4.36E-06
GO:0009581	detection of external stimulus	4.50E-07	GO:0015824	proline transport	5.27E-06
GO:0019748	secondary metabolic process	7.89E-07	GO:0034754	cellular hormone metabolic process	7.16E-06
GO:0048584	positive regulation of response to stimulus	1.37E-06	GO:0015804	neutral amino acid transport	9.11E-06
GO:0010260	animal organ senescence	1.40E-06	GO:0004364	glutathione transferase activity	9.31E-06
GO:0019825	oxygen binding	1.54E-06	GO:0042343	indole glucosinolate metabolic process	1.36E-05
GO:0031667	response to nutrient levels	2.07E-06	GO:0009873	ethylene-activated signaling pathway	1.43E-05
GO:0031349	positive regulation of defense response	5.79E-06	GO:0009310	amine catabolic process	1.77E-05
GO:0004364	glutathione transferase activity	5.79E-06	GO:0042402	cellular biogenic amine catabolic process	1.77E-05
GO:0019199	transmembrane receptor protein kinase activity	7.67E-06	GO:0044249	cellular biosynthetic process	1.77E-05
GO:0035304	regulation of protein dephosphorylation	8.70E-06	GO:0009682	induced systemic resistance	2.53E-05
GO:0009873	ethylene-activated signaling pathway	8.75E-06	GO:0006576	cellular biogenic amine metabolic process	2.68E-05
GO:0035303	regulation of dephosphorylation	1.01E-05	GO:0009408	response to heat	3.17E-05
GO:0002684	positive regulation of immune system process	1.36E-05	GO:1901576	organic substance biosynthetic process	3.53E-05
GO:0050778	positive regulation of immune response	1.36E-05	GO:0009063	cellular amino acid catabolic process	3.65E-05

b1	IDs	p.adj.	*f1*	IDs	p.adj.
GO:0071369	cellular response to ethylene stimulus	1.60E-05	GO:0009646	response to absence of light	3.99E-05
GO:0009816	defense response to bacterium, incompatible interaction	1.90E-05	GO:0052482	defense response by cell wall thickening	4.03E-05
GO:0031669	cellular response to nutrient levels	2.15E-05	GO:0052544	defense response by callose deposition in cell wall	4.03E-05
GO:0022857	transmembrane transporter activity	2.40E-05	GO:0000160	phosphorelay signal transduction system	5.19E-05
GO:0016773	phosphotransferase activity, alcohol group as acceptor	2.80E-05	GO:0009058	biosynthetic process	6.08E-05
GO:0009991	response to extracellular stimulus	2.95E-05	GO:0044106	cellular amine metabolic process	7.32E-05
GO:0008144	drug binding	3.55E-05	GO:0044237	cellular metabolic process	8.52E-05
GO:0015802	basic amino acid transport	4.64E-05	GO:0031323	regulation of cellular metabolic process	9.15E-05
GO:0000160	phosphorelay signal transduction system	4.97E-05	GO:1901606	alpha-amino acid catabolic process	1.22E-04
GO:0044281	small molecule metabolic process	5.84E-05	GO:0071369	cellular response to ethylene stimulus	1.22E-04
GO:0015075	ion transmembrane transporter activity	6.70E-05	GO:0015075	ion transmembrane transporter activity	1.27E-04
GO:0006995	cellular response to nitrogen starvation	6.73E-05	GO:0009733	response to auxin	1.30E-04
GO:0006470	protein dephosphorylation	7.77E-05	GO:0006464	cellular protein modification process	1.31E-04
GO:0019438	aromatic compound biosynthetic process	7.77E-05	GO:0036211	protein modification process	1.31E-04
GO:0015662	ATPase activity, coupled to transmembrane movement of ions, phosphorylative mechanism	1.03E-04	GO:0009072	aromatic amino acid family metabolic process	1.60E-04
GO:0006857	oligopeptide transport	1.04E-04	GO:0015802	basic amino acid transport	2.06E-04
GO:0005788	endoplasmic reticulum lumen	1.16E-04	GO:0019825	oxygen binding	2.54E-04
GO:0009267	cellular response to starvation	1.17E-04	GO:0009269	response to desiccation	3.27E-04
GO:0072507	divalent inorganic cation homeostasis	1.30E-04	GO:0009308	amine metabolic process	3.30E-04
GO:0015696	ammonium transport	1.51E-04	GO:0005516	calmodulin binding	3.64E-04
GO:0009963	positive regulation of flavonoid biosynthetic process	1.57E-04	GO:0010260	animal organ senescence	3.64E-04
GO:0004675	transmembrane receptor protein serine/threonine kinase activity	1.94E-04	GO:0006862	nucleotide transport	4.07E-04
GO:0009695	jasmonic acid biosynthetic process	2.00E-04	GO:0015696	ammonium transport	4.75E-04
GO:0016311	dephosphorylation	2.09E-04	GO:0019222	regulation of metabolic process	5.92E-04
GO:0042594	response to starvation	2.14E-04	GO:0006984	ER-nucleus signaling pathway	6.32E-04
GO:0019220	regulation of phosphate metabolic process	2.25E-04	GO:0015748	organophosphate ester transport	6.66E-04
GO:0051174	regulation of phosphorus metabolic process	2.25E-04	GO:0032101	regulation of response to external stimulus	7.84E-04
GO:0031668	cellular response to extracellular stimulus	2.25E-04	GO:0015318	inorganic molecular entity transmembrane transporter activity	8.83E-04
GO:0009962	regulation of flavonoid biosynthetic process	2.26E-04	GO:0016491	oxidoreductase activity	0.0013

b1	IDs	p.adj.	*f1*	IDs	p.adj.
GO:0019375	galactolipid biosynthetic process	2.32E-04	GO:0006888	ER to Golgi vesicle-mediated transport	0.0014
GO:0009682	induced systemic resistance	2.35E-04	GO:0042344	indole glucosinolate catabolic process	0.0017
GO:0009646	response to absence of light	2.36E-04	GO:0051186	cofactor metabolic process	0.0018
GO:0045089	positive regulation of innate immune response	2.38E-04	GO:0019199	transmembrane receptor protein kinase activity	0.0019
GO:0071496	cellular response to external stimulus	2.38E-04	GO:0009991	response to extracellular stimulus	0.0021
GO:0019374	galactolipid metabolic process	2.70E-04	GO:0031667	response to nutrient levels	0.0039
GO:0005516	calmodulin binding	2.83E-04	GO:0008794	arsenate reductase (glutaredoxin) activity	0.0039
GO:0015748	organophosphate ester transport	2.88E-04	GO:0009975	cyclase activity	0.0039
GO:0032101	regulation of response to external stimulus	2.89E-04	GO:0030613	oxidoreductase activity, acting on phosphorus or arsenic in donors	0.0039
GO:0015085	calcium ion transmembrane transporter activity	2.89E-04	GO:0030614	oxidoreductase activity, acting on phosphorus or arsenic in donors, disulfide as acceptor	0.0039
GO:0140096	catalytic activity, acting on a protein	3.09E-04	GO:0022857	transmembrane transporter activity	0.0047
GO:0016798	hydrolase activity, acting on glycosyl bonds	3.09E-04	GO:0030611	arsenate reductase activity	0.0057
GO:0022804	active transmembrane transporter activity	3.09E-04	GO:0006796	phosphate-containing compound metabolic process	0.0062
GO:0006862	nucleotide transport	3.09E-04	GO:0046423	allene-oxide cyclase activity	0.0064
GO:0031399	regulation of protein modification process	3.64E-04	GO:0005623	cell	0.0066
GO:0072503	cellular divalent inorganic cation homeostasis	3.97E-04	GO:0044464	cell part	0.0066
GO:0043412	macromolecule modification	4.04E-04	GO:0035304	regulation of protein dephosphorylation	0.0110
GO:0009694	jasmonic acid metabolic process	4.20E-04	GO:0007623	circadian rhythm	0.0110
GO:0042631	cellular response to water deprivation	4.97E-04	GO:0048511	rhythmic process	0.0110
GO:0071462	cellular response to water stimulus	4.97E-04	GO:0043295	glutathione binding	0.0110
GO:0034605	cellular response to heat	5.12E-04	GO:0072341	modified amino acid binding	0.0110
GO:0004553	hydrolase activity, hydrolyzing O-glycosyl compounds	5.40E-04	GO:1900750	oligopeptide binding	0.0110
GO:0048193	Golgi vesicle transport	6.83E-04	GO:0035303	regulation of dephosphorylation	0.0118
GO:0042626	ATPase activity, coupled to transmembrane movement of substances	7.37E-04	GO:0031225	anchored component of membrane	0.0128
GO:0043492	ATPase activity, coupled to movement of substances	7.37E-04	GO:0005618	cell wall	0.0143
GO:0006664	glycolipid metabolic process	7.53E-04	GO:0030312	external encapsulating structure	0.0143
GO:0005215	transporter activity	7.68E-04	GO:0009267	cellular response to starvation	0.0154
GO:0016036	cellular response to phosphate starvation	9.28E-04	GO:0004553	hydrolase activity, hydrolyzing O-glycosyl compounds	0.0154
GO:0009813	flavonoid biosynthetic process	9.55E-04	GO:0003700	DNA binding transcription factor activity	0.0163

b1	IDs	p.adj.	*f1*	IDs	p.adj.
GO:0006812	cation transport	9.89E-04	GO:0010120	camalexin biosynthetic process	0.0163
GO:0009247	glycolipid biosynthetic process	9.89E-04	GO:0052317	camalexin metabolic process	0.0163
GO:0016787	hydrolase activity	0.0010	GO:0031668	cellular response to extracellular stimulus	0.0173
GO:1903509	liposaccharide metabolic process	0.0011	GO:0002831	regulation of response to biotic stimulus	0.0173
GO:0004568	chitinase activity	0.0011	GO:0000162	tryptophan biosynthetic process	0.0178
GO:0042430	indole-containing compound metabolic process	0.0012	GO:0046219	indolalkylamine biosynthetic process	0.0178
GO:0055074	calcium ion homeostasis	0.0012	GO:0071496	cellular response to external stimulus	0.0179
GO:0010120	camalexin biosynthetic process	0.0013	GO:0071704	organic substance metabolic process	0.0179
GO:0052317	camalexin metabolic process	0.0013	GO:0022804	active transmembrane transporter activity	0.0193
GO:1901362	organic cyclic compound biosynthetic process	0.0015	GO:0030551	cyclic nucleotide binding	0.0207
GO:0005509	calcium ion binding	0.0017	GO:0042594	response to starvation	0.0207
GO:0042435	indole-containing compound biosynthetic process	0.0018	GO:0016765	transferase activity, transferring alkyl or aryl (other than methyl) groups	0.0214
GO:0006643	membrane lipid metabolic process	0.0018	GO:0000302	response to reactive oxygen species	0.0221
GO:0016192	vesicle-mediated transport	0.0019	GO:0009403	toxin biosynthetic process	0.0223
GO:0009812	flavonoid metabolic process	0.0020	GO:0009700	indole phytoalexin biosynthetic process	0.0223
GO:0004888	transmembrane signaling receptor activity	0.0021	GO:0046217	indole phytoalexin metabolic process	0.0223
GO:0005216	ion channel activity	0.0022	GO:0052314	phytoalexin metabolic process	0.0223
GO:0002218	activation of innate immune response	0.0022	GO:0052315	phytoalexin biosynthetic process	0.0223
GO:0002253	activation of immune response	0.0022	GO:0004564	beta-fructofuranosidase activity	0.0223
GO:0052031	modulation by symbiont of host defense response	0.0023	GO:0004675	transmembrane receptor protein serine/threonine kinase activity	0.0223
GO:0052173	response to defenses of other organism involved in symbiotic interaction	0.0023	GO:0015145	monosaccharide transmembrane transporter activity	0.0223
GO:0052200	response to host defenses	0.0023	GO:0015291	secondary active transmembrane transporter activity	0.0245
GO:0052255	modulation by organism of defense response of other organism involved in symbiotic interaction	0.0023	GO:0140110	transcription regulator activity	0.0247
GO:0052552	modulation by organism of immune response of other organism involved in symbiotic interaction	0.0023	GO:0044248	cellular catabolic process	0.0247
GO:0052553	modulation by symbiont of host immune response	0.0023	GO:0006793	phosphorus metabolic process	0.0271
GO:0052555	positive regulation by organism of immune response of other organism involved in symbiotic interaction	0.0023	GO:0042631	cellular response to water deprivation	0.0275
GO:0052556	positive regulation by symbiont of host immune response	0.0023	GO:0071462	cellular response to water stimulus	0.0275

b1	IDs	p.adj.	*f1*	IDs	p.adj.
GO:0052564	response to immune response of other organism involved in symbiotic interaction	0.0023	GO:0031669	cellular response to nutrient levels	0.0323
GO:0052572	response to host immune response	0.0023	GO:0009055	electron transfer activity	0.0325
GO:0075136	response to host	0.0023	GO:1901658	glycosyl compound catabolic process	0.0335
GO:0009403	toxin biosynthetic process	0.0023	GO:0015085	calcium ion transmembrane transporter activity	0.0335
GO:0009700	indole phytoalexin biosynthetic process	0.0023	GO:0031226	intrinsic component of plasma membrane	0.0339
GO:0046217	indole phytoalexin metabolic process	0.0023	GO:0016829	lyase activity	0.0339
GO:0052314	phytoalexin metabolic process	0.0023	GO:0016054	organic acid catabolic process	0.0344
GO:0052315	phytoalexin biosynthetic process	0.0023	GO:0046395	carboxylic acid catabolic process	0.0344
GO:0000041	transition metal ion transport	0.0024	GO:0010421	hydrogen peroxide-mediated programmed cell death	0.0344
GO:0044432	endoplasmic reticulum part	0.0025	GO:0036474	cell death in response to hydrogen peroxide	0.0344
GO:0002831	regulation of response to biotic stimulus	0.0028	GO:0050691	regulation of defense response to virus by host	0.0344
GO:0008061	chitin binding	0.0031	GO:0097243	flavonoid binding	0.0344
GO:0016298	lipase activity	0.0040	GO:2001147	camalexin binding	0.0344
GO:0010193	response to ozone	0.0046	GO:2001227	quercitrin binding	0.0344
GO:0038023	signaling receptor activity	0.0050	GO:0005216	ion channel activity	0.0344
GO:0060089	molecular transducer activity	0.0050	GO:0034284	response to monosaccharide	0.0355
GO:0005794	Golgi apparatus	0.0050	GO:0080167	response to karrikin	0.0355
GO:0046467	membrane lipid biosynthetic process	0.0051	GO:0006812	cation transport	0.0365
GO:0006796	phosphate-containing compound metabolic process	0.0060	GO:0005215	transporter activity	0.0368
GO:0004871	signal transducer activity	0.0081	GO:0006995	cellular response to nitrogen starvation	0.0397
GO:1900055	regulation of leaf senescence	0.0085	GO:0080043	quercetin 3-O-glucosyltransferase activity	0.0397
GO:0004674	protein serine/threonine kinase activity	0.0090	GO:0006470	protein dephosphorylation	0.0469
GO:0015318	inorganic molecular entity transmembrane transporter activity	0.0096	GO:0006498	N-terminal protein lipidation	0.0473
GO:0005388	calcium-transporting ATPase activity	0.0097	GO:0006499	N-terminal protein myristoylation	0.0473
GO:0042436	indole-containing compound catabolic process	0.0100	GO:0009642	response to light intensity	0.0475
GO:0004683	calmodulin-dependent protein kinase activity	0.0106			
GO:0006874	cellular calcium ion homeostasis	0.0117			
GO:0034754	cellular hormone metabolic process	0.0118			
GO:0009409	response to cold	0.0119			
GO:0051186	cofactor metabolic process	0.0119			
GO:0009612	response to mechanical stimulus	0.0130			

b1	IDs	p.adj.	*f1*	IDs	p.adj.
GO:0099023	tethering complex	0.0132			
GO:0015405	P-P-bond-hydrolysis-driven transmembrane transporter activity	0.0139			
GO:0009684	indoleacetic acid biosynthetic process	0.0143			
GO:0015399	primary active transmembrane transporter activity	0.0149			
GO:0009683	indoleacetic acid metabolic process	0.0160			
GO:0017119	Golgi transport complex	0.0179			
GO:0030001	metal ion transport	0.0186			
GO:0005217	intracellular ligand-gated ion channel activity	0.0211			
GO:0071214	cellular response to abiotic stimulus	0.0219			
GO:0104004	cellular response to environmental stimulus	0.0219			
GO:0016765	transferase activity, transferring alkyl or aryl (other than methyl) groups	0.0222			
GO:0006569	tryptophan catabolic process	0.0225			
GO:0046218	indolalkylamine catabolic process	0.0225			
GO:0010112	regulation of systemic acquired resistance	0.0226			
GO:0010204	defense response signaling pathway, resistance gene-independent	0.0226			
GO:0043167	ion binding	0.0226			
GO:0009733	response to auxin	0.0254			
GO:0009838	abscission	0.0256			
GO:0022853	active ion transmembrane transporter activity	0.0261			
GO:0042625	ATPase coupled ion transmembrane transporter activity	0.0261			
GO:0009851	auxin biosynthetic process	0.0265			
GO:0008194	UDP-glycosyltransferase activity	0.0273			
GO:0009850	auxin metabolic process	0.0281			
GO:0006968	cellular defense response	0.0296			
GO:0010185	regulation of cellular defense response	0.0296			
GO:0006793	phosphorus metabolic process	0.0344			
GO:0009074	aromatic amino acid family catabolic process	0.0365			
GO:0006882	cellular zinc ion homeostasis	0.0371			
GO:0015297	antiporter activity	0.0393			
GO:0016491	oxidoreductase activity	0.0417			
GO:0004806	triglyceride lipase activity	0.0426			

b1	IDs	p.adj.	*f1*	IDs	p.adj.
GO:0042343	indole glucosinolate metabolic process	0.0481			
GO:0098771	inorganic ion homeostasis	0.0485			
GO:0015824	proline transport	0.0490			

Tab. S2 Enhanced gene expression of stress responsive genes in the* ugt *triple mutant (b1f1f2) under control conditions

Values represent log2 fold changes compared to the wild type untreated with adjusted p-values smaller than 0.05.

ATG	*b1f1f2*	annotation	ATG	*b1f1f2*	annotation
AT4G11600	1.61	glutathione peroxidase	AT4G07820	1.33	cysteine-rich secretory proteins, antigen 5 and pathogenesis-related protein 1 domain-containing protein
AT2G48150	1.49	glutathione peroxidase	AT3G22231	2.34	pathogen and circadian controlled 1
AT3G63080	1.13	glutathione peroxidase	AT1G78780	1.96	pathogenesis-related protein
AT1G63460	1.02	glutathione peroxidase	AT2G14610	5.84	pathogenesis-related protein 1
AT3G03670	4.72	peroxidase	AT1G75040	4.36	pathogenesis-related protein 5
AT2G37130	1.49	peroxidase	AT4G36010	1.20	pathogenesis-related thaumatin family protein
AT1G14540	1.39	peroxidase 4	AT1G20030	1.61	pathogenesis-related thaumatin-like protein
AT2G38390	2.49	peroxidase 23	AT1G13340	3.58	Regulator of Vps4 activity in the MVB pathway protein
AT3G49120	2.34	peroxidase 34	AT1G14880	5.36	cadmium resistance protein 1
AT4G08770	2.61	peroxidase 37	AT1G14870	2.82	cadmium resistance protein 2
AT4G08780	3.14	peroxidase 38	AT1G58390	2.80	CC-NBS-LRR class disease resistance protein
AT4G36430	1.27	peroxidase 49	AT1G15890	1.72	CC-NBS-LRR class disease resistance protein
AT4G37530	1.43	peroxidase 51	AT5G66910	1.70	CC-NBS-LRR class disease resistance protein
AT5G05340	3.72	peroxidase 52	AT1G12290	1.65	CC-NBS-LRR class disease resistance protein
AT5G06730	2.14	peroxidase 54	AT1G17615	6.91	Disease resistance protein (TIR-NBS class)
AT5G19880	4.52	peroxidase 58	AT1G17610	1.42	Disease resistance protein (TIR-NBS class)
AT5G39580	1.21	peroxidase 62	AT1G33560	1.04	disease resistance protein ADR1
AT5G64100	1.36	peroxidase 69	AT1G12210	2.17	disease resistance protein RFL1
AT5G64120	1.73	peroxidase 71	AT4G26090	3.94	disease resistance protein RPS2
AT2G29460	3.95	glutathione S-transferase	AT3G50950	1.23	disease resistance RPP13-like protein 4
AT1G65820	1.15	glutathione S-transferase	AT5G24530	4.06	downy mildew resistance 6 protein / oxidoreductase
AT1G02930	3.23	glutathione S-transferase 1	AT3G48080	3.78	lipase class 3 family protein / disease resistance protein-related protein
AT1G02920	2.99	glutathione S-transferase 11	AT1G58602	1.00	LRR and NB-ARC domain-containing disease resistance protein

ATG	*b1f1f2*	annotation	ATG	*b1f1f2*	annotation
AT2G02930	1.49	glutathione S-transferase 16	AT1G30410	1.25	multidrug resistance-associated protein 13
AT5G44990	3.77	Glutathione S-transferase family protein	AT3G13090	2.86	multidrug resistance-associated protein 8
AT4G02520	2.57	glutathione S-transferase PM24	AT4G27220	2.60	NB-ARC domain-containing disease resistance protein
AT2G29470	7.06	glutathione S-transferase tau 3	AT5G66890	4.13	putative disease resistance protein
AT3G09270	3.23	glutathione S-transferase TAU 8	AT4G11170	3.74	putative disease resistance protein
AT5G62480	2.94	glutathione S-transferase tau 9	AT5G47250	1.18	putative disease resistance protein
AT1G74590	2.10	glutathione S-transferase TAU 10	AT5G45440	1.07	putative disease resistance protein
AT1G69930	4.50	glutathione S-transferase TAU 11	AT4G33300	1.69	putative disease resistance protein ADR1-like 1
AT1G69920	2.94	glutathione S-transferase TAU 12	AT1G58410	1.18	putative disease resistance protein RXW24L
AT1G78340	5.22	glutathione S-transferase TAU 22	AT3G14470	1.43	putative disease resistance RPP13-like protein 1
AT1G17170	1.78	glutathione S-transferase TAU 24	AT3G25510	2.60	putative TIR-NBS-LRR class disease resistance protein
AT2G02390	1.81	glutathione S-transferase zeta-class 1	AT3G26470	2.73	RPW8 domain-containing powdery mildew resistance protein
AT2G30750	2.38	cytochrome P450 71A12	AT1G72870	2.68	TIR-NBS class of disease resistance protein
AT3G26830	4.11	cytochrome P450 71B15	AT1G72950	2.16	TIR-NBS class of disease resistance protein
AT3G26170	3.02	cytochrome P450 71B19	AT5G18350	8.31	TIR-NBS-LRR class disease resistance protein
AT3G26180	1.43	cytochrome P450 71B20	AT5G38350	6.31	TIR-NBS-LRR class disease resistance protein
AT3G26210	3.06	cytochrome P450 71B23	AT1G63870	5.16	TIR-NBS-LRR class disease resistance protein
AT3G26230	2.12	cytochrome P450 71B24	AT5G45000	4.13	TIR-NBS-LRR class disease resistance protein
AT3G26220	2.90	cytochrome P450 71B3	AT4G23510	3.96	TIR-NBS-LRR class disease resistance protein
AT2G02580	7.34	cytochrome P450 71B9	AT4G11340	3.96	TIR-NBS-LRR class disease resistance protein
AT2G45570	3.10	cytochrome P450 76C2	AT3G04220	2.30	TIR-NBS-LRR class disease resistance protein
AT5G36220	1.23	cytochrome P450 81D1	AT2G16870	2.22	TIR-NBS-LRR class disease resistance protein
AT4G31500	1.72	cytochrome P450 83B1	AT5G41750	2.18	TIR-NBS-LRR class disease resistance protein
AT2G44890	5.66	cytochrome P450, family 704, subfamily A, polypeptide 1	AT4G14370	2.12	TIR-NBS-LRR class disease resistance protein

ATG	*b1f1f2*	annotation	ATG	*b1f1f2*	annotation
AT2G45510	3.47	cytochrome P450, family 704, subfamily A, polypeptide 2	AT2G17060	2.02	TIR-NBS-LRR class disease resistance protein
AT2G14100	3.69	cytochrome P450, family 705, subfamily A, polypeptide 13	AT3G44400	1.97	TIR-NBS-LRR class disease resistance protein
AT1G50560	1.32	cytochrome P450, family 705, subfamily A, polypeptide 25	AT5G41550	1.93	TIR-NBS-LRR class disease resistance protein
AT1G50520	1.42	cytochrome P450, family 705, subfamily A, polypeptide 27	AT1G17600	1.91	TIR-NBS-LRR class disease resistance protein
AT3G20960	2.02	cytochrome P450, family 705, subfamily A, polypeptide 33	AT1G65850	1.83	TIR-NBS-LRR class disease resistance protein
AT2G30770	5.33	cytochrome P450, family 71, subfamily A, polypeptide 13	AT5G46520	1.70	TIR-NBS-LRR class disease resistance protein
AT2G34500	2.80	cytochrome P450, family 710, subfamily A	AT1G63730	1.61	TIR-NBS-LRR class disease resistance protein
AT5G24910	5.69	cytochrome P450, family 714, subfamily A, polypeptide 1	AT5G46260	1.53	TIR-NBS-LRR class disease resistance protein
AT3G14680	2.68	cytochrome P450, family 72, subfamily A, polypeptide 14	AT4G16960	1.52	TIR-NBS-LRR class disease resistance protein
AT3G14620	1.75	cytochrome P450, family 72, subfamily A, polypeptide 8	AT4G36150	1.40	TIR-NBS-LRR class disease resistance protein
AT1G33730	5.76	cytochrome P450, family 76, subfamily C, polypeptide 5	AT5G36930	1.37	TIR-NBS-LRR class disease resistance protein
AT1G33720	2.33	cytochrome P450, family 76, subfamily C, polypeptide 6	AT5G38340	1.36	TIR-NBS-LRR class disease resistance protein
AT5G35920	3.95	cytochrome P450, family 79, subfamily A, polypeptide 4 pseudogene	AT5G41740	1.21	TIR-NBS-LRR class disease resistance protein
AT4G37340	3.83	cytochrome P450, family 81, subfamily D, polypeptide 3	AT4G16940	1.08	TIR-NBS-LRR class disease resistance protein
AT4G37370	1.93	cytochrome P450, family 81, subfamily D, polypeptide 8	AT1G63740	1.07	TIR-NBS-LRR class disease resistance protein
AT5G67310	2.34	cytochrome P450, family 81, subfamily G, polypeptide 1	AT4G19520	1.07	TIR-NBS-LRR class disease resistance protein
AT4G31970	3.09	cytochrome P450, family 82, subfamily C, polypeptide 2	AT5G48770	1.06	TIR-NBS-LRR class disease resistance protein
AT3G03470	2.40	cytochrome P450, family 87, subfamily A, polypeptide 9	AT4G12010	1.06	TIR-NBS-LRR class disease resistance protein
AT2G27690	1.06	cytochrome P450, family 94, subfamily C, polypeptide 1	AT1G52900	4.72	Toll-Interleukin-Resistance domain-containing protein
AT2G27690	1.06	cytochrome P450, family 94, subfamily C, polypeptide 1	AT5G38344	4.11	Toll-Interleukin-Resistance domain-containing protein
AT2G21910	2.92	cytochrome P450, family 96, subfamily A, polypeptide 5	AT1G57630	3.79	Toll-Interleukin-Resistance domain-containing protein
AT5G46350	1.72	putative WRKY transcription factor 8	AT2G20142	3.55	Toll-Interleukin-Resistance domain-containing protein
AT2G30250	2.03	putative WRKY transcription factor 25	AT5G44920	2.07	Toll-Interleukin-Resistance domain-

ATG	*b1f1f2*	annotation	ATG	*b1f1f2*	annotation
					containing protein
AT1G69810	1.18	putative WRKY transcription factor 36	AT1G72900	1.12	Toll-Interleukin-Resistance domain-containing protein
AT5G22570	5.28	putative WRKY transcription factor 38			
AT4G11070	4.88	putative WRKY transcription factor 41			
AT2G46400	2.71	putative WRKY transcription factor 46			
AT4G01720	1.20	putative WRKY transcription factor 47			
AT5G49520	1.20	putative WRKY transcription factor 48			
AT5G26170	3.15	putative WRKY transcription factor 50			
AT5G64810	4.59	putative WRKY transcription factor 51			
AT4G23810	1.21	putative WRKY transcription factor 53			
AT2G21900	4.39	putative WRKY transcription factor 59			
AT2G25000	2.28	putative WRKY transcription factor 60			
AT1G18860	4.45	putative WRKY transcription factor 61			
AT5G01900	4.33	putative WRKY transcription factor 62			
AT1G66600	4.68	putative WRKY transcription factor 63			
AT1G29280	1.64	putative WRKY transcription factor 65			
AT1G66550	4.73	putative WRKY transcription factor 67			
AT3G56400	2.15	putative WRKY transcription factor 70			
AT1G29860	1.22	putative WRKY transcription factor 71			
AT5G15130	4.01	putative WRKY transcription factor 72			
AT5G13080	5.12	putative WRKY transcription factor 75			
AT5G07100	1.40	WRKY DNA-binding protein 26			
AT5G24110	1.13	WRKY DNA-binding protein 30			
AT4G22070	4.57	WRKY DNA-binding protein 31			
AT3G01970	1.74	WRKY DNA-binding protein 45			
AT2G40750	3.08	WRKY DNA-binding protein 54			
AT3G01080	3.70	WRKY DNA-binding protein 58			
AT4G31800	2.31	WRKY transcription factor 18			
AT2G40740	4.07	WRKY transcription factor 55			
AT1G62300	1.30	WRKY transcription factor 6			
AT1G01010	2.21	NAC domain-containing protein 1			
AT1G02220	1.48	NAC domain-containing protein 3			
AT1G02230	3.60	NAC domain-containing protein 4			
AT5G39610	2.40	NAC domain containing protein 6			
AT1G25580	1.11	NAC domain-containing protein 8			
AT1G34180	3.47	NAC domain containing protein 16			
AT1G52890	3.43	NAC domain-containing protein 19			
AT2G17040	2.28	NAC domain containing protein 36			
AT2G24430	5.41	NAC domain containing protein 38			
AT2G43000	3.74	NAC domain-containing protein 42			
AT3G04060	2.63	NAC domain containing protein 46			
AT3G04070	4.25	NAC domain containing protein 47			

ATG	*b1f1f2*	annotation	ATG	*b1f1f2*	annotation
AT3G04420	1.39	NAC domain containing protein 48			
AT3G10500	1.53	NAC domain containing protein 53			
AT3G15500	1.75	NAC domain-containing protein 55			
AT3G44350	4.35	putative NAC domain-containing protein 61			
AT4G01540	1.02	NAC domain-containing protein 68			
AT5G14490	6.93	NAC domain containing protein 85			
AT5G18270	1.91	NAC domain containing protein 87			
AT5G39820	4.25	NAC domain containing protein 94			
AT5G22380	4.71	NAC domain-containing protein 90			
AT5G61430	2.45	NAC domain containing protein 100			
AT2G30140	1.90	UDP-glucoronosyl/UDP-glucosyl transferase-like protein			
AT4G34131	1.40	UDP-glucosyl transferase 73B3			
AT2G36780	2.46	UDP-glucosyl transferase 73C			
AT3G53150	5.13	UDP-glucosyl transferase 73D1			
AT2G26480	3.66	UDP-glucosyl transferase 76D1			
AT5G59580	5.80	UDP-glucosyl transferase 76E1			
AT4G34135	1.44	UDP-glucosyltransferase 73B2			

***Tab. S3: 217 SA responsive genes identified by Blanco* et al. *(2009) were compared to the expression in wild type BTH treated,* ugt76b1 ugt74f1 ugt74f2 *(b1f1f2)*, ugt76b1 *(b1) and* ugt74f1 ugt74f2 *(f1f2)*.**

Values represent log2 fold changes compared to the wild type untreated with adjusted p-values smaller than 0.05.

ATG	Blanco *et al.* 2009	WT BTH	*b1f1f2*	*b1*	*f1f2*
AT3G16150	1.75	-2.31	-1.80	-	-2.03
AT1G32120	1.05	-1.68	-1.19	-1.02	-
AT3G15520	1.13	-1.42	-	3.58	1.03
AT4G15550	1.99	-1.19	-1.08	-	-
AT5G14730	1.07	-1.09	-	3.74	-
AT4G18950	1.01	1.07	-	3.60	-
AT3G44190	1.30	1.10	-	2.89	2.15
AT4G11900	1.49	1.11	1.05	1.13	-
AT1G66970	2.52	1.11	-	3.46	1.07
AT1G05170	1.05	1.15	-	4.08	-
AT2G16430	1.16	1.16	-	3.15	2.18
AT3G26690	1.32	1.19	-	3.85	-
AT1G77120	1.19	1.21	1.12	-	-
AT4G13180	2.31	1.22	-	3.95	1.17
AT3G14840	1.38	1.24	1.09	-	-
AT4G38550	1.33	1.27	1.26	1.02	-
AT2G23200	1.56	1.29	1.13	1.23	-
AT5G11970	1.04	1.30	-	3.98	1.35
AT5G19440	1.05	1.30	-	4.47	-
AT2G39220	1.53	1.31	-	4.24	-
AT5G03320	1.00	1.32	-	4.40	-
AT3G04480	1.57	1.34	-	4.52	1.50
AT1G11330	1.16	1.36	1.28	1.20	-
AT3G21630	1.06	1.36	-	4.32	1.54
AT1G70740	1.01	1.37	-	4.72	-
AT4G35310	1.10	1.37	-	3.11	-
AT1G25580	1.03	1.38	1.11	-	-
AT4G25940	1.10	1.39	1.22	1.40	-
AT3G50950	1.53	1.39	1.23	1.10	-
AT1G53710	1.28	1.39	1.01	-	-1.05
AT1G70530	1.16	1.40	1.04	-	-
AT3G21810	1.12	1.42	1.15	1.14	-
AT5G36930	1.61	1.45	1.37	1.55	-
AT1G69730	1.36	1.46	-	4.43	1.93
AT5G19930	1.03	1.47	-	4.98	-
AT5G03610	1.27	1.48	-	4.16	-
AT5G56230	1.20	1.48	1.59	1.66	-
AT4G23570	1.08	1.49	1.02	-	-
AT3G29240	2.26	1.49	-	4.43	1.10
AT1G07400	1.05	1.52	-	5.52	1.41

ATG	Blanco *et al.* 2009	WT BTH	*b1f1f2*	*b1*	*f1f2*
AT4G19660	2.44	1.52	1.07	-	-
AT4G36150	1.46	1.52	1.40	1.26	-
AT3G12040	1.04	1.56	1.32	1.22	-
AT3G59570	1.10	1.58	-	5.49	-
AT5G27920	1.25	1.59	1.29	-	-
AT5G07360	1.09	1.66	1.32	1.29	-
AT3G14990	1.46	1.67	1.17	-	-
AT1G07630	1.07	1.68	1.06	1.00	-
AT1G65800	1.86	1.68	1.54	1.30	-
AT1G03370	1.26	1.70	1.16	1.19	-
AT5G64370	1.01	1.75	1.29	-	-
AT1G52780	1.76	1.78	1.27	1.29	-
AT5G19980	1.09	1.82	1.02	-	-
AT3G11840	1.08	1.83	1.32	1.49	-
AT2G25460	1.08	1.84	-	5.14	-
AT4G27740	1.01	1.86	1.54	1.43	-
AT4G02380	1.06	1.86	-	5.66	-
AT5G51830	2.18	1.88	-	5.03	1.57
AT4G14400	2.69	1.89	1.67	1.43	-
AT4G23810	1.97	1.90	1.21	1.20	-
AT5G05410	1.00	1.92	3.05	2.72	1.01
AT2G44180	1.06	1.92	1.35	-	-
AT4G28490	1.48	1.93	1.08	-	-
AT5G45500	1.16	1.96	1.48	1.15	-
AT1G11310	1.77	1.98	1.27	1.05	-
AT3G63030	1.19	1.98	1.64	1.16	2.82
AT1G14790	1.15	1.99	1.63	1.40	-
AT4G26070	1.74	1.99	1.51	1.27	-
AT5G25930	1.21	2.01	1.19	-	-
AT5G53550	1.89	2.02	1.80	1.69	-
AT4G32870	2.10	2.04	1.35	1.87	-
AT5G05190	1.09	2.04	1.19	1.04	-
AT5G45510	1.23	2.04	1.62	1.07	-
AT3G09830	1.11	2.05	1.43	1.54	-
AT4G02220	1.16	2.09	1.32	1.12	-
AT1G49000	1.13	2.10	1.23	-	-
AT3G08870	1.33	2.11	1.53	1.32	-
AT4G14220	1.18	2.16	1.12	1.07	-
AT4G33300	1.21	2.16	1.69	1.52	-
AT5G42440	1.26	2.16	1.62	2.27	-
AT4G23470	1.16	2.17	1.40	1.93	-
AT4G36090	1.32	2.18	1.46	1.17	-
AT3G16990	1.55	2.19	1.41	1.50	-
AT1G31580	3.17	2.20	1.65	1.51	-
AT4G23260	1.09	2.23	2.14	1.73	-

ATG	Blanco *et al.* 2009	WT BTH	*b1f1f2*	*b1*	*f1f2*
AT3G28480	1.37	2.23	1.50	1.30	-
AT4G15530	1.09	2.25	-	6.00	-
AT1G12940	1.58	2.27	3.84	2.23	-
AT1G80160	1.43	2.31	2.82	2.55	-
AT1G16670	1.46	2.32	1.49	1.20	-
AT5G61010	1.16	2.32	1.36	1.37	-
AT1G03290	1.20	2.33	1.55	1.67	-
AT1G72060	1.38	2.34	2.57	2.08	-
AT3G26600	1.90	2.34	1.70	1.50	-
AT2G17120	1.08	2.38	1.53	1.38	-
AT1G65040	1.01	2.45	1.47	1.26	-
AT3G01290	1.24	2.48	1.89	1.63	-
AT2G39210	2.01	2.50	1.82	1.65	-
AT4G08470	1.39	2.50	2.31	1.83	-
AT2G44370	1.39	2.52	2.06	1.69	-
AT5G54860	1.40	2.61	1.62	-	-
AT3G50470	1.47	2.62	2.62	2.61	-
AT5G18780	1.35	2.67	1.96	1.30	-
AT3G51890	1.17	2.68	1.80	1.81	-
AT1G07000	1.50	2.71	1.91	1.54	-
AT2G25510	3.71	2.71	2.32	2.19	-
AT5G08380	1.21	2.77	2.33	2.11	-
AT4G01870	1.55	2.79	-	5.75	1.61
AT3G45620	1.39	2.80	1.95	1.81	-
AT3G07195	1.52	2.87	2.08	1.90	-
AT1G17860	1.35	2.87	2.79	-	-
AT5G24210	2.13	2.91	1.97	1.74	-
AT3G14620	1.34	2.92	1.75	1.53	-
AT1G34750	2.11	2.93	2.05	1.58	-
AT2G40750	2.84	2.96	3.08	2.53	-
AT5G18270	1.31	2.97	1.91	1.73	-
AT5G48380	1.07	2.98	2.21	1.81	-
AT1G51790	1.30	2.99	2.94	3.06	1.46
AT3G56710	2.92	3.00	1.83	1.47	-
AT4G31800	1.93	3.05	2.31	1.63	-
AT1G76970	1.36	3.05	1.78	1.54	-
AT3G05660	1.46	3.10	3.14	2.68	1.18
AT5G03350	7.57	3.12	2.40	2.06	-
AT2G31880	1.40	3.16	2.19	2.90	2.26
AT2G46430	1.64	3.18	2.50	2.87	1.08
AT5G05460	2.09	3.20	2.52	2.04	-
AT1G02850	1.11	3.26	1.47	1.23	-
AT2G25000	1.48	3.34	2.28	2.68	1.51
AT5G54610	3.56	3.34	2.52	2.06	-
AT3G50260	1.36	3.35	2.86	2.18	1.07

ATG	Blanco *et al.* 2009	WT BTH	*b1f1f2*	*b1*	*f1f2*
AT3G54960	1.11	3.39	2.07	1.66	-
AT3G60140	1.36	3.43	4.36	2.91	-
AT1G72680	1.51	3.49	2.11	1.88	-
AT3G09010	2.80	3.54	1.93	1.74	-
AT1G04980	1.14	3.57	2.21	2.11	-
AT2G30550	1.86	3.58	2.18	1.85	-
AT5G39050	1.35	3.59	1.99	1.86	-
AT1G66880	1.26	3.65	2.46	1.90	-
AT1G51800	1.92	3.65	2.83	2.62	-
AT3G46230	1.34	3.78	1.80	1.54	-
AT4G25110	2.06	3.78	3.39	2.62	-
AT3G08970	1.16	3.79	2.31	1.83	-
AT5G37600	1.61	3.82	3.61	-	-
AT3G62780	2.12	3.82	3.55	2.26	2.34
AT1G70690	1.07	3.83	2.46	2.25	1.54
AT5G26920	1.12	3.85	2.27	1.83	-
AT5G13330	1.13	3.89	2.66	-	-
AT1G03850	3.39	3.95	2.24	1.77	-
AT2G46400	1.55	3.97	2.71	2.16	-
AT4G13510	1.94	3.99	2.79	2.63	-
AT5G26340	1.42	4.01	3.42	2.05	-
AT4G14365	1.20	4.03	2.83	3.23	1.41
AT3G61190	1.26	4.09	2.64	1.88	1.22
AT5G64510	1.42	4.09	3.04	2.50	-
AT4G26090	1.69	4.22	3.94	3.15	1.52
AT3G50480	1.60	4.33	3.07	2.39	3.37
AT2G27660	1.38	4.36	3.52	3.26	-
AT3G48640	1.62	4.38	3.05	2.34	-
AT4G26270	1.12	4.56	3.61	2.36	-
AT1G08050	1.27	4.68	3.07	2.79	-
AT3G28540	1.22	4.73	3.52	3.41	-
AT3G04070	1.10	4.76	4.25	2.89	1.89
AT1G28480	3.49	4.85	2.83	2.49	-
AT4G20110	1.23	4.94	3.82	2.50	-
AT3G25882	5.66	4.97	3.74	2.26	-
AT5G24530	3.70	5.03	4.06	3.58	1.21
AT3G47480	1.30	5.20	3.82	2.74	-
AT2G45220	1.29	5.22	4.10	3.04	-
AT1G10340	1.22	5.28	4.43	2.46	-
AT4G11890	1.47	5.32	3.96	3.35	-
AT5G01900	4.32	5.33	4.33	3.27	2.33
AT2G34500	1.02	5.40	2.80	2.50	-
AT1G02450	5.79	5.44	4.78	-	-
AT5G11920	1.43	5.48	4.69	3.33	-
AT1G65610	1.15	5.85	3.82	2.64	-

ATG	Blanco *et al.* 2009	WT BTH	*b1f1f2*	*b1*	*f1f2*
AT2G24850	1.17	6.03	3.86	2.73	-
AT5G22570	4.96	6.08	5.28	3.13	-
AT5G10760	1.06	6.08	5.20	3.11	-
AT3G13950	1.67	6.45	4.45	2.57	2.07
AT1G14880	3.55	6.81	5.36	3.81	-
AT3G11340	5.72	6.91	4.61	2.90	1.02
AT3G60420	1.38	7.38	6.03	2.67	2.40
AT5G13080	1.71	8.63	5.12	2.52	2.24
AT1G70520	1.00	-	-	-	-
AT1G76520	1.00	-	-	-	-
AT5G38530	1.01	-	-	-	-
AT2G39200	1.03	-	-	-	1.17
AT2G46450	1.06	-	-	-	-1.18
AT3G23175	1.08	-	-	-	-
AT1G52290	1.11	-	-	1.05	-
AT3G25190	1.13	-	-1.06	-1.01	-
AT5G44070	1.15	-	-	-	-
AT5G39580	1.16	-	1.21	-	2.56
AT2G39740	1.16	-	-	-	-
AT4G21990	1.17	-	-	-	-1.36
AT3G25070	1.20	-	-	-	-
AT1G21670	1.22	-	1.33	-	1.49
AT3G62370	1.23	-	-	-	-
AT5G14470	1.26	-	-	-	-
AT5G19750	1.26	-	-	-	-
AT3G29230	1.31	-	-	-	-
AT5G38980	1.32	-	-	-	-
AT2G29420	1.37	-	-	-	-
AT5G11250	1.38	-	-	-	-
AT1G15045	1.40	-	-	-	-
AT3G57700	1.42	-	-	-	-
AT3G11280	1.46	-	-	-	-
AT5G64250	1.51	-	-	-	-
AT1G76600	1.52	-	-	1.08	-
AT5G05090	1.55	-	-	-	-
AT2G02800	1.61	-	-	-	-
AT4G01070	1.74	-	-	-	-
AT1G49750	1.77	-	-	-	-
AT1G16260	1.80	-	1.08	1.20	-
AT3G04210	1.86	-	-	1.22	-
AT1G73800	2.33	-	-	-	-
AT5G63790	2.41	-	-	-	-

***Tab. S4: ROS responsive genes identified by Gadjev* et al*. (2006) were compared to the expression in wild type BTH treated (WT BTH)*, ugt76b1 ugt74f1 ugt74f2 *(b1f1f2)*, ugt76b1 *(b1) and* ugt74f1 ugt74f2 *(f1f2)*.**

Values represent log2 fold changes compared to the wild type untreated with adjusted p-values smaller than 0.05.

ATG	WT BTH	*b1f1f2*	*b1*	*f1f2*
AT4G22530	1.39	-	-	-
AT2G43510	1.53	1.53	1.74	-
AT1G19020	1.76	-	1.26	-
AT3G53230	2.11	-	1.37	-
AT1G62300	2.58	1.30	1.62	-
AT1G22400	2.78	1.10	1.70	-
AT4G01870	2.79	-1.21	-	-
AT1G10585	3.02	-	1.07	-
AT1G26380	3.30	3.03	2.69	-
AT2G32190	3.34	-1.16	-	-1.56
AT2G41380	3.39	1.90	2.18	-
AT4G37990	3.39	2.42	2.63	-
AT4G37370	3.49	1.78	2.32	-
AT3G54150	3.56	2.84	3.05	1.35
AT1G17170	3.60	1.74	2.29	-
AT3G08970	3.79	2.41	2.94	1.36
AT1G26420	3.86	2.31	3.04	-
AT1G05340	4.26	1.93	2.54	-
AT3G28210	4.92	2.63	3.13	1.64
AT1G13340	5.27	4.11	3.92	2.29
AT4G39670	5.36	3.95	4.22	1.86
AT1G57630	5.77	3.58	3.97	-
AT3G26830	5.84	2.84	3.31	-
AT2G29460	5.91	3.79	4.21	-
AT3G11340	6.91	-	-	1.18
AT5G13080	8.63	4.61	5.03	1.57
AT2G29470	9.17	5.12	5.75	1.61
AT2G21640	-	7.06	6.65	-
AT3G49620	-	-	-	1.68

***Tab. S5: ROS responsive genes identified by Vaahtera* et al.** ***(2014) were compared to the expression in wild type BTH treated (WT BTH),* ugt76b1 ugt74f1 ugt74f2 *(b1f1f2)*, ugt76b1 *(b1) and* ugt74f1 ugt74f2 *(f1f2)*.**

Values represent log2 fold changes compared to the wild type untreated with adjusted p-values smaller than 0.05.

ATG	WT BTH	*b1f1f2*	*b1*	*f1f2*
AT4G23290	-2.87	-1.39	-	-
AT5G47230	-1.59	-	-	-
AT4G17490	-1.58	-	-	-
AT2G29450	-1.58	-1.37	-	-
AT5G28630	-1.52	-	-	-
AT1G27130	-1.16	-	-	-
AT5G27760	1.24	-	-	-
AT2G33710	1.25	-	1.23	-
AT3G50970	1.28	2.14	1.02	2.36
AT3G45640	1.37	-	1.12	-
AT3G12740	1.73	-	1.18	-
AT3G11840	1.83	1.32	1.43	-
AT4G02380	1.86	-	-	-
AT1G05100	1.97	-	-	-
AT1G30370	1.98	1.39	2.20	-
AT2G29500	2.04	-	1.80	-
AT1G80820	2.37	-	1.60	-
AT5G46080	2.47	1.27	1.62	-
AT3G01290	2.48	1.89	2.19	-
AT2G44370	2.52	2.06	2.25	1.54
AT4G12720	2.58	1.37	1.76	-
AT3G25250	2.59	-	1.62	-
AT5G20230	3.60	2.41	2.55	-
AT3G46230	3.78	1.80	3.35	-
AT3G61190	4.09	2.64	3.13	-
AT5G22530	5.48	3.72	4.13	1.67
AT3G28580	5.55	4.17	4.43	-
AT4G10500	7.21	5.32	6.61	-
AT2G40000	-	-	1.17	-

Tab. S6: Candidate genes of transporters positively regulated in* ugt76b1*, which were not regulated in* ugt74f1*, with their localisation according to the TAIR database.

ATG	*ugt76b1*	annotation	located in
AT2G34960	1.04	cationic amino acid transporter 5	integral component of membrane, mitochondrion, plasma membrane
AT1G53270	1.05	ABC transporter G family member 10	mitochondrion, plasma membrane
AT5G09710	1.06	putative magnesium transporter MRS2-9	NA
AT1G67940	1.09	ABC transporter I family member 17	plasma membrane, vacuolar membrane
AT1G68570	1.12	putative nitrite transporter, NPF3.1	cytoplasm, integral component of membrane, intracellular vesicle, plasma membrane
AT3G60160	1.21	ABC transporter C family member 9	chloroplast, membrane, plant-type vacuole, plasmodesma, vacuolar membrane
AT2G32830	1.30	putative inorganic phosphate transporter 1-5	cytoplasm, integral component of membrane
AT5G19980	1.30	golgi nucleotide sugar transporter 4	Golgi apparatus, Golgi trans cisterna, chloroplast
AT1G78000	1.33	sulfate transporter 1	chloroplast, integral component of plasma membrane, plasma membrane
AT1G30420	1.36	ABC transporter C family member 11	cytoplasm, membrane, nucleus, plant-type vacuole, vacuolar membrane
AT2G41190	1.39	transmembrane amino acid transporter-like protein	nucleus, plasma membrane, vacuolar membrane
AT1G14360	1.69	UDP-galactose transporter 3	integral component of Golgi membrane, integral component of endoplasmic reticulum membrane
AT4G23010	1.74	UDP-galactose transporter 2	cytoplasm, integral component of Golgi membrane, integral component of endoplasmic reticulum membrane, plasma membrane
AT1G69480	1.76	phosphate transporter PHO1-10	Golgi apparatus, cytoplasm, plasma membrane, trans-Golgi network
AT5G53550	1.81	metal-nicotianamine transporter YSL3	cytoplasm, extracellular region, membrane, plasma membrane
AT1G55910	1.86	zinc transporter 11	chloroplast, membrane, nucleus
AT5G40240	1.98	nodulin MtN21/EamA-like transporter family protein	plasma membrane
AT3G13080	2.11	ABC transporter C family member 3	apoplast, chloroplast, membrane, plant-type vacuole, plasmodesma, vacuolar membrane, vacuole
AT2G47800	2.14	ABC transporter C family member 4	Golgi apparatus, chloroplast, cytosol, membrane, plant-type vacuole, plasma membrane, plasmodesma, vacuolar membrane, vacuole
AT2G02810	2.21	UDP-galactose transporter 1	chloroplast, endoplasmic reticulum membrane, integral component of Golgi membrane, integral component of endoplasmic reticulum membrane
AT1G72125	2.57	putative peptide/nitrate transporter, NPF5.13	integral component of membrane
AT3G03700	2.64	Plasma-membrane choline transporter family protein	integral component of membrane, plasma membrane
AT5G40230	2.72	nodulin MtN21/EamA-like transporter family protein	plasma membrane
AT3G47780	2.86	ABC transporter A family member 7	intracellular membrane-bounded organelle, mitochondrion, plasma membrane, plasmodesma
AT1G65730	3.25	putative metal-nicotianamine transporter YSL7	membrane, nucleus, plasma membrane
AT3G60970	3.76	putative ABC transporter C-15	membrane, plant-type vacuole, vacuolar membrane
AT3G01760	3.99	Lysine histidine transporter-like 4	plasma membrane

Tab. S7: Comparison of mobile RNAs identified from Thieme* et al. *(2015) with significantly changed genes with a fold change higher than two in* ugt76b1 *(b1).

Values represent log2 fold changes compared to the wild type untreated with adjusted p-values smaller than 0.05. 22 genes showed negative, whereas 273 showed positive regulation in ugt76b1 *background.*

ATG	shoot to root	root to shoot	*b1*
AT2G01520	shoot to root	root to shoot	-5.66
AT5G26260	shoot to root	root to shoot	-4.04
AT3G44540	shoot to root		-3.10
AT4G11320	shoot to root	root to shoot	-1.84
AT3G44550	shoot to root		-1.61
AT1G14250		root to shoot	-1.56
AT4G37410	shoot to root	root to shoot	-1.55
AT5G03545	shoot to root	root to shoot	-1.54
AT3G50300	shoot to root		-1.37
AT1G67105	shoot to root		-1.33
AT2G05440	shoot to root	root to shoot	-1.31
AT1G27030	shoot to root	root to shoot	-1.20
AT3G53480	shoot to root		-1.17
AT5G65700	shoot to root		-1.11
AT5G44530	shoot to root		-1.10
AT3G16240	shoot to root	root to shoot	-1.06
AT2G25790	shoot to root		-1.04
AT3G27690	shoot to root		-1.04
AT4G37220	shoot to root		-1.02
AT3G21420	shoot to root	root to shoot	-1.01
AT1G12010		root to shoot	-1.01
AT2G38760		root to shoot	-1.01
AT2G37940	shoot to root		1.00
AT1G77420		root to shoot	1.01
AT5G47420		root to shoot	1.02
AT2G04400	shoot to root	root to shoot	1.02
AT3G50970	shoot to root	root to shoot	1.02
AT4G24690	shoot to root	root to shoot	1.03
AT2G24180	shoot to root	root to shoot	1.03
AT3G06300	shoot to root	root to shoot	1.03
AT4G33920	shoot to root		1.03
AT3G19190	shoot to root		1.03
AT1G24530		root to shoot	1.03
AT4G37520	shoot to root		1.03
AT2G46600	shoot to root	root to shoot	1.03
AT4G18930	shoot to root		1.03
AT5G03320	shoot to root	root to shoot	1.04
AT2G47470		root to shoot	1.05
AT1G59580		root to shoot	1.05
AT4G04960	shoot to root		1.06
AT4G02370	shoot to root		1.06
AT5G10610		root to shoot	1.06
AT5G16880	shoot to root		1.06
AT3G14840	shoot to root	root to shoot	1.07
AT2G17760		root to shoot	1.07
AT5G51070	shoot to root	root to shoot	1.07

ATG	shoot to root	root to shoot	*b1*
AT4G04570	shoot to root	root to shoot	1.07
AT4G15260	shoot to root	root to shoot	1.07
AT1G65820	shoot to root		1.07
AT1G58602	shoot to root	root to shoot	1.07
AT2G38250	shoot to root		1.08
AT1G76600	shoot to root		1.08
AT4G28710	shoot to root	root to shoot	1.09
AT1G09970	shoot to root	root to shoot	1.09
AT1G09480	shoot to root		1.09
AT1G67940		root to shoot	1.09
AT4G01370	shoot to root		1.09
AT5G04720	shoot to root	root to shoot	1.10
AT1G66090	shoot to root		1.10
AT3G17410	shoot to root		1.10
AT2G19710		root to shoot	1.11
AT1G51660	shoot to root		1.11
AT2G05520	shoot to root		1.11
AT1G62422	shoot to root		1.11
AT3G03610	shoot to root		1.11
AT5G23510	shoot to root		1.12
AT3G45640	shoot to root	root to shoot	1.12
AT2G45910	shoot to root		1.12
AT2G37110	shoot to root	root to shoot	1.13
AT3G05500	shoot to root		1.13
AT2G23200		root to shoot	1.14
AT5G03460	shoot to root	root to shoot	1.14
AT5G39000		root to shoot	1.15
AT4G28570		root to shoot	1.15
AT3G14990	shoot to root	root to shoot	1.15
AT2G35810	shoot to root		1.16
AT2G28570	shoot to root	root to shoot	1.16
AT5G05410	shoot to root		1.16
AT4G20830	shoot to root	root to shoot	1.17
AT2G03120	shoot to root	root to shoot	1.17
AT3G12740	shoot to root	root to shoot	1.18
AT1G69610	shoot to root		1.18
AT1G61610		root to shoot	1.18
AT2G41100	shoot to root	root to shoot	1.19
AT3G28450	shoot to root	root to shoot	1.19
AT3G50950	shoot to root	root to shoot	1.20
AT1G59870	shoot to root	root to shoot	1.20
AT2G31945	shoot to root		1.20
AT1G72900	shoot to root		1.21
AT5G44580	shoot to root	root to shoot	1.23
AT5G61380	shoot to root		1.23
AT3G20510		root to shoot	1.23
AT4G20860	shoot to root		1.24
AT1G22930	shoot to root		1.25
AT5G07830	shoot to root		1.25
AT1G56510	shoot to root	root to shoot	1.26
AT5G46520	shoot to root	root to shoot	1.26

ATG	shoot to root	root to shoot	*b1*
AT5G18310	shoot to root		1.28
AT4G39950	shoot to root	root to shoot	1.28
AT5G39785	shoot to root		1.28
AT2G36890	shoot to root		1.28
AT4G11530	shoot to root		1.28
AT4G21980	shoot to root		1.29
AT1G72910	shoot to root		1.30
AT1G65800	shoot to root	root to shoot	1.30
AT5G19240	shoot to root		1.30
AT4G14220	shoot to root		1.30
AT3G44720	shoot to root	root to shoot	1.31
AT3G15500	shoot to root		1.32
AT1G50520	shoot to root		1.32
AT3G52710	shoot to root	root to shoot	1.32
AT1G18570	shoot to root		1.32
AT2G39420	shoot to root	root to shoot	1.33
AT3G28880		root to shoot	1.34
AT5G39030	shoot to root		1.34
AT3G15760	shoot to root		1.34
AT5G58120	shoot to root		1.34
AT1G69490	shoot to root		1.35
AT2G40095	shoot to root		1.35
AT1G32700		root to shoot	1.36
AT5G21090		root to shoot	1.36
AT3G19930	shoot to root		1.36
AT3G53230	shoot to root		1.37
AT1G30700	shoot to root		1.37
AT5G37070	shoot to root		1.38
AT1G52780	shoot to root	root to shoot	1.38
AT5G24230	shoot to root		1.39
AT1G51760	shoot to root	root to shoot	1.43
AT1G80840	shoot to root	root to shoot	1.43
AT4G28490	shoot to root	root to shoot	1.43
AT4G16660	shoot to root	root to shoot	1.44
AT3G20600	shoot to root		1.44
AT1G61250		root to shoot	1.45
AT2G22860	shoot to root		1.45
AT5G66620	shoot to root		1.45
AT4G21534	shoot to root		1.45
AT2G37970	shoot to root	root to shoot	1.46
AT5G05190	shoot to root	root to shoot	1.47
AT1G64360	shoot to root		1.48
AT4G01740	shoot to root		1.49
AT5G27420	shoot to root	root to shoot	1.50
AT3G17700	shoot to root		1.50
AT5G45110	shoot to root	root to shoot	1.51
AT1G64065	shoot to root	root to shoot	1.52
AT4G35600	shoot to root		1.52
AT4G09750		root to shoot	1.52
AT5G37740	shoot to root	root to shoot	1.52
AT2G19130	shoot to root	root to shoot	1.52

ATG	shoot to root	root to shoot	*b1*
AT5G17330	shoot to root	root to shoot	1.52
AT5G42050	shoot to root	root to shoot	1.53
AT2G17290	shoot to root	root to shoot	1.53
AT5G25930	shoot to root		1.54
AT5G38210	shoot to root		1.55
AT3G10500	shoot to root		1.55
AT4G25900	shoot to root		1.56
AT1G06620	shoot to root	root to shoot	1.57
AT4G17500	shoot to root	root to shoot	1.59
AT4G23885		root to shoot	1.60
AT5G23850	shoot to root		1.60
AT1G70810	shoot to root	root to shoot	1.61
AT2G41640	shoot to root		1.61
AT3G29000	shoot to root	root to shoot	1.61
AT1G65250	shoot to root		1.61
AT3G25250	shoot to root		1.62
AT2G17710	shoot to root	root to shoot	1.62
AT5G45510	shoot to root	root to shoot	1.63
AT4G21930	shoot to root		1.64
AT1G27330	shoot to root	root to shoot	1.65
AT1G02520	shoot to root		1.66
AT5G48560	shoot to root	root to shoot	1.66
AT1G09560	shoot to root	root to shoot	1.66
AT2G32210	shoot to root		1.67
AT3G23510		root to shoot	1.67
AT5G49520	shoot to root	root to shoot	1.67
AT5G56870	shoot to root	root to shoot	1.67
AT3G63010	shoot to root		1.68
AT1G30730		root to shoot	1.73
AT1G61120		root to shoot	1.74
AT3G51540	shoot to root		1.76
AT1G72120	shoot to root	root to shoot	1.77
AT1G16150	shoot to root	root to shoot	1.77
AT2G41090	shoot to root		1.78
AT3G09020	shoot to root	root to shoot	1.78
AT1G59590	shoot to root	root to shoot	1.78
AT2G13790	shoot to root	root to shoot	1.80
AT1G17745		root to shoot	1.80
AT3G44860	shoot to root	root to shoot	1.80
AT2G37710	shoot to root		1.81
AT5G61210	shoot to root	root to shoot	1.83
AT4G34390	shoot to root		1.83
AT5G59820	shoot to root		1.83
AT4G24026		root to shoot	1.85
AT5G43420	shoot to root		1.86
AT3G49120	shoot to root	root to shoot	1.88
AT1G12160	shoot to root		1.88
AT5G54860	shoot to root		1.90
AT3G04720	shoot to root		1.90
AT1G31580	shoot to root		1.90
AT4G11000	shoot to root	root to shoot	1.93

ATG	shoot to root	root to shoot	*b1*
AT5G04930	shoot to root	root to shoot	1.93
AT5G10625	shoot to root	root to shoot	1.94
AT4G01610	shoot to root	root to shoot	1.97
AT2G46440	shoot to root		1.97
AT1G02220	shoot to root		2.01
AT2G40113	shoot to root		2.01
AT4G39675	shoot to root	root to shoot	2.06
AT3G60450	shoot to root	root to shoot	2.08
AT1G21750	shoot to root		2.13
AT2G47800		root to shoot	2.14
AT5G47120	shoot to root	root to shoot	2.14
AT5G58940	shoot to root		2.16
AT5G37540	shoot to root		2.18
AT3G25780	shoot to root	root to shoot	2.21
AT1G54575	shoot to root		2.22
AT1G56660	shoot to root	root to shoot	2.22
AT4G01750	shoot to root	root to shoot	2.23
AT5G59570	shoot to root		2.25
AT4G23170	shoot to root	root to shoot	2.25
AT3G50260	shoot to root		2.26
AT5G20400	shoot to root	root to shoot	2.28
AT5G52750	shoot to root		2.29
AT1G58190	shoot to root		2.33
AT1G65500	shoot to root		2.34
AT1G67810	shoot to root		2.49
AT5G24210		root to shoot	2.50
AT5G41750	shoot to root		2.51
AT5G35580	shoot to root		2.51
AT2G17040	shoot to root	root to shoot	2.54
AT4G12290	shoot to root		2.54
AT5G20230	shoot to root	root to shoot	2.55
AT3G14620	shoot to root	root to shoot	2.55
AT3G44300	shoot to root	root to shoot	2.58
AT3G02840	shoot to root		2.58
AT3G09010	shoot to root		2.64
AT4G26090	shoot to root	root to shoot	2.67
AT4G31800	shoot to root		2.72
AT1G66880	shoot to root	root to shoot	2.73
AT1G07900		root to shoot	2.82
AT5G52640	shoot to root	root to shoot	2.83
AT5G44480		root to shoot	2.85
AT3G47780	shoot to root		2.86
AT5G52810	shoot to root		2.94
AT3G52430	shoot to root	root to shoot	2.97
AT1G31885	shoot to root		2.99
AT3G50930	shoot to root	root to shoot	3.01
AT1G51800	shoot to root		3.15
AT1G34420	shoot to root		3.16
AT1G21250	shoot to root	root to shoot	3.24
AT5G53110		root to shoot	3.25
AT5G15130	shoot to root		3.33

ATG	shoot to root	root to shoot	*b1*
AT5G59680	shoot to root		3.35
AT5G44585	shoot to root		3.35
AT3G26210	shoot to root		3.42
AT3G26470		root to shoot	3.42
AT5G25250	shoot to root	root to shoot	3.44
AT5G07780	shoot to root		3.45
AT4G15610	shoot to root	root to shoot	3.47
AT5G59670		root to shoot	3.55
AT2G44290	shoot to root		3.58
AT5G55450	shoot to root		3.62
AT1G35710	shoot to root	root to shoot	3.63
AT1G35230	shoot to root		3.65
AT3G21520	shoot to root		3.70
AT2G18690	shoot to root	root to shoot	3.71
AT4G21120	shoot to root		3.73
AT3G50770	shoot to root	root to shoot	3.74
AT3G01420	shoot to root	root to shoot	3.74
AT1G61800		root to shoot	3.81
AT5G10380	shoot to root		3.87
AT3G26830	shoot to root	root to shoot	3.92
AT5G39670	shoot to root		3.99
AT2G35980	shoot to root		4.02
AT5G45380	shoot to root		4.05
AT5G38344	shoot to root		4.11
AT1G30900	shoot to root		4.25
AT4G39670	shoot to root		4.30
AT5G66690	shoot to root	root to shoot	4.31
AT5G27060		root to shoot	4.36
AT2G14560	shoot to root	root to shoot	4.37
AT3G28580	shoot to root		4.43
AT5G24530	shoot to root	root to shoot	4.47
AT2G26820	shoot to root	root to shoot	4.62
AT3G51860	shoot to root	root to shoot	4.98
AT3G13950	shoot to root		5.14
AT2G32680	shoot to root		5.14
AT2G04495	shoot to root		5.18
AT1G21240	shoot to root		5.20
AT1G75040	shoot to root	root to shoot	5.35
AT4G14630	shoot to root	root to shoot	5.41
AT3G13610	shoot to root	root to shoot	5.53
AT3G28510	shoot to root	root to shoot	5.55
AT5G44460		root to shoot	5.63
AT4G00700	shoot to root	root to shoot	5.67
AT3G15536	shoot to root		6.49
AT4G10500		root to shoot	6.61

Tab. S8: Comparison of mobile RNAs identified from Deeken* et al. *(2008) with significantly changed genes with a fold change higher than two in* ugt76b1 *(b1).

Values represent log2 fold changes compared to the wild type untreated with adjusted p-values smaller than 0.05.

ATG	*b1*
AT2G31880	2.53
AT1G35710	3.63
AT4G21400	1.32
AT2G13790	1.80
AT2G13800	1.47
AT1G21250	3.24
AT1G09210	1.44
AT1G18210	1.11
AT2G46600	1.03
AT4G33050	2.11
AT2G41090	1.78
AT2G41100	1.19
AT3G56800	1.23
AT3G57330	1.06
AT4G34390	1.83
AT4G29810	1.54
AT3G45640	1.12
AT4G01370	1.09

***Tab. S9: Ethylene response factors (ERFs) regulated in* ugt76b1**

Values represent log2 fold changes compared to the wild type untreated. Adjusted p-values smaller than 0.05.

ATG	*ugt76b1*	annotation
AT2G22200	-2.02	ERF056
AT1G12630	-1.16	ERF027
AT1G01250	-1.09	ERF023
AT1G64380	-1.05	ERF061
AT1G33760	1.02	ERF022
AT1G28370	1.04	ERF11
AT2G33710	1.23	ERF112
AT1G77640	1.25	ERF013
AT5G65130	1.35	ERF057
AT4G28140	1.43	ERF054
AT4G17500	1.59	ERF1A
AT5G47220	1.81	ERF2
AT1G71520	2.01	ERF020
AT1G43160	2.23	RAP2-6
AT3G50260	2.26	ERF011
AT3G23240	2.45	ERF1B/ERF1
AT5G13330	2.57	ERF113
AT5G51190	25.30	ERF105

7 Acknowledgement

I would like to pay special thankfulness, warmth and appreciation to the persons below who made my research successful and assisted me at every point to cherish my goal. This thesis would not have been possible without the help, support and guidance of many people:

Firstly, I would like to thank my direct supervisor PD Dr. Anton Schäffner for the guidance and continuous support during my PhD study. I'm extremely grateful for his confidence in my research and his constitutive criticism, which helped me to develop new and interesting questions.

I would like to especially acknowledge Prof. Dr. Jörg Durner, PD Dr. Dietmar Martin, and the members of the examination committee for their willingness to review this work. I am very grateful to Prof. Dr. Jörg Durner for valuable advices to my projects during the institute seminars, the thesis committee meetings and his comments and corrections of my thesis.

I am deeply grateful to Dr. Corina Vlot for the positive impact, suggestions, and feedback, especially for the Pip-related part of my thesis. Her meticulous comments were an enormous help to me. Prof. Dr. Jörg-Peter Schnitzler, Dr. Andrea Ghirardo, Baris Weber, and Felix Antritter for their support and providing me the access to the GC-MS instrument.

Special thanks to Birgit Geist and Birgit Lange for the crucial technical assistance in different laboratory issues. My deep thanks go to Dr. Inonge Gross and Jennifer Sales for correction of this thesis and proofreading. I'm deeply indebted to Dr. Jin Zhao, Dr. Elisabeth Georgii, and Eva-Esther Rudolf for interesting discussions and ideas throughout my whole PhD. I like to thank my flatmate Christoph Schmid for statistical advice and help.

I wish to extend my sincere gratitude to former and current members of Anton Schäffner's group: Dr. Wei Zhang, Dr. Rafał Maksym, Dr. Andre Schmiesing, Dr. Jin Zhao, Jessica Lehnert, Emily Klein, Valentin Haury, Daniel Eberl, Dr. Elisabeth Georgii, Dr. Dereje Mekonnen, Franziska Bottler, Birgit Geist, Komal Jhala, Birgit Lange, and Thayssa Schley.

I am really grateful for the best girls of BIOP family, which I could imagine, and for our not only scientific discussions and activities. All the best for you, girls! For the tea discussion with Birgit Lange about work, but also other problems. "Live long and prosper!"[1] For the coffee breaks with Anna Sommer. „Hier fängt die Geschichte an."[2]

1 Star Trek, Explained in "Journey to Babel"

2 Walter Moers; Die Stadt der Träumenden Bücher

And I am grateful to all other former and present BIOP colleagues for advices, the good cooperation, pleasant working atmosphere in the institute, the encouragement, and beyond:

PD Dr. Frank Gaupels, PD Dr. Karin Pritsch, Dr. Alexandra Ageeva-Kieferle, Dr. Stephan Dräxl, Dr. Ulrike Frank, Dr. Martin Groth, Dr. Katharina Kempkens, Dr. Miriam Lenk, Dr. Christian Lindermayr, Dr. Fabian Weikl, Dr. Barbro Winkler, Gabriele Barthel, Kornelia Bauer, Evi Bieber, Lena Frank, Lucia Gößl, Valentin Hankofer, Claudia Knappe, Diana Lochner, Elke Mattes, Patrizia Thoma, Marion Wenig, Florian Wilsch, Christoph Wurm, and all others.

Finally, I have to say 'thank-you' to: my boyfriend, my table tennis trainer, all my friends and family. Thank you for listening, offering me advice, and supporting me through this entire process.